Author:
Harrison, Aime Thomas

Title:
A performance framework for the soil strengthening properties of fibre-reinforced sand

Department of Civil Engineering

A performance framework for the soil strengthening properties of fibre-reinforced sand

A dissertation submitted to the University of Bristol in accordance with the requirements of the degree of Doctor of Philosophy in the Faculty of Engineering, Department of Civil Engineering by

Aime Thomas Harrison

April 2006

Abstract

Traditional methods of soil reinforcement consist of introducing continuous inclusions into an earth mass. Soil-improvement techniques of reinforcing soils with tension-resisting elements are now an accepted practice in civil engineering projects. However, less research has been done of the non-traditional reinforcement elements in the form of short fibres. Fibres can improve the strength of a granular cohesionless soil mass, as reinforced soils resemble traditional earth reinforcement with plant roots in many shear strength characteristics.

This study investigates the soil strengthening properties of randomly distributed fibre-reinforcement in granular soil. A range of fibre concentrations was hand-mixed with Hostun sand and the samples were fabricated by pluviation, tamping, spooning and vibration. One-dimensional compression and direct shear tests were undertaken to compare the stress- deformation response of un-reinforced sand samples and sand reinforced with ***LokSand*** fibres under static and shear stresses.

The addition of fibre content increased the peak shear strength of samples compared with un-reinforced sand samples in small-scale direct shear tests under a small range of normal stress values. The peak stress ratio and critical state stress ratio values were higher for fibre-reinforced Hostun sand samples than plain sand samples, which demonstrated the fibres' ability to increase the peak shear strength and reduce post-peak deformation in shear. The enhanced shear strength of fibre-reinforced sands was analysed with respect to the tensile strength of the fibres and the fibre content. A relationship between the samples' density values and the critical stress ratio values was determined and compared with the direct shear tests results.

The engineering properties related to the interface region between fibres and soil was of significant importance. The results of the laboratory tests demonstrated that the behaviour of sand with fibre reinforcements of random orientations were more ductile than plain sand in shear, depending on the method of preparation adopted. The enhanced shear stress values and the strain-softening properties were modelled and verified by the laboratory test results. The inclusion of fibres enhanced the shear stresses and reduced the strain localisations in Hostun sand samples. This research placed quantifiable values to the geotechnical parameters for the test sands based on their initial densities, fibre contents and normal stress values.

Acknowledgements

During this work I was supported by a grant by the Needham Cooper Trust, for which I am extremely grateful.

I would like to give special thanks to my supervisor, Professor David Muir Wood, and all my colleagues in the Geomechanics Group and the Soil Mechanics Laboratory. I have greatly enjoyed the discussions and knowledge that we have shared. I feel honoured to have been a part of a dynamic team of individuals, both technical and research staff.

I must thank my family and friends for their support during the completion of my research thesis. I dedicate this work to my parents, my aunts and my chosen family. I only hope that this dissertation can make them as proud of me as I am of them.

Declaration

I declare that the work in this dissertation was carried out in accordance with the *Regulations of the University of Bristol*. The work is original except where indicated by special reference in the text and no part of this dissertation has been submitted for any other degree.

Parts of the work have been published. This would not have been possible without the contributions of Prof. David Muir Wood in the preparation of the following papers:

Harrison, A. (2004) Fibre-Reinforced Soil: Soil Mechanics, Proceedings of the Young Geotechnical Engineering Symposium, University of Birmingham, June 2004

Harrison, A. (2002) Sample Preparation Methods for Fibre-Reinforced Soil, Proceedings of the Young Geotechnical Engineering Symposium, University of Dundee, July 2002

Any views expressed in the dissertation are personal and in no way represent those of the University of Bristol.

The dissertation has not been presented to any other University for examination either in the United Kingdom or overseas.

Signed:  Date: 1 NOVEMBER 2006

Aime Harrison

Contents

Contents

Contents

Contents

Nomenclature

Symbol	Definition
a	angle between the directions of plane deformation and the major principal stress
A_f	area of a sample occupied by fibres
A_r	area of shear plane occupied by roots
A_s	area of soil in shear
c'	cohesion
C_v	coefficient of variation
d	diameter
dv	change of dilation angle
dx	change of horizontal displacement
dy	change of vertical displacement
$d\gamma$	change of shear strain (percentage)
D_{50}	mean grain size
e	void ratio
$e_{0\%}$	void ratio value of un-reinforced samples at critical confining stress ratio
e_{cs}, e_{cv}	void ratio at critical state
e_{fc}	void ratio values of fibre-reinforced samples at critical state
e_i	initial void ratio
e_{max}	maximum void ratio
e_{min}	minimum void ratio
e_p	peak void ratio
e_{ss}	void ratio values at steady state
e_λ	void ratio to mean normal stress slope intercept
EA	stress ratio and volume change for sand reinforced with flexible strips
F	force
G_f	specific gravity of a fibre
h_t	final (total) height of a specimen
h_n	height of compacted material at the top of the layer being considered
H'	strain-softening parameter
H'_e	void ratio parameter
I_1	normal stress value
I_p	mean normal stress

l	length
I_p	mean normal stress
M_f	weight of fibres
M_s	weight of soil
n	number of the layer being considered
n_t	total number of sample layers
p	crushing strength of a soil
P_s	probability of particle survival of a crushing test
p'	mean principal stress (in triaxial tests)
q'	principal stress difference (in triaxial tests)
R_f	wall friction ratio
RD	relative density
S_{1D}	constant stress level in one-dimensional compression test
S_{1Dmin}	minimum constant stress level in one-dimensional compression test
S_r	increased shear stress due to root reinforcement
T_o	axial tensile load value
T_{cr}	Cartesian coordinate for critical tension
T_{max}	ultimate tension of reinforcement
T_p	pre-tension value
T_r	maximum tensile stress of a root
U	stress ratio and volume change for un-reinforced sand
U_n	percentage under-compaction for the layer being considered
v_o	initial volume
V_f	volume of fibres
V_{total}	total sample volume
X	distance from centre of loading to point of consideration
z	anchor length of reinforcement
α, ε, ε_1	strain
γ_d	dry density
γ_w	density of water
δ	anchor displacement
ε_v,	volumetric strain
θ	angle of root or fibre orientation
λ	angles of inclination from the shear plane
ξ	normal to the shear plane

ϕ'	angle of internal friction
ϕ'_{ds}	angle of internal friction in direct shear
ϕ'_{p}	peak angle of internal friction
ϕ'_{ps}	angle of internal friction in plane strain
ϕ'_{ld}	angle of internal friction at large displacements
ϕ'_{cv}, ϕ'_{cs}	angle of internal friction at critical value
ψ	angle of dilation
ψ_{rate}	dilation rate
ψ_{p}	peak angle of dilation
ψ_{A}, ψ_{SP}	state parameter
σ, σ_{1}, σ_{n} and σ_{yy}	normal stress
σ_{2}, σ_{3}	confining stresses (in triaxial tests)
σ_{crit}	critical normal stress
σ_{min} and σ_{max}	normal stress (minimum and maximum values)
σ_{avg}	average normal stress
σ_{yield}	normal stress at yield
τ	shear stress
τ_{yx}	shear stress in the direction *yx* in Cartesian co-ordinates
v_{x}	horizontal shear displacement

List of Figures

List of Tables

1.0 Introduction

"Nature is just enough; but men and women must comprehend and accept her suggestions."

Antoinette Brown Blackwell *(1825-1921)*

1.1 Overview of soil reinforcement methods

In nature, soils are usually reinforced by plant and tree roots. These roots spread as they grow and friction is created between the soil particles and the roots below the surface. The ability of the tallest trees to resist toppling under the weight of their expansive branches is a measure of the success of the friction interacting between the tree roots and the surrounding soil. In the case of soil slopes, plant roots provide a greater cohesion to the soil mass, thus the soil is better equipped to resist shear forces.

Many experiments have been performed on soils permeated with roots to study the soil-root interaction. The results showed significant strength increases in the soil mass, thereby improving the soil stability. The materials used in the reinforcement of soils have progressed from natural fibres to metallic, rubber and glass fibres as well as polypropylene monofilament fibres and mesh elements. Laboratory investigations have confirmed the same reinforcing effects for natural fibres can be found with monofilament fibres.

Fibres are used in geotechnical engineering because their high strength and stiffness properties are advantageous in many engineering applications. The interface formed between the fibre and the surrounding material maintains a bond for the transference of loads. The properties of the interface region can be changed significantly as a result of the consolidation and volumetric changes that take place in the fabrication process, as highlighted in this thesis.

In engineering projects, geosynthetics are used by engineers to stabilise soils by improving their bearing capacity and/or shear strength. Some typical applications include anchoring sheets of geotextiles in between layers of soil in an embankment; improving the ground conditions for foundations by employing geogrids; lining deposits of contaminated soils deep within soil with geomembranes; et cetera. Fibres strengthen the bearing capacity of soils, while also allowing improved drainage away from the surface layer of the soil bed to lower soil strata, compared with other geotextile types. The soil reinforcements investigated for sands in this thesis are randomly-distributed synthetic fibre inclusions called *LokSand.*

The *LokSand* fibres are currently mixed with granular soils to underlie grassed areas that experience repeated high vertical stresses in use, in order to improve the bearing capacity (FibreTurf brochure, 2000). The fibres provide improved drainage from the grass surface (compared with geotextile layers, for example) as well as being non-corrosive and weather-resistant. The addition of *LokSand* fibres enables a soil mass to resist vertical deformations, but the basic shear resistance that they contribute is dependent on factors such as the type of soil, the density of the soil mass and the amount of normal stress they experience. The stress states in direct shear have already been proven to be dependent on these variables in literature. Tables 1.1 and 1.2 are simplified tables of previous research on the soil parameters of reinforced soils investigated with respect to soil strength. Some of the kernel papers on root-reinforcement research have been included for completeness. Fibres have provided greater resistance to large loads than un-reinforced granular soils in practice. What is required to evaluate the increased amount of shear resistance the fibres impart to sand is a study that accounts for the variables of a fibre-soil mix and quantifies the effects that these variables have on the soil strength parameters.

1.1.1 The benefits of fibre-reinforced soil

The main advantage of fibre reinforcements is the tensile strength that the fibres can bring to compressive materials. It is widely documented that fibres are used to reinforce concrete (Burgoyne, 2001; Concrete Society, 1973; Hollaway & Leeming, 1999; Karihaloo, 2000). Fibre reinforcement in soils is a relatively new concept in modern day engineering projects, but there are advantages that fibres have over geotextiles and geomembranes. These advantages include greater flexibility, better weather-resistance, low cost, comparatively easy placement and drainage allowance. Later in this thesis the particular soil-reinforcing attributes of the crimped *LokSand* fibres will be discussed further.

A good example of the ground improvement features of *LokSand* fibres is sports pitches, like the Millennium Stadium, Cardiff. The pitch in the stadium was a collection of removable pallets containing grass-soil turf (see Figure 1.1) that were placed on a concrete slab with small openings for air vents and surface runoff drains. Depending on the condition of the grass, warm air could be expelled up into the soil layer to avoid frost or the drainage openings could be opened to dry the turf in moist conditions. The turf was subjected to repeated dynamic loading as well as vertical stresses with torque, but the surface recovered the vertical deformations and the roots of the grass were sufficiently confined by the granular soil in the sub-surface layer. (This system using pallets has recently been replaced, as the plastic pallets were injuring the players.)

Lightweight polypropylene fibres such as *LokSand* fibres are also ideal for reinforcing embankments or slopes. The improved cohesion that the fibres give to soil can translate as a steeper incline of an embankment face. The improved bearing capacity that the fibres bring to soils also accounts for cost savings in construction including lower materials costs (compared with other types of earth reinforcements), fewer man hours of labour and more usable space saved either at the bottom or top of the embankment.

1.2 Soil mechanics of fibre-reinforced soils

1.2.1 Basic concepts of fibre-reinforcement

Reinforced soils exhibit higher peak stresses and greater volume expansion than plain soils (McGown et al, 1985; Jewell and Wroth, 1987; Jones, 1985; Qiu et al, 2000). The tensile strength of the fibres is mobilised when the soil grains confine the fibres. At this point the fibres are deforming in order to sustain the forces. The forces in the fibres are transferred onto the soil grains in order to sustain stress and a more dense packing order is formed between the soil particles (depending on the amount of stress being applied). Sand samples can expand in reaction to direct shear forces throughout a sample's shear zone (Bauer and Zhao, 1993; Saada et al, 1999; Scarpelli and Wood, 1982). The effects of the interactions of fibres and soils have been compared with soils of different particle shape as the particle shape can affect the ability of the fibres to bond with soil particles (Al-Refeai, 1990; Jones, 2001). Varying moisture and fibre contents were also tested in this thesis in order to compare the strength of this bond as discussed later.

The increase in the soil strength due to the inclusion of fibres has been described by the basic soil strength parameters of the volumetric strain characteristics, angle of internal friction and the critical state conditions in this thesis.

1.2.2 Volumetric strain characteristics

Fibre-reinforced soil subjected to large compressive stresses has improved bearing capacity in the field. In laboratory experimentation, one-dimensional compression and dynamic compaction showed *LokSand*-reinforced Hostun sands to be more compressive than plain sand in the oedometer cell and Light Proctor compaction tests, respectively (see Chapters 3 and 4). In shear, fibre-reinforced soils show greater volumetric expansion than plain soils.

Fibres provide tension to a soil-fibre mix, which produces an increased resistance to shear as well as greater ductility in the mix when compared to plain sand. The post-peak shear stresses that accompany significant volume expansion are sometimes called 'strain-softening' as the fibre-reinforced samples continue to dilate as the shear stress values decrease. The presence

of fibres allows greater shear stresses to be achieved, despite the volumetric expansion. In this case a distinct peak stress is not always apparent.

1.2.3 The angle of internal friction

A strength envelope is a graphical representation of the combinations of shear and normal stress at failure where points below the envelope represent stresses below peak and points on the envelope represent failure stresses for a particular soil. The angle of internal friction (ϕ') is the angle between the strength envelope and the normal stress axis. This angle is defined as the angle of shearing resistance within a soil and will be denoted by its behavioural condition by a subscript (e.g. ϕ'maximum = ϕ'_{max}, ϕ'critical state = ϕ'_{cs}, etc.).

There is uncertainty whether to quantify the effect of fibres on shear strength by the cohesion or the angle of friction. To quantify the amount that the fibres can resist shear stress, the angle of internal friction is sometimes used as an indication of improved soil strength. There is much divergence in literature over whether the angle of internal friction is altered by the inclusion of fibre reinforcement. Di Prisco and Nova (1993) and Wu et al, (1988_a) thought that that the angle of internal friction was unaffected while Al-Refeai (1991), Gray and Ohashi (1983), Maher and Gray (1980), Michalowski and Zhao (1996), Waldron (1977) and Zornberg (2004) stated the opposite was true, to name just a few. The angles of internal friction for fibre-reinforced sands will be compared with plain sands in shear tests in order to assess the relevance of this strength parameter in the proposed fibre-reinforced sand model.

1.2.4 Critical state conditions

The shear strength of a soil as measured in tests depends mainly on the density of the soil at the start (see Figure 1.2). Dense samples usually have a steep stress-displacement curve up to a peak value then decline to a 'steady' or critical stress value. In loose samples the peak value may not be reached, or the stress-deformation curve may flatten out at the highest stress value. In these cases the critical and ultimate stress states are one and the same. The critical state for fibre-reinforced sands is extremely dependent on the sample density at all stress ratio values during shear.

A model for the critical state for fibre-reinforced sands based on initial sample density has not yet been reported to the knowledge of the Author. All features of the fibre-soil mix variables have been considered with respect to the states of stress attempted.

1.3 Aims and objectives of this research project

The aim of this research project is to investigate the effects of fibre reinforcement on the engineering properties within sand in high quality laboratory tests. Soil parameters such as particle size, shape and grading, moisture and fibre content, sample density, normal stress, internal angle of friction and dilatancy were defined from the geotechnical experiments conducted in the University of Bristol's Geomechanics Laboratory. It is the aim of this research project to apply the knowledge gained from the sample preparation techniques, the results of these preliminary tests and the direct shear test results to model the different stress states created for Hostun sand reinforced with *LokSand* fibres.

The main scope of work involves determining the enhanced amount of shear resistance that the fibres impart to sand samples. The internal angle of friction has been used as a measure of increased strength within reinforced samples, but it is possible that increasing the normal stress value does not always produces a linear failure envelope for fibre-reinforced sample. Samples with different initial densities can require different confining stresses to mobilise the pull-out resistance of the fibres in the shear zone. It is of great importance what amount of shear displacement is required to take place in order to mobilise the peak shear stress in fibre-reinforced samples and how much the stress ratio increases. The attainment of a critical state has also been found to be dependent on the initial sample density (Chapters 3 & 5). The fibre content is usually used as a determinant of the strength parameters, so a correlation must exist amongst the normal stress, fibre content and sample density.

1.3.1 Thesis overview

Chapter Two sets out the background of the technical approaches used in this thesis. A brief discussion of the typical compression characteristics of fibre-reinforced soils and the significance of the stress history is undertaken to establish the deformational behaviour of reinforced soils with respect to normal stresses. Idealised reinforced soil behaviour follows to outline the effects of the fibres' properties on the basic soil strength parameters and the general design concepts of reinforced soils are explained. This section continues with a description of common interpretations of direct shear data in order to clarify the representation of typical soil parameters.

The analytical approach to this research work is then established. Key issues of performance modelling pertaining to shear stress-deformation, sample density variations and the critical state parameter are presented to broaden the basis of understanding of the problems related to general direct shear soil mechanics for fibre-reinforced sands. The inclusion of randomly-distributed fibres offers much non-uniformity within a sample volume in which strains can

become localised in shear. Subsequent volumetric changes can resemble un-reinforced sand samples, but the overall sample expansion tends to be greater in reinforced samples. During the volumetric expansion, a critical stress value may not always be reached for fibre-reinforced samples due to their initial density values. The model performance of reinforced sand samples in direct shear is presented to describe the methodology used to obtain the major objectives.

The laboratory experimentation includes dynamic compaction, one-dimensional compression and direct shear tests. The greatest amount of relevant information for this research model will result from the direct shear tests, although the other two tests reveal interesting deformation behaviour. The one-dimensional compression tests will generally be presented and discussed before the direct shear tests in Chapters 3 and 5, while the dynamic compaction tests can be found in Chapter 4.

Chapter Three gives details of the various sample preparation techniques utilised for fibre-reinforced sands. A study of traditional and modified preparation techniques is included as well as the effects they had on the initial sample densities. The testing programme is set out with reference to error corrections as required. It was found from initial laboratory tests that sample preparation methods of fibre-reinforced sand samples are a highly sensitive experimental process that can dramatically affect test results. To resolve the correction factors used in the presentation of strength parameters, the methods of data manipulation are explained.

Chapter Four provides information of the compaction of test samples with varying moisture and fibre contents. The optimum dry density values achieved for samples are compared with test data of Berry Hill sands reinforced with similar fibres. Again the method of sample preparation is shown to affect the samples' test performance.

Chapter Five sets out the investigation of the shear strength values that were achieved in fibre-reinforced sands. The shear strength contribution of fibre-reinforcements was determined according to the shear strength and volume change increases they mobilise within the sand samples. Peak and critical states of stress are considered and a model for the sample behaviour is introduced.

Chapter Six compares the peak and critical stress states for plain sand samples to fibre-reinforced soil behaviour. The correlation of samples' stress-strain behaviour according to their initial void ratio values and fibre contents under a range of different stress conditions

suggest the existence of a critical void ratio at which the tensile strain of the fibres is resisted. This critical void ratio was found to be dependent on the initial samples density, the normal stress value and the fibre content.

Chapter Seven draws together all the conclusions that originated from the model approach. Further work to be undertaken to develop the findings of the experimentation is proposed.

1.4 Introduction figures

Reference	Type of test	Sample parameters investigated
Waldron (1977)	Direct shear of plant roots	Plant root pullout strength
Waldron & Dakessian (1981)	Direct shear of plant roots	Plant root stretching and aspect ratio in shear strength
Waldron (1983)	Direct shear (creep) of plant roots	Plant root orientation and pull-out resistance
Wu & Tatsuoka (1989)	Direct shear of plant roots	Plant root orientation and pull-out resistance
Wu et al (1988_a)	Direct shear of plant roots	Initial sample density, the confining stress of the samples and the physical properties of the roots
Wu et al (1988_b)	Direct shear and triaxial tests of plant roots	Initial sample density, the confining stress of the samples and the physical properties of the roots

Table 1.1: Root-reinforced soil tests in literature

Reference	Type of test	Sample parameters investigated
Bailey (2000)	Direct shear and triaxial tests of *Loksand* fibre-reinforced sands	Peak shear strength, critical value of confining stress, internal angle of friction and fibre content
Bauer and Zhao (1993)	Direct shear of polyester geogrid-reinforced soils	Geogrid orientation and the relationship between peak shear strength and dilation
Gray & Ohashi (1983)	Direct shear of fibre-reinforced sands	Area ratio of fibres, fibre modulus, initial fibre orientation, friction angle
Jewell & Wroth (1987)	Direct shear of sand reinforced with close-coiled springs	Critical value for confining stresses
Maher & Woods (1990)	Direct shear of fibre-reinforced sands	Critical confining stress and fibre orientation
McGown et al (1978)	Direct shear of fibre-reinforced sands	Critical value for the confining stress and fibre orientation
Michalowski & Zhao (1996)	Direct shear and triaxial tests of fibre-reinforced sands	Critical value for the confining stress
Palmeira & Milligan (1989)	Direct shear of fibre-reinforced sands	Internal angle of friction and the relationship between particle size and shear box dimensions
Qui et al (2000)	Direct shear of fibre-reinforced sands	Roughness of fibres' surface and relationship between peak shear strength versus dilation
Vaid et al (1981)	Direct shear of fibre-reinforced sands	Relationship between peak shear strength versus dilation
Zornberg (2002_a)	Direct shear of fibre-reinforced sands	Fibre content, fibre aspect ratio, pull-out resistance and angle of friction

Table 1.2: Reinforced soil tests in literature

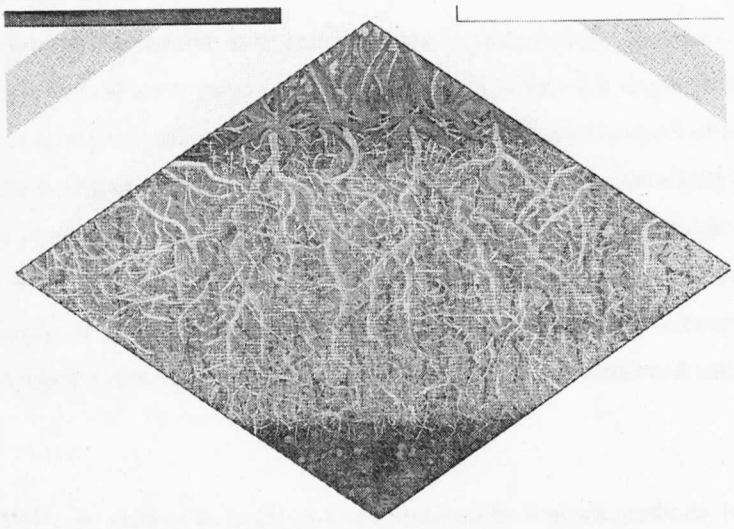

Figure 1.1: Section drawing of fibre-reinforced granular soil underlying a grass surface
(from a FibreTurf brochure, 2000)

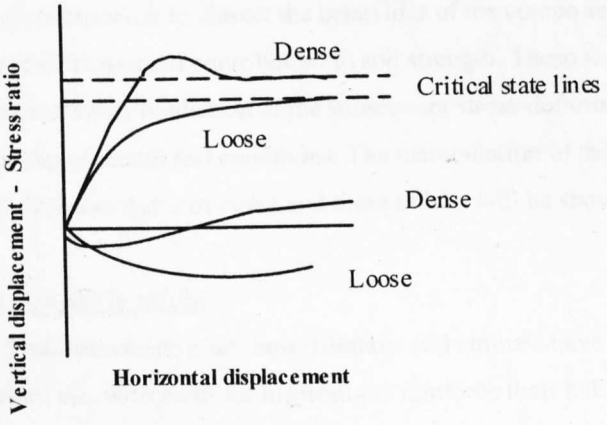

Figure 1.2: Stress – displacement for dense and loose soil behaviour in shear

2.0 Research framework for fibre-reinforced soils

2.1 Introduction

The framework for this investigation considers many geotechnical aspects of fibre reinforcement, from plant roots as reinforcing elements within soil slopes to engineered fibres as load-transfer mechanisms within foundations. The key elements of the fibre's geometry and mechanical properties are evaluated as physical characteristics that enhance the stress-deformation response of cohesion-less soils under a range of loading conditions. The stress-deformation behaviour of fibre-reinforced sands at critical states of stress is outlined. Finally, the established numerical models that have been used to rationalise typical soil behaviour and their application to fibre-reinforced soils are presented.

Reinforcements are utilised to improve soil conditions by various methods. In this review, the conventional testing procedures and properties are explained. The mechanical bond between reinforcements and soils is explored as determined by the parameters of the fibres and soils both independently and together. The variables of reinforced soil mixes are highlighted. The expected performance in traditional soil tests is demonstrated and the engineering qualities intrinsic to fibre-reinforcement are introduced.

The objectives of this section are to dissect the behaviour of the components of fibre-reinforced soils for their individual contribution to soil strength. These same variables will ultimately combine into a prediction of the subsequent stress-deformation response based on a range of experimental test conditions. The manipulation of the composite variables generates different states of stress and these effects will be shown.

2.1.1 Soil reinforcement in nature

The concept of soil reinforcement is not new. Humans and animals have mixed tree roots, reeds, branches, etc. with earth for millennia to reinforce their habitats in much the same way that tree roots reinforce soil (e.g. the Tower of Babylon in Ur completed circa 550 BC was constructed of clay bricks and woven reeds; the Chinese constructed the Great Wall of China by mixing clay and gravel with branches and the Romans supported the quay earth walls of the Port of Londinium with tree trunks (Jones, 1996)). Readily available plant fibres of various weights and sizes were strategically placed within a soil mass or woven together for a more dense composition. Early

structures utilised natural materials to give stability to soil and some of these materials have proven to resist centuries of environmental impact.

Many experiments have been performed on soil permeated with roots to study the soil-root interaction for soil stability and shear strength. Engineers have built in situ test equipment around naturally occurring root systems, they have tested dismembered branches in laboratories and seedlings have been planted and grown inside purpose-built test containers (Waldron, 1977; Waldron and Dakessian, 1981and Waldron, 1983). These experiments were executed to discover the strength parameters for reinforced soil samples such as shear strength, compressive/tensile strength, the angle of internal friction and creep. The results showed significant strength increases in the reinforced soil mass, thereby enhancing the soil stability for slopes and embankments.

Soil slopes appear to be stabilised by the presence of naturally occurring plant roots particularly those of woody vegetation. The failure surface of the slope corresponds to zones of weakness in the earth. As the random roots anchor topsoil into the denser earth below, the potential failure surface has an improved resistance to shear. A direct shear test device, in which a sample of soil is sheared along a plane perpendicular to the axis of the container, is particularly suitable for the study of the effect of plant roots on soil shearing resistance. Shearing resistance is a good indication of the potential slope stability of a soil.

Direct shear test results have been used to compare the shear resistance of plant roots. Alfalfa, barley, and yellow pine roots were planted within soil sample test containers and tested in compacted layers of silty clay loam by Waldron (1977). The roots were naturally neither randomly oriented nor placed by design to resist stresses in the soil. Roots proved to be very effective in finding firm anchorage as a result of the high ratio of roots to soil in the cross-section and the high shear stress required to reach a root pullout value. However, the maximum shear stress value at pullout may have been a limiting factor in the reinforcement because of the observed rupture of the soil-root interface contact.

Waldron deduced the root pullout strength value from the maximum tangential stress that the soil puts on the root where root slippage occurs. Figure 2.1 shows a simple model for root reinforced soil that can be applied to fibre-reinforced soil. The model uses the angle of deformation of a root (β) from its original position (a) to its position during shear strain (b). This angle (β) was included in the determination of the shear

stress values. The soil shearing resistances observed in the direct shear test results were classified by the displacement range between observed "peak" and "residual" stresses. The average shear resistance was 20.6 kPa. The shear resistance and the relative strength increases were recorded as +16.7 kPa and 420% respectively. Compared with un-reinforced soil, roots appeared to increase the shear resistance by increasing apparent cohesion with little or no effect on the angle of internal friction. The roots strengthened the soil by providing greater resistance to tensile strain in a normally cohesion-less material.

The soil-root behaviour model developed in the previous tests was extended to predict the increase of soil shear resistance that resulted from stretching, slipping and breaking roots of various sizes. It was found that the strength decreased with increasing root diameters (Waldron and Dakessian, 1981). There was no root tensile failure (root breakage) during the shear tests. It was concluded that root slippage rather than breakage was the most common condition limiting the reinforcement or strengthening of saturated fine-textured soil by roots. The limitation of the soil-root bond strength for the test materials was found to be due to the root interface properties (i.e. the type of soil and the roughness of the fibres) rather than the plant species, root morphology, or root strength. The calculations of the change of shear stress of the reinforced soil considered the deformation of the root reinforcement due to the stretching and slipping of roots and the aspect ratio (length to width ratio) of the roots as parameters affecting the soil strength.

These geotechnical experiments discovered the improved strength values that reinforcement offers to granular soils. Modern materials have developed in such a way that the effects of soil strengthening by roots have been imitated and improved upon with alternative types of reinforcing materials. Geotextiles and geosynthetics are widely used in industry. The direct shear tests presented in this thesis used crimped polypropylene fibres as soil reinforcement in direct shear tests.

2.1.2 Fibre reinforcements used in soil strengthening

Some of the first soil-strengthening laboratory experiments that now form the basis of fibre reinforcement as a geotechnical technique were conducted by Casagrande (1938) and Vidal (1969). Casagrande introduced the concept of reinforcing weak soil with layers of high-strength membranes. Vidal established the modern concept of earth reinforcement in the 1960's for a composite material consisting of flat reinforcing strips laid horizontally in a granular soil. The main principle with horizontal inclusions in soil

is that gravity generates friction at the interface region between the reinforcing material and the soil, which ultimately stabilises a soil mass.

In the present day engineers improve the stability of retaining walls or embankments by means of horizontal layers of inclusions in aggregates and/or gravel. Geotextiles have also been used to improve the bearing capacity and drainage of road sub-grades. Granular soil or fill with a less cohesive soil can interlock with the geosynthetics as it is the frictional forces between the soil and textile that anchor the reinforced soil structure. Most geotextiles in use today are sheets of fabric anchored within a mass of soil. Polymer grids have also been used for reinforcement of soil structures in recent years. The soil-polymer grid frictional interaction primarily controls the soil reinforcement mechanism. These reinforcement grids have also proven successful against dynamic loading conditions (McGown et al, 1995). Polymer grid reinforcement reduces the earth pressures acting on a retaining wall as well as the wall deformation.

In geotechnical design, the choice of reinforcement material depends on the application, but the economical preference is to adapt regular construction materials for the reinforcement or anchorage of a soil mass. The mechanical principles for all engineered inclusions are similar: the inclusions react in tension to any extensional deformation, which gives an artificial confinement to the soil. Both stiffness and strength increase as a consequence. Fibre reinforced soil is a composite material in which fibres of relatively high tensile strength are embedded in a soil mix of zero tensile strength for enhanced strength under a range of loading conditions.

Fibres are now used because their increased peak strength and stiffness properties are advantageous in many engineering applications. The interface of the fibres with other materials creates mechanical characteristics that are unique for each matrix composition. A mix, therefore, has a combination of strength and deformation properties that cannot be achieved by either of the mix components on their own due to the increased strength that forms within the interface. The advantages of randomly distributed fibres over continuous inclusions, like geogrids or geomembranes, include the maintenance of strength isotropy and the absence of the potential planes of weakness that can develop parallel to continuous planar reinforcement elements. The phenomenon of strain localisation will be analysed in greater detail later in this thesis.

Polypropylene fibres improve the strength of a granular cohesion-less soil mass as the reinforced soils resemble traditional earth reinforced by plant roots in many soil

strength characteristics (Gray & Ohashi, 1983 and Jones, 1996). They are lightweight and cheap to manufacture. As the fibres are flexible, the increased strength they bring is associated with the amount of strain. Ductility is defined as the ability to deform without having brittle or sudden failure. Reinforced soil is more ductile than plain sand with respect to shear deformation. This is shown by the significant strains and deformations that take place within the soil mass in shear before the full strength of the material is realised (Bailey, 2000; Bauer & Zhao, 1993; Gray & Ohashi, 1983; Maher & Woods, 1990; Qui et al, 2000; Waldron, 1977).

Texsol is a process by which continuous synthetic threads are introduced into a soil as reinforcements during compaction. Leflaive (1985) originally tested the performance of continuous synthetic threads in sand subjected to cyclic loads. An increased peak static strength was observed and this study led to the development of the *Texsol* process that is now widely used in the manufacture of geotechnical materials for soil reinforcement. The deformation pattern of earthworks where this technique is employed was analysed by Di Prisco and Nova (1993) and the stress-strain behaviour observed in Leflaive's triaxial compression tests was reproduced in their laboratory tests. The increased soil strength was attributed to the apparent cohesion that resulted from the contact between the soil and the threads.

2.1.3 Description of soil properties that enhance the fibre-soil bond

The shearing stress that develops in fibre-reinforced sand mobilises tensile resistance in the fibres via friction at the fibre-sand interface. A peak shearing resistance will occur either at the onset of greatest mobilisation between the sand and the reinforcement surface or when there is tensile breakage within the fibre. The amount of tensile stress that develops in a fibre at the shear plane depends upon a number of material parameters including fibre length and diameter as well as content, modulus or longitudinal stiffness, current fibre orientation, fibre content, the surface roughness or friction of the fibre, the sand particle shape and size, the sand friction angle and the initial density of the samples. The test variables that affect the strength of the interface between the materials include the sample preparation method, the vertical confining stress and the volume ratios of the dimensions of the fibres compared to the test mould dimensions. Gray and Al-Refeai (1986) decided that fibres should be long enough and "frictional" enough to avoid pull-out; conversely the confining stress must be high enough so that pullout forces do not exceed the shear forces due to surface friction along the fibre. A tensile strain distribution along the length of the fibre was also

assumed which results in a transfer of loads from the fibres to the remainder of the soil mass.

Figure 2.2 shows the increased compression of the fibre and sub-angular soil grains from the (a) "as placed" soil-fibre composition to the (b) compressed soil-fibre composition. The normal forces and the resultant forces acting on the soil particles cause a compression of the soil grains as the air voids decrease. The confinement of the fibre within the soil sample increases as the soil grains lock the fibre into a confined position. In general, the "as placed" sample section represents a specimen that has been compressed by nothing other than the self-weight of the sample. The normal force depicted in position (b) represents the mass of a top cap, a steam roller, a plate or any compaction device while the resultant forces are the forces generated by the underlying sample mass and/or the bottom of a test mould. Depending on the mix variables and normal stress value, the tensile forces of the fibres can be mobilised by their confinement between soil particles.

The skin friction between the fibre's surface and the adjacent sand grains resists shear due to the axial displacement of the fibres. An increased confining stress on the failure plane can mobilise additional shear resistance in the sand, which impedes bond failure between the soil and reinforcement. Reinforcements have shown a deformed shape at large displacements and fibres in particular are assumed to be thin enough that they offer little if any resistance to shear displacement from bending stiffness (Palmeira and Milligan, 1989). Randomly oriented fibres are considered to provide an optimum shearing resistance within a failure plane as the small, localised displacements of the soil grains generated in shear can be minimised by the presence of fibres. The placement and orientation of reinforcements within soil can affect the mechanical properties of the mix as a whole.

Much experimentation has been done on fibre and root reinforcement shear tests to investigate the significance of the reinforcement orientation and placement. Gray and Ohashi (1983) analysed the fibre deformation in direct shear tests of sand reinforced by fibres oriented at different angles to the shear plane and placed at equal spacing from each other. The amount of shear resistance was affected by a number of soil-fibre variables including area ratio, fibre modulus, initial fibre orientation, and the sand friction angle. Analysis of test data revealed that less than 25% of the tensile strength of the fibres was mobilised at the shear plane, even for long fibres. They also suggested that the fibre length should be adjusted according to the dimensions of the test mould

and the particle size of the soil grains for optimum shear resistance. These were the factors that affected the mechanical behaviour of the mix variables in the shear failure plane. Randomly placed fibres tested by Maher and Woods (1990) showed a similar shear modulus as that of vertically oriented fibres, an orientation of 90° with respect to the horizontal shear plane. The orientations of fibres within test moulds were proven to affect the shear strength of a sample in shear.

The preferred fibre content or length for randomly distributed fibres for a particular test depends on the volume of the test material. Optimum fibre content has been reported as being between 0.6% and 1.0% dry weight in many previously published studies. Santoni et al (2001) reported the upper and lower limits of fibre length with respect to the dimensions of both the soil particle and the triaxial test mould. Six different soil types were tested for their ability to bond with fibres of different deniers. The results were highly dependent on the specimen's preparation. The performance of the different soil types was similar, but optimum silt content of 8% was found to be beneficial for fibre-reinforced sands. Depending on the soil sample size, the soil particle size and fibre content can work in partnership for soil strength.

Higher compaction energies are required in reinforced soils to achieve the same initial density as un-reinforced soils. Hoare (1979) found that for a given compactive energy, fibres resisted compaction causing a less dense packing order of soil particles with increasing amounts of reinforcement. Fibre-reinforced sand samples showed greater resistance to penetration than un-reinforced sand under large stresses in California Bearing Ratio tests (see Figure 2.3 after Lawton et al, 1993). In the laboratory, preparing a dry fibre-reinforced sand sample to a particular initial density value for small-scale tests was challenging. A fibre-sand mix should be compressed in a manner that provides uniform density with the least amount of air voids in order to provide sufficient confinement to the fibres. The initial density of the mix determines the amount that the fibres reinforce soil through their tensile strength.

The conclusions of many experiments are that sufficient normal load is required to mobilise the reinforcing effect of fibres within a soil. A critical confining stress has been described as a defining value for the strength of a fibre-reinforced soil. Below this value the fibres tend to pull out without contributing a significant amount to the soil's strength (Maher and Woods, 1990). This slip or pullout in turn affects the shear envelope and, at low confining stresses, results in apparent friction angles which are higher for the reinforced sand compared to the sand alone. Jewell and Wroth (1987)

monitored the plastic flow of reinforced soil in a direct shear apparatus and proved that extensible reinforcements (in this case, close-coiled polymer tension springs) demonstrate almost no influence until the mobilised shearing resistance in the sand exceeds a critical value. These tests emphasise the importance of conducting direct shear tests on reinforced sands over a range of confining stresses in order to adequately define the stress-deformation response at peak stresses.

Previous researchers have discovered the strength parameters for reinforced soils to include higher shear resistance and reduction of post-peak stress deformation due to the tensile strength of the reinforcements. The deformation at residual stresses can be as influential to shear strength as deformations at the peak stress values. The factors that contribute to samples' strength and volume change have been included and a summary of the mechanical properties of the interface region between the fibres and sand grains follows. The stress-strain response of reinforced samples in compression and direct shear is also introduced and the established formulae related to this behaviour are presented.

2.2 Model Description

2.2.1 General description

Stress-deformation modelling for fibre reinforcement and fibre-soil interactions is very complex. Many of the parameters required for modelling the effects of fibre-reinforced soil can be difficult to quantify such as the stress history, the development of strain localisations and the amount of confinement the fibres give to the sand grains. In many cases these types of parameters are assumed to be negligible with respect to peak and critical shear stresses. By contrast, the parameters of initial density, the fibre content of the sample volume and shear-dilatancy values can be measured directly with a high degree of confidence.

The soil strength variables are described and represented in this section. Further details of soil testing procedures will be illustrated in the following sections with the emphasis on the particular contribution that reinforcements potentially make. The inherent strength of reinforced soil has been shown to come from the bond between the reinforcements and the surrounding soil (see, for example Al-Refeai, 1991). The effects of the bond strength as represented in the strength parameters are discussed.

A study of fibre-reinforced soil strength properties is required to obtain accurate data on the stress-deformation behaviour in shear for soils reinforced with varying percentages of reinforcements confined by a range of normal stresses. The experimental data for reinforced soils can then be investigated based on the patterns of behaviour for un-reinforced soils in order to observe to what extent the fibres have strengthened a soil mass. The mechanical response that can be expected of a soil sample in direct shear will be based on its initial density, fibre content and normal stress value.

The laboratory data deemed necessary to study the reinforced soil properties in direct shear include the initial sample density, the internal angle of friction, the dilatancy characteristics, the peak and critical shear stress values and the sample densities that correspond to these stress values. This section discusses the significant aspects of direct shear testing for reinforced soils.

2.2.2 Common interpretations of direct shear data

The direct shear test is commonly used to interpret the load transfer mechanism between reinforcements and soil. This mechanism can be modelled from the tests by relating the soil deformation to the amount of reinforcements. The stress ratio is defined as the ratio of the shear stress to the normal stress in a direct shear test. For comparing the soil strength increase that results from adding reinforcements to sands, the equivalent stress ratio is used which is the ratio of the peak shear stress of reinforced sand to the corresponding un-reinforced sand for the same normal stress and initial void ratio. The shear strength increases for *LokSand*-reinforced Hostun sand samples will be compared based on the amount of fibre reinforcements added to the soil samples.

The investigations of shear resistance for soil reinforced with plant roots emphasize the fundamental strength parameters of fibre reinforcements. Waldron et al (1983) designed a moveable frame for direct shear tests of plant roots that grew in purpose-built containers and tests were executed either with both constant shear stress rate or with constant displacement rate. A striking result of the shear-displacement modulus was the continual increase in shear resistance over the entire displacement range shown by the pine-rooted samples. In Figure 2.4 the shear stress to shear displacement is shown for pine- and alfalfa-rooted soils as well as fallow soil. The solid lines show stresses resulting from constantly maintained shear displacement, and the points

connected by dashed lines represent the applied stresses in creep shear (displacement rates as shown). This work-hardening behaviour of the pine-rooted soil was very favourable for improving stability due to the increased resistance to displacements.

The objective in the shear testing of fibre-reinforced soil presented here is to investigate the amount of strength increase that the fibres provide effectively (i.e. before strain failure) to a sand sample in shear. The determining factors of the soil strength are contained in the soil-fibre interface region. An attempt to discover optimum conditions for soil improvement depends on the soil type as well as the fibre content, length, orientation, aspect ratio and pullout resistance. From these studies it can be concluded:

- the limitation of the soil-root/fibre bond strength is determined by both the soil properties including grain shape and density, and the fibre properties;
- roots/fibres appeared to increase shear resistance by increasing apparent cohesion;
- the resistance contributed by the reinforcements depends on the orientation and length of the fibres;
- the pullout resistance of a fibre is an ultimate value of tensile force;
- fibres may decrease strain localisation within the shear zone; and
- there is a correlation between the confining stress and the dilatancy and fibre pullout resistance.

Figure 2.5 shows a typical plot of the shear stress to deformation relationship for dry uniform sand with and without fibre reinforcement subjected to a constant normal load. As the samples experience small values of shear stress, the corresponding displacements are linear and recoverable. The recoverable phase exists in the region from the origin up to point "A" while an initial compression occurs within the samples. In the region after point "A" the reinforced sample is considered to be work-softening (plastic phase) up to the peak stress at point "B" due to the localised shear forming between the soil grains. The peak stress for the samples is reached when the shear resistance of the sand reaches its ultimate state, or yield. At the peak stress ratio the applied stresses are constant so there are no recoverable strains within the sample volume. Compared with fibre-reinforced sand, the plain sand reaches its peak sooner and the peak stress value tends to be less than the reinforced sand. In the region labelled "C", the stress ratio increases in the reinforced samples for as long as the normal stress is maintained, while the plain sand stress ratio tends towards a constant value. The residual stress is defined as the constant shear stress value in region "C". The

reinforced samples have a higher residual stress value than the plain sand samples. The reinforced sample's behaviour tends to show less of a reduction in the residual stress from peak stress ratio compared to un-reinforced samples. The fibre-reinforced soil is more dilatant than the plain soil.

2.2.3 The significance of initial density and confining stress

The deformation properties of sand under a variety of confining stresses are related to the void ratio limits (e_{max} and e_{min}) as it is possible to estimate the degree of confining stress dependency of sand deformation properties and shear strength from these limits (Maeda and Miura, 1999). The e_{max} is defined as the void ratio generally achieved by quickly inverting a measuring cylinder containing the dry soil (BS 1377: Part 4, 1990), and e_{min} is generally achieved by compaction of a known mass under saturated conditions without causing particle crushing. The densest condition for compacted soil is represented by e_{min}. Figure 2.6 shows a representation of how an assembly of soil particles traps water and air within the volume of the voids. The deformation behaviour of angular sands in particular is dependent on the confining stress, but the confining stress value at which critical state conditions are achieved is not constant for all granular materials.

Analysis of the stability of hillside slopes by Wu et al (1987) considers the actions of vegetation roots as soil reinforcement. The shear resistance contributed by the roots depended on both the orientation of the roots and the dimensions of the shear box. One of the limitations of comparisons between direct shear and slope stability tests is that the deformation conditions in the shear test differed from those along a potential slip surface in a slope failure. The conclusion was to estimate the difference between the measured shearing resistance and the shearing resistance along a potential slip surface. Wu et al (1988) continued analysis of the shear strength of soil-root systems in direct shear tests and in triaxial tests by measuring the shear strength of hemlock tree roots. The results indicated that the shear resistance developed in the reinforced sand at large displacements was slightly less than the ultimate strength value compared to plain sand. Although the roots could withstand high normal stresses in compression, low confining stresses could not mobilise the tensile strength of the plant roots for shear resistance.

An increase in confining stress results in increased peak shear strength and deformation of a sand-geotextile system. This phenomenon studied by McGown et al (1981) is

based on the fact that when the confining stress increases, the sand grains are packed closer and come into closer contact with the filaments that oppose their sliding and reorientation. It is the normal stress that anchors the soil grains and fibres as a composite system and the magnitude of this confining stress affects the shear resistance of the soil-fibre composite.

Fibres tend to slip or pull out at confining stresses less than a threshold confining stress. In direct shear tests, less than 25% of the tensile strength of fibres could be mobilised in the shear plane (Gray and Ohashi, 1983). The "threshold" confining stress corresponds to the transition in the principal stress envelope from a steep angle of inclination towards a constant stress value (see Figure 2.7). Randomly placed fibre reinforced samples produced larger deformations at peak strength than soil reinforced with the same proportion of reinforcement in the form of geotextile layers (10% at 100 kPa and 12% at 400 kPa) in triaxial tests (Bouazza et al, 1994). The threshold confining stress was the same for both systems (110 kPa $<\sigma_{crit}<$ 125 kPa). In the case of $\sigma_3 < \sigma_{crit}$, the sand fails before the reinforcements pull-out because of the extensibility of the latter (Schlosser et al, 1985). It was observed that due to the introduction of the reinforcements, the angle of internal friction increased by up to 12° from an original angle of 39°. The shear envelopes suggest that the reinforcements increased the value of cohesion. The 1% fibre inclusion gave approximately the same cohesion as reinforcement with 3 layers of geomembrane reinforcement. In all cases, larger axial strains were achieved at peak stresses with fibre reinforcement.

The initial linear stress-deformation relationship shown in direct shear is similarly represented for triaxial test results. The volumetric strain of fibre-reinforced sand in triaxial tests shows an initial contraction followed by dilation, but the transition from one state to the other occurs at a higher axial strain than for the un-reinforced sand. The failure envelope in terms of σ_1' and σ_3' showed a transition at a certain "critical" confining stress (see Figure 2.8), as demonstrated by Maher and Gray (1990), Ranjan et al (1996) and Bailey and Knox (1997). A representation of the threshold confining stress in direct shear for dense and loose sands was shown in Figure 2.7.

At high confining stresses or fibre aspect ratios an increase in strength is almost linear with increasing fibre content (see, for example, Maher and Gray, 1990). At lower confining stresses or fibre aspect ratios, samples approach a higher upper limit of stress compared with un-reinforced soils. Figure 2.8 showed the effect of fibre inclusion on

the failure envelope of sand tested in the triaxial apparatus. From this figure, the assumption is the principal stress envelope for reinforced soil is similar to un-reinforced sand above a critical confining stress but with an offset. The maximum strength increase was found to be constant in tests with confining stresses greater than the critical stress value. From this observation, it is possible to achieve optimal reinforcement for particular stress environments and soil particle shape.

As with the strength under static loads, the contribution of fibres to stiffness is more pronounced at lower confining stresses and drops sharply with an increase in the applied normal stress. The inter-granular friction of the sand dominates the failure stress of a fibre-reinforced composite and reduces the importance of the contribution of the fibres at higher stresses. In Figure 2.9 the shear stress values were plotted against the shear strain according to samples' fibre contents. The fibre-reinforced soil's shear stress modulus (stress ratio $_{reinforced}$ / stress ratio $_{un\text{-}reinforced}$) increased to a maximum value regardless of the soil particle grain size when the confining stresses were less than the critical stress value in triaxial tests. The shear strength modulus increased linearly according to the increased fibre contents as the shear strain increased. Figure 2.10 (a) and (b) shows the shear modulus versus shear strain for triaxial test samples. The isotropic confining stress for low- and high-strain measurements respectively, were found to be in the range of 3-7 psi (21-48 kPa) in tests of 3% fibre content with Muskegon dune sand (a sand of similar soil properties as the test sand in this study: specific gravity, 2.65; D_{50}, 0.41; e_{max}, 0.78, e_{min}, 0.50). These results showed an increase in the confining stresses beyond the optimum range generally results in less effective fibre contribution to shear stiffness.

The shear strength envelopes for reinforced soil showed a threshold confining stress value, below which the fibres tended to slip or pull out due to low confinement and above this value tensile failure of the fibres occurs. The fibre-reinforced soils also exhibit a higher residual strength compared with un-reinforced soil. Ranjan et al (1996) performed triaxial tests to determine the effects of confining stress, fibre properties, (i.e., fibre content and aspect ratio), soil-fibre surface friction and the soil characteristics on the shear strength of soils. The conclusion was that fibre-reinforced soils must be confined by a stress great enough to mobilise tensile stress without breaking or pulling the fibres.

The shear strength envelopes for reinforced sand decreased with an increase in confining stress in triaxial tests performed by Maher and Gray (1990) and Maher and Woods (1990). Therefore the reinforced sand samples' internal angles of friction reduced with increased confining stresses in shear. In the laboratory experimentation presented in this thesis, three different confining stresses were used for *LokSand*-reinforced Hostun sand in direct shear to observe the changes in the internal angle of friction with respect to the normal stress value. The confining stress dependency of internal angle of friction was related to the initial void ratio values and fibre contents of the test sands in later chapters.

2.2.4 Stress-strain response for fibre-reinforced soils

The stress-strain response of fibre-reinforced soils can be tested in direct shear and triaxial tests. In direct shear tests, the sample is forced to shear in a predetermined horizontal shear plane. However, this may not actually be the weakest plane of a sample. There is an unequal distribution of stress over the shear surface; however stress measurements are usually taken as an average of measurements over the entire surface area (Dietz, 2000). The shear stress in the failure plane represents the overall soil shear strength of a sample volume.

Triaxial tests are often used in the determination of the shear strength of fibre-reinforced soils. Many examples exist in published literature (see, for example, Bailey and Knox, 1997; Gray and Al-Refeai, 1986; Hoare, 1979; Jones et al, 2001; Maher and Gray, 1990; McGown et al, 1985; and Ranjan et al, 1996). The results of a triaxial test can provide more information than is generally given by the direct shear failure envelope. For similar soils the internal angle of friction determined by triaxial tests is lower than that obtained by the direct shear test up to 3° (Rethatí, 1998). However, the accurate estimation of the direct shear strength from the triaxial strength is in general rather difficult. The soil grains in a triaxial test have considerably greater freedom to deviate laterally than those in a plane strain test, and in these circumstances a smaller enhancement of strength due to dilatancy might be expected (Bolton, 1986).

Let us consider the direct shear test for the investigation of the shear strength properties of sands. The following observations are typical for direct shear test results for loose, medium and dense sands (see Figure 2.11):

- Shear stress increases with shear displacement to a maximum or peak value and then decreases to an approximately constant value at large shear displacements in dense and medium sands.
- Shear stress increases with shear displacement to a maximum value, then remains constant for loose sands.
- The volume of dense and medium dense specimens initially decreases then increases with shear displacement. The volume remains approximately constant at large shear displacements.
- The volume of loose specimens gradually decreases to a certain value and then remains approximately constant during the continued testing.

It has been explained that the principal stress failure envelope for fibre-reinforced sand has a confining stress below which the reinforcing mechanism is not fully mobilised. Depending on its initial density and the consolidating stress, fibre-reinforced sand could reach the critical state as it dilates following yield. In order to observe a marked difference between the peak stress and the critical state for test samples, dense samples are preferable. Jewell and Wroth (1987) made the following assumptions for reinforced dense sand at peak shearing resistance:

- there is sufficient uniformity for the deforming sand to be described in terms of a single state of stress and incremental strain,
- the orientation of the principal axes of stress and incremental strain coincide,
- the incremental strains at the peak stress ratio are plastic and
- there is zero linear incremental strain in the horizontal direction.

Randomly distributed fibres provide strength isotropy in a soil composite. Fibre inclusions increase the shear strength within a reinforced soil mass, by an amount sometimes referred to as the 'equivalent' shear strength. Gray and Ohashi (1983) found that low modulus fibre reinforcements increased peak shear strength and limited the amount of post peak reduction in shear resistance in dense sand. They compared reed, plastic (PVC) fibres, Palmyra palms, and copper wires as reinforcing inclusions. The same or higher shear strength increases could be achieved with a modest increase in the number of fibres or area ratio of relatively low modulus reed fibres compared to stiffer and stronger copper wires with the same initial area ratio. The effects of the fibres' slip or pullout led to apparent larger angles of internal friction within the reinforced soil composites.

Dense Leighton Buzzard sand was tested with and without reinforcements oriented at 25° to the horizontal shear plane by Jewell and Wroth (1987). Figure 2.12 shows the stress ratio and vertical deformation of reinforced and un-reinforced dense sand in direct shear. The inclusions demonstrated almost no influence until the stress ratio in the sand exceeded a critical value for the first time. The reinforced samples had greater peak stress ratio values than the un-reinforced, and the reinforced samples continued to dilate throughout the test. The tests show a comparison between extensible and inextensible reinforcements. A conclusion of this comparison was that the stiffness of the inclusion dictates the shear displacement behaviour. As the graph shows, the inextensible reached a distinct peak value at approximately the same shear displacement as un-reinforced sand while the extensible reinforcements gradually achieved a peak value after greater shear displacement. The extensible reinforcements thereby limited the volumetric deformation in shear while sustaining greater shear stresses. The post-peak stress values were identical for both types of reinforcements.

The inclusion of fibres increases the peak shear strength and limits the amount of post-peak reduction in the shear resistance of dense sands. Previous research (Noorany and Uzdavines, 1989 and McGown et al., 1985) found that fibres improve the soil stiffness in situations of repeated loading. Noorany and Uzdavines (1989) stated that polypropylene fibres absorbed the strain deformation that is generated by repeated loading in triaxial tests. McGown et al. (1985) noticed an improvement in the elasticity of soil-mesh mixtures where repeated loading is involved.

Lawton et al (1993) compared unreinforced sand with sand reinforced with layers of polypropylene fibres in California Bearing Ratio and triaxial tests. The fibres provided the greatest resistance to CBR penetration at large loads. Lawton's conclusions agreed with other researchers (Bailey, 2000; Gray and Al-Refeai, 1986; Maher and Woods, 1990; Gray and Ohashi, 1983 and 1986; and Hoare, 1979) that large deformations are required to mobilise the reinforcing effect of fibres within a soil.

Reinforced soil tests by other researchers were sometimes sheared with much larger normal stress values and/or by much larger horizontal displacements than the *LokSand*-reinforced Hostun sand samples in this thesis, but similar stress-deformation behaviour was seen in all test results. These studies showed that the inclusion of fibres in uniform sand causes an increase in the maximum shear strength of the sand.

2.2.5 The relevance of the internal angle of friction in sands

The internal angle of friction is the parameter that describes the soil strength characteristics. In the direct shear test an interpretation is given for the angle of friction of sand. The determination of the angle of shearing resistance was based on the assumption that the horizontal plane is the plane of the maximum stress ratio. In a direct shear sample, the stresses assumed acting on an element of soil in the shear plane after a horizontal displacement increment of v_x are shown in Figure 2.13. The normal stress acting on the central plane (σ'_1) is defined as σ'_{yy} and the shear stress on the central plane is defined as τ_{yx}. The ratio between these stresses in direct shear is the tangent known as the angle of internal friction ϕ'_{ds}.

$$\tan \phi'_{ds} = \frac{\tau_{yx}}{\sigma'_{yy}}$$

In the direct shear test the major (σ'_{yy}) and minor (σ'_{xx}) principal stresses (σ'_1 and σ'_3 respectively) are imposed on a sample prior to the commencement of horizontal deformation, v_x. During the horizontal deformation, the sample is sheared and the directions of σ'_1 and σ'_3 are rotated. Zero deformation in the intermediate principal stress σ'_2 direction is assumed for plane strain direct shear tests.

The angle of internal friction is a representation of soil strength as it is the angle of shearing resistance in plane strain. The Mohr-Coulomb theory of shear stress and strain for soil states that the maximum possible ratio of shear stress to normal stress is equal to the soil's angle of friction, ϕ'_{ds}, when there is zero cohesion. As the direct shear test measures the frictional resistance across the sample's central plane, the stress ratio on the shear plane is considered to be the sample's maximum value.

$$\sin \phi'_{ds} = \frac{\sigma'_1 - \sigma'_3}{\sigma'_1 + \sigma'_3}$$

The angle of dilation ψ is defined by the ratio of incremental volume change $d\varepsilon_{yy}$ and incremental shear strain $d\gamma_{yx}$.

$$\tan \psi = \frac{-d\varepsilon_{yy}}{d\gamma_{yx}}$$

The incremental strain observed in a direct shear sample shearing with peak resistance illustrates the direction of plastic strains in a Mohr's circle in Figure 2.14. The

directions along which the sand does not elongate make an angle of $\pm (45 - \psi/2)$ with the direction of the major principal strain increment. Jewell and Wroth (1987) reported on a series of direct shear tests using artificial crushed glass to represent a granular material where the direction of principal stresses could be observed. Measuring the observed strains during shear led to the conclusion that the principal axes of stress and strain rate coincided.

Critical state can be described as the condition of unchanging stress value at large displacements where the constant stress continues without volume changes ($\psi = 0$). The peak and critical stress states are related by the following:

$$\sin\phi'_{ps} = \frac{\tan\phi'_{ds}}{\cos\psi + \sin\psi\tan\phi'_{ds}}$$

which relates the peak shear angle of internal friction of a soil to the angle of internal friction obtained in direct shear and

$$\sin(\phi'_{ps})_{crit} = \tan(\phi'_{ds})_{ld}$$

where the peak internal friction angle at critical state is related the angle of internal friction mobilised on the shear plane at large displacements in a direct shear test.

The angle of friction at critical state can be expressed as:

$$\sin\phi'_{critical} = \tan(\phi'_{ds})_{ld}$$

Due to the interaction between the soil and the reinforcement surface, greater frictional resistance is made apparent by an increased internal angle of friction in most reinforced soil tests. The internal friction angle determined by a Mohr-Coulomb failure envelope is a universal representation of soil strength. Waldron developed many models for root-reinforced soil strength in shear tests (Waldron et al, 1983; Waldron and Dakessian, 1981; and Waldron 1977). The inclusion of plant roots increased the internal angle of friction for the reinforced soil samples, thus the increased internal strength of plant root-reinforced soils compared to un-reinforced soils was measured by the increased internal angle of friction.

The addition of mesh elements increases the principal stress at failure significantly in triaxial tests. Based on the observations of Al-Refeai (1991), it can be assumed that the shear strength of reinforced sand with bond failure was characterised by an apparent friction angle larger than that of the soil alone due to the inclusions. Increasing the fibre length resulted in increasing the apparent cohesion of the sample. The ultimate strength values were governed by the fibre content and the geometry of the fibres.

The measured friction angles of *Texsol* reinforced soil varied with the orientation of the bed of soil with respect to the principal axes of stress in triaxial tests. Di Prisco and Nova (1993) postulated that the internal angle of friction for reinforced soil is essentially the same as for un-reinforced soil. Figure 2.15 shows increased peak stress values and, as seen from the intercept on the q axis, a greater apparent cohesion for the reinforced sample compared to the un-reinforced sample (for which the apparent cohesion is zero). The way in which the material is placed in the test mould gives the reinforced soil an ordered structure. The main conclusions for the *Texsol* triaxial test results are that peak stress values and the dilatancy at failure were strongly attributed to the fabrication method. For this reason, the sample preparation methods described in Chapter 3 were given careful consideration. The friction angle and apparent cohesion will be used for strength interpretations in the results chapters.

2.2.6 The effect of fibres on the shear zone

A definite shear zone is developed around the failure plane of soil during direct shear. Common assumptions about the shear zone in soil follow:

- The thickness of this zone depends on soil particle size. The zone height is estimated as 20 to 25 percent of the height of the sample in a standard shear box.
- The soil on either side of the horizontal shear zone behaves like rigid blocks in which the reinforcement is firmly embedded.
- The dilatancy or contraction of the soil and the interaction between the soil and the reinforcement only occurs in the shear zone.

(Jewell and Wroth, 1987)

The volume of fibres within a sample can be described by the volume fraction: the ratio of the volume of fibres and the total volume of sand in a sample. The volumetric representation of the fibre content is more accurate than stating the weight of fibres as a percentage of the total sample weight, since it accounts for the length, diameter and

number of fibres. Common assumptions about soil reinforcements in the shear zone follow:

- The reinforcement is sufficiently long to prevent pullout.
- The reinforcements are flexible and, as such, have no bending stiffness.
- Full bonding exists between the soil and reinforcement.

(Jewell and Wroth, 1987)

These assumptions may not fully represent the behaviour of randomly distributed fibre-reinforced soils. For example, it would be unrealistic to consider the soil surrounding the shear zone as a rigid block when the fibres are distributed evenly throughout the sample. It is also unrealistic to assume that all dilatancy and contraction within the sample occurs only in the shear zone as the tensile strains in the fibres can extend beyond this imagined boundary. However the assumptions made by Jewell and Wroth for the behaviour within the shear zone have been adopted to consider the fibre reinforcements as anchored in the top and bottom halves of a "rigid" (i.e. non-deforming) soil. By doing, so the entire shear box sample represents the shear zone of a larger reinforced soil mass experiencing shear.

Localised deformations in the form of narrow shear bands are often observed to develop after large deformations occur in materials. Within this shear band, the material behaviour is inelastic. The width and orientation of these shear bands depend on material parameters, geometry, boundary conditions and loading conditions (Liu et al, 2005). Liu et al concluded that based on their studies, the shear band patterns depend on the thickness of the specimen. In direct shear tests the localisation of large inelastic strains at the shear zone divides the specimen into well-defined blocks that, at the final stages of specimen response, move with respect to each other like rigid bodies. The transition among shear band patterns is smooth and is always associated with the specimen thickness variation.

Figure 2.16 shows a density profile for a shear band in a dense triaxial Hostun sand sample. The inset photograph shows a shear band depicted as a trench across the centre of an otherwise homogeneous sample. The thickness of the shear band was measured as 2mm, which is much smaller than the estimated shear band thickness of 6-9mm by (20-30 times the mean grain size). In the experiments undertaken by Desrues et al (1996), the scatter of the void ratio values were found to be approximately ±0.02 for dense Hostun sand. The graph in Figure 2.16 shows the density within a shear band as the

radiographic density measured by tomography (set to approximately -300 Modified Hounsfield Units) plotted against the displacement in millimetres. The figure shows MHU values ranging from approximately 155 to 245 in the shear band pictured, which measured 30mm in cross-section. The graph shows the fluctuation of the volume changes during testing although it is possible that at a resolution so close to the grain sizes, only an average measure over the shear band has a physical meaning at the continuum level.

For an even distribution of fibres with random orientations, the shear resistance of fibres may extend within a soil sample beyond the shear plane. The orientation of reinforcements in soils has been documented as a dominant feature of the shearing resistance within the shear zone. For this reason, random distribution of fibres has been the orientation of choice for this set of direct shear samples in order to reduce the deformation effects of the shear bands that develop during tests. Three categories of shear bands were identified by Karakouzian et al (2001), which were based on the orientation and development location of the shear bands. Primary bands form in the direction of shearing in granular materials. Secondary shear bands are oriented at an acute angle approximately 40° to the direction of shearing (depending on the angle of dilation) and are further classified as either continuous or terminating, where "continuous" secondary shear bands form a visible band that is continuous across the passive side of the specimen and "terminating" secondary shear bands end when the shear band ceases to continue to form or the shear band encounters another material layer. Tertiary shear bands form off of primary or secondary shear bands, typically in the direction of shearing. A random distribution of flexible fibres can impede and prevent these types of shear band development by confining the soil grains to create a ductile mass that rearranges the sand particle packing order while it deforms in shear due to its tensile properties, as observed in Chapter 5.

What is required for the investigation of the improved strength of fibre-reinforced soils is a relationship between the normal stress value and the sample density at which the sample is in its critical state during direct shear.

2.2.7 The state parameter

The critical state for sand is sometimes called a "steady" state because the shear stresses are constant without changes in the effective stresses or volume. The state parameter was defined by Been and Jefferies (1985) as a change of void ratio and stress

level with reference to a critical state for sand behaviour. Their research suggests that the mechanical properties of sand cannot be expressed in terms of relative density without also describing the stress level. It was also suggested that this state parameter (ψ_A) depends on a repeatable particle arrangement at the steady state condition. From Figure 2.17 the following formulas emerge:

$$\psi_A = e_\lambda - e_{ss}$$

$$\text{and} \quad e = e_\lambda - \lambda \log I_1$$

where the mean normal stress (I_p) was plotted against the void ratio values at steady state (e_{ss}) and the slope intercept (e_λ). The figure shows the steady state line (SSL) for Kogyuk sands. For convenience, the state parameter will be denoted as ψ_{SP} from this point onwards in this thesis.

The shear stress at critical state was related to the normal stress value in Figure 2.17 by a function of the steady state angle of friction, which was approximately 31° for Kogyuk sand (D_{50} = 350μm, $e_{min\ (average)}$ = 0.486, $e_{min\ (average)}$ = 0.851). Similarity between the internal angle of friction and the angle of dilation exists in the behaviour of sands. The state parameter concept provides the relationship of dilation rate and angle of friction to a physical condition or state (Been and Jefferies, 1985).

The relationship between void ratio and effective stress for a sample at critical state can be ascertained by employing the following steps (see Figure 2.18):

1. determine the in situ critical or steady state line of the material from basic soil tests
2. determine the sample density and stress level
3. by assuming undrained (constant volume) behaviour, determine the ultimate steady state of the sample
4. compare the steady state shear stress with the applied experimental stresses to determine the factor of safety of samples.

(adapted from Been, 1999)

This procedure was used by Been to determine the liquefaction potential of sands. (Please note that the critical shear stress values found at critical void ratios in laboratory experimentation may not be applicable to field conditions.) Factors that inhibit the repeatability of the critical state line for sands in experimentation include

sampling variations, the impact of the fines content and inconsistencies between natural soils and reconstituted laboratory samples. Indeed it is more difficult to determine a critical state line for fibre-reinforced sands due to samples' non-homogeneity, preparation variations and differences in fibre characteristics.

The main principle of the critical state line and its central purpose for use in this thesis is that it is a unique relationship, independent of test conditions or the stress-deformation path followed to reach the critical state values. Although there are disparities in literature about the test conditions that best represent the critical state line (Been et al, 1991; Vaid et al, 1990; Ishihara et al, 1975), the overriding fact is that the minimum or maximum shear strength of a sample depends greatly on the initial density of the sample and the loading conditions. Especially in the case of fibre-reinforced sands, the samples pass through a transformation state and are still dilating at the end of the tests, thus it is not clear what the true ultimate critical state of the samples might be. Many of the problems and differences of opinion on the critical state line and its uniqueness are related to shear localisation. The size of the test sample and size of the grain particles determine the width of the shear zone (in both direct shear and triaxial tests), so any dissimilarity in the thickness of a sample's shear zone will create a different impact on soil samples of different scales. The inclusion of fibres usually alters the width of shear zones in soil, which has implication for the shear displacements.

2.2.8 Strain-localisation in reinforced soil

Reinforced soil is more ductile than plain sand with respect to deformation. This is shown by the significant strains and deformations that take place before the full strength of the material is realised. Dilatancy is usually measured as the volume change that occurs in the shear failure zone at peak stress ratio values. The soil in shear zones will dilate fully to achieve a critical state, at which shear deformation can continue in the absence of volume change (Bolton, 1986). The fibre-reinforced sand samples' dilatancy behaviour post-peak is demonstrative of the density value of the sample during the residual stress state. Dilation characteristics at both peak and large displacements must be examined in order to assess the amount that the fibre reinforcements have contributed to the soil strength. The localised strains that occur in the shear zone of reinforced soil will be explained in this section.

The angle of dilation for sand in plane shear is characterised by the tangent of volume expansion where dv is the change of the dilation angle over the change of shear strain (percentage) $d\gamma$.

$$\tan\psi_{rate} = -\frac{dv}{d\gamma}$$

Figure 2.19 shows the mechanical significance of the angle of dilation in a plane strain deformation, which can be applied to direct shear test conditions. In 2.19a the shear zone of two sliding rigid soil blocks is shown as *ZZ*. For compatibility *ZZ* must be a zero extension line so that $d\varepsilon_z = 0$. The angle of dilation as shown in 2.19b is equal to the instantaneous angle of motion of the sliding blocks in relation to the shear surface where the following formula applies.

$$\tan\psi = -\frac{d\varepsilon_y}{d\gamma_{yz}} = \frac{dy}{dz}$$

Figure 2.19c shows the Mohr circle of strain increment for the shear sample. If the soil above the zero extension line *ZZ* is assumed as one rigid mass sliding upwards an angle of ψ over a lower rigid soil mass, and that the angle of shearing at zero dilation remains at critical state (ϕ'_{cs}) then the formula for the observed angle of shearing on the rupture surface would be as follows.

$$\phi = \phi'_{cs} + \psi$$

This expression assumes that any angle of shearing greater than the friction angle of loose earth is seen to be solely due to the geometry of the volumetric expansion that is necessary before shearing can to take place (Bolton, 1986).

Figure 2.20 shows the volume change behaviour of Ottawa sand in drained simple shear. Vaid et al (1981) determined the dilation angle to be a function of both the relative density (D_r) and confining stress (σ_{vo}) where an increase in σ_{vo} resulted in a decreased angle of dilation. For a series of tests, the dilation angle decreased linearly at each relative density value at a constant rate with confining stress.

The rate of volume expansion with shear strain is generally larger for dense sand than for loose sand. Figure 2.21 compares triaxial compression test results for Toyoura sand (σ_1 = 100 kPa) with a model that predicted the dilatancy behaviour based on three initial densities. The samples with lower void ratio values reached higher peak stress states and greater dilatancy as expected for dense samples. The samples with higher

void ratio values showed no change in dilatancy after the peak stress value until the end of the tests, as would be the expected behaviour of loose samples. The objective of these triaxial tests (Li and Dafalias, 2000) was to predict the void ratio values at critical state based on the confining stresses by the state parameter.

An illustration of the relationship between void ratio at critical state and the dilatancy trends for undrained triaxial tests is shown in Figure 2.22. When the state parameter ψ_{SP} is equal to zero, the plastic dilatancy value d in Figure 2.22(b) is also equal to zero. Soil states denser than critical are negative with ψ_{SP} and states looser than critical value are positive. Although the state parameter can be defined throughout direct shear tests, the volume changes that occur at large shear displacements deserves special consideration.

For sands initially in either a dense or loose state, the critical state of shear failure is where the volumetric expansion rate is zero (Roscoe et al, 1958). Li et al (1999) found that dilatancy was not only a function of the state of stress, but also a function of the material's ultimate state, and in particular of the proximity of the material state to the critical state (e.g. the state parameter). To achieve a given angle of dilatancy, the particle structure should be both dense and not so highly stressed that the soil grains would fracture.

The angle of dilation is seen to be equal to the instantaneous angle of motion of the box halves relative to the rupture surface. A great deal of attention has been focussed on the relation between the peak internal angle of friction (ϕ'_p) and the peak angle of dilatancy (ψ'_p). Bolton (1986) developed expressions for plain sand that state that any angle of shearing in excess of the critical state friction angle for loose sand is seen to be due solely to the geometry of the volumetric expansion which is necessary before shearing can take place. Table 2.1 shows typical values for the internal angle of friction for soils and Table 2.2 presents the derivations for the angles of friction (ϕ) and dilatancy (ψ).

It should be recognised that the angle of dilatancy becomes a meaningless parameter in an axisymmetric triaxial compression test, as a more useful measure of triaxial dilatancy rate ($-d\varepsilon_v/d\varepsilon_1$) can be determined from the peak stress ratio. The relationship that develops in triaxial test sand data can display the following:

- The variation in the peak angle of shearing resistance, and the rate of dilatancy, with relative density at a particular stress level.

- The variation in peak angle of shearing resistance with stress level, at particular relative densities.
- The combined variation for particular sands in those few studies where both density and stress level effects were studied.
- The comparison in behaviour displayed between plane strain and triaxial test behaviour.

(Bolton, 1986)

In the direct shear test the soil in the shear zone will dilate fully to achieve a critical state, at which shear deformation can continue in the absence of a volume change. The volume change in the shear zone is measured by the angle of dilation of plane strain deformation. Dense sands tend to dilate when sheared. In reinforced soil, the shearing soil transfers loads to the fibre reinforcement and the tension of the fibres is mobilised as a result. An increase in the tension in the fibres will increase the "apparent cohesion" and the internal angle of friction of the soil-fibre composite as seen in the Mohr-Coulomb failure envelope (see Figure 2.23). The tensile stress contributes to additional shear strength in the composite; hence the mobilisation of tensile strength in the reinforcement is related to the amount of soil dilatancy.

The average dilatancy of a soil is tan ψ = (vertical displacement / horizontal displacement) where ψ is the soil dilatancy angle. The soil volume increase that occurs in direct shear tests is assumed to take place in the shear plane. The angle of orientation of reinforcements relative to the shear plane influences the dilatancy behaviour of the soil (this is discussed further in section 2.3.3). The magnitude of normal stress was observed to have an affect on the dilatancy of fibre-reinforced sands in direct shear tests.

We have seen evidence in this chapter that the inclusion of fibres increases both the soil strength as represented by the angle of internal friction and the apparent cohesion of a sand sample. An illustration of the reinforcing effect of 0.5% fibres (by weight) on un-reinforced sand proposed in this model is given in Figure 2.24. We assume increased peak shear stress values for reinforced samples corresponding to the same normal stress values of un-reinforced samples, in order to increase the angle of internal friction. An element of apparent cohesion is provided by the tensile properties of the fibres. According to the diagram, the fibre content provides an amount of tension that

increases the friction angle and cohesion of the sample. The volume changes activate this tension in direct shear.

During the loading stages before shear and the start of strain, reinforced specimens may not deform homogeneously due to the effect of tensile-reinforcing. Strain localisation will occur at different points of particle contact depending on the reinforcements. After the start of strain localisation, both reinforced and unreinforced soils will not deform homogeneously. Before the onset of strain localisation, a sand mass that is more effectively tensile-reinforced becomes less dilative due to the restraint to the development of strains in the sand (Peng et al, 2000). The numerical analysis of the behaviour of reinforced soils should therefore consider the strain-softening properties of soil particles that are associated with strain localisation.

Strain localisation is a phenomenon where the response of a specimen is no longer representative of unique material properties, because the deformation mode (and the evolution of properties) is no longer uniform. The shear zone is seen as the region of shearing material where the strains are considerably greater than those in the surrounding regions. The angle of dilation is defined by $\sin \psi = -dv_\varepsilon / d\gamma_\varepsilon$ where dv_ε and $d\gamma_\varepsilon$ represent the increments of volumetric and shear strain in the shear zone respectively. For fibre-reinforced sand samples, it is assumed that the fibres distribute the shear strains to the entire volume in shear bands. To quote Scarpelli and Wood (1982):

> "Where a number of shear bands divide a region into small sub-regions an incremental strain field parameter (such as the angle of dilation) is calculated as the average of values for the several sub-regions."

This will be the case in the dilatancy analysis of fibre-reinforced samples, as the angle of dilation represents average values for the stresses and strains experienced by the sample in the shear zone.

Some assumptions for the shear zone in fibre-reinforced samples in direct shear include:

- the fibres are distributed evenly throughout the shear zone;
- the effects of tensile strains in the fibres extend beyond the boundary of the shear zone;

- the strain localisation will occur at different points for reinforced and unreinforced samples; and
- the angle of dilation represents the average values of volumetric and shear strain that takes place in the shear zone.

Strain softening is characterised by decreasing shear stress with a corresponding increase in strain. Strain hardening is characterised by a mobilisation of tensile stress in the fibres with a corresponding increase in both stress and strain in the case of fibre-reinforced soils. The strength increases with the strain increase up to a peak stress value. The post-peak strain is of great importance for the behaviour of fibre-reinforced sands in shear.

Strain localisation is assumed to commence at the peak stress state as the increase in shear strength for reinforced sands is generally related to volume expansion in shear testing. Larger dilation from shear deformation in reinforced sands is then suppressed by volume contraction at the peak shear strength. Soil in shear zones will dilate fully to achieve a critical state, at which point shear deformation can continue in the absence of a volume change. Both the normal stress and soil density affect the angle of dilatancy of soils as well as their shear strength values.

To achieve a given angle of dilatancy in plane strain, the particle structure should be both dense and not so highly stressed that particle breakage should occur. The accepted definition for the state of compaction of granular materials is relative density. It has generally been found that relative density offers a superior correlation compared with voids ratio for the strength of sands in direct shear tests, presumably since it compensates for effects of particle grading and shape that can influence e_{max} and e_{min}.

The peak shear stress values are greater in dense, angular soil samples. Strain localisation occurs in the shear failure zone, which can lead to greater dilations at peak stress values. The resistance to dilation of sand is known to depend on factors such as void ratio, stress level, grain size distribution and grain angularity (as seen in Figure 2.25 which compares angular with round sand). One method used to influence the amount of dilation, is to set the initial density of a test sample by its fabrication method. In the next chapter, details about setting the initial density of samples will be explained in more detail.

2.3 Test material variables

2.3.1 Mechanical effects of the mix variables

The interactions between soil and reinforcement are dependent on the characteristics of the individual components of the mix. Some studies have evaluated the stress-strain behaviour of fibre-reinforced soils as a composite of two independent materials (Gray & Ohashi, 1983), while others consider the composite simply as a reinforced soil with its own unique characteristics (Di Prisco & Nova, 1993). The interaction of the fibre and soil will demonstrate different behaviour depending on the proportions of the variables of the fibre-soil mix.

The interface region between the fibres and the surrounding material maintains the bond for the transference of loads. Factors such as the surface texture of the reinforcements and the length to diameter fibre aspect ratio as well as the soil grading and particle shape of the soil control the effective area of the reinforcement over which a bond may develop. There are numerous examples in literature that the strength of the bond between the sand particles and the reinforcing fibres has been shown to affect the strength properties of tests samples. Previous research has found that the strength of the interface region varies according to factors such as the amount of the initial density, the confining stress of the samples and the physical properties of the fibres (see, for example, Al-Refeai, 1991; Gray and Al-Refeai, 1986; Gray and Ohashi, 1983; Maher and Gray, 1990; Michalowski and Zhao, 1996; Nooray and Uzdavines, 1989; Waldron, 1977; Waldron and Dakessian, 1981; Waldron et al, 1981; Wu et al, 1988_a and 1988_b). The material variables and their properties that contribute to shear strength for reinforced soils will now be explored.

The angularity or roundness of the shape of the sand grains can create preferred orientations for the movement of soil particles and the flow of fluids (when a moisture content exists) within a soil mass. For example, Mukegon dune sand particles are round and Mortar sand particles are angular. It is expected that the way in which these two sands react to deformation would be different due to their different grain shape. Figure 2.25 shows the major principal stresses at failure, as a function of the confining stress in triaxial tests of Muskegon and Mortar sands with different grain shape, and fibre aspect ratios. The fibre aspect ratio is defined as the ratio of the fibre length to diameter. A higher fibre aspect ratio translated into an increased fibre surface area and improved sand-fibre interaction in the study shown. The fibres had a random

orientation and the fibre content was 3% by weight for all the samples. The test results differed according to the shape of the sand grains.

In Figure 2.25 rounded sands exhibit a curved-linear envelope and angular sands exhibit a bilinear envelope. The angular sands clearly show the critical confining stress at the point where the two lines of differing gradient meet. The rounded sands show a more curved-linear envelope. The distinctive transition of the envelope tangents occurs at a threshold confining stress, referred to in this study as a critical confining stress. From these results it was ascertained that the grain shape of a type of sand would affect not only the initial settlement characteristics of a sample, but also the stress values. From this observation, it is possible to predict the optimal reinforcement for particular stress environments based on soil granulometry, the aspect ratio and type of fibre.

The bond strength between the soil grains and fibre reinforcements will be investigated in compression and shear. The reinforcing effects of the fibres can be observed as a combination of sustained higher peak stress values and a delayed commencement of plastic deformation in a sample. The tensile and compressive properties of both materials will be taken into consideration for the determination of the soil strength with respect to the amount of confining normal stress, according to the fibre content and initial density values of the samples.

2.3.2 The significance of the fibre content and length

Strength increase is generally proportional to the amount of reinforcement up to a limiting content for dry soil samples. At higher plastic fibre contents in direct shear, the strength increases tend to approach an asymptotic upper limit at 2% (Gray and Al-Refeai, 1986). Figure 2.26 shows the principle stress value for failure increasing with the increasing fibre contents in triaxial compression tests. Different loading conditions obviously result in significantly different shear strength behaviour for reinforced samples, but this figure demonstrates the effects of different confining stresses. The higher confining stress curves (392 kPa) showed more than twice the failure strength increase than the lower stress samples (98.1 kPa) as the fibre content increased.

Increasing the amount of reinforcement may increase the failure stress of the fibre-soil mixture, but the amount of pre-stress applied by sample preparation required to achieve a dense sample must be altered accordingly. An increase in porosity occurs with increasing reinforcement and the inherent decrease in soil strength. As detailed earlier in this thesis, the confining stress must be great enough to allow the pull-out strength of

the fibres to be mobilised. Jones et al (2001) suggested that at a low confining pressure, a minimum fibre content of between 0.05% and 0.10% by dry mass would be required to increase the fibre-reinforced soil strength. Beyond that minimum fibre content, the increase in strength with increasing amount of fibre is almost linear up to 2% of fibre content. The stress ratio of sand increases with increased fibre content and fibre aspect ratio to a limiting value termed the weight fraction. The weight fraction is the weight of the fibre content divided by the soil weight (Maher and Woods, 1990), so optimum fibre content depends on the types of fibre, the type of soil that are to be mixed, and the fibres' length to width ratio.

The fibre aspect ratio (length to diameter) is a factor that affects the strength increase versus fibre content relationship. In Figure 2.27 the peak failure stress increased with an increase in the fibre aspect ratio (l/d) in triaxial tests (after Ranjan et al, 1996). Gray and Ohashi (1983) found that an increase in the fibre length tended to yield higher shear resistance, but did not lend greater stiffness to the sand fibre composite. The dimensions of the test mould have been mentioned (Wu et al, 1988) as one determinant for the fibre length in order to mobilise the tensile strength of the fibres, and the confining stress is the other.

In reinforced earth, cohesion is imparted to soil by the linear reinforcing elements. Stress is carried within the mix by forces tangential to the fibres, which produces differing tensions along the fibre lengths. These tangential forces can be carried by friction between the fibres and the surrounding soil. Shorter fibres required a greater confining stress to prevent bond failure, regardless of size or shape of sand particles. Fine sands have shown a more favourable response to fibre reinforcement than medium sands. The amount of strength increase induced by short fibres depends on the fibre content and aspect ratio, and soil grain size. Figure 2.28 plots the average shear strength increase of different inclusions against the length of the inclusion. The conclusions that can be drawn from this graph are the values of the optimum fibre lengths that are required to obtain an increase in shear strength (at the same stress levels) for the granular materials listed.

Comparisons can also be made among the reinforcing materials based on their strength enhancing behaviour. At the same aspect ratio, confining stress, and weight fraction, rougher fibres tend to be more effective in increasing strength (Jones et al, 2001; Gray and Al-Refeai, 1986) as rougher surfaces provide a larger surface area with which the

soil can attach. Some geomembrane sheets are manufactured with roughened surfaces (O'Rourke et al, 1990) specifically for improved cohesion.

Let us consider, for a moment, how the reinforcing properties of geotextiles are tested. Most geotextiles are sheets of fabric anchored within a mass of soil where the geotextile is anchored while vertical stresses are applied. The sand-geotextile element acts as a frictional material with an increased internal friction and improved strength, but usually with no cohesion. The most practical orientation of a geotextile is horizontal, so the effect of the reinforcement can easily be measured by experimentation in triaxial tests with horizontally placed layers of reinforcement.

Because many published studies on fibre-reinforced soils have been conducted in the triaxial apparatus, the length of the fibre is not usually given much consideration as any extremely long fibres could have the same effect as the fibre content value in a triaxial test mould. To ensure the tension of the fibres is mobilised, the fibre length will depend on the dimensions of the test apparatus and the soil granulometry. If the fibres are too short to gain anchorage with the surrounding soil grains, the fibres may be pulled out in tension and fail.

In order to quantify the amount of shear resistance or tensile strain experienced by the fibres within a sand laboratory sample, the volume fraction was considered. The volume fraction was calculated together with the tensile strength of the fibres to define the amount of increased shear strength within test samples. The ability of the fibres to confine the soil grains depends on the quantity and quality of the fibres' dispersion within the test samples.

2.3.3 Orientation of the reinforcing fibres

Direct shear tests have mainly been used to test the orientation of natural root reinforcements and geotextiles as a determining parameter of soil strength. This has especially been the case in the stabilising of soil slopes (Waldron, 1977; Wu, 1979; Wu et al, 1988_1 and 1988_2). The objective of the slope stability tests was to study the interaction between the soil and reinforcement and the shearing resistance along a potential slip surface. Roots that intersected a shear plane at an angle greater than 90° were subjected to compression during shear and therefore did not contribute greatly to the shearing resistance. Figure 2.29 compares the failure envelopes of sand reinforced with reed fibres of random and perpendicular orientation sheared within the shear box. The random fibre orientation shows almost identical shear strength values to the fibres

oriented at 90° to the shear plane. Thus, the shear resistance of randomly oriented fibres was as resistant in the shear plane as fibres oriented at 90° to the shear plane.

Figure 2.30 shows the normal and shear forces for fibres oriented at 90°and 63 or 64° to the shear plane at displacements of approximately 4cm from Wu et al (1988_b). The peak and ultimate shear strength trend lines are also shown. The test results indicated that the shearing resistance of the soil-root samples was slightly less than the ultimate strength at larger displacements. The results showed that the roots allowed the reinforced samples to withstand greater shear stresses than plain sand for all root orientations mentioned before experiencing failure by buckling. The soil-root interaction was used by Wu et al (1988_a) to compute the shearing resistance of roots in soil from in situ direct shear tests. The in situ tests showed that in the test conditions described, unless the angle of root orientation exceeds 80° with respect to the shear surface, roots with diameters greater than 0.7cm would not fail in tension. This agrees with observations of excavated roots, as all of those that failed in tension had diameters of 0.7cm or less. The test boxes were constructed around naturally-occurring root systems and measured 30 x 30 x 60cm. The force generated in the roots and its contribution to the shearing resistance as measured in the in situ test were said to be dependent on the length of the roots with respect to the dimensions of the test box.

Randomly oriented reed fibres at 3% by weight showed a slightly higher stiffness (labelled as a shear modulus ratio) than fibres oriented at 90° to the shear plane in Figure 2.31. The stress ratio shown in the graph is the reinforced shear value over the un-reinforced shear value. At a confining stress of 138 kPa, the random orientation of 3% reed fibres demonstrated slightly higher shear strength than the reed fibres originally oriented at 90° to the horizontal shear plane as the shear strain increased.

The mechanical properties of randomly distributed fibres have proven to resemble the behaviour of fibres orientated at 90° to the shear plane (Maher and Woods, 1990 and Gray and Ohashi, 1983). Maher and Gray (1990) noticed planar failure surfaces oriented in the same manner predicted by Mohr-Coloumb theory in triaxial tests of randomly distributed fibre-reinforced sand that suggested an isotropic reinforcing action with no development of preferred planes of weakness or strength.

Initial fibre orientations of 60° with respect to the shear surface gave the greatest shear strength increases in triaxial compression tests for Netlon-reinforced sand (Al-Refeai,

1991). McGown et al (1985) cut Netlon mesh into elements 50 x 50mm and mixed with sand at 0.18% of mesh by dry weight of soil. Model footing tests were also undertaken and the improvements were very similar to those measured in the triaxial tests in terms of both strength and deformation characteristics. Leflaive (1988) found that for soil reinforced with continuous yarn, *Texsol*, the geometrical arrangement of the yarn within the soil may vary due to the method and equipment used for production. These limitations in preparation create anisotropic samples for small-scale testing. The strength of a soil having an anisotropic fabric is a function of the angle between the major principal stress direction and the axes of anisotropy in the soil.

To illustrate a reinforcement inclined with respect to the failure surface, Figure 2.32 shows the strain increment diagram for sand in direct shear with a reinforcement oriented 60° to the shear plane. An angle of internal friction for plain sand ($\phi' = 35°$) is shown in the Mohr-Coulomb model plus the angles of inclination for a fibre orientation from the shear plane ($\lambda = 25°$) and normal to the shear plane (ζ). Tatsuoka (1987) stated that the maximum efficiency of reinforcement should be expected when the orientation of the reinforcements coincides with the angle of shearing resistance of the soil. This can be regarded an underestimation of the problem as the optimum orientation for reinforcements depends on many material parameters of both the soil and the reinforcements.

The angle of orientation of fibres must be assumed or estimated within 0° and 180° to the shearing surface. This boundary condition is reasonable given that the fibres contributing to shear strength can only be pulled along normal to the shear plane, along the shear plane, or at some angle in between. At the optimum fibre orientation, the combined effect of shear displacement and soil dilatancy will mobilise the most tension in the reinforcement. Ola (1989) and Gray and Ohashi (1983) found that the direction of principal strain for fibre-reinforced samples in direct shear coincided with the direction of maximum tensile strain, which was 60° to the shear plane.

The efficiency of reinforcements is highly dependent on the orientation of the reinforcements with respect to the shear plane as increases in the shear resistance of reinforced soils are generated by the tensile stress in the reinforcements. As random orientations of fibres resemble the same strength-deformation characteristics as fibres orientated normal to the shear plane, randomly distributed *LokSand* fibres provide additional shearing resistance to plain sand samples through tensile strength.

The interaction mechanism that mobilises the tensile stress in soil reinforcement is not yet fully understood. Direct shear tests are suitable for the study of the reinforced soil bond because they can simulate the shear mechanism along a potential failure plane in a reinforced soil. Bauer and Zhao (1993) studied the shear mechanism of geogrid-reinforced granular soils in direct shear. The bond between the soil and reinforcement was strengthened by the bearing resistance of the transverse members of the geogrid as well as the interlock of the soil particles with the geogrid. The main conclusion drawn from the testing of geo-textile reinforced soils is that the maximum efficiency is expected when the orientation of the reinforcement coincides with the direction of the maximum tensile strain increment of the soil.

Figures 2.33 and 2.34 show the increased peak and residual stresses and vertical movement (respectively) for coarse sand reinforced with geogrids inclined at 0°, 45°, 60° and 90° to the horizontal shear plane at 28 kPa normal stress. It can be observed that at small horizontal displacements the stress ratio increased linearly until a peak value was reached. Geogrid samples denoted as having 0° inclination to the horizontal shear plane were sliding tests whereby the geogrid was anchored in place by clamping the geogrid to the stationary half of the shear box after the sand had been compacted to this level. The residual shear strength of the mechanically compacted sand labelled "un-reinforced" was approximately 25% lower than the peak strength. The samples with 90° orientation also experienced a post-peak stress ratio reduction. In contrast, the sand reinforced at angles of 60° or 45° to the shear plane yielded high peak shear strength values that were sustained until the end of testing,

The vertical displacement of the samples was monitored in order to evaluate the soil dilatancy. Figure 2.34 shows similar dilatancy characteristics for the sands reinforced at angles of 60° and 45° to the shear plane compared with the "un-reinforced" sands. The samples with reinforcement inclined at 0° showed little vertical displacement as the peak stress was reached quickly and thereafter and did not substantially resist shear along the horizontal surface of the geogrid. The post-peak vertical displacement of the 90° geogrid samples increased more than the 0° angle of orientation, although it was less that the un-reinforced samples due to the non-uniformity the geogrid introduced to the shear plane.

The increase of shear stress with increasing normal stress is shown in Figure 2.35 for the test samples. In the normal stress range of 20 to 35 kPa, an increase in shear strength occurred for all samples and the reinforcements at 60° proved to be the

optimum angle of orientation for increased shear strength. The test results in Figure 2.36 show the stress ratio and horizontal displacement for reinforced crushed limestone aggregate. For this soil, the specimen with the geogrid originally inclined at 90° showed a constant stress ratio value of 1.5 with continued shear displacement and again the 60° and 45° orientations showed the greatest shear stress increases. The high stress ratio values of reinforced aggregate were sustained at large shear deformations until the end of the tests.

The orientation of the reinforcement relative to the horizontal shear plane had a significant influence on the volume change behaviour. The normal stress value significantly increased the shear strength behaviour, although for the narrow range of normal stresses investigated it was considered to have little effect on the soil dilatancy. The dilatancy of the un-reinforced samples (0°) tended to reach a plateau while the reinforced samples continued to dilate even at the end of the tests. Bauer and Zhao concluded that the volume expansion of the soil was directly related to the magnitude of the tensile strain within the geogrid and thereby indicates the contribution of the fibres to the shear strength increase.

2.3.4 Fibre pull-out resistance

All soil reinforcement models assume the tensile strength of fibres to be fully mobilised at failure. This assumption requires fibres to be either fixed at their ends or the inclusions are assumed to be long enough for frictional bonding strength between the fibres and soil grains to exceed the tensile strength of the fibres. Another common assumption for the tensile strength is the existence of a coefficient of friction between the soil grains and the fibres. This assumed coefficient is further influenced by the orientation of the fibres. The fibre pull-out resistance has been shown to be dependent on the confining stress in shear tests of randomly-distributed fibre- or root-reinforced soils. The tensile stress that develops in the fibres at the shear plane is mainly a function of the fibres' response to tensile deformation. This response can manifest itself in the forms of stretching, slipping, or breaking.

Direct shear tests are conventionally used as a test method for measuring the angle of bond friction for soil reinforcement. This applies only to the bonding through shear between the soil and the surface of the reinforcement. In a pullout test the reinforcement is displaced with respect to a stationary mass of soil. Volume expansion in the deforming soil immediately surrounding the reinforcement can cause additional confining stresses to be generated in the pull-out test, and the reinforcement being

pulled with respect to the soil might allow an angle of friction greater than the peak angle of friction found from direct shear test (ϕ_{ds}) to be mobilised on a rough reinforcement surface. However, the higher bond stresses which result would only apply in the field under loading conditions that reproduced those in the pull-out test. If the interface friction were greater than the soil friction, then failure would be expected to take place in the soil.

The magnitude of the fibre-induced distributed tension within a soil is defined by the properties of the individual fibres. The interface shear resistance of individual fibres is characterised as a function of the adhesive component of the interface shear strength between the soil and the fibre, the frictional component of the interface shear strength and the average normal stress acting on the fibres. The experimental results from Zornberg et al (2000) confirm that the fibre-induced soil tension increases linearly with fibre content and fibre aspect ratio when failure is characterised by pull-out of individual fibres.

Most polymers tend to creep when subjected to a tensile force, and this tendency increases rapidly as the tensile force is increased. The allowable tensile force must therefore be greater than the required tensile resistance of the reinforcement. Many tests of the pull-out resistance limits of reinforcements are cited in literature. Figure 2.33 schematically shows that the relative displacement of reinforcements varies along the reinforcement length. The anchor displacement (δ) and the Cartesian coordinate for critical tension (T_{cr}) is coincident with the anchor length of reinforcement (z) and ultimate tension (T_{max}). T_o refers to the axial tensile load value. The pull-out resistance/breakage strength of the reinforcement, according to Leshinsky and Boedeker (1989), depends in part on the factor of safety of a given reinforced structure. Within the formula for factor of safety, the interface shear is considered fully mobilised along the embedded length of reinforcement beyond the point of maximum tensile force. Juran and Christopher (1989) and Wu and Tatsuoka (1989) introduced equations for the amount of displacement that occurs within a reinforced soil sample at the point of maximum tensile force. The interface angle for reinforced Toyura sand in pullout tests decreases with confining stresses higher than 50 kPa (Peng et al, 2000). In direct shear tests, increasing confining stresses can increase the internal angle of friction up to a limiting value. The discoveries made from pull-out tests in literature demonstrate the existence of a threshold confining stress, beyond which the reinforcements may break or pull-out.

2.4 Experimentation

2.4.1 The effects of dynamic compaction

Fibre-reinforced granular soil tends to resist vertical stress deformation. The application of *LokSand* fibres in the sub-grade layer of soil beneath vegetation reduces the amount and penetration of soil by compaction with large loads, so the optimum moisture content for laboratory samples was determined by light Proctor compaction tests in this thesis. In the case of fibre-reinforced Hostun sand, dynamic compaction tests like the Proctor test lend an insight into both the compaction characteristics and the effects of moisture content on the samples.

There is an increase in the volume of air voids that occurs within samples of increasing fibre reinforcement during the mixing of the two materials. An inherent decrease in strength properties results from the increased air voids, however heavy compaction in the form of California Bearing Ratio tests can overcome the compactive resistance of the fibres and it produces a stronger, more ductile material as a result. Lawton et al (1993) found that reinforcement provides resistance to the dynamic compaction of reinforced soil in the CBR test, as was seen in Figure 2.3. Bailey (2000) also discovered that the presence of fibres in sand could increase the penetration resistance in CBR tests. Greater fibre contents gave higher stress-penetration values for fibre contents up to 1% by weight.

When considering the compression characteristics of moistened fibre-reinforced sands, we are aware that the inclusion of fibres allows a granular soil to be more ductile. The enhanced ductility due to fibres is represented by larger plastic deformations at larger normal stresses. The moisture content also increases the ductility of sand. Observations from the Proctor tests results will show to what extent the moisture and fibre contents affect the ductility of the Hostun sand samples.

The moisture content effects are very important to soil strength due to the presence of capillary forces at the particle contacts. Soil permeability affects the degree of coupling between the solid and fluid phases and it plays an important role in the initiation and development of strain localisation (Liu et al, 2005). The lower the permeability, the higher the load increment taken by water, and the slower the transfer of the load to the solid soil skeleton becomes. Hence coupling effects increase as the permeability decreases.

From the different aspects of compression discussed in this section, the settlement characteristics of a reinforced sample were found to be dependent on the following factors:

- Fibre reinforcements can make a soil more ductile depending on the density of the mix.
- Pre-loading of reinforced soils can provide a greater confining stress as well as initial mobilisation of the tensile resistance of the reinforcement through increased bond strength.
- Granular soils inherently contain an amount of tensile strength due to the concept of sand grains consisting of semi-spherical particles held together by tension bonds that resist particle breakage in one-dimensional compression.
- The yield stress of a granular soil in compression (taken as a point of maximum curvature on void ratio to normal stress plot) can be approximated as a function of the particle size and a percentage of its probability of survival in a particle breakage test.

The direct shear experimentation presented in this thesis includes an estimation of the expected vertical deformation for samples for fibre-reinforced sands based on the one-dimensional compression of the sample materials.

2.4.2 One-dimensional compression

The one-dimensional compression test measures the sample deformation due to vertical stresses. Not only is the method of laboratory experimentation of this relationship important, so is the methodology used in investigating this relationship. The influence of the initial state of a soil, including stress and strain histories, cannot be ignored in the investigation of the subsequent performance under normal stress. In the case of small-scale tests, the fibre-reinforced sand samples are more sensitive to sample disturbance and pre-compression from normal stresses before final placement. For this reason, the test samples for this thesis were labelled according to their initial density values.

Inter-granular friction is the dominant mechanism affecting the mechanical response of fibre-reinforced soils. The stress-strain behaviour is affected by a critical combination of contacts within the soil grains and the resulting force interactions. Thevanayagam (1999) stated that the stress-strain behaviour and deformation resistance a soil can offer under different loading conditions is dictated by the active participation (or lack

thereof) of different types and sizes of particles within the soil matrix in the transfer of inter-particle forces. Such effects must be specified when dealing with sands to understand the mechanisms contributing to the load transfer from fibres to the soil. The shape of the soil particle and the amount of normal stress imposed on a sample at any moment affects the volume of voids between the soil and fibres as well as the stress history of the mix.

The results of one-dimensional compression tests tend to be plotted as void ratio versus vertical stress. As the void ratio values decrease with increasing vertical stresses a representation of the deformation of the soil composite is given (see, for example, Figure 2.38). The particle diameter size of a soil sample can affect the compression behaviour of a sample. For cohesionless soils, particle crushing at high stresses is a significant deformation mechanism. Figure 2.39 shows the vertical deformation of plain soil samples under three different normal stresses. The points of particle breakage were highlighted in order to test the ultimate strength of the soil particles. This failure mechanism for the soil particles is similar to fibre breakage, as in both cases one of the mix materials has permanently deformed its physical shape.

Figure 2.40 shows the schematic definition of S_{ID}, the dimensionless stiffness coefficient for one-dimensional strain where the reciprocal of the void ratio ($1/e$) is plotted against effective stress raised to the power p ($p = 0.5$ approximates the crushing strength of a wide range of normally consolidated cohesionless soils). For granular soils S_{ID} is constant below the stress level where particle crushing is a significant deformation mechanism. S_{ID} has been used to model the effects of void ratio, relative density, and particle shape and size distribution with respect to one-dimensional strain. The stress levels chosen for the fibre-reinforced Hostun samples in this thesis would not be great enough to allow particle crushing, and likewise the shear displacement will not be great enough to result in fibre breakage, in order to avoid inaccuracies in test results due to permanent material degradation. The vertical deformation of samples in compression tests with normal loads up to 200 kPa will be plotted as void ratio versus normal stress.

In sports pitches and grassed surface roads reinforced with fibres, the fibre reinforcements allow granular soils to resist compression deformation from large loads (Bailey, 2000 and Jones, 2004). A sand-fibre mix can sustain larger axial loads than plain sand and the increased resistance to deformation is found with the increase in the concentration of fibres. One important consideration for the deformation characteristics

of fibre-reinforced soils is the unequal distribution of loads. The fibres transfer loads from the point of contact to areas of less stress, so any small variations in the load application of a small-scale laboratory test can affect the deformation behaviour of the sample (Waldron, 1977). Figure 2.41 shows the localisation of deformations for plain sand samples in axisymmetric tests. The angle α is the angle between the directions of plane deformation and the major principal stress. The presence of fibres would certainly alter the both the direction of α as well as the amount of displacement required to mobilise the reinforcing effect of the fibres.

In one-dimensional compression tests, an initial pre-load compression was imposed upon dry *LokSand*-reinforced Hostun sand by the weight of the top cap and load hangar. Further vertical deformations were measured relative to this initial pre-load compression. Pre-loading granular soil shear test samples can encourage the mobilising of tensile force within reinforcement at less horizontal displacement than non-pre-loaded samples of low initial density. The peak shear stress of a pre-loaded soil can be greater than a sample that was not pre-loaded.

Some geosynthetics are pre-stressed by stretching for greater tensile strength within a soil to enhance the bearing capacity of a soil. The mobilised surface friction between the soil and reinforcement provides a stronger interlock between the two materials. Compactive forces are applied and the reinforced soil deforms while internal stresses build up. Upon removal of the applied forces, the reinforcements may attempt to return to their original configuration, but the majority of soil particles in the interlock will prevent this contraction. The result is an internal (compressive) confining stress built into the interface bonds. Figure 2.42 shows the settlement within a loaded region ($X \leq 1.0$) reduces as the pre-stress in the geosynthetic layer is increased, although there is an increase in settlement slightly beyond the loaded region. Values of the pre-tension per unit length applied to the geosynthetic reinforcement are labelled as T_p in the legend. This indicated that the reductions in the amount of settlement due to pre-stressing were more significant at the centre of the loading than at the edges of the reinforced footings. The pre-stress reduced the differential settlements of a loaded footing due to the transference of loads to the surrounding soil. The load carrying capacity of reinforcements operate best with large loads, so pre-stressing the reinforcements increases the strain resistance to smaller loading conditions.

Pre-stress and pre-compression refer to any elements of a sample's stress history that take place before a soil mechanics test begins. Waldron and Dakessian, 1981 conducted

direct shear tests of soils permeated by roots of grasses, legumes, and young trees. The clay loam samples were pre-wet to a moisture content, which produced the highest bulk densities ranging from 1.20 to 1.90 g/cm^3 depending on the soil mix. In test columns with smaller diameter, more of the soil overburden at shear depth was supported by wall friction and arching. When a space was created between the two box halves (the upper and lower loading collars) at the shear plane prior to shearing (Waldron, 1977), relatively more vertical load was transferred to the soil in the smaller columns than in the columns of larger diameter (see Figure 2.43 for a diagram of the test apparatus). In the smaller diameter columns without roots the vertical load formerly carried by the wall was transferred to soil particles. Therefore, the vertical normal inter-particle stress at the beginning of shear was less in the rooted soil and resulted in an observed shear resistance that was initially smaller. Pre-compression of the soil reinforced with vertical roots would delay the onset of root reinforcing in the clay loam model and might well have had a similar effect in experimentation. In order to address these pre-compression effects on the shear strength values, the vertical deformation of dry fibre-reinforced Hostun sand samples was observed and the shear behaviour compared with non-pre-compressed samples.

2.4.3 Direct shear

Most direct shear tests of reinforced soil in literature are predominantly concerned with either the angle of orientation of the fibre (see, for example, Waldron, 1977; Wu et al, 1979; Wu et al, 1987 and 1988; Tatsuoka, 1987; Maher and Woods, 1990; Maher and Gray, 1990; McGown et al, 1985; Gray and Ohashi, 1983) or the method of anchoring the fibre reinforcements in soil (Zornberg, 2001; Leshinsky and Boedeker, 1989; Wu and Tatsuoka, 1989; Juran and Christopher, 1989). However, it can be difficult to achieve either a specifically arranged or a completely uniform fibre distribution within a laboratory fibre-soil mix for small-scale testing.

It will be seen in the test results that the peak strength of reinforced sand and un-reinforced sands are mobilised at different shear deformation. The difference in the peak stresses indicates that the stress state of reinforced samples is a consequence of the tensile stress of the fibres being mobilised. According to Qui et al (2000) reinforced sand in general becomes stronger:

- as the total contact area between the sand and reinforcement increases;
- as the roughness of the reinforcement surface increases; and

- as the degree of spatial dispersion of the reinforcement increases.

The consideration of a load-transfer mechanism for reinforced soils indicates that the dilatancy is restrained by the factors mentioned above. Figure 2.44 shows the strength ratio of Toyura sand reinforced with flexible strips of phosphor-bronze as the peak shear strength for reinforced sand at the shear displacement where the corresponding un-reinforced sand experienced peak as $(\tau_{vh})_{RP}/(\tau_{vh})_{UP}$ under 50 kPa normal stress. This ratio is plotted against the vertical displacement of the reinforced sand when the un-reinforced sand experienced the peak shear strength. The test sand had an initial void ratio of 0.617, which relates to a relative density of 94.8% for un-reinforced sand and 91.8 - 95.6% for reinforced sand. From the dashed average vertical displacement line on the graph, the rougher reinforced samples showed much higher averaged strength ratio and less total dilation compared with the smoother reinforced sand samples (strength ratio = 1.1 occurring at 0.66mm dilation at greatest value). The rougher (sand-glued) reinforcements showed a general decline in vertical displacement with increasing stress ratio values.

The residual stress refers to the stress of a sample at the post-peak "steady state". The peak stress and residual stress values are used to describe the strength of soils. Reinforced samples can reach the residual stress and continue to dilate, as dilatancy characteristics are usually considered for incremental response. The residual angle of internal friction value has been shown as a function of confining stress (Siddiquee et al, 1999). The residual stress and angle of friction tend to decrease with an increase in the confining stress. More effectively reinforced sands show larger peak and residual strengths.

Reinforced samples become more dilatant than un-reinforced samples at the residual stress state. Figure 2.45 shows the stress ratio and volume change for un-reinforced sand (U) and sand reinforced with flexible strips of different stiffness (EA). The reinforced sand exhibits a larger volume expansion at the residual state and higher peak stresses at large shear deformations with larger surface areas of reinforcement. In general, the phosphor-bronze-reinforced soils exhibit high strength, behaving in a brittle way as the deformation becomes large.

The laboratory test results presented here are the first to relate the normal stress and initial density values to the increased shear strength values and volumetric changes for

Hostun sand reinforced with crimped polypropylene fibres. The quantities required to estimate the increase of shear strength for this model include the fibre content, the initial density, the normal stress and the volume of the shear zone being considered. The effect of the initial one-dimensional compression on fibre-reinforced test samples was also considered with respect to the sample's volume changes both during sample placement in the shear box as well as while the shear tests took place.

2.5 Summary

The aspects of a research model for fibre-reinforced sand in direct shear have been described. The variables of a fibre-soil mix have been explored in order to establish their relevance to the strength parameters of test samples. The inclusion of fibres, their placement and geometry, and the tensile strength properties that they impart to granular soil has been reviewed. The initial compression from normal stress and subsequent volume changes during direct shear has been explained with respect to the initial samples' densities. The idealised behaviour of reinforced soil in one-dimensional compression and direct shear has been described.

The shear resistance in the shear zone governs the mechanical behaviour of direct shear samples. Fibres provide an increased confinement for the soil grains of a sample through tensile strength. The increased peak and residual strengths of samples due to the fibres result from the dilatancy trends in the shear zone. Angles of internal friction and dilatancy will be used along with the state parameter to investigate the relationship between the normal stress values, sample densities and the shear strength values. The intrinsic mechanical properties of fibre reinforcements such as tensile strength, stiffness and surface properties were discussed in order to propose sample preparation methods and a testing programme for the analysis of fibre-reinforced sands in the following chapter. A framework is produced that enables prediction of the shear strength of fibre-reinforced sands by their initial density range, fibre content and normal stress value.

2.6 Figures: Research Framework for Fibre-reinforced Soils

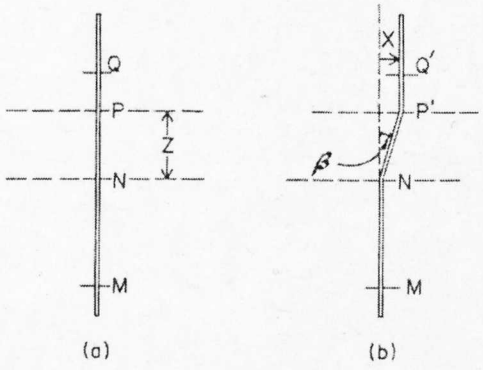

Figure 2.1: Model of a flexible elastic root extending vertically across a horizontal shear zone of thickness Z for (a) undisturbed soil and (b) upper mass of soil above N, displaced a distance X, with root segment MNPQ extended to length MNP'Q'
(after Waldron, 1977)

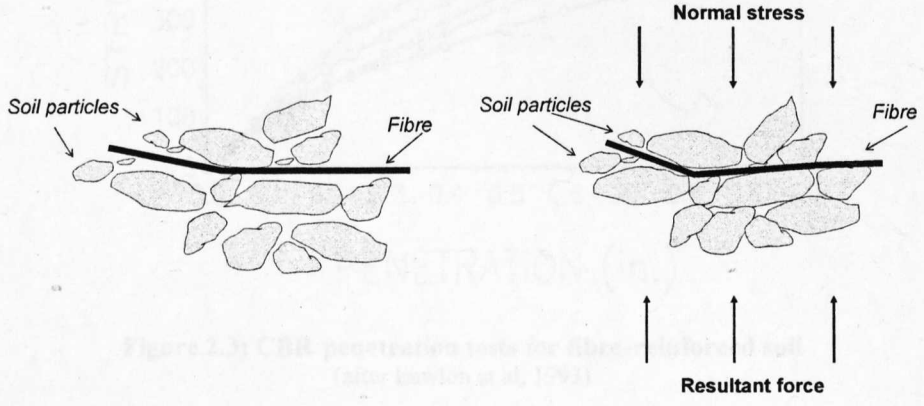

Figure 2.2: Fibre-reinforced sample section

(a) "as placed" sample section (b) sample section in compression

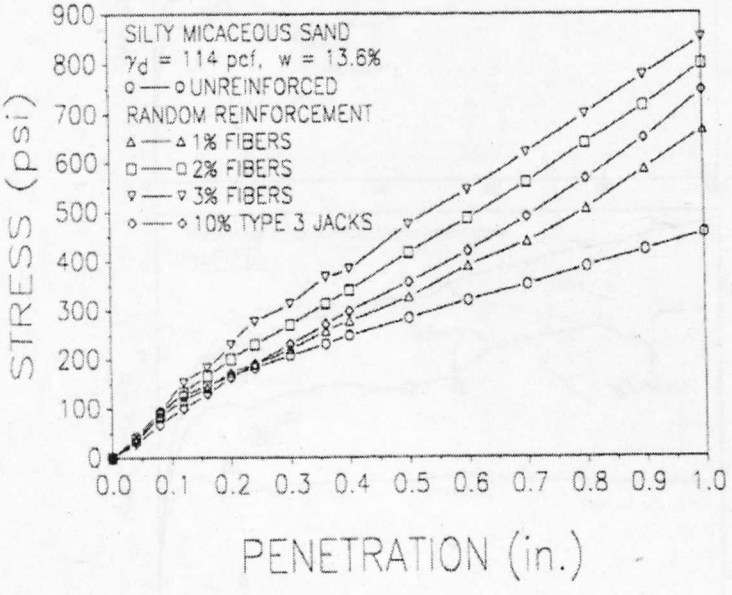

Figure 2.3: CBR penetration tests for fibre-reinforced soil
(after Lawton et al, 1993)

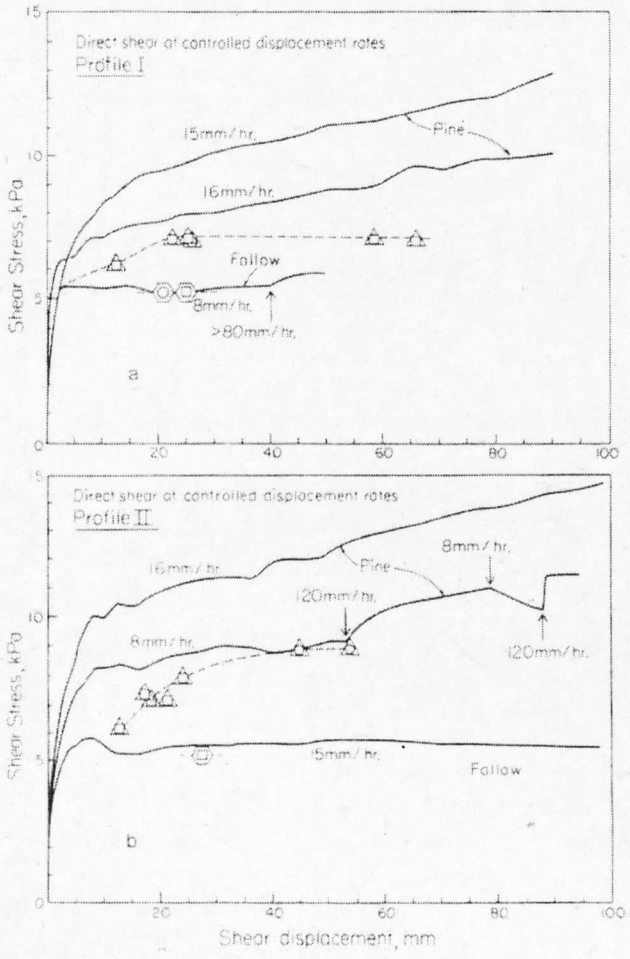

○ fallow, 14 months; △ alfalfa-rooted soil, 14 months; □ 8 mm/h; ○ 16 mm/h.

Figure 2.4: Shear stress versus shear displacement for root-reinforced and fallow soils
(after Waldron et al 1983)

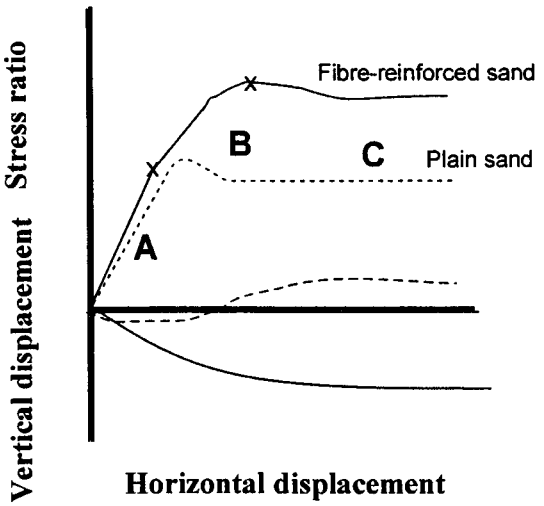

Figure 2.5: Stress-strain response of fibre-reinforced sand in direct shear

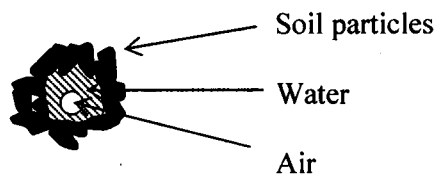

Figure 2.6: Assembly of soil particles with voids filled with mixture of air and water

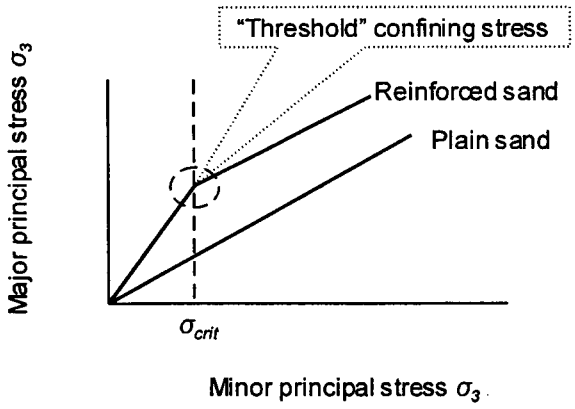

Figure 2.7: "Threshold" confining stress diagram

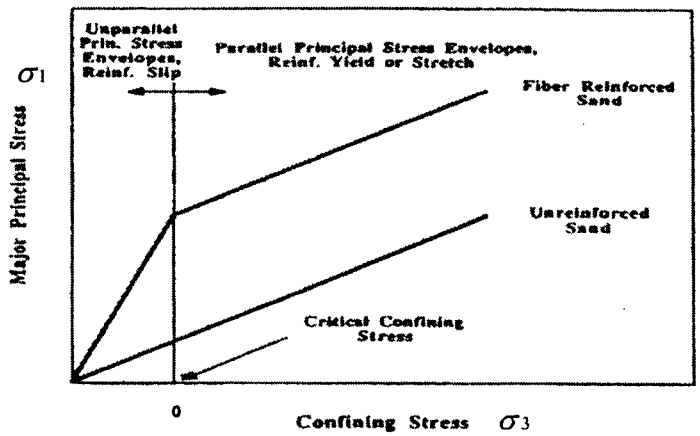

Figure 2.8: Idealised failure envelope (triaxial test)

(after Maher and Gray, 1990)

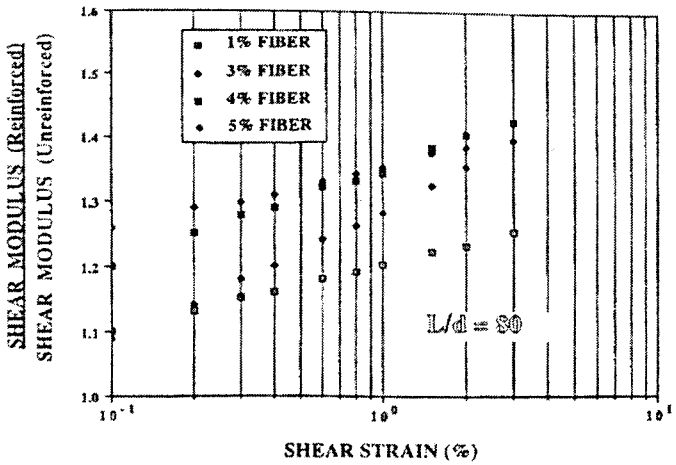

Figure 2.9: Failure stresses for fibre contents
(after Maher and Gray, 1990)

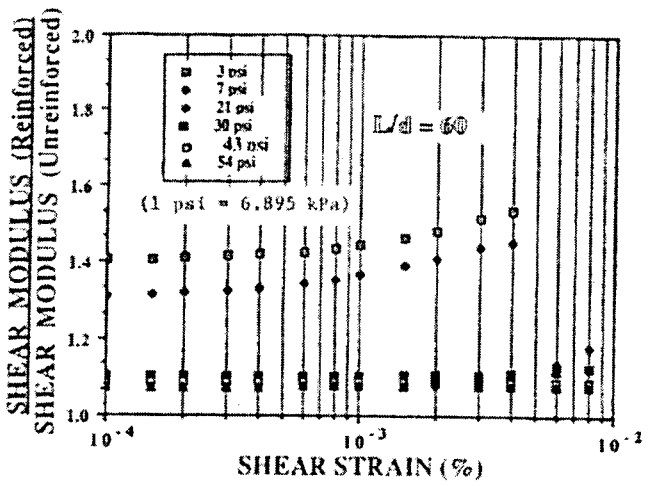

(a)

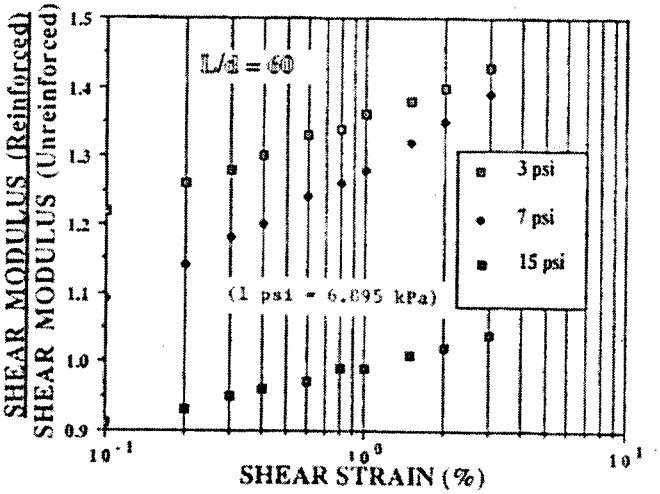

(b)

Figure 2.10: Confining stress (triaxial test)
(after Maher and Woods, 1990)

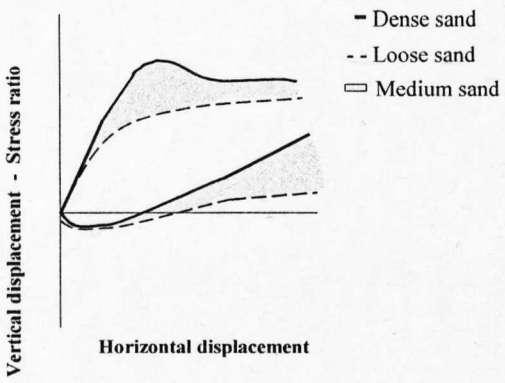

Figure 2.11: Stress-deformation behaviour of dense, medium and loose sands

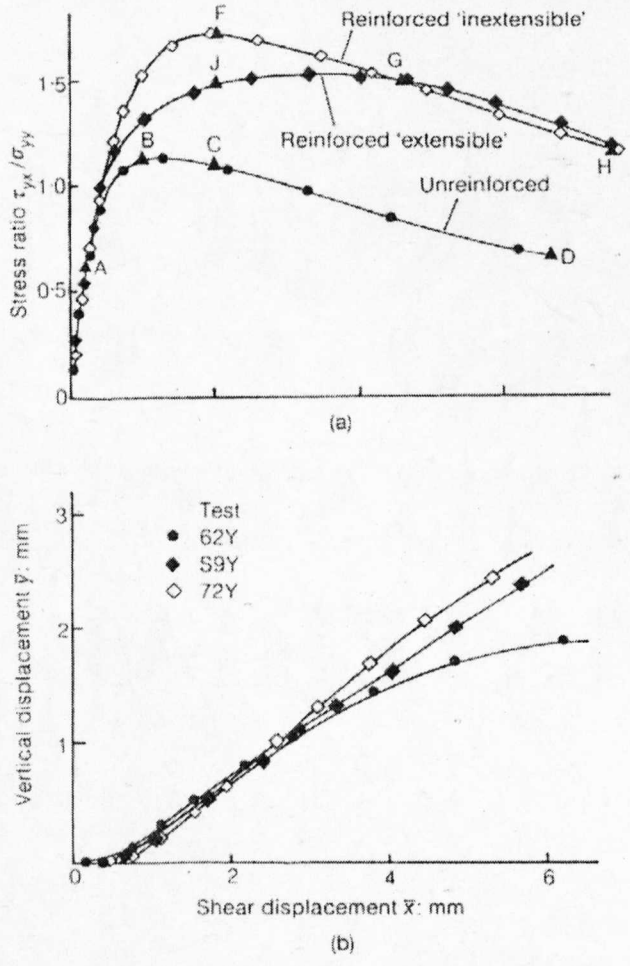

Figure 2.12: Direct shear test results on sand reinforced with extensible and inextensible reinforcements
(after Jewell and Wroth, 1987)

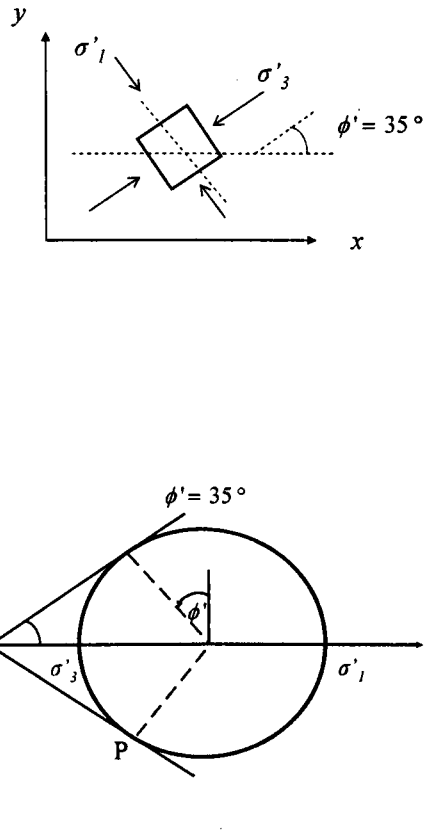

Figure 2.13: The principal stresses acting on a soil element in direct shear

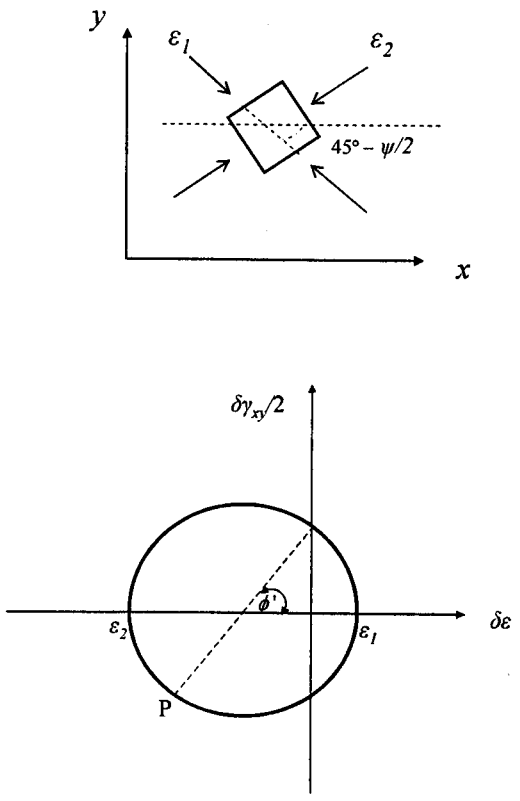

Figure 2.14: The incremental strain on a soil element in direct shear

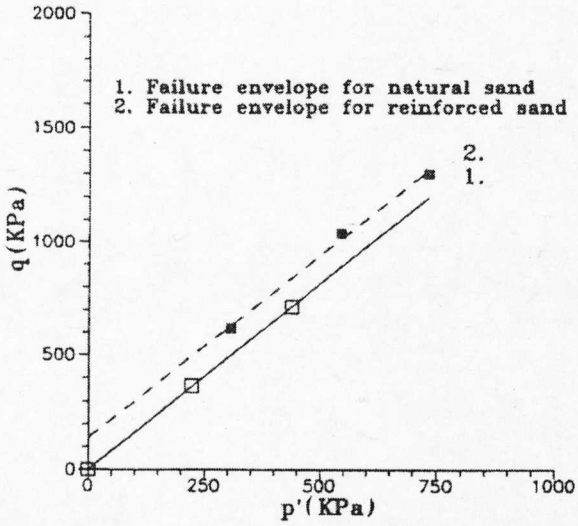

Figure 2.15: Failure envelope comparison (triaxial test)
(after Di Prisco and Nova, 1993)

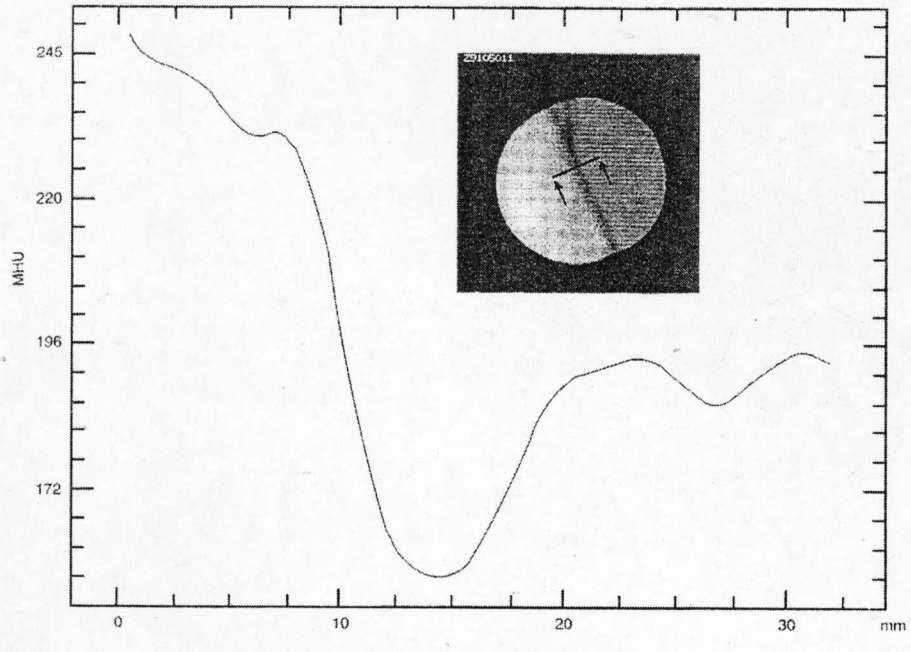

Figure 2.16: Shear band deformation

(after Desrues et al, 1996)

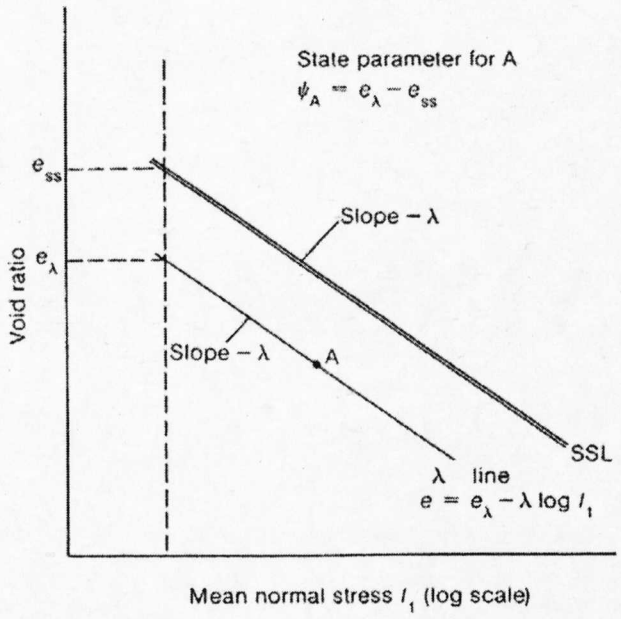

Figure 2.17: State parameter

(after Been and Jefferies, 1985)

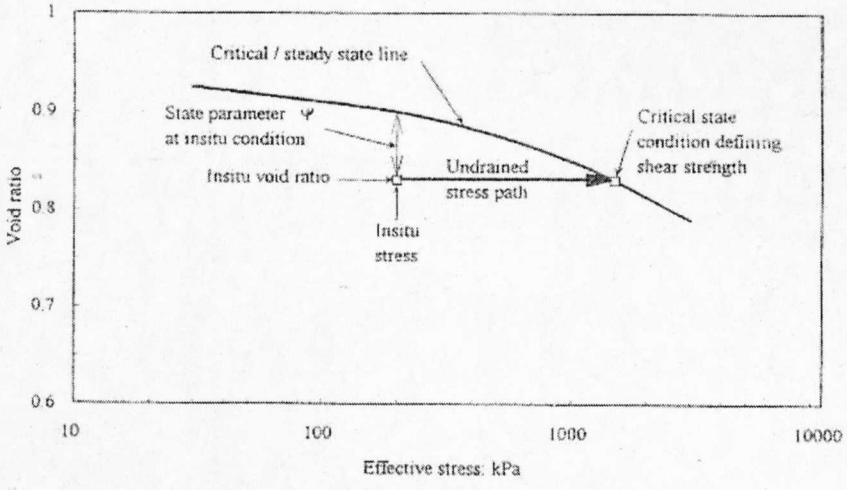

Figure 2.18: Void ratio - effective stress relationship with critical state

(after Been, 1999)

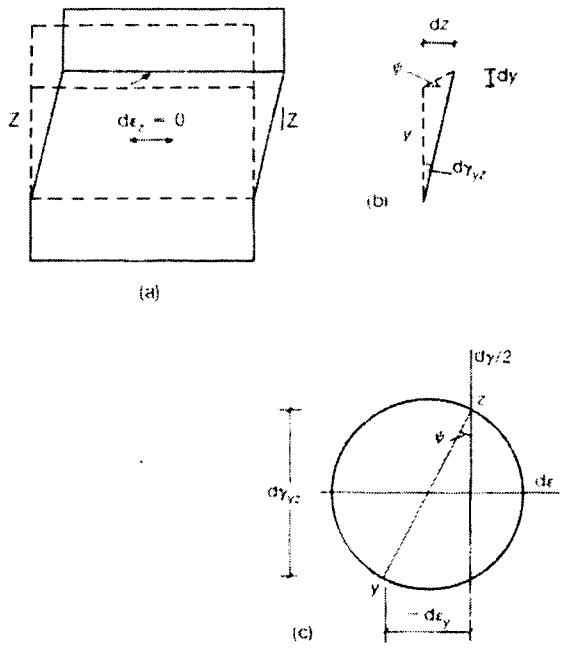

Figure 2.19: Angle of dilation for sand in plane strain deformation

(after Bolton, 1986)

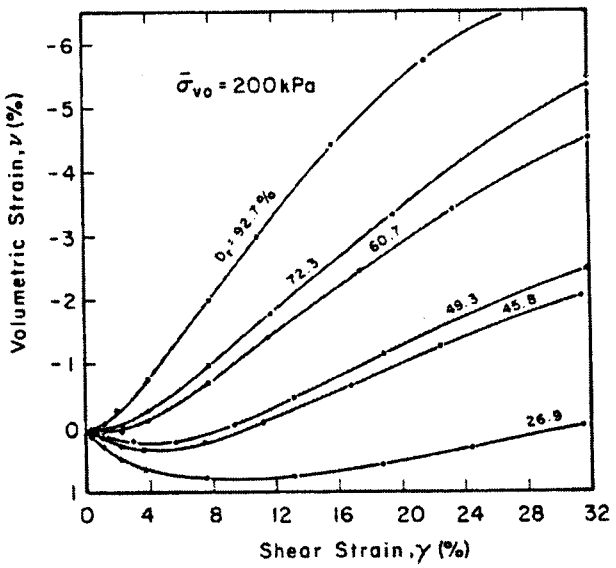

Figure 2.20: Volume cha nge behaviour of Ottawa sand in drained simple shear

(after Vaid et al, 1981)

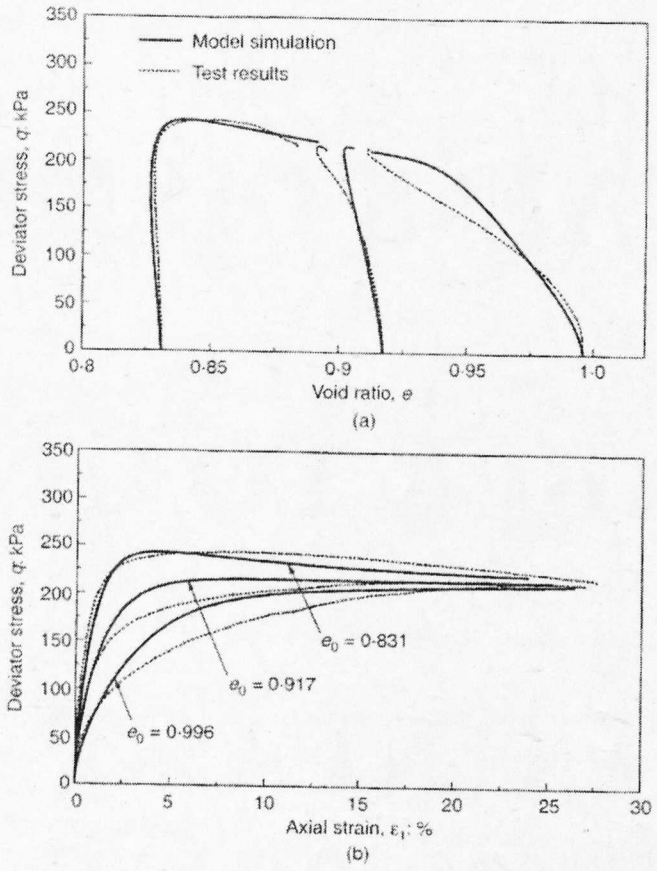

Figure 2.21: Triaxial compression test results for σ_1 = 100 kPa

(after Li and Dafalias, 2000)

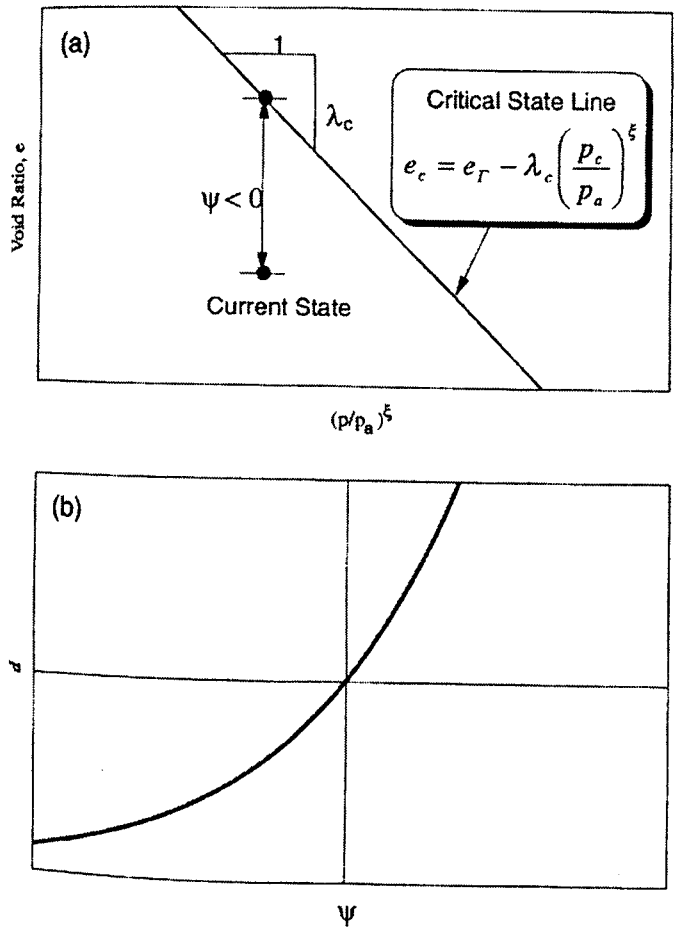

Figure 2.22: Dilatancy parameter *d* versus state parameter ψ

(after Li et al, 1999)

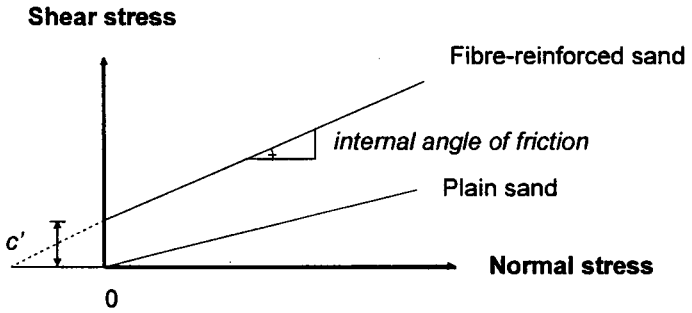

Figure 2.23: Mohr-Coulomb stress envelope with cohesion (*c'*)

Type of soil	ϕ, degrees	ϕ_{cv}, degrees
Sand: round grains		
Loose	28 to 30	
Medium	30 to 35	26 to 30
Dense	35 to 38	
Sand: angular grains		
Loose	30 to 35	
Medium	35 to 40	30 to 35
Dense	40 to 45	
Sandy gravel	34 to 48	33 to 36

Table 2.1 Typical values of ϕ and ϕ_{cv} for granular soils
(after Das, 1983)

	Description	Derived using formula:
ϕ'_{ds}	The angle of friction mobilised on the central plane	$\phi'_{ds} = \tan(\tau_{yx} / \sigma'_{yy})$
ϕ'_{ld}	The angle of friction mobilised on the central plane at large displacements	$\phi'_{ld} = \tan(\tau_{yx} / \sigma'_{yy})_{ld}$
ψ	The angle of volumetric shear strain (dilatancy)	$\tan\psi = -(dv_y / dv_x)$
ϕ'_{ps}	The maximum stress deviation in horizontal or vertical direction	$\phi'_{ps} = \sin[\tan\phi'_{ds} / (\cos\psi + \sin\psi \tan\phi'_{ds})]$
ϕ'_{crit}	The angle of friction at critical state	$\phi'_{crit} = \sin(\tau_{yx} / \sigma'_{yy})_{crit}$

Table 2.2: Derivations of the angles of friction and dilatancy

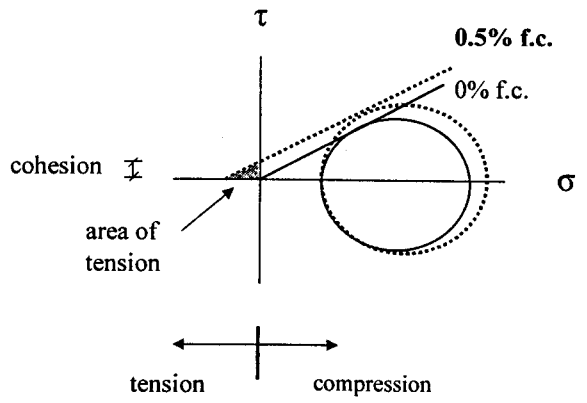

Figure 2.24: A model for the increased soil strength due to fibre reinforcement

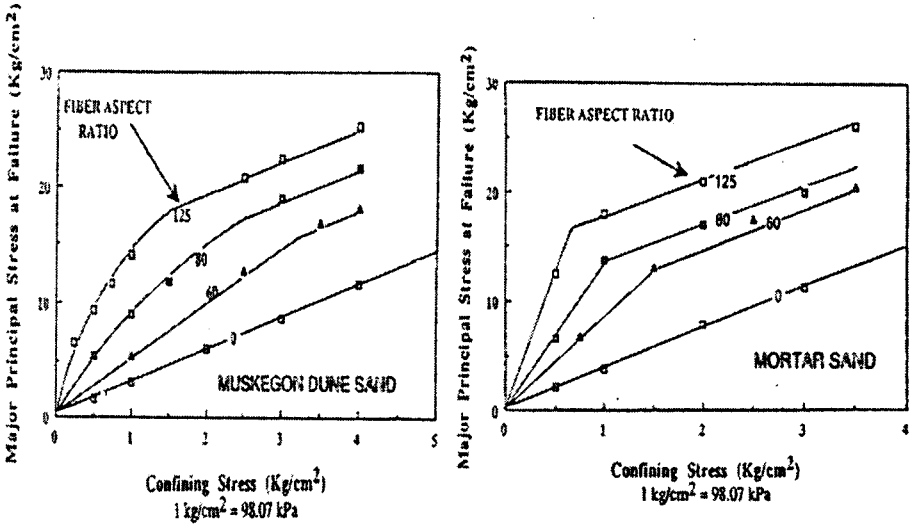

(a) depicts round sand

(b) depicts angular sand

Figure 2.25: Failure stresses for two different fibre-reinforced sands
(after Maher and Gray, 1990)

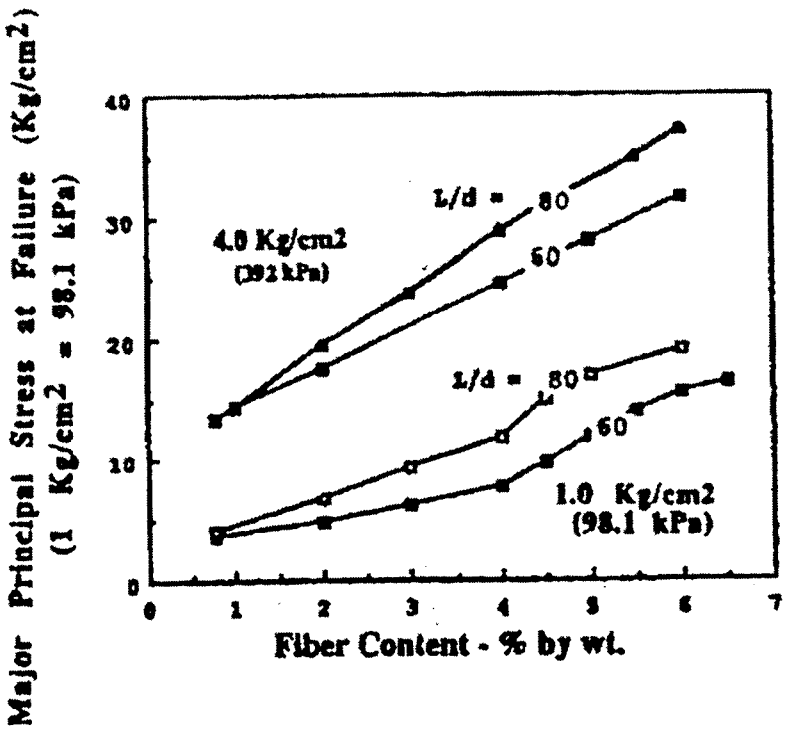

Figure 2.26: Failure stresses for different fibre contents (triaxial tests)
(after Maher and Gray, 1990)

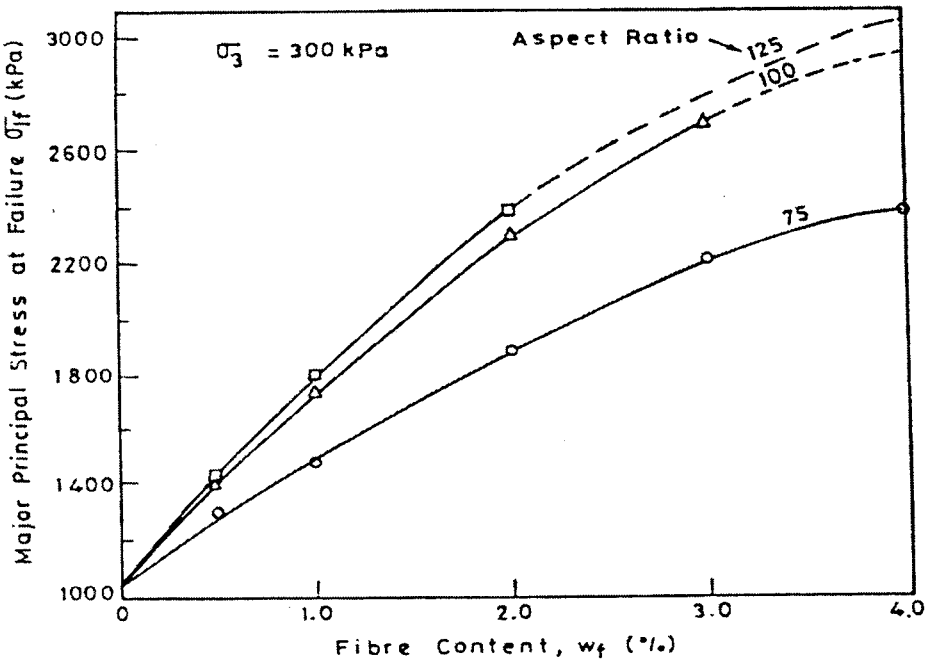

Figure 2.27: The effect of fibre content on the strength of plastic fibre-reinforced sand
(after Ranjan et al, 1996)

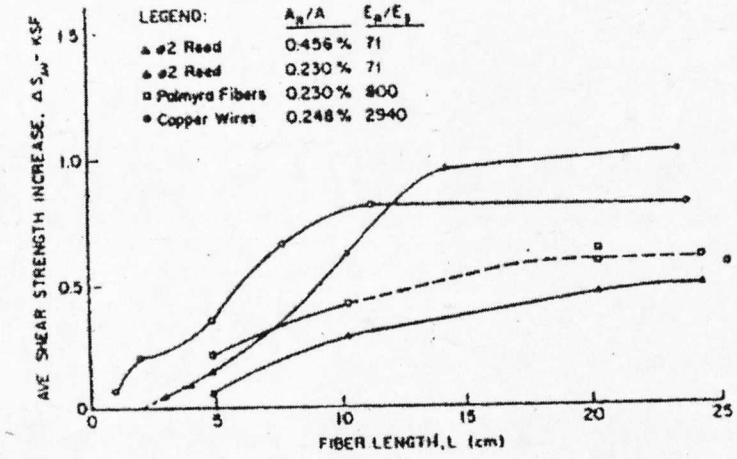

Figure 2.28: Fibre length (direct shear)
(after Gray and Ohashi, 1985)

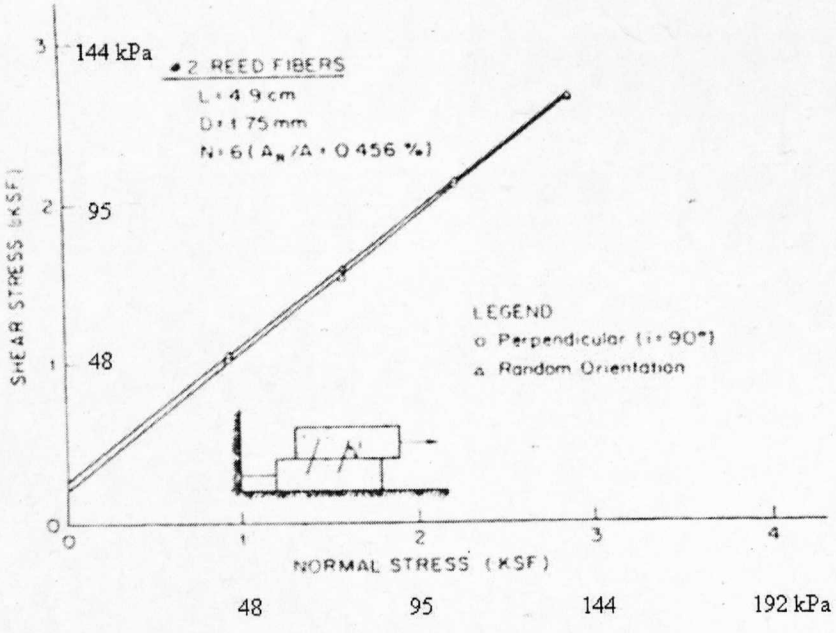

Figure 2.29: Fibre orientation (direct shear)
(after Gray and Ohashi, 1983)

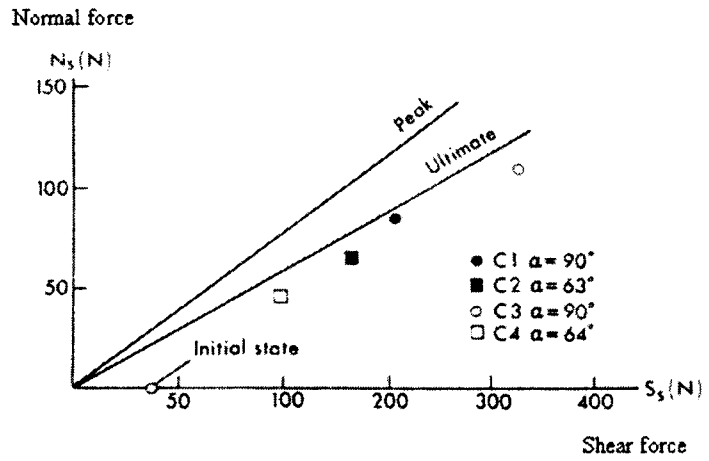

Figure 2.30: Fibre orientation comparisons (direct shear)

(after Wu et al, 1988_2)

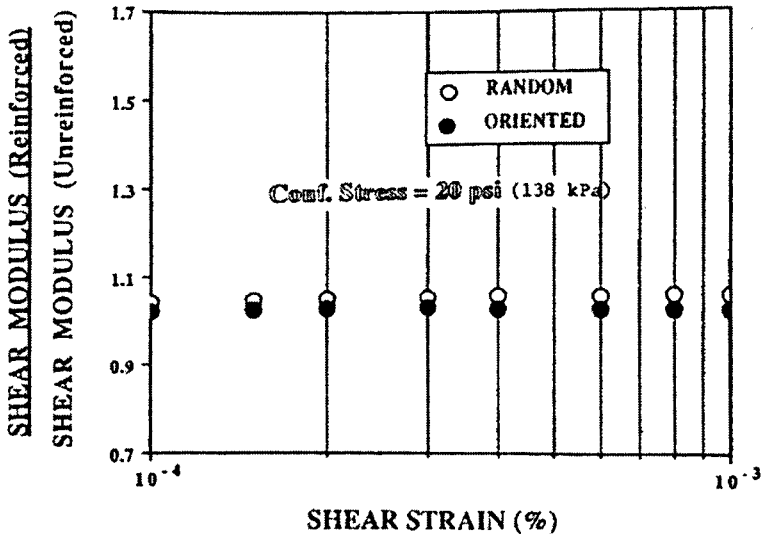

Figure 2.31: Fibre orientation (triaxial)
(after Maher and Woods, 1990)

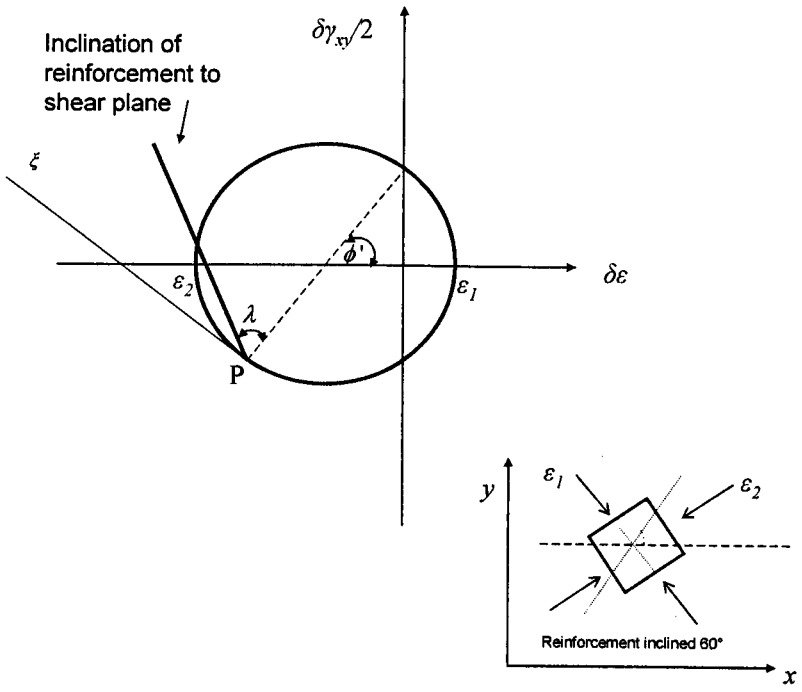

Figure 2.32: Strain diagram for reinforcements of 60° orientation

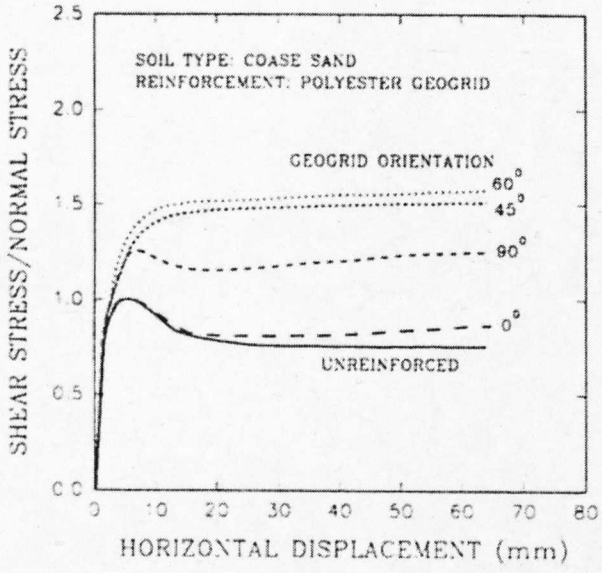

Figure 2.33: Stress-deformation curve for geogrid-reinforced coarse sand
(after Bauer and Zhao, 1993)

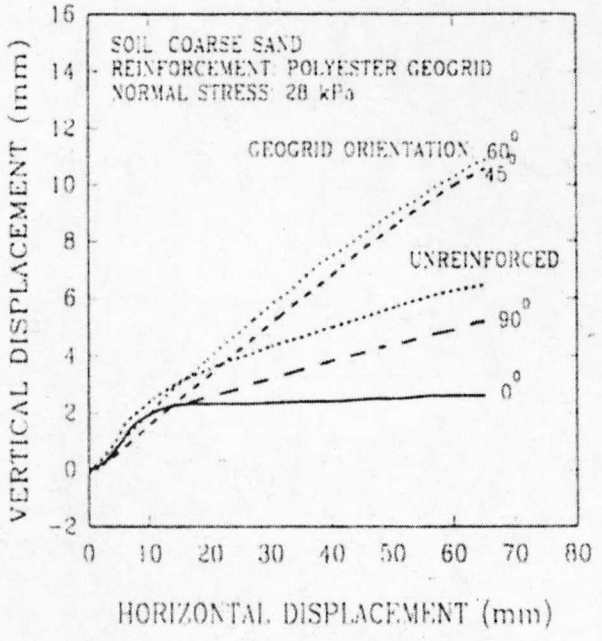

Figure 2.34: Dilatancy behaviour of geogrid-reinforced coarse sand
(after Bauer and Zhao, 1993)

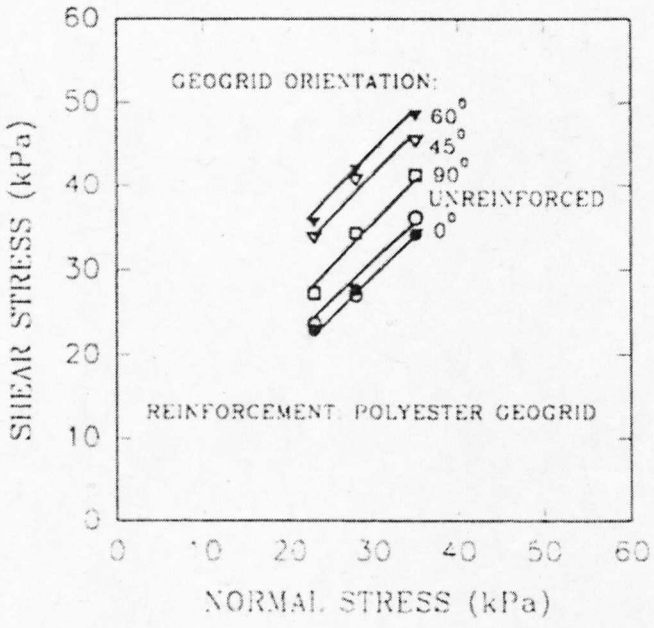

Figure 2.35: Shear stress increases for geogrid-reinforced soils
(after Bauer and Zhao, 1993)

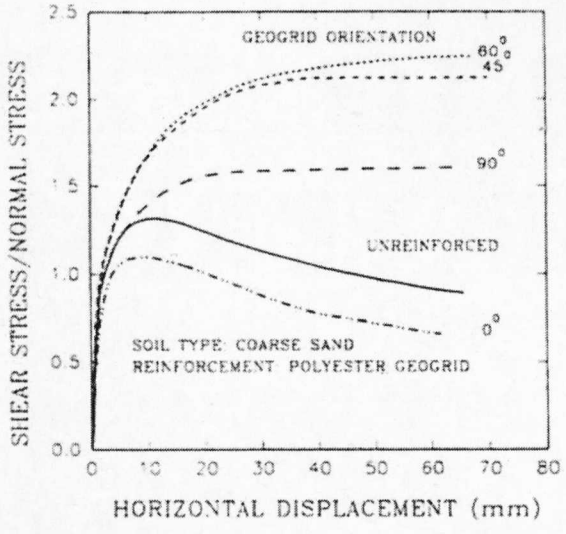

Figure 2.36: Stress-deformation curve for geogrid-reinforced crushed limestone aggregate
(after Bauer and Zhao, 1993)

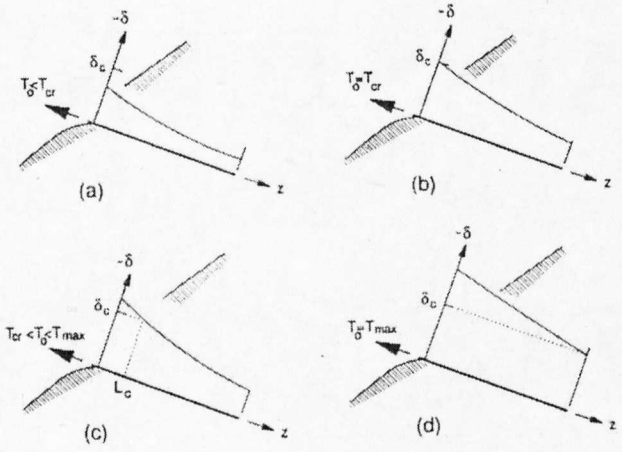

Figure 2.37: Fibre pullout resistance

(after Hryciw and Irsyam, 1993)

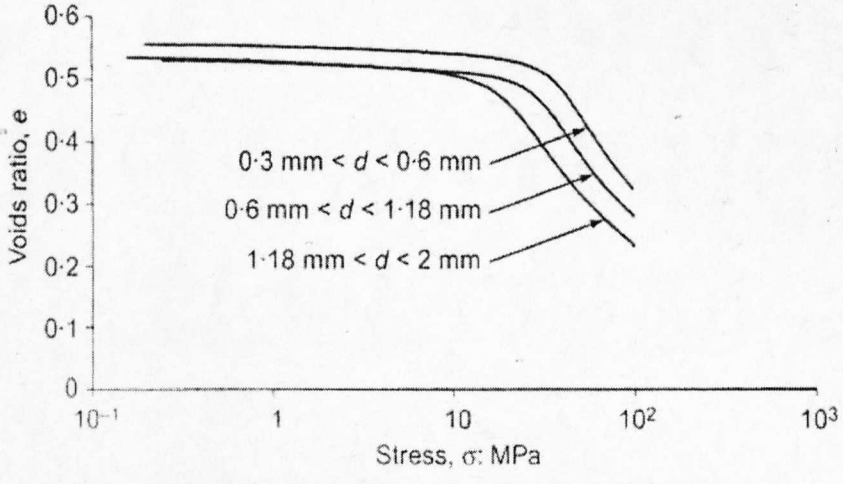

Figure 2.38: Compression plots for silica sands according to diameter *d*

(after McDowell, 2002)

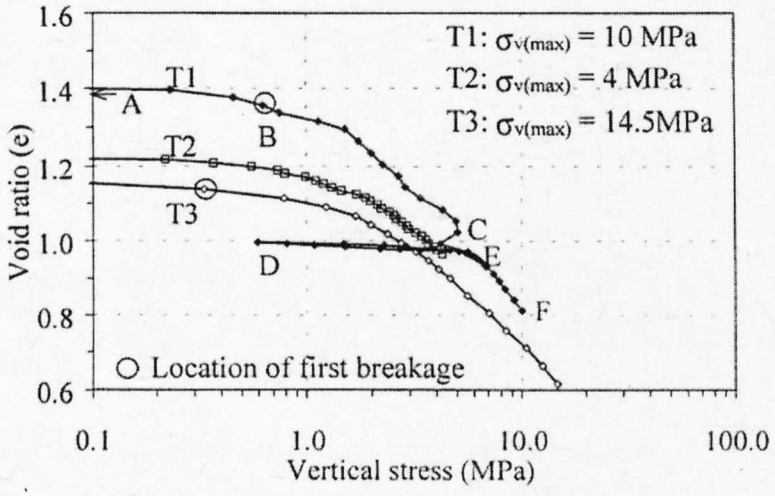

Figure 2.39: One-dimensional compression tests for three normal stresses

(after Cheng et al, 2001)

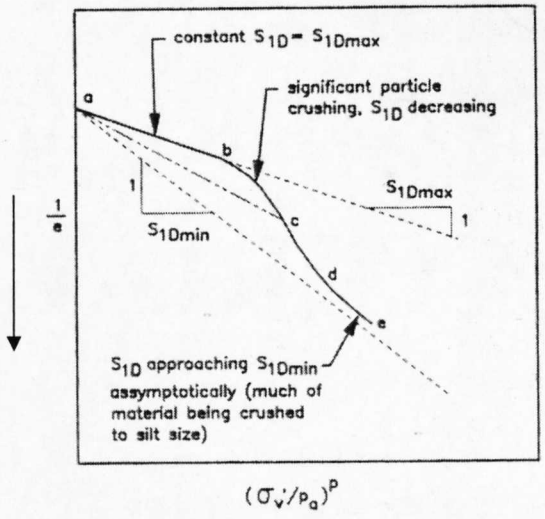

Figure 2.40: A compressive strain model

(after Hardin, 1987)

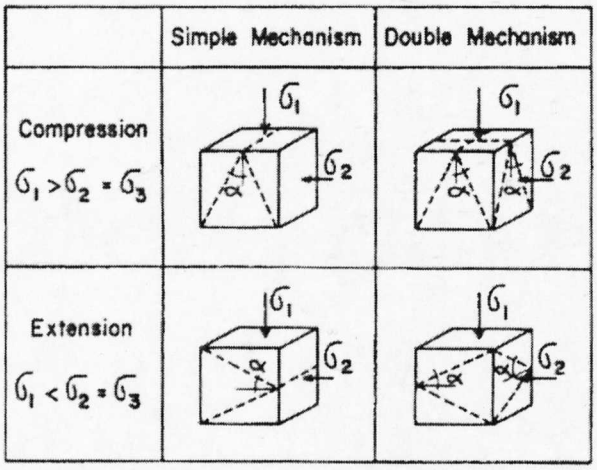

Figure 2.41: Localisation of deformation of sand samples in axisymmetric tests

(after Desrues et al, 1985)

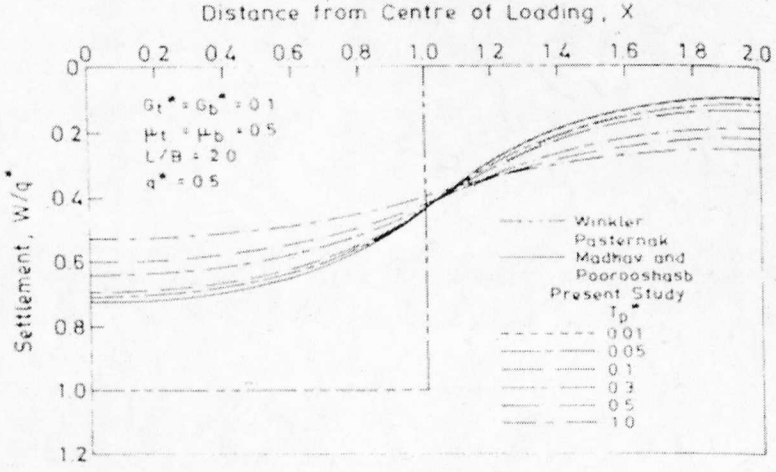

Figure 2.42: Settlement profiles

(after Shukla and Chandra, 1994)

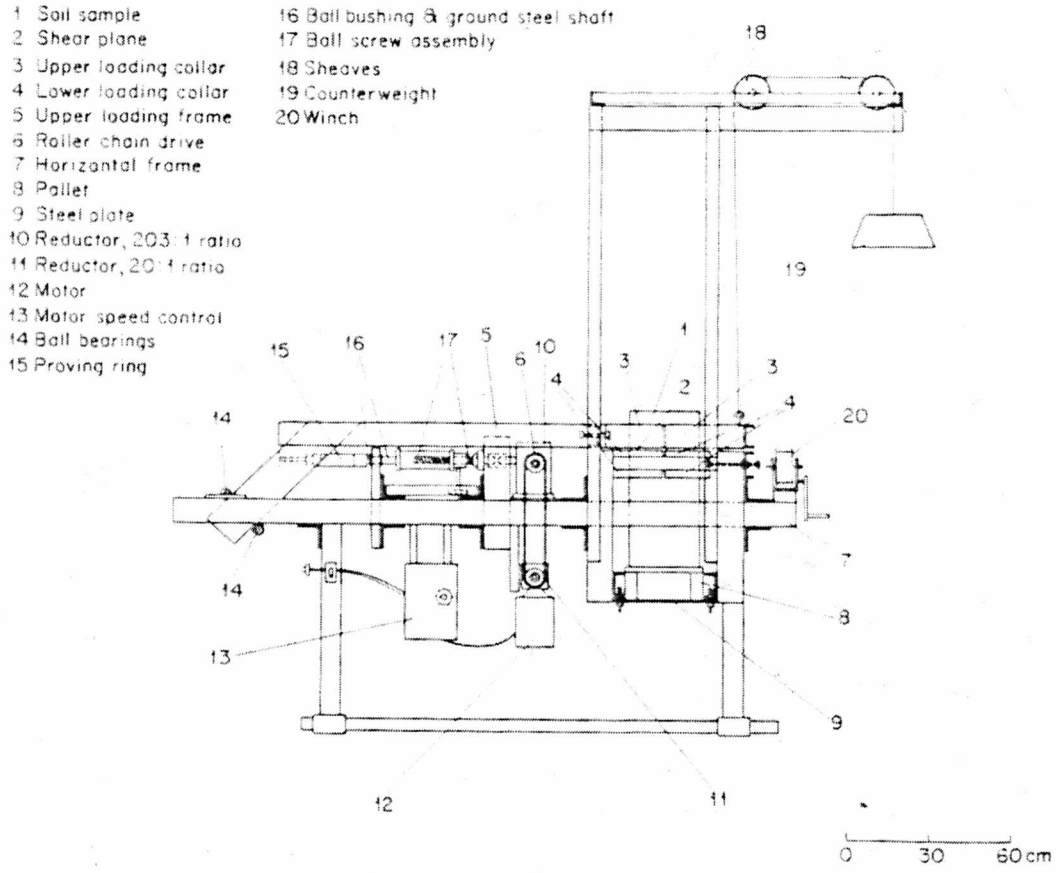

Figure 2.43: A direct shear box apparatus with soil sample positioned for shear plane at 15cm depth

(after Waldron, 1977)

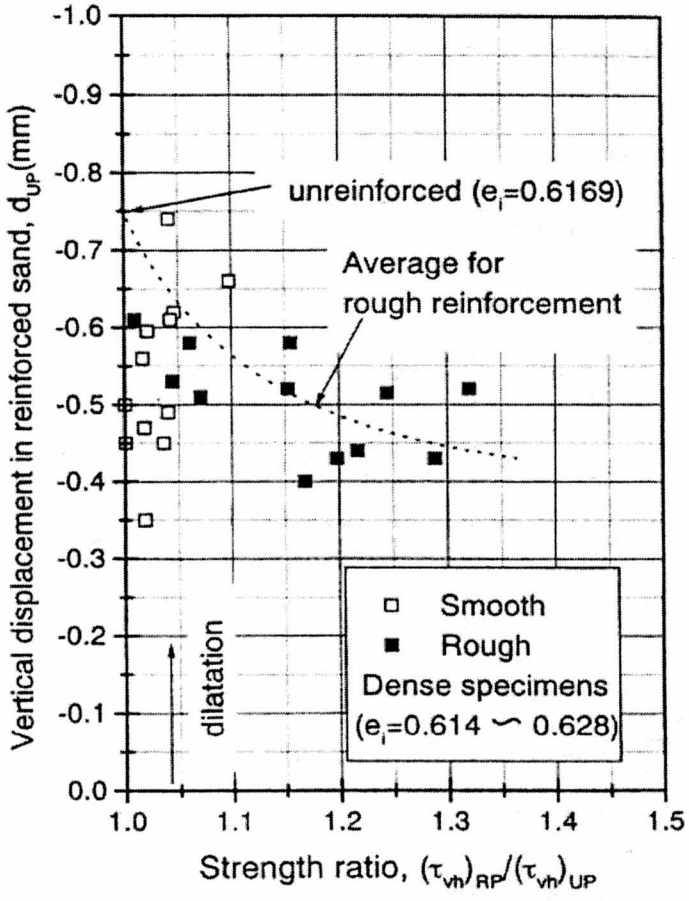

Figure 2.44: Relationship of strength ratio to vertical displacement

(after Qui et al, 2000)

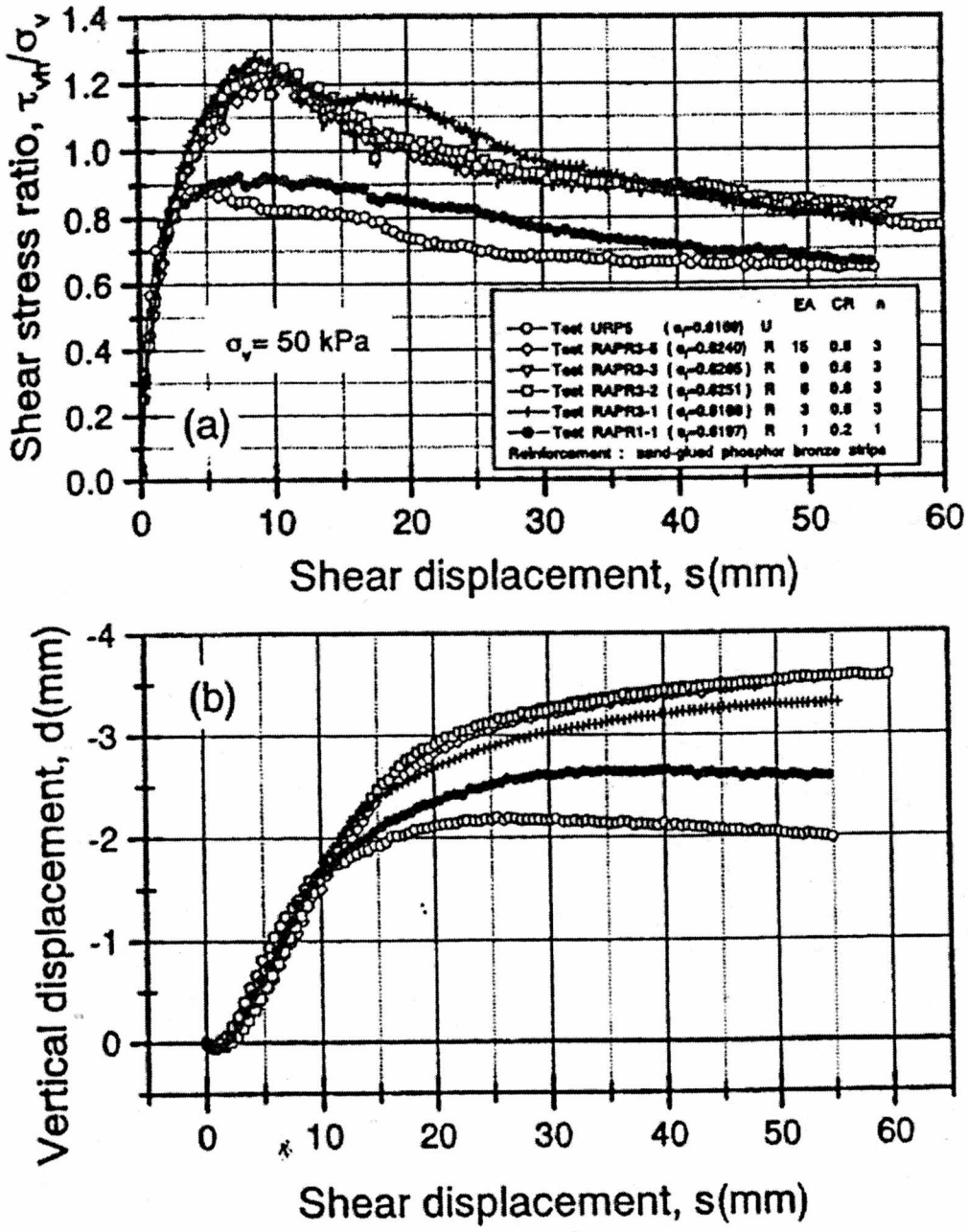

Figure 2.45: Results from constant pressure tests

(after Qui et al, 2000)

3.0 Sample preparation techniques for fibre-reinforced sand

3.1 Introduction

There is a dearth of experimental data that define the mechanisms that regulate the distribution of the fibres and the homogeneity of reinforced samples in the fabrication process. Tatsuoka et al (1986a) and Mulilis et al (1977) studied various sample preparation techniques for sand samples to observe the effects of fabrication methods on stress-strain behaviour and density. Similar studies into the various effects of the fabrication process of randomly-distributed fibre-reinforced sand samples complement existing research and will particularly contribute to future research projects of sand reinforced with randomly distributed fibres.

It was found from laboratory tests that the sample preparation method of fibre-reinforced sand samples is a highly sensitive experimental process that can dramatically affect test results. An investigation of the shear strength and stability of fibre-reinforced sand prepared by various techniques follows. A study of four different preparation techniques is included as well as the effects they have on the soil parameters. The expected outcomes of the preparation methods are shown in Figure 3.1.

During the testing of samples in one-dimensional compression and shear tests, the repeatability of the test results was monitored. Once the initial density values were established, the one-dimensional compression characteristics of samples were compared. Once the deformation behaviour under normal loads were understood, it was possible to investigate the initial density values of test samples as the basis of comparison for the peak and critical stress states in direct shear.

3.1.1 Basic considerations

The preparation method of compression and shear tests must ensure uniform density throughout the sample volume to produce the most accurate results. The ability of the volume of fibres to expand when they are separated causes problems in the preparation of both moist and dry samples. Stirring usually causes the fibres to cluster together rather than disperse, and the fibres do not physically adhere to the sand grains. The volume of air in a fibre-soil mix expands as the air voids between the fibres and the sand grains expand during mixing. In industry *LokSand* fibres are supplied pre-mixed with granular soil and experience densification by a number of passes of a steamroller in order to address compaction resistance issues. Sample placement in laboratory experimentation requires a methodical approach to static or dynamic compression in

order to fully confine the fibres by the soil particles. When placing the sample into the test apparatus, the mix must be compacted to force the trapped air to escape. This also increases the sample's density.

Previous research confirms the benefits of fibre reinforcement in granular soil, but it poses many questions regarding the volumetric changes that the fabrication process creates and the subsequent implications on the mechanical properties. Light compaction of some type is necessary to achieve an optimum density value for test samples, but Hoare (1979) found that for a given compactive energy, fibres resisted compaction causing less dense packing with increasing reinforcement. Consequently, higher compaction energies are required to achieve the same density in reinforced soils than in un-reinforced soils. Al-Refeai (1991) also noticed greater difficulty in achieving completely uniform fibre distributions as the fibre content and fibre length are increased.

An extensive study of various sample preparation methods follows for high quality small-scale tests. The initial density values of fibre-reinforced sand samples with a range of fibre contents and lengths are used to compare the repeatability of these fabrication processes in this section.

In order to present test results, a sample labelling system was created and used throughout the project. The labelling was used to uniquely identify a sample in the laboratory and to compare the test results based on the initial density and fibre content. The principal labelling system used for a test sample used the following format:

V670.3

where **V** indicates the sample preparation procedure of **V**ibration was used
67 indicates the initial void ratio was 0.**67** and
0.3 indicates the fibre content was **0.3**% by weight.

Other label prefixes included **100-50** or **200-50** (kPa) to indicate the amount of pre-load of test samples.

The mechanical effects of the sample variables are quantified in Chapters 5 and 6.

3.2 Test materials

3.2.1 Test sands

The type of soil used in this research project is sand. According to British Standard (BS 1377), sands are classified as soils whose dominant particles range in sizes between 0.06 and 2mm. Soils with a smaller or larger particle size are silts and gravel, respectively. Sands are then categorised as either fine (0.06-0.2mm), medium (0.2-0.6mm) or coarse (0.6-2mm).

The grading curves of the test sands are represented on Figure 3.2. The sands used are Grenoble sand, Medium Golden Sand (MGS) and Hostun sand. The MGS sand is termed "Medium Golden Sand" due to its colour. As is shown, the three materials used were all in a similar range. They are all classified as uniformly graded medium sand, although they differ in particle shape. The sands range in particle shape from sub-angular (Hostun sand) to sub-rounded (MGS and Grenoble sands). They share the same specific gravity (Dietz, 2000 and Benahmed, 2001), as seen in Table 3.1.

The grain angularity can create preferred orientations for particles within a soil mass. These orientations can in turn result in anisotropic mechanical properties. Muller (1967) classified the shapes of sand and silt-sized particles ranging from angular to well-rounded. The mechanical effect of the soil grain shape was shown in Figure 2.13 in the previous chapter. The peak internal angles of friction for Hostun sand were found to range from 34.4° for loose samples (e_i = 0.906) and 40-42° for dense samples (e_i = 0.655) in triaxial tests with 300 kPa cell pressure (Schanz and Vermeer, 1996). A unique angle of friction for Hostun sand at critical state was found to be 34.4° by Schanz and Vermeer (1996), which existed independently of the strain conditions. The range of internal angles of friction for Hostun sand direct shear samples can be estimated by adding up to 3° to the angles determined from triaxial tests (Rethatí, 1998).

Hostun sand was the preferred material for the laboratory tests. Figure 3.3 shows photographs of the Hostun sand particles as seen through a scanning electron microscope. In order to practise sample preparation techniques, Grenoble and MGS sands were used for both comparison and as substitute sands for Hostun sand. A supply of the MGS sand was found in the Soils Laboratory of the University of Bristol's Department of Civil Engineering.

3.2.2 *LokSand* fibres

LokSand is a crimped polypropylene fibre currently used in sports grounds for improved bearing capacity and drainage. In the past lack of uniformity in inclusion size, strength and fibre degradation behaviour has restricted the use of fibre reinforcement materials in industry and research. The polypropylene fibre test material used in this study is manufactured to have a constant length, cross-section and density, and the fibres are unique in that they are crimped to aid in soil stabilisation.

The fibres are approximately 35mm in un-crimped length and measure approximately 0.1mm in diameter as supplied by the manufacturer which gives the fibres an aspect ratio of 350. They are water-resistant and are resistant to corrosion. A photograph of the crimped fibres is shown in Figure 3.4.

The tensile strength and behaviour of the fibres are important factors when considering the stress-strain characteristics of fibre-reinforced soil. The fibres used in this study were tested by Bailey (2000) in a high tensile testing machine. The results of constant strain tests are shown in Figure 3.5 for straight (non-crimped) fibres of 35mm average length and 0.1mm diameter. The crimping or straightness of fibres may affect the tensile strain readings in this type of tensile test (due to the slight reduction of fibre length that crimping causes), but the intrinsic tensile strength of the *LokSand* fibres in the constant strain test shown in the figure would not be affected by their shape. Using the yield stress state shown in the test results, the fibres have a tensile strength of 3.2 N/mm with no fracture apparent. (No test results were recorded for fibres that failed by fracture.)

Some disadvantages of the test fibres should also be mentioned. Polypropylene has a tendency to creep under constant loading. Bell (1993) stated that the creep strain of an earth wall reinforced by a layer of polypropylene would theoretically amount to approximately 12% based on a 50-year life-span of use. These polypropylene fibres, therefore, may not be suitable for earth-reinforced walls. Strength could also be lost by UV degradation, so care should be taken for sun protection during field placement or laboratory preparation. In general, these fibres are used in ground improvement by means of improved bearing capacity beneath roads and other surface sub-grades.

3.2.3 Test equipment

Two test moulds are used in the analysis of fibre-reinforced soil behaviour: the oedometer cell and the shear box. The test moulds were of different shape and size. The

sample preparation methods had to reflect the differences of the moulds' geometries and volumes. The circular oedometer cell was used for the compression tests and a small shear box was used for direct shear tests. The oedometer cell has a 75mm interior diameter and 20mm total sample height. The load hanger is suspended from the end of a counter-balanced lever arm. A dial gauge is in contact with the top of a stabilising screw that rests on an indentation in the cell's top cap. Figure 3.6 is a photograph of the oedometer apparatus.

The shear box mould is 60mm square and the total internal height of the two halves of the shear box is 44mm. The separation of the two halves of the shear box is the shear plane at a height of 19mm from the base. When building samples in layers, it is imperative that the layer nearest this height provides thorough sample coverage as the boundary between layers is a major potential zone of weakness. The steel top cap has an indentation on its top surface where between the load hanger and the top cap, a steel ball sits. The dial gauge for the measurement of vertical movement is placed after the load hanger is balanced on the steel ball. The top half of the shear box is fixed to a proving ring and the lower half of the box is pulled by a motorised gearing system that provided movement at a rate of 1.27mm/minute. The carriage that contains the shear box mould rests on "frictionless" ball bearings that support the mould during shear. Figure 3.7 is a photograph of the shear box apparatus.

3.3 Sample variables

3.3.1 Soil type

Other researchers have studied clay and low-grade soils reinforced with fibres; however, test soils other than sand are outside the context of this research. The type of soil that is normally reinforced by fibres tends to be granular. The granular layer in a soil mass provides a compressive layer that provides drainage for the surface vegetation layer. The fibres pervade the voids within the granular layer. The ability of the sand grains to adhere to the fibres and form an interlock is affected by the shape of the soil particles in the same way that the shape and size of grains can determine the packing order of the soil particles.

Figure 2.2 showed the increased compression of the fibre and sub-angular soil grains from the (a) "as placed" soil-fibre composition to the (b) compressed soil-fibre composition. The normal forces and the resultant forces acting on the soil particles cause a compression of the soil grains as the air voids decrease. The confinement of the

fibre within the soil sample increases as the soil grains lock the fibre into a confined position. In general, the "as placed" sample section represents a specimen that has been compressed by nothing other than the self-weight of the sample. The normal force depicted in position (b) represents the mass of a top cap, a steam roller, a plate or any compaction device while the resultant forces are the forces generated by the underlying sample mass and/or the bottom of a test mould.

When sands have uniform particle size distributions, the contact efficiency is better if the angularity is greater. A rounded shape of the sand grains would allow greater movement during shear compared to sub-angular sand. Shear tests results from identical sample preparation methods were compared for sub-rounded (Grenoble) and sub-angular (Hostun) sands under 100kPa normal stress. The initial void ratio of the Grenoble and the Hostun sands was 0.65 (relative densities of 0.78 and 0.92, respectively) as set by the preparation technique. Figure 3.8 shows the stress ratio and vertical displacement versus horizontal displacement relationship, whereby the Hostun sand exhibits dense behaviour with elastic deformation until a peak value. The Grenoble was in a loose state as it did not exhibit a critical value separate from the peak stress. It must be mentioned that the full background of the Grenoble test sand is unknown as it may have been reconstituted after some other types of soil tests in the laboratory. Grenoble sand was not used in any subsequent experimentation; nonetheless, these test sands exhibit the dependency that strain-deformation behaviour has on the soil grain shape as highlighted by Maher and Gray (1990).

3.3.2 Initial density

Non-uniformities of strain can develop within samples from the beginning of a test. Loose samples are sensitive to vibrations, so it is logical to expect that for loose samples there are always large initial contractions as the particle structure collapses and reorganises itself to withstand the shear stress. In dense sands the initial contraction is eventually followed by the usual expansion of sands. Zones of preferential dilation are formed during the course of tests, thus samples with uniform density gave more accurate experimental results.

The density packing of a soil mass is usually quoted as the void ratio, a ratio of the volume of voids over the volume of soil grains. The initial density of a laboratory sample is considered to be a physical characteristic from which a stress-strain relationship evolves. In order to achieve the same initial density values for un-reinforced and reinforced sands, some sort of compaction is necessary to compress the

reinforcements within a sample volume. The higher strains achieved by fibre-reinforced sand compared with un-reinforced sand indicate that reinforced samples are not as heavily compacted by the same sample preparation methods as the un-reinforced sand (Hoare, 1979; Al-Refeai, 1991; Santoni et al, 2001; Lawton et al, 1993). The inference is that the presence and/or action of the fibres can affect the density of a sample, perhaps through v_o, the reduced initial specific volume of the sand. Atkinson and Bransby (1978) indicated that v_o strongly influences the behaviour of sands and the same sand can demonstrate different types of compression depending on v_o, and the applied stress levels.

The elements of sample preparation procedures that affect the initial density values have been considered and are summarised below.

- Settlements due to self-weight occur almost as rapidly as a sample is placed.

- The magnitude of the initial vertical strain experienced by laboratory samples during testing is highly dependent upon the values of pre-load established by the fabrication process of the sample and by any weight-bearing components of the test apparatus that are placed upon the sample during assembly.

- The creation of an opening between the two halves of the shear box generally generates friction and strains within a sand sample, depending on the type of machinery used.

- Bedding of the tops caps can result from the application of the load hangers before dial gauges are positioned. The surface area of the top cap and configuration of the shear test equipment were constraints in the positioning of additional dial gauges for samples before the load hanger was applied (see Figure 3.9). There was not enough clear space on the top surface for a single LVDT (linear variable differential transformer). Consequently, an unknown amount of vertical strain can be imposed upon a sample of a known initial density and all subsequent measurements of the sample's densities are recorded relative to a false initial density value. This opportunity for inaccurate measurement of initial densities has been resolved in the experimentation results as will be highlighted later in this chapter.

- The deposition process of a sample creates an inherent non-uniformity that can be attributed to the grain characteristics of a soil mass. Casagrande and Carillo (1944) defined this as "a physical characteristic inherent in the material and entirely independent of the applied stresses and strains". As a result, the placement method of the laboratory samples within tests moulds was executed with the utmost care in order to cause the least disturbances to the soil particles during all sample preparations.

The initial densities chosen for experimentation have been selected to represent "dense", "medium" and "loose" states for the test sands. The initial densities will be achieved by the different sample preparation techniques and they will also form a major aspect for the basis of comparison in laboratory tests.

3.3.3 Moisture content

The moisture content increases the volume of the voids of a sample, thus decreasing the initial density value. Preliminary tests were prepared with MGS sand and moisture content of 2% by weight as this was a nominal value chosen to represent the moist condition in compression and shear tests. Bailey and Knox (1997) and Jones et al (2001) both added 6% moisture content to soil samples reinforced with fibres, but even the moisture content value of 2% proved to create unsuitable Hostun test samples for this small-scale experimentation. The Medium Golden Sand was chosen as a test material due to its similarity to Hostun sand in specific gravity and particle size distribution. Figure 3.10 shows the one-dimensional compression characteristics for the MGS sand samples. The samples were compacted according to the under-compaction method (see section 3.4.3) for three initial densities (e_0=0.67, 0.72 and 0.76) set by initial dry soil weights of 104, 110 and 120g respectively (as seen in the figure). The initial void ratio values were above the limits for this sand type and as a result, the compression characteristics were unreliable. The addition of 2% moisture content for MGS sand gave an initial void ratio above the upper limit for this sand type, so the individual grains did not initially have enough contact with their neighbours to sustain equilibrium throughout the sample volume.

What is apparent from the compression curves in Figure 3.10 is that the void ratios began to converge once the values were within the void ratio limits for MGS sand. The comparison curves for samples 110 and 120g intercepted the e_{max} value of 0.78 (relative density 0%) at approximately 400 kPa vertical stress. Samples of 120g dry weight with 0.0 and 0.5% fibre content were the densest with the lowest void ratio values at the end

of the test. These sets of compression tests prove that the moisture content can dramatically increase the volume of voids in a fibre-reinforced sand sample.

In sample preparation moisture content facilitates the cohesion of fibres and granular particles during mixing, but in fact the bond between the two materials appeared to weaken with the addition of water. Figure 3.11 shows the stress-strain relationship for moistened and dry Grenoble samples in direct shear (the same dry Grenoble sample was compared with Hostun sand in Figure 3.8). The dry sample (e=0.65) shows the expected stress-dilatancy relationship for medium density sand compared to the moist sample (e=0.68). The one-dimensional compression and direct shear investigations will be concentrating on the mechanical features of dry samples only in order to eliminate any discrepancies due to moisture effects for fibre-reinforced test sands, with the Proctor compaction tests as the only obvious exceptions.

3.3.4 Fibre content

Greater difficulty in achieving both completely uniform fibre distributions and uniform initial densities is experienced as the fibre content and length are increased. The amount of *LokSand* fibre that is generally used in practice is approximately 0.45 - 0.60% by dry weight. Fibre reinforcements of more than 1 or 2% are not generally used with soil mixes in practice.

Preliminary one-dimensional and shear tests were conducted with fibre contents ranging from 0.0 to 1.0% by weight. The majority of the tests were conducted on samples of 0.0, 0.3 and 0.5% fibres by weight to compare the effects of varying fibre contents as a major factor for strength and dilatancy comparisons when subjected to a range of normal loads. Figure 3.12 shows the fibre content limits for Grenoble sand under-compacted (see section 3.4.3) in its most dense state from initial void ratio (e_i= 0.52) to its maximum void ratio value. The error bars show the range of void ratio value variance for samples prepared with five different fibre contents by weight.

Figure 3.13 shows a two-dimensional drawing of Hostun sand particles reinforced with 17.5mm long *LokSand* fibres with 0.3% fibre content in order to show the scale of the sand particles to the crimped fibres. A fibre content of 0.3% by weight (weight fraction of the total sample weight) equates to 0.5% fibre in the total volume by the following formula for the volume of fibres:

$$\text{Volume fraction} = V_f = \frac{M_f \times V_{total}}{0.001 \times G_f}$$

where V_f is the volume of the fibres, V_{total} is the total sample volume, M_f is the weight of the fibres, G_f is the specific gravity of the fibres (G_f = 0.91) and 0.001 is a conversion factor. Samples with 0.3% and 0.5% fibre contents by weight had 0.5% and 0.8% volume fraction for initial void ratio in the range of 0.67-0.76 according to calculations, as this formula does not account for air voids. The volume fractions for the fibre contents and initial densities for the shear box are shown below.

$e_{initial}$	**Weight fraction (%)**	**Volume of fibre (mm^3)**	**Volume fraction (%)**
0.67	0.3	828	0.5
0.67	0.5	1379	0.8
0.72	0.3	801	0.5
0.72	0.5	1335	0.8
0.76	0.3	784	0.5
0.76	0.5	1307	0.8

The volume fraction is a useful soil parameter to describe the amount of the total sample volume that the fibres occupy. In Chapter 6 the volume fraction will be used to describe the amount of fibre content in the shear zone.

3.3.5 Fibre length

Initial tests were run with the fibres as provided by the manufacturer, of length 35mm, but the tensile force of the fibres was not fully mobilised in the 60mm square shear box with 44mm sample height. Bailey (2000) tested 35mm long *Loksand* fibres in a shear box measuring 305mm square, with a sample height of 150mm. The test fibres described here were cut to an average length of 17.5mm in order to achieve an optimum fibre length that exploits the pull-out strength for the experimental stress range. Comparisons between samples reinforced with fibres of the original 35mm length and 17.5mm are given in Chapter 5.

3.3.6 Fibre Orientation

The orientation of the fibres was a random placement with an overall even distribution, as judged by eye during the sample preparation. *LokSand* fibres, being extremely

flexible and fine, are placed in a random distribution in the field after mechanical mixing with granular material. In order to achieve the most valuable test results, random distribution is the chosen fibre orientation for this thesis. The uniformity of the fibre distribution was judged by eye during the sample preparation and placement.

3.3.7 Skin Friction

The fibres' ability to bond with soil is the skin friction between the two materials. Skin friction is a resultant of the individual properties of the test materials when combined to provide a structure that possesses unique attributes that the individual materials would not possess on their own. The *LokSand* fibres used in the experimentation are crimped for the purpose of better interlock within the surrounding soil mass. The crimped fibres produce a rough surface for the soil grains to bond with in the same fashion that fibrous plant roots bond with soil. The crimped shape may also offer a greater amount of pull-out strength than straight *LokSand* fibres, but due to the manufacturing process being identical for straight and crimped fibres, the tensile strength shown in Figure 3.5 will be assumed for the crimped fibres henceforth. The pull-out ultimate strength is not expected to be reached in this set of experiments; therefore it is assumed to be negligible in this set of tests.

3.3.8 Normal stress

Normal stresses are sometimes used during sample preparation in order to pre-load or apply an initial confining stress upon a sample. The normal stress also increases the density of the sample volume after fabrication. It is important to account for any pre-loading in the sample preparation in order to effectively assess the fibres' contribution to a sample's strength.

Normal stress was used in fabrication to pre-compress the samples' volume so that identical initial densities are achieved. All additional weights that are built into the test apparatus have been incorporated into the calculation of the total normal stress values. The initial density, fibre content and normal stress values will be core variables for comparing the sample preparation techniques for this study.

3.4 Traditional preparation techniques

3.4.1 General sample preparation considerations

The technique of preparing fibre-reinforced samples requires careful consideration as fibre-reinforced soil is a mix of two very different materials. The variables of the soil

include the classification and shape of the soil grains and the water content while the fibre variables consist of the fibre content, the fibre length and the fibre orientation. The interaction between the sand grains and fibres is of paramount importance for the strength of the materials in both compression and shear and this interaction is created during the fabrication process. Traditional sample preparation methods for granular soils include pluviation, tamping and vibration. Pluviated sand samples can produce a range of different initial densities for laboratory tests. Tamped samples were prepared according to the under-compaction method introduced by Ladd (1978) in order to fabricate samples having the same initial density values both with and without fibre reinforcement. Vibration was used to densify reinforced and un-reinforced samples in layers. A description of these sample preparation methods follows.

3.4.2 Pluviation

Pluviation is a standardised sample preparation technique for un-reinforced sands. Pluviation was chosen as a sample preparation for a control set of un-reinforced, dry sand samples to test in compression and shear. The pluviation process allows sand grains to fall through the air like rain (as the Latin word *pluvia* translates to English to mean "rain"). The result is a sample undisturbed by external forces other than the self-weight of the grains. An advantage of this process is that a range of initial density values can be obtained for samples.

Most pluviators used in laboratories are modelled on Miura and Toki's (1982) Multiple Sieve Pluviator (MSP) shown in Figure 3.14. They consist of a cylindrical receptacle and funnel that discharge sand by gravity through a number of sieves positioned at a known height of drop above a test mould. The uppermost sieves used by Miura and Toki were square opening sieves of aperture 1.41mm for the uppermost sieves and 3.66mm for the lower six sieves. The funnel had a nozzle of an aperture that regulates the rate of discharge into the sieves and it is the diameter of the nozzle aperture that has been found to influence sample density. The vertical distance between the final sieve and the sample mould is termed the height of drop, which has also been documented in literature as a factor that affects sample density significantly (Tatsuoka et al, 1982), to a lesser extent (Mulilis et al, 1975) and insignificantly (Miura and Toki, 1982). Vaid and Negussey (1984) studied different heights of drops and found that samples with a drop less than 300mm were less dense, while samples with a height of drop between 300 and 700mm showed little difference in density. The energy of sand particles at impact during deposition has also been considered to control the relative density value (Vaid and Negussey, 1984). Beneath the final sieve, a second cylinder connects the bottom of

the lowest sieve to the test mould. It is in this final cylinder that the deposition energy can cause rebound effects depending on the height of drop.

Figure 3.15 shows the configuration of the multiple sieve pluviator used in the laboratory. This pluviator allows for the adjustment of the height of fall, the nozzle aperture size or the sieve size if required. The nozzle apertures for these tests ranged from 8 to 32mm for dense to medium dense samples respectively. Lo Presti et al (1993) found an increased mesh size produced less dense samples, so different sieve sizes were tested in the MSP apparatus and a singular sieve (SS) apparatus (2.0mm diameter). The sample densities were compared based on the test equipment parameters of height of fall, nozzle aperture and sieve size.

The nozzle diameters used in sample preparation tests were 8, 24 and 32mm. The test results determined the 8mm as the nozzle diameter that creates the most repeatable density values, so it was the preferred size in subsequent tests. An MSP apparatus was used in this study with six sieves of 3.35mm aperture. Figure 3.16 shows the densities for different heights of drop and nozzle diameters in Hostun sand pluviation tests (denoted by their nozzle diameter in the legend) and Miura and Toki's pluviation test results for Toyoura sand from their 1982 paper. The Toyoura sand results are included for comparison with the heading "M&T" next to the nozzle diameter size in Figure 3.17. The Toyoura test sand used by Miura and Toki has the same specific gravity as Hostun sand, with a mean particle size of 0.18mm.

The M&T 23 and M&T 25mm nozzle data are in the same density range as the Hostun sand tests with nozzle diameter 24mm. The smaller diameter nozzles produced the more dense samples. The relative density achieved by M&T 10mm was approximately 0.1% lower than the densities achieved with the 8mm nozzle. The 32mm diameter nozzles produced samples with initial densities more loose than desired for the experimental design.

The sample weight is usually determined by starting with a known mass, pluviating the sample, levelling the top surface and weighing the remaining sand deposited outside the mould. This method can provide the most accurate weight measurement with the least disturbance to the test sample.

The uniformity of the pluviated sands' relative density was investigated with respect to natural placement in test moulds. A single 2.0mm sieve was used in this set of tests to

give an improved uniformity distribution over the six 3.35mm sieves, due to a smaller relative diffuser ratio (RDR) as discovered by Lo Presti et al (1992). The RDR is the sieve opening size of the uppermost sieve divided by the mean grain size (D_{50}). A comparison of the sieve sizes' relative diffuser ratios follows:

$$RDR_{3.35mm\ sieve} = 3.35mm \div D_{50} = 3.35mm \div 0.4mm = \mathbf{8.35}$$

$$RDR_{2.0mm\ sieve} = 2.0mm \div D_{50} = 2.0mm \div 0.4mm = \mathbf{5}$$

The relative diffuser ratios affect the relative density of a sample in that they affect the amount of inter-particle interference which occurs following the exit of particles from the diffuser (in this case the sieve). The inter-particle interference increases as the RDR decreases and, consequently, the relative density of samples increases.

Inter-particle interference was observed in all tests that had the height of drop enclosed between the lowest sieve and the test mould. These 'rebound' effects from the sides of the shield were verified by placing six steel (non-porous) cups in the same configuration for a number of tests. The 35mm diameter cups were arranged in the formation shown in plan in Figure 3.17. The differing densities due to the cups' position under the sieve (see Figure 3.18), suggest that there were either rebound effects between the height of drop of the 40mm tall container and the deposited sand particles, or the diffuser failed to sufficiently diffuse the sand. Tests were also run without the outer cylinder for the height of fall. The maximum density was found to be in the central cup. The two main results of those tests were that less sand fell into the outer cups than before and the maximum density was again found in the central cup. These test results are labelled SS in the legend.

Tests that incorporated a single 2.0mm aperture sieve with the 8mm diameter nozzle were labelled SS. These were used for comparison with multiple sieve test results with the same small diameter nozzle. The overall height of fall from the hopper was reduced accordingly for "SS" tests. The height of drop was positioned at 350mm for all tests and compared with results from a third pluviation test apparatus, the perspex column.

The Perspex pluviator, shown in Figure 3.19, has a fixed 2.0mm mesh positioned at a 350mm height of drop to the cup. It consists of a container area of 120 x 120mm with a container wall 120mm high that holds the sand. The sand is released by opening a square 110 x 110mm grid of circular holes. The grid consists of two plates of Perspex

(one fixed and one free) with holes evenly spaced at an aperture of 10mm diameter. The holes are shielded by the plate parts in between the holes before the two plates slide from the blocked position. The sand pluviation begins when the free-sliding plate is moved to the 'open' position and the holes are aligned to open the full 10mm diameter.

If loose samples are required, a relatively small pouring height (height of drop) is needed. In such cases the position of the pouring tip must be continuously raised as the thickness of the deposit builds up in order to maintain a constant height drop at all times. This brings an additional complexity to the sample deposition process.

3.4.3 Moist under-compaction

In order to establish a consistent density range for moist samples both with and without fibre reinforcement, wet-tamped samples were tested in compression. In preliminary investigations, a range of moist samples were compared with dry samples with the aim of comparing the workability of the fibre-reinforced sands as well as testing the soil strength properties. According to Tatsuoka et al (1986) wet-tamped sand samples have the greatest strength compared to other preparation techniques including air-pluviation, wet-vibration and water-vibration methods. One improvement on the traditional wet-tamping technique is the under-compaction method.

The under-compaction method was developed by Ladd (1978): the sample is prepared by tamping in layers. Each layer is lightly compacted to a predetermined height value, which denotes a selected percentage of the total density. The additional compaction due to subsequent layers is taken into account so that the first layers are not over-compacted. The ratio of the density of the layers to the sample's final desired density value indicates the percentage of under-compaction.
The required height of the specimen at any given top layer surface is calculated from the following formula:

$$h_n = \frac{h_f}{n_f}\left[(n-1)+\left(1+\frac{U_n}{100}\right)\right]$$

where h_n = height of compacted material at the top of the layer being considered,
h_f = final (total) height of the specimen,
n_f = total number of sample layers,
n = number of the layer being considered and
U_n = percentage under-compaction for the layer being considered.

The benefits of the procedure of under-compaction were outlined by Ladd as follows:

- specimens are produced that have a relatively uniform stress-strain response and
- most types of coarse-grained soils can be used with a relative density ranging between very loose and very dense.

The aim of this procedure for Ladd (1978) was to improve the consistency and repeatability of cyclic strength testing results, compared to conventional wet-pouring preparation methods. Under-compaction is a widely used sample preparation technique for moistened laboratory samples in shear; therefore it was employed in this study. The preliminary samples were compacted in layers with a steel bar 15 x 2.5 x 2.5mm weighing 785.5g found in the Soil Laboratory (see Figure 3.20). After the nature and amount of the necessary compaction were determined, a tamping device was designed and fabricated for use in all subsequent experiments. The device is in two parts. The main part is a steel rod with interchangeable bases to fit inside different test samples for compaction at the surface layer as shown in Figure 3.21a and b. This rod has a screw stop that is positioned at different points along its length to allow the rod to fall to a predetermined height. The rod passes through two thick Perspex discs that hold the rod upright in order to produce a level sample surface, but also allow the rod to fall smoothly in the vertical direction. The secondary part of the apparatus is a larger Perspex disc that allows greater freedom of movement of the rod around the horizontal surface of the different shapes of test moulds.

The sample preparation by under-compaction of the fibre-reinforced samples was as follows. Loose to dense samples were prepared with 2% moisture content for better workability when mixing with the fibres. Fibre contents were measured by weight and slowly introduced to the moist sand in extremely small quantities during hand mixing with a metal spoon. By placing small groups of the fibres in the mix separately, the uniformity of the finished sample mix was regulated. The total weight was then divided into three equal weights for separate layer placements.

Each layer was compacted to predetermined but different heights in order to take into account the additional compaction due to subsequent layers. The sample layer heights for 110g and 120g samples are shown in Figure 3.21, while the dimensions of under-compacted sample layers for all compression test moulds follow:

- One-dimensional compression sample assembly

M_s = 104g	M_s = 110g	M_s = 120g
Layer 3 h_n = 8mm	Layer 3 h_n = 6mm	Layer 3 h_n = 6mm
Layer 2 h_n = 5mm	Layer 2 h_n = 6mm	Layer 2 h_n = 6mm
Layer 1 h_n = 7mm	Layer 1 h_n = 8mm	Layer 1 h_n = 8mm

The difference of U_n values between layers is relative to the number of layers and desired sample density. Three layers were chosen as the total height of the test sample is 20mm. U_n values of between 0% and 30% for the first two layers all provide the same sample heights for such a shallow sample, so based on the under-compaction theory, Layer 1 had 15%, Layer 2 had 10% and Layer 3 had 0% under-compaction.

Void ratio values greater than e_{max} were achieved by the under-compaction technique for the moist samples, therefore negative relative density values were recorded before the load cap and hanger loads were applied and the sample was compressed. Moist-tamped MGS fibre-reinforced sand samples were tested in one-dimensional tests. Figure 3.10 shows the compression behaviour of the moist under-compacted samples for three initial densities set by the dry weight of the mix at 104, 110 and 120g of sand with 2% moisture content and fibre contents of 0.0, 0.1, 0.3, 0.5 and 0.7% by weight. The moisture content increased the volume of the voids in the samples with and without fibres considerably.

Heavier compaction than that used during sample preparation for these tests would be necessary to suitably compress the low moisture content samples to the same initial density as dry samples. Dry compression tests were prepared to set density values by the under-compaction method to assess the effects of adding 2% moisture content to the samples.

3.4.4 Dry under-compaction

Low initial density values for the moist MGS samples raised the question of the effect the moisture content has on the sample's amount of compaction during preparation and the subsequent compression behaviour. Void ratio values greater than e_{max} were achieved by the moist under-compaction technique, so the same amount of under-compaction was applied to moist and dry samples of Grenoble sands for comparison.

Figure 3.22 shows the initial densities of pluviated Hostun sand and moist under-compacted and dry-tamped Grenoble sand samples in terms of relative density. The

different samples were plotted according to their preparation methods on the horizontal axis. The pluviated Hostun samples for all nozzle sizes were included and labelled. The densities of the 8mm nozzle samples had the best repeatability of the preparation methods shown and provided the densest samples (relative density approximately 92%). The under-compaction method was used for Grenoble sand with 2% moisture content to produce a range of relative density values (approximately 33%) that relate to void ratios of between 0.66 and 0.69. This method showed favourable repeatability for the initial density values. The dry-tamped samples had the least favourable repeatability of the three techniques. The dry samples were all prepared with the same sample heights used for the moist samples, but the initial density values had a relative density of approximately 20%. Due to their loose state, the initial bedding of the top cap during test assembly altered significantly. The initial void ratio values for moist- and dry-tamped samples were in the region of 0.68-0.69.

3.4.5 Traditional techniques compared

The initial density ranges for samples prepared by pluviation, moist under-compaction and dry tamping were compared. One-dimensional compression tests compared the repeatability of the sample preparation method as well as the density changes that result in compression for samples reinforced with differing fibre contents. The repeatability and reliability of the initial density values were the first obstacles that a preparation technique must surmount in order to establish optimum soil parameters for shear test samples. Indeed Vaid et al (1999) stated that shear behaviour can be affected by the type of preparation method utilised, even when similar initial densities are achieved for test samples.

The Medium Golden Sand was chosen as a preliminary test material due to its similarity to Hostun sand in specific gravity and particle size distribution, although the details of its origin were unknown. Grenoble was readily available in the lab as representative sub-rounded sand and the sub-angular Hostun sand is widely used in European soil laboratories. The difficulty in obtaining similar tests results from the same sample preparation methods illustrates the behaviour of sub-rounded and sub-angular sands reinforced with fibres. The rounded shape of the sand grains allowed greater movement during compaction than sub-angular sand would. This rolling movement impedes the formation of interlock between the sub-rounded sand grains and the fibres.

In Figure 3.23 the relative densities for dry-tamped and moist-tamped Grenoble sand with 2% moisture content by weight were shown. Pluviated Hostun sand was plotted for the comparison of the traditional sample preparation method for direct shear tests. The dry and moist Grenoble samples were both under-compacted to the relative density values of 30% within a shear box mould. Moist samples showed more volume contraction in shear tests.

The samples prepared by pluviation with 8mm nozzle diameter gave favourably repeatable initial densities. Spurious data resulted from the moist under-compacted samples in direct shear tests as the repeatability of this method was unfavourable. Dry tamping produced the densest samples with fibres, so samples with 0% moisture content will provide information about the effects of the fibre reinforcements more clearly. A more sophisticated sample preparation method than these conventional techniques is therefore necessary to achieve a wider range of initial density values for dry fibre-reinforced samples with improved repeatability.

3.5 Preparation techniques for fibre-reinforced sand

3.5.1 Preparation considerations for fibre-reinforced soil samples

The conventional sample preparation techniques used on fibre-reinforced sands confirmed that a certain amount of compaction is necessary to achieve an initial density range from loose to dense conditions. The addition of moisture content can increase the volume of the voids within a mix until compacted to a set density. Dry samples will be tested in compression and shear to observe the soil strengthening that the fibres impart to sand according to the preparation techniques used.

For a set of control tests, un-compacted samples were fabricated by spooning. This was simply a process of spooning portions of the hand-mixed sample so that the compression characteristics could be compared with other preparation techniques. The calculation of sample layer heights used in the under-compaction method is a useful technique for the preparation of samples with uniform density (by any technique). For random fibre placement, the distribution of the fibre content can be closely controlled by visual inspection. The spooned assembly allows the experimenter to monitor the uniformity of the fibre content. Vibration techniques can sometimes allow fibres to "float" to the surface while the soil grains settle at the base of a sample. To assemble fibre-reinforced sand samples with uniform fibre content throughout as

well as a range of initial densities, a technique of vibration in layers was developed. The layer heights were determined with the effects of over-compaction and granular settlement in mind.

3.5.2 Spooned assembly

When fabricating a fibre-reinforced sample, the fibres need to be separated before mixing by hand with the test sand. Stirring usually causes the fibres to clump together rather than to disperse due to frictional effects. The volume of the matrix expands as air becomes trapped between the fibres and the soil grains during mixing and deposition, so compression tests were adopted where the samples were assembled completely by spoon-placement and then compressed by vertical loads. The objective was to create a sample with a visibly uniform density and to then observe the repeatability of the vertical compression.

The spooned assembly set of experimental samples was prepared without any compaction or pre-load. The samples were deposited in three layers by the same procedure as the dry-tamped samples. Each layer was levelled with a straightedge to aid in the uniformity of density and accuracy of the height measurements. Light dry-tamping of sample Layers 2 and 3 with the back of the spoon was the only form of under-compaction used for the samples with void ratio values 0.67 and 0.72 to maintain equal layer heights.

- Shear box test mould (dry-tamped and spooned)

M_s = 251g	M_s = 238g	M_s = 243g
Layer 3 h_n = 12mm	Layer 3 h_n = 12mm	Layer 3 h_n = 12mm
Layer 2 h_n = 18mm	Layer 2 h_n = 18mm	Layer 2 h_n = 18mm
Layer 1 h_n = 14mm	Layer 1 h_n = 14mm	Layer 1 h_n = 14mm
e = 0.67	e = 0.72	e = 0.76

The samples in Figure 3.24 show one-dimensional compression tests results from the shear box mould with the initial void ratio values at the first load equal to 10.5 kPa, which is the combined weight of the top cap and load hanger before weights are applied. Dry Hostun sand with 0.0 and 0.3% fibre content by weight was tested with identical vertical loads.

Although all samples were spooned to the same initial density, the fact that the reinforced samples compressed more than the un-reinforced samples raises questions

regarding the compression behaviour for this fibre-soil mix preparation method. There is also disparity between the compression curves for the two fibre-reinforced specimens, so repeatability was a problem with 0.3% fibre content.

To investigate this phenomenon further, samples were pre-loaded by vertical loads of 50, 100 and 200 kPa to verify the amount of the vertical deformation. The range of initial densities was attributed to the weight of the load hanger compressing some of the samples to lower void ratios before the actual weights were applied. Samples were pre-loaded to either 100 or 200 kPa and then the load was removed to detect any strain recovery that might take place. These samples were denoted as (100-50) and (200-50) in the graph legend in Figure 3.25. The samples were then tested in direct shear to examine the effects of the pre-load with respect to peak stress values.

The compression test results for the spooned samples do not share an original void ratio value due to the initial bedding of the test apparatus for the reinforced samples. As the samples were not pre-loaded or pre-compacted in a methodical way, the initial bedding of the top caps was variable among the test samples. The samples were not all loaded in the same sequence due to the different hangar weights available, which were believed to affect the intermediate stages of compression. An alternative sample preparation was deemed necessary to suitably compress the fibre-reinforced samples for the testing of soil in dense conditions.

Samples with 0.0 and 0.3% fibre content prepared by pluviation and dry-tamping have been included for comparison. Another preparation method that appears in Figures 3.25 and 3.26 includes samples vibrated with a static load that was equal in weight to the top cap of the test apparatus. This preparation method is explained further in the following section. The densest samples were fabricated by this method and the values in compression from 0 to 50 kPa were nearly identical for 0.0 and 0.3% fibre content.

3.5.3 Vibration with a Perspex top cap

It has been generally recognised that vibration or dynamic impact can be used to densify cohesionless soils. These densification practices have often been applied in laboratory tests to establish the maximum density of sand. When dense samples are required, Vaid and Negussey (1984) suggest that they can be obtained by dry vibration. However, for moistened fibre-reinforced samples, vibrational techniques tend to allow the fibres to float to the surface of sand test specimens. By incorporating the under-

compaction formula for layer heights, light vibration was attempted on layers of dry sand samples with and without fibres to achieve more repeatable initial densities and more dense samples than those realised by previous techniques.

Three layers of sample were spooned into the test mould. A Perspex top cap (weighing 55.7g, σ_v' = 1.24 kPa) was placed on the surface of each layer during vibration to produce a level sample surface from which the layer height may be measured. The surface cap was made of Perspex due to its light weight compared to the steel top cap used in testing (weighing 380.8g, σ_v' = 8.46 kPa). Vibration was applied vertically to the Perspex top cap until the sample reached a set density. In the same way that the percentage of under-compaction determines the amount of compression for each layer, the vibration was applied until each layer achieved a set height within the test mould. A small amount of horizontal vibration was applied to the exterior of the test moulds as well. Figure 3.25 included the compression characteristics of samples prepared by this method, denoted as "vibrated" in the legend.

The highest initial densities were obtained for dry fibre-reinforced and un-reinforced samples by this preparation technique. The Perspex top cap was intended to act as a light yet rigid surface through which the vibrator made contact with the sample surface. This preparation method was attempted in order to avoid an initial pre-load to the surface of the sample layers that was greater than the weight of the top cap.

3.5.4 Vibration with a steel top cap

In this set of test results a load approximately equal to the steel top cap of the apparatus (374.1g) was applied to the top of each layer and the samples were vibrated to a set density. Figure 3.25 shows the one-dimensional compression behaviour of samples that have been pre-stressed, pluviated or vibrated. By applying a static load during the fabrication process, a higher density was achieved than for samples vibrated without this load as shown in Figure 3.25 by the results titled "vibrated with plate" in the legend. Samples with and without fibres were spooned into the test mould in layers as before. In the same way that the percentage of under-compaction determines the amount of compression for each layer, light vibration was applied by an electric engraver until each layer achieved a set height within the mould.

Samples denoted as (100-50) and (200-50) in the graph legend were pre-loaded to either 100 or 200 kPa and then the load was removed as shown in Figure 3.26. The samples were then tested in direct shear to examine the effects of the pre-load with

respect to peak stress values. The densest condition for the initial void ratio values for fibre-reinforced and un-reinforced Hostun sand was obtained by this preparation method. The slight variance in the void ratio values between 10 and 55 kPa normal stress was due to the amount of weight applied at each stage. The samples with higher void ratios in the first two load increments were loaded in two stages from 10 to 38 to 65 kPa, while the more loose behaviour is shown when loaded directly from 10 to 55 kPa. This stress difference is due to the amount of space available on the load hanger for the required number of weights for a given loading sequence. The density and the repeatability of this sample preparation method proved to be the most favourable of the ones tested.

3.5.5 Determination of the density of a fibre-soil mix

The density of a soil structure is determined by the volumetric packing of its grains. The soil skeleton is composed of soil particles of differing size, shape and grading. The voids between the particles contain air voids and water as shown in Figure 2.21. The proportions of the solid particles that occupy the voids, as well as the proportions of air and water in those voids determine the density of a soil. The proportion of voids between soil particles determines the density of the soil structure that significantly affects the volume changes that occur when a soil deforms.

The density of a fibre-soil mix is described either as a void ratio (e) or relative density (RD). The relative density of a sample is a ratio of the difference between e_{max} and $e_{initial}$ values divided by the void ratio limits of the dry soil. Formulae for the determination of e and RD are as follows:

$$e = \frac{Volume_{total} \cdot G_s \cdot \gamma_w}{M_s} - 1 \quad \text{as} \quad e = \frac{Volume_{total} - Volume_{soil}}{Volume_{total}} \quad \text{for dry soil}$$

$$\text{and} \quad RD = \frac{e_{max} - e_i}{e_{max} - e_{min}}$$

Consistent with engineering practice, the weight of fibres as a percentage of the total dry soil weight is used to define the fibre content. It is common practice to disregard the fibre content when calculating the void ratio of a fibre-reinforced sample. For this reason, the placement and compaction of the fibres is an important feature of the initial density value of a fibre-reinforced sample. Any inclusion will add to the volume of a

soil mass and increase the voids between the soil grains. The challenge when introducing fibres into a soil mass lies in the fabrication of a material with uniform density. The homogeneity of a soil sample with fibre content is affected by all variables of a fibre-soil mix. Light vibration under a small load is the favoured sample preparation technique for one-dimensional compression and direct shear tests.

3.6 Experimental procedures

3.6.1 Basic considerations of the shear box test

Stroud (1971) listed the basic considerations for sample preparation of simple shear samples as the following:

(a) The sand must be [placed] into the apparatus in such a way that the voids ratio is uniform throughout (within certain prescribed limits).

(b) The contact developed between the sand and the top and bottom shear faces of the apparatus must be strong enough to develop the full frictional resistance of the sand.

(c) The upper surface of the sand must be moulded as closely as possible to the shape and position of the contact faces of the [top cap]. 'Lack of fit' will result in local stress and strain concentrations that may lead to more serious non-uniformities later in the test.

(d) The sample must be disturbed as little as possible after [placement] and during surface preparation. Local disturbances should obviously be avoided. Perhaps less obviously, care must be taken to ensure that the sample is not prematurely over-loaded, however temporarily. This is a particular problem for tests at low stress levels.

These sample preparation considerations assume a pluviated deposition. What has not been emphasised enough is the particular care that must be taken for sample uniformity in the shear plane. The uniformity of the area surrounding the shear zone can have serious implications for the stress-strain behaviour shown in direct shear test results. This has especially been the case for fibre-reinforced sand samples.

The samples were built in layers that occupied at least 4mm above and below the shear plane to avoid the creation of a pre-determined shear plane by means of the preparation.

The height from the base of the shear box to the shear plane is 19.0mm. The samples were prepared with a top surface at 44mm height in order to ensure a level surface.

3.6.2 Testing preparations

The experiments conducted in this research project used both standardised and modified sample preparation laboratory methods. Basic soil tests defined the properties of the test materials. The pluviation, tamping, spooning and vibration of samples achieved a range of initial densities from which further analysis has been made. These sample preparation techniques produced a range of initial densities for samples from which the effects of preparation method were compared and tested for repeatability.

Laboratory tests were done in order to further develop an understanding of the void ratio-stress state significance and how the various densities can be achieved by the chosen preparation techniques. The main features of the tests and the sample properties are presented.

3.6.3 Sample disturbance and stress history

The vertical and shear deformations of fibre-reinforced samples in pre-loaded conditions were linked with the amount of load and type of stress history. Samples with an initial pre-load were loaded up to 200kPa, the loads removed, and then subsequent loads of 50, 100 and 200kPa were imposed on the samples. This confining stress served to reduce the air voids in the test samples so that the reinforcing effects of the fibres could be initiated before shear stress was applied.

In the field, passes of heavy rollers both compress and vibrate fibre-reinforced soil surfaces. Heavy vibration could disturb fibre-reinforced samples enough to weaken the interlock between the fibres and the soil grains in small-scale tests, but light vibration was applied and monitored in the sample preparation in order to densify the samples.

3.6.4 Fibre contents

The fibres contents used in tests were 0.0, 0.3 and 0.5% by weight. The fibres were all cut to 17.5mm length in order to suit the small-scale test moulds (unless otherwise specified). The fibres were then hand-mixed by a metal spoon with the dry Hostun sand in a small ceramic mixing cup to reduce friction between the fibres and the mixing implement.

3.6.5 Void ratio values

The initial void ratio values for Hostun test sand were 0.67 (dense), 0.72 (medium) and 0.76 (loose). The uniformity of the void ratio values was controlled during the preparation method regardless of the fibre content. In order to achieve the same initial density for samples with 0.0 and 0.5% fibre content, the duration of the vibration applied would be altered, but the sample layer heights would be the same.

3.6.6 Normal stress levels and loading procedure

The upper portion of a sample will often experience deformation during shear under low confinement. The net vertical displacement is a summation of this repeated event combined with the compressions that occur deeper in the sample.

The normal stress range for the compression tests and the shear tests was between 0 and 200 kPa. Normal loads were applied by adding weights to the load hanger. Shear loads are introduced using a constant strain motor. The load hanger for the shear box rests directly on the top cap while the oedometer load hanger is counter-balanced, so once a test was completed the apparatus was dismantled in the reverse order of setting up. Accurate interpretation of soil parameter measurements relies upon the uniformity of stress and strain throughout the test. The stress distribution was assumed to be constant throughout the sample, due to the reinforcing effects of the fibres between the two halves of the sample. The rigidity of surface loads on a sample determines the uniformity of the subsequent stress distribution. For this reason, the bending stiffness of the top caps was assessed for their possible flexural effects (see Appendices).

3.7 One-dimensional compression

3.7.1 Description of the oedometer cell

The oedometer cell consists of two shallow bronze cylinders: one that serves as case for the inner cell and the porous stone at the base; and one that contains the sample as shown in Figure 3.27. Once the sample is prepared the steel top cap, weighing 300.8g, is placed on the sample surface and the load hanger is set by the adjustment of a stabilising rod. The load hanger is suspended from the lever arm, which is set at a position that intensifies the normal stress value by a factor of 9. The weight of the load hanger is counter-balanced for vertical positioning by the stabilising rod that rests on the top of the top cap. The dial gauge is placed on the top surface of the rod after the test cell is positioned and the lever arm balanced.

3.7.2 Procedure of vibrating samples to chosen densities for compression cell

The volume of the compression test cells was much smaller than the shear box so only two layers of the sample (equal to half the weight) were placed in the cell and vibrated in turn. Upon the surface of each layer, the Perspex top cap was positioned to provide a level surface for a brief duration of light vertical vibration in order to achieve a set height. An extra surface load was unnecessary to obtain the desired layer heights.

Fibre contents of 0.0, 0.3 and 0.5% by weight were used to reinforce dry sand test sands prepared to each of the three initial void ratio values: 0.67, 0.72 and 0.76.

3.7.3 Initial compression

The one-dimensional compressive behaviour of fibre-reinforced soils was tested for two purposes. Firstly the vertical displacement measurements under known normal stresses were used to predict the initial deformations that occur in the direct shear samples when the load hanger and top load cap are applied. Secondly, the samples' vertical displacements under a range of normal loads provided information about the repeatability of particular preparation methods for the range of initial sample densities tested. Therefore the one-dimensional compression tests were conducted using first small loads to measure the initial deflection of the load cap, and then larger loads were used so that the changes in void ratio could be determined throughout a range of normal loads.

All test samples had an unfixed top cap of known weight placed upon the top surface, which produces a small vertical deformation. In small-scale laboratory experimentation, there is usually an initial compression that a sample will experience when the top cap or load hanger is placed upon it. The initial compression could not be measured due to the configuration of the dial gauges with respect to the top cap. In the tests presented here, load hangers are then positioned which increased the vertical deformation before dial gauges were placed. The results from one-dimensional compression tests with a lightweight top cap provided the missing information about the small initial deformation.

One-dimensional compression tests with a lightweight Perspex top cap were undertaken to determine the amount of vertical settlement that occurs within a shear sample before the dial gauge is positioned. For the direct shear box, after the unfixed top cap is placed upon the surface of the sample, the load hanger balances on a steel ball that fits into a spherical indentation in the top cap and the dial gauge is placed on

top of the hanger. From the one-dimensional compression test results, the initial void ratio values for shear test samples were corrected.

To investigate the effects of loading on soil stiffness, the void ratio is plotted against normal stress in Figure 3.28. The vertical compression from an initial void ratio value of 0.67 is plotted for un-reinforced samples and samples reinforced with 0.3% fibre content by weight. The normal stress readings begin with 10 kPa due to the weight of the load hanger. A vertical displacement equal to approximately 0.004 was observed between the start of the test and 14 kPa normal stress for all samples, the value of the weight of the shear box load hanger arrangement. The vertical deformation shows good repeatability for both fibre contents. Figure 3.28 shows the repeatability of the loosest sample (e=0.76) with 0.0% and 0.3% fibre contents. The reinforced samples deformed slightly more than the un-reinforced samples (void ratio changes of -0.005 and -0.004 respectively) at larger normal stresses despite having an initially higher void ratio before the compression began. The range of disparity for the void ratio values was recorded and is shown by error bars (± 0.004).

The first load increment in Figure 3.29 shows the test results for compression starting from 1 to 11 kPa to show the small stress compression characteristics that are lost during the placement of the shear box top cap and load hanger. The initial densities of the test samples will take these results into account and the values of the initial void ratios for the shear test samples will be referred to as e_i, ($e_{initial}$) although they are in fact $e_{corrected}$.

$$e_{corrected} = e_{11\ kPa} \text{ for shear tests and}$$

$$e_{corrected} = e_{1\ kPa} \text{ for one-dimensional compression tests}$$

3.8 Shear box tests

3.8.1 Procedure of vibrating samples to chosen densities for shear box

The sample layer heights for vibrated samples have already been stated. Providing sufficient sample coverage above and below the shear plane was integral to the sample layer height design, as was the concept of under-compaction for the sake of uniform density throughout the sample volume. Each plan dimension of the shear box is approximately 150 times the mean grain size (D_{50}) of the sand tested, which is in the ideal range recommended in specifications and by other researchers (Jewell and Wroth, 1987; Palmeira and Milligan, 1989). Vibration with a small load, in this case a steel plate of equal weight to the shear box top cap, ensured a level sample surface for the

application of the test top cap and eliminated the bedding effects normally associated with the application of the top cap.

3.8.2 The size of the opening between box halves

Side friction is increased in the apparatus assembly when a gap of approximately $5D_{50}$ is made to reduce the metal-metal frictional forces of the two box halves in shear. In the case of the Hostun sand, $5D_{50}$ equates to 2mm, which was introduced by the rotation of the separating screws positioned at two diagonal corners of the test mould (see Figure 3.30). One-half rotation is equal to 0.5mm. The screws are then retracted and removed while the sample holds the top half of the box by friction. The top half of the box brings the upper portion of sample with it and produces an increment of shear displacement from a portion of the sample immediately beneath the upper box half.

An initial settlement of the sample height results from the application of the load hanger after this movement of the mould. In moist samples, the shear box mould movement can sometimes cause dilation. For the dry shear tests samples, no noticeable vertical movement was observed.

3.8.3 Initial vertical deformation from the load hanger application

The specimen height after the addition of the load hanger is usually taken as datum from which subsequent vertical movements are measured (Head, 1990). To resolve the unknown vertical deformation value, one-dimensional tests in an oedometer measured the settlement of samples under a load equal to the weight of the load hanger and the results were used to correct the initial vertical deformation values (see Figure 3.31). The total normal load imposed onto the sample consists of the following items:

- the load hanger = 3.622kg
- the steel top cap = 364.0g
- the steel balancing ball = 16.0g
- the top half of the shear box = 1.045kg
- the weight of the top half of the sample ~ 120g

In Figure 3.31 the vertical deformation of vibrated samples in one-dimensional compression was measured according to the initial void ratio value. The densest samples showed the least deformation (Δe~0.03) while the loosest samples showed the greatest deformation (Δe ~0.04). The greater the fibre content, the greater the vertical

deformation was observed for all samples. This test served as an example of the fibre-reinforced sands' improved flexibility compared to un-reinforced sands with the same initial density.

3.9 Manipulation of the test data

3.9.1 Correction factors for test data

Recorded test results for soils are usually estimates of the stress-deformation properties of the soil under shear stresses. In literature there is often uncertainty of how the test results have been derived and interpreted. As the determination of the estimated error in test data relies on the accuracy of the laboratory equipment employed, the main soil strength parameters and their error corrections are presented here.

The greatest possible error could arise from the error in measurements of sample height and weight. A dial gauge was used to measure the samples' vertical displacement in test data including the change in void ratio. The dial gauge measured to 0.002mm confidence, which gave an error of ±0.0045 for void ratio calculations. It was assumed that any errors within the dial gauge were evenly distributed throughout all readings and therefore were not of a large magnitude for vertical and horizontal displacements. A balance with 0.1g resolution was used for all tests; however a reading of ±0.1g of soil could result in an error of approximately ±0.001 on the void ratio calculations. The estimated error for the void ratio values were determined by the following formula.

$$\text{estimated error} = (\text{error} / \text{average value}) \times 100\%$$

Therefore, the standard variation for samples prepared to have the void ratio value of 0.67 is calculated as (0.001/ 0.67) x 100% = 0.149%.

Initial void ratio value (e_i)	Error (±)	Standard variation (±)
0.67	0.00149	0.149%
0.72	0.00139	0.139%
0.76	0.00132	0.132%

The intrinsic normal stress values of the laboratory consist of the weight imposed onto the top cap via the load hanger as well as the inherent weight of components of the apparatus. The normal stress in shear tests usually also includes the self-weight of the upper portion of sample that lies above the shear plane. British Standards state that a

calculation of the normal stress component of a shear test sample that does not include the sample self-weight leads to underestimation of the σ_n value and, hence, overestimation of the stress ratio τ/σ_n.

The initial void ratio values were determined by the usual formula and as mentioned earlier, where the weight of the soil solids (M_s) did not include the weight of the fibre content. The initial void ratio (e_i) for samples is a numerical calculation as prepared in the laboratory. The void ratio values at critical state, e_{cs}, and steady state, e_{ss}, were determined from test data as void ratio values representative of the stress states.

The errors for the derived test parameters τ and σ were given careful consideration. The shear stress was determined from the reading of a dial gauge that monitored the direct stress transmitted to the proving ring via the motor that drives the halves of the shear box apart. Each dial gauge digit represented ±0.328 kPa shear stress. The standard variations are less than 1% for 50, 100 and 200 kPa stress values, so the shear stress values are quoted with confidence. The normal loads were calibrated by measuring the individual weights on a balance. Masses less than 0.5kg were measured to 0.001g accuracy, and masses greater than 0.5kg were measured to 1g accuracy.

3.9.2 The volume change calculations

The changes in volume of a sample are usually represented as the changes in vertical displacement (*dy*) plotted against the changes in horizontal displacement (*dx*). Great care was taken in the sample preparation stage to not disturb samples at any time prior to the commencement of tests. The initial volume changes of the samples were measured as a change from the measured volume in its original state as prepared and placed in the test equipment. For one-dimensional compression and shear tests, dial gauges measured the *dy* and *dx* displacements and the units were converted in the traditional way for the initial void ratio values.

The volume change in direct shear tests is represented in terms of *dy*. The vertical displacement (*dy*) was gauged from the central point of contact between the centre of the shear box top cap and the load hanger. The horizontal displacement (*dx*) was calculated based on the recorded speed of the separation of the box halves, which was 1.27mm per minute. As mentioned earlier, the top cap was not fixed so it was assumed that *dy* as measured at the centre of the top cap represented the vertical displacement of the sample as a whole. Should a noticeable difference in the elevation of one section of the top cap develop, the test would have been discounted on grounds of non-

homogeneity of the mix. Non-homogeneity in the deformation could represent unreliable test results with respect to shear strength and poor repeatability of the sample behaviour.

The bending stiffness of top caps in testing can affect the vertical deformation in plain sand. It was assumed that the fibre-reinforcements transferred the normal top cap load throughout the sample volume, as there were no obvious discrepancies between the vertical deformations of the Perspex and bronze top caps (see Appendices).

3.9.3 Wall friction

Wall friction is sometimes deemed to be the cause of considerable non-uniformity in the sand immediately adjacent to the interior walls of the shear box and could significantly affect the parameters measured (Stroud, 1971). The separation of the two halves of the shear box used in this study occurs when the sand is in a loaded state. The following was observed for dense sand in an unloaded state:

> "This movement is sufficient to disturb the grains in contact with the wall which in turn brings about a local collapse of the sand structure near the wall. On applying a shear force the [anticlockwise] rotation of the top boundary, noted in dense tests, compounds this local disturbance."
>
> Stroud (1972)

The general pattern of deformation in shear at low confining stresses includes a small separation between the sample and the test mould at two particular points. There was a small separation between the top of the front box wall and the top cap as well as at the lower back box wall and the sample base. This behaviour originates from the wall friction that the separation of the box halves generates. In Figure 3.32, the wall friction as a percentage of the horizontal shear force (R_f) is plotted against strain α for dense and loose sand samples.

Stroud found that the error in stress ratio values due to the wall friction in the simple shear apparatus was below the general level of accuracy of measurement for the test equipment, and therefore deemed tolerable. Fibres have the ability to absorb small strains within a soil mass (especially under stress), so the localised disturbances generally caused by this stage of the sample placement were considered minimal for this small-scale study.

3.9.4 The internal angle of friction

The angle of internal friction is often more correctly referred to as the angle of shearing resistance. The angle ϕ' is not a true angle of friction, but instead it is the slope of the line representing shear strength in terms of effective normal stress on the failure surface, based on Coulomb's failure condition for soils. Schultze (1975b) published data for the angle of friction, specifically its tangent for granular soils in shear. He found for a population of less than 30 experiments the coefficient of variation of tan ϕ' is in the range of 0.05-0.14, which is the standard deviation divided by the arithmetic mean. The mean values and the coefficients of variations of the angle of friction were obtained in direct shear tests. The calculated mean values and coefficients of variations of the angle of friction in gravelly sand (for a population of 29 experiments) are based on the initial void ratio (e_i)

$$\cot\phi = 3.36e_i + 0.005$$

where variance is defined as the index of variability of the measured physical characteristics of the soil. The calculated error for the angles of friction reported here will include the appropriate coefficients of variance as ± (value).

In shear tests the standard variation increases with decreasing particle grain size due to the higher number of grains and the greater number of points of contact between the grains; and for the compacted state the variation is higher than that of the loose state. For direct shear tests, Harr (1977) found a coefficient of variation $C_v = 0.14$ for tan ϕ' in silty sand. The standard variation of ϕ' for cohesive and semi-cohesive soils is somewhat higher than that for granular soils. Generally the standard variation of the angle of internal friction is most likely a consequence of test procedures, rather than a predetermined relationship based on any one soil parameter.

3.9.5 The calculations of the shear zone

A characteristic shear zone width was assumed based on the shear deformation and dilatancy characteristics within the shear zone. It is assumed that the direction of the majority of shear strains within the sample coincide with the direction of maximum shear strain. The shear zone that forms in the middle section of a specimen in direct shearing consists of infinitesimal multiple shear bands (Shewbridge and Sitar, 1996). The thickness of the shear zone is generally assumed to be 10 – 20 times as large as the mean diameter of particle D_{50}. However, the number of shear bands may increase with the increase in the ratio of the shear box size to the size of the sand grains (Palmeira

and Milligan, 1989). Such a complex shear zone formation is enhanced by the addition of reinforcements. More dilatant behaviour is observed at large shear displacements for reinforced soil due to the development of multiple shear bands (Shewbridge and Sitar, 1996).

The shear zone for an un-reinforced sand sample in a standard shear box is generally assumed to be 2mm in height due to the height of the gap between the two halves of the shear box. Due to the load transference that the fibres impart to the sand, the shear zone width for fibre-reinforced Hostun sand samples in this investigation will be considered as the total height of the sample. This calculation accounts for the shear volume both above and below the shear plane. This may seem to be an over-estimation of the shear zone for a 60 x 60 x 44mm shear box, but with the random distribution of fibres, the shear strains are expected to extend throughout the total sample volume.

A formula for the contribution of fibres to shear strength relies on an area fraction for calculation. In equations that include the fibre content as a soil strength parameter in the shear plane, an area fraction is often used. The area fraction for a fibre-reinforced soil is simply the area of a sample occupied by fibres (A_f) divided by the area of the soil being considered (A_s) as shown below.

$$\text{Area fraction} = \frac{A_f}{A_s} \text{ x } 100\%$$

The area of the shear plane for the shear box was 60 x 60 mm. As the mean Hostun sand particle diameter can be assumed to be D_{50}, we can approximate there are a maximum 9000 grains of sand with a diameter of 0.40mm in the shear plane (as $3600\text{mm}^2 \div 0.40\text{mm} = 9000$). The approximation of the amount of the shear plane occupied by the fibres is inherently more complex as the fibres have either 35 or 17.5mm length, up to 360° of orientations and the fibres could conceivably be interwoven around any number of sand grains' surfaces. One 0.9mm diameter *LokSand* fibre of 17.5mm length has an area that is 0.44% of the shear area by the following calculation:

$$\text{Area fraction} = \frac{(17.5 \times 0.9)}{3600} \times 100\% = 0.4375\%$$

This area fraction accounts for fibres that would lie horizontal on a shear plane. With the multitudinous possible orientations of randomly-distributed fibres in the shear plane, an area fraction does not represent an accurate representation of the fibre content within a planar area. Therefore, in the model presented in this thesis the volume fraction will be considered for the increased shear strength of test samples.

The orientations of random reinforcements within a soil are difficult to determine, although many shear strength calculations for reinforced soils rely on the angle of reinforcement orientation. Wu et al (1979) investigated the shear strength of soils reinforced by plant roots based on the roots' area ratio and orientations and devised the following formula

$$\Delta\tau = S_r = T_r \frac{A_r}{A_s}\left[\cos\theta\tan\phi + \sin\phi\right]$$

where the parameters included S_r as the increased shear stress due to root reinforcement, T_r as the maximum tensile stress of a root, A_r as the area of shear plane occupied by roots, A_s as the area of soil in shear, θ as the angle of root orientation and ϕ as the angle of internal friction of the soil. The bracketed term was estimated by Wu et al (1979) based on field and laboratory data. A parametric equation was used to vary the angles of θ and ϕ so that the range of the term was approximated to be 1.12 (with a range of 0.92 to 1.21). The range of values for the two angle terms was determined as follows:

$$40^\circ \leq \theta \leq 70^\circ$$

$$\text{and } 20^\circ \leq \phi \leq 40^\circ$$

The volume fraction of fibre-reinforced Hostun sands samples will be used in order to become a planar quantity in the following formula:

$$\Delta\tau = S_r = T_r \times V_f \times 1.12$$

3.10 Summary

Different data manipulation techniques are employed in American and British standards for laboratory experimentation. In literature there is often uncertainty of how the test results have been derived and interpreted as recorded test results for sands are merely estimates of the stress-deformation mechanical changes of behaviour under

compressive and shear stresses. The laboratory experiments were described, the sample preparation procedures were compared, a discussion of the data interpretation followed and any assumptions they contain were identified.

Modified sample preparation techniques used the under-compaction method to determine sample layer heights for spoon assembled and vibrated samples. The spooned assembly and pluviated samples represented the control specimens for comparison in the same manner in that they were the control tests of the traditional techniques; however, the range of sample densities was very limited. Although spooned samples provided one-dimensional compression information for samples with only the smallest amount of pre-load, they produced neither repeatable initial densities nor totally reliable direct shear samples.

As the density distribution was seen to be a concern in test samples when using pluviation, sample deposition by pluviation was not as successful a preparation technique as vibration in terms of uniform density. The vibrated samples provided the most accurate initial densities and the densest samples. By applying a small load in the form of a steel plate, the compression and shear test results were reliable and repeatable.

A predetermined density for these materials was attempted for various sample soil particle sizes and shapes. The initial density range and subsequent mechanical behaviour of samples were compared in one-dimensional compression and direct shear tests according to their initial deformation characteristics. It was found that the parameters which increased the void ratios in these sand samples can have a negative affect on the repeatability of test results. The results of the sample preparation analysis are summarised in Figure 3.33. Notable conclusions include the following:

- Added moisture content can increase the void ratio of sand samples and can greatly increase the voids of fibre-reinforced samples depending on the compaction process.

- The fibre content, length and orientation can influence the initial sample density and subsequent stress-deformation behaviour, depending on the compaction process used. Therefore, fibre contents lower than 1% by weight were used, the fibres used in small-scale tests were cut to 17.5mm length and a random orientation was adopted.

- Samples that were prepared by vibration under a small load produced the best repeatability for initial density values.

- An optimum sample preparation method for direct shear tests of fibre-reinforced soils was found by a combination of light vibration and a small normal load.

- The one-dimensional compression behaviour of samples was reported for normal loads up to 200 kPa. The normal stresses of 50, 100 and 200 kPa for direct shear test samples will be loaded onto test samples before the dial gauges are placed, so the compression of samples by the direct shear test equipment can be compared with the one-dimensional compression test results.

The testing methodology and the samples' response to dynamic compaction are described in the following chapter. The stress-deformation behaviour of the samples prepared by the methods described here will be explored further in Chapters 5 and 6.

3.11 Figures for sample preparation techniques for fibre-reinforced sand

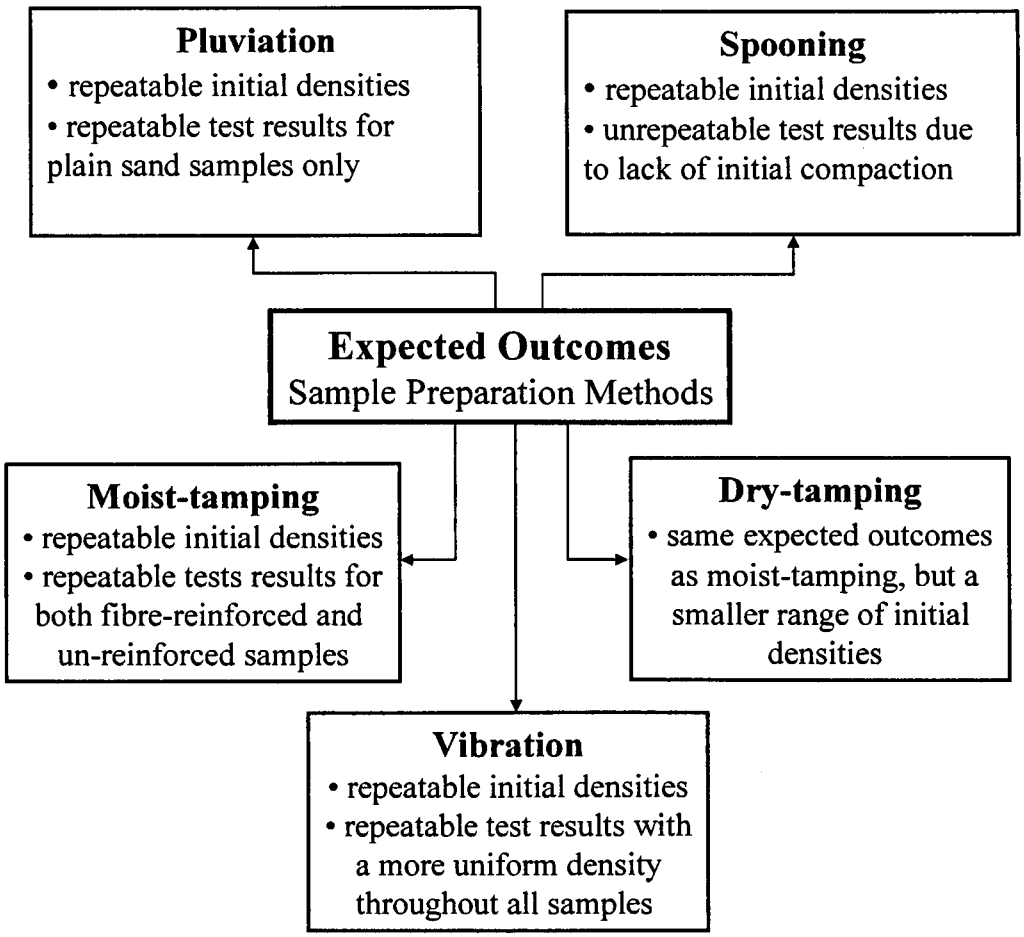

Figure 3.1: Expected outcomes of sample preparation methods

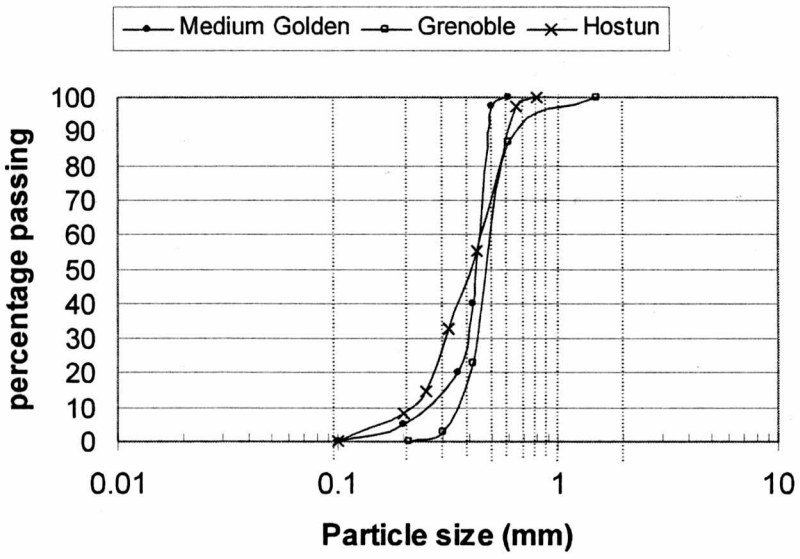

Figure 3.2: Particle size distribution chart for test sands

Sand	G_s	e_{min}	e_{max}	D_{10} (mm)	D_{50} (mm)	D_{60} (mm)	Cu	Shape
MGS	2.66	0.49	0.806	0.34	0.44	0.45	1.32	Sub-rounded
Grenoble	2.65	0.42	0.776	0.35	0.48	0.50	1.43	Sub-rounded
Hostun	2.65	0.62	1.014	0.23	0.40	0.45	2.0	Sub-angular

Table 3.1: Physical properties of the test sands

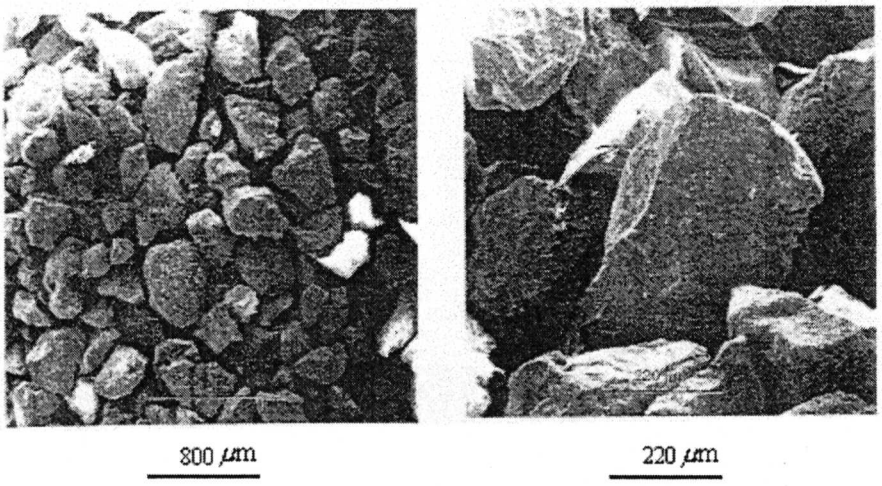

Figure 3.3: Microscope photographs of Hostun sand particles

(after Benahmed, 2001)

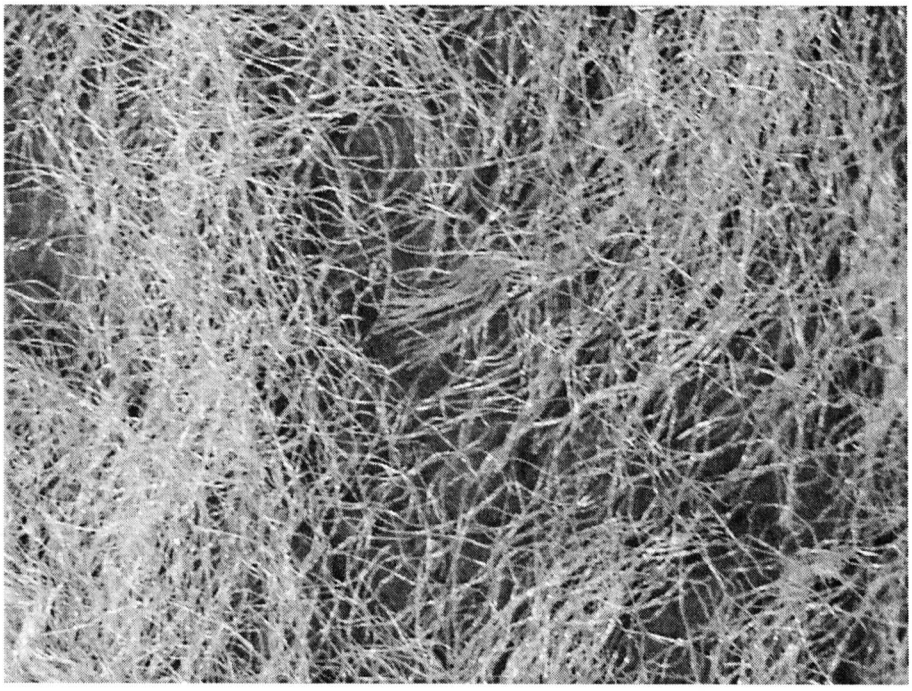

Figure 3.4: Photograph of test fibres

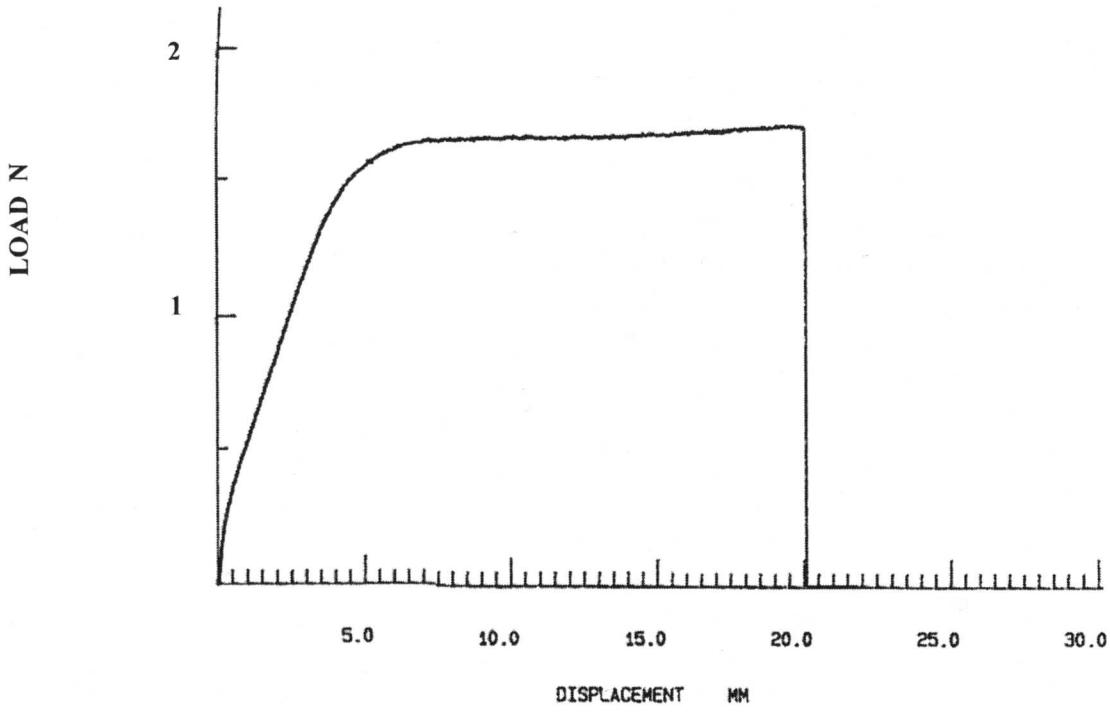

Figure 3.5: Fibre tensile strength

(after Bailey 2000)

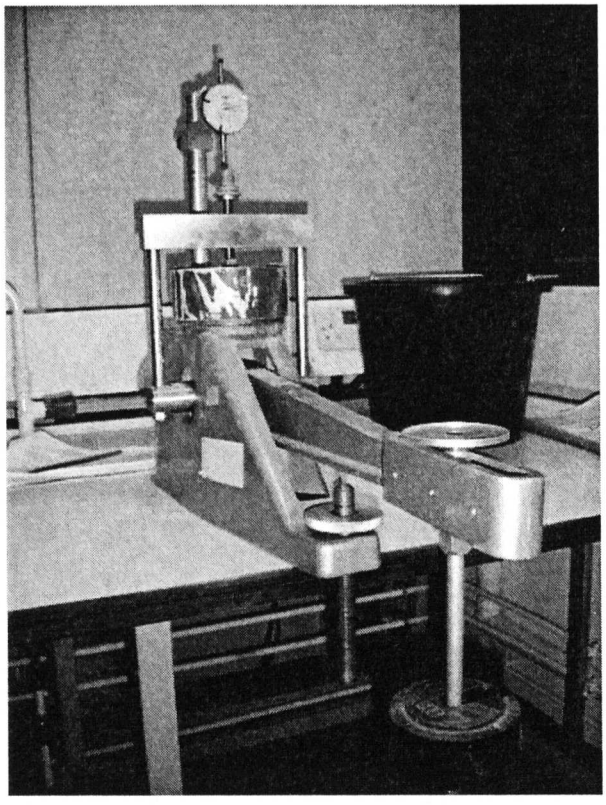

Figure 3.6: Oedometer apparatus

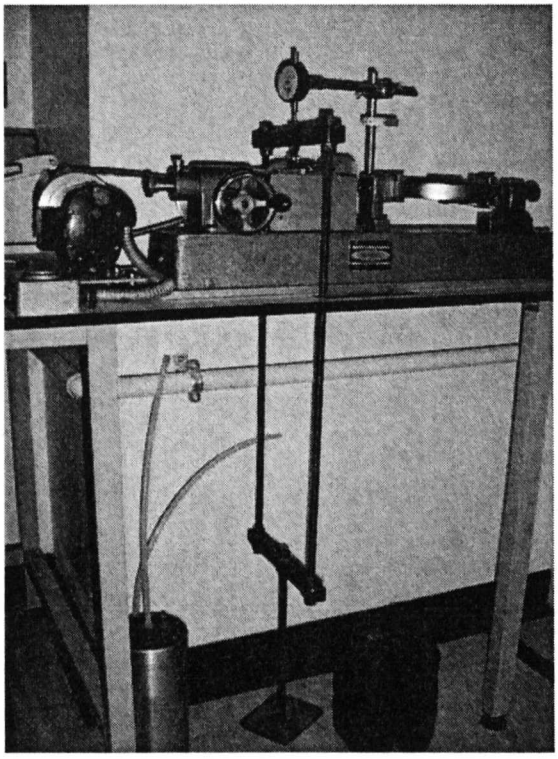

Figure 3.7: Shear box apparatus

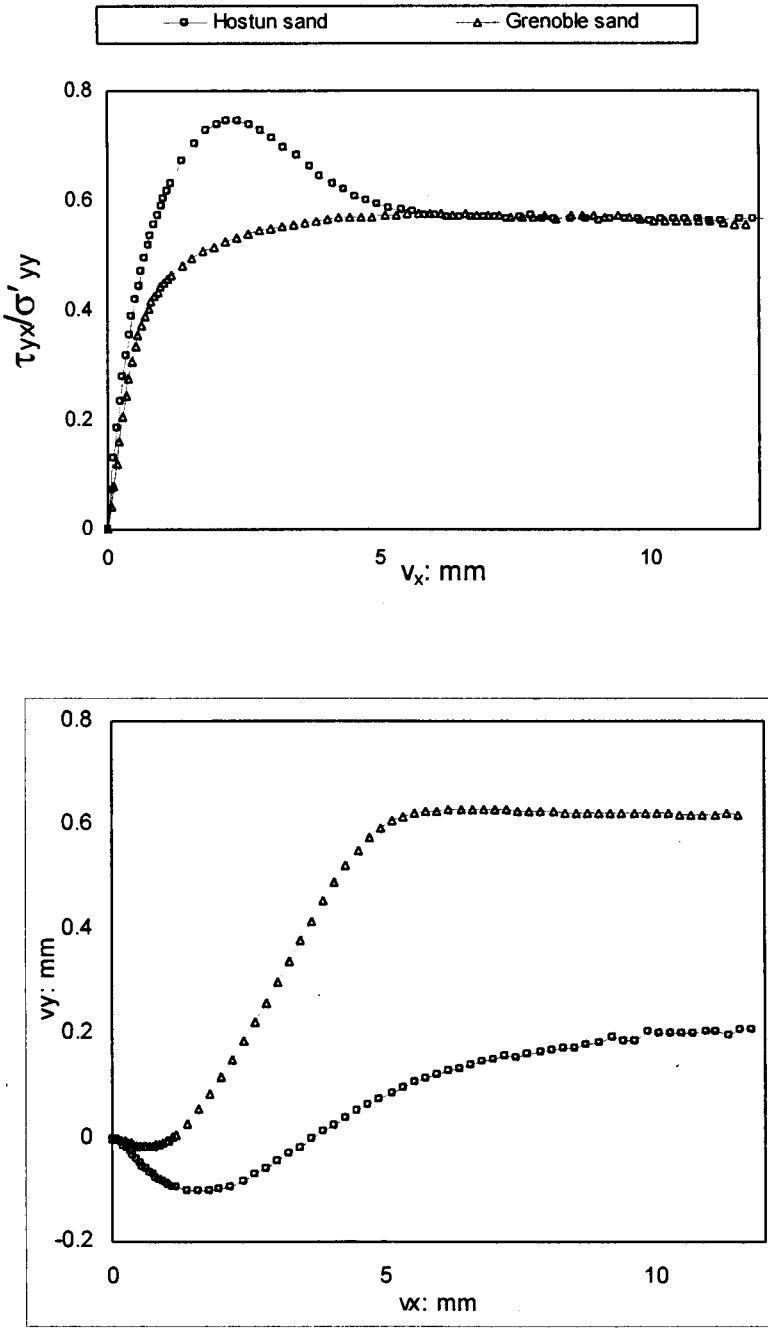

Figure 3.8: Hostun and Grenoble sands in direct shear (100 kPa normal stress)

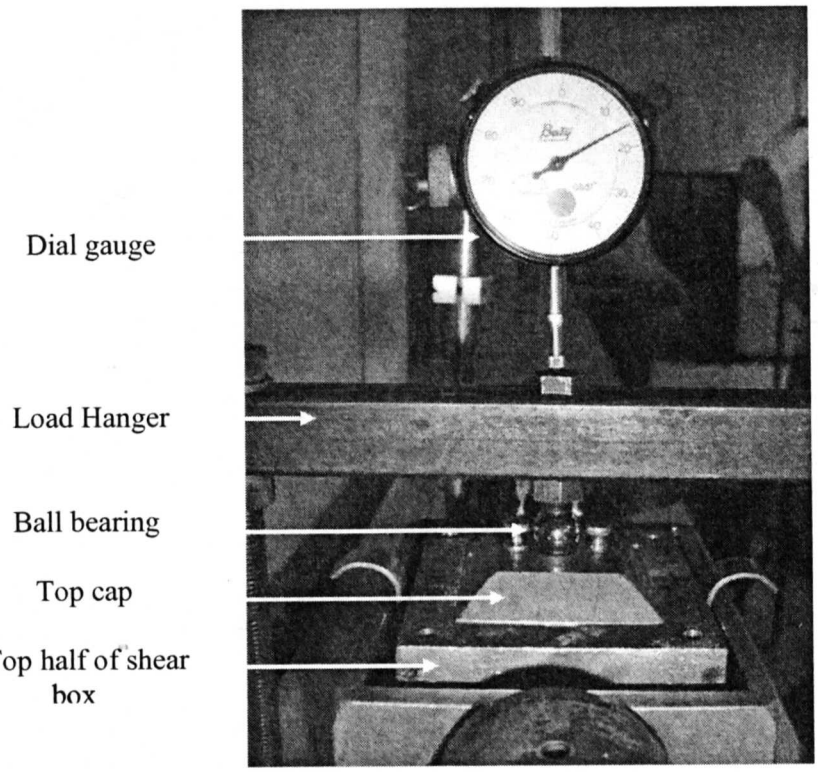

Figure 3.9: Load hanger-dial gauge configuration for the shear box test

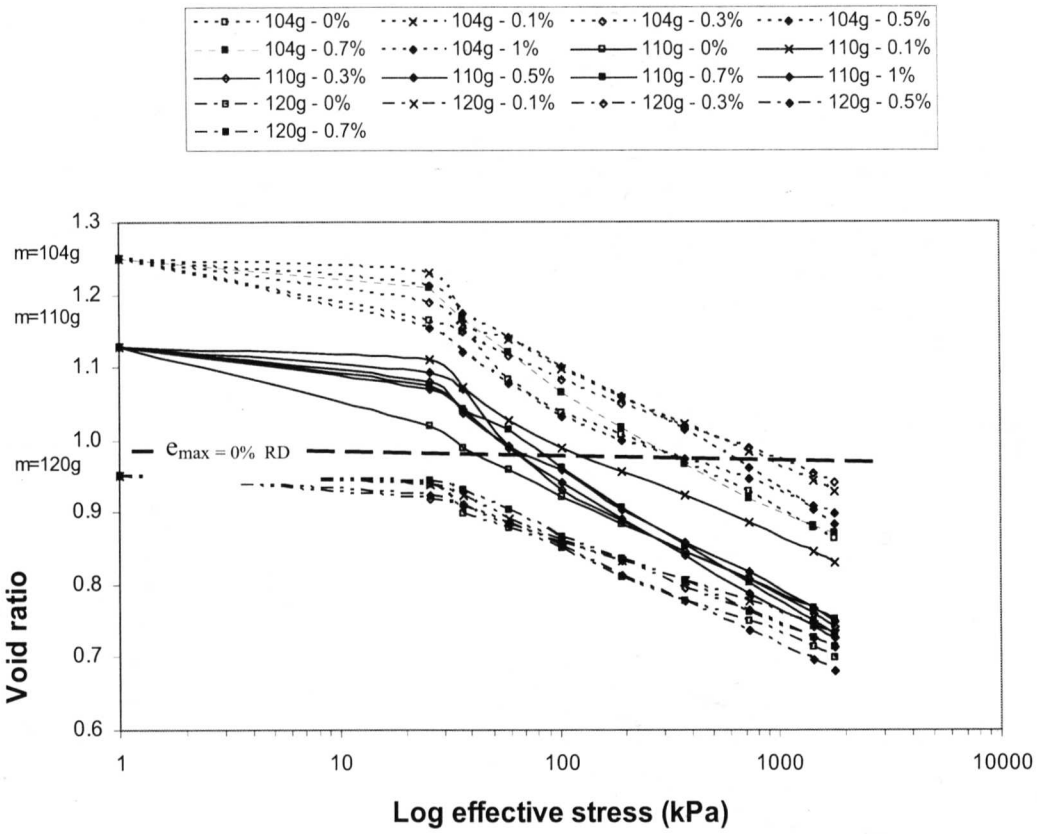

Figure 3.10: One-dimensional compression tests for MGS sand with 2% moisture content

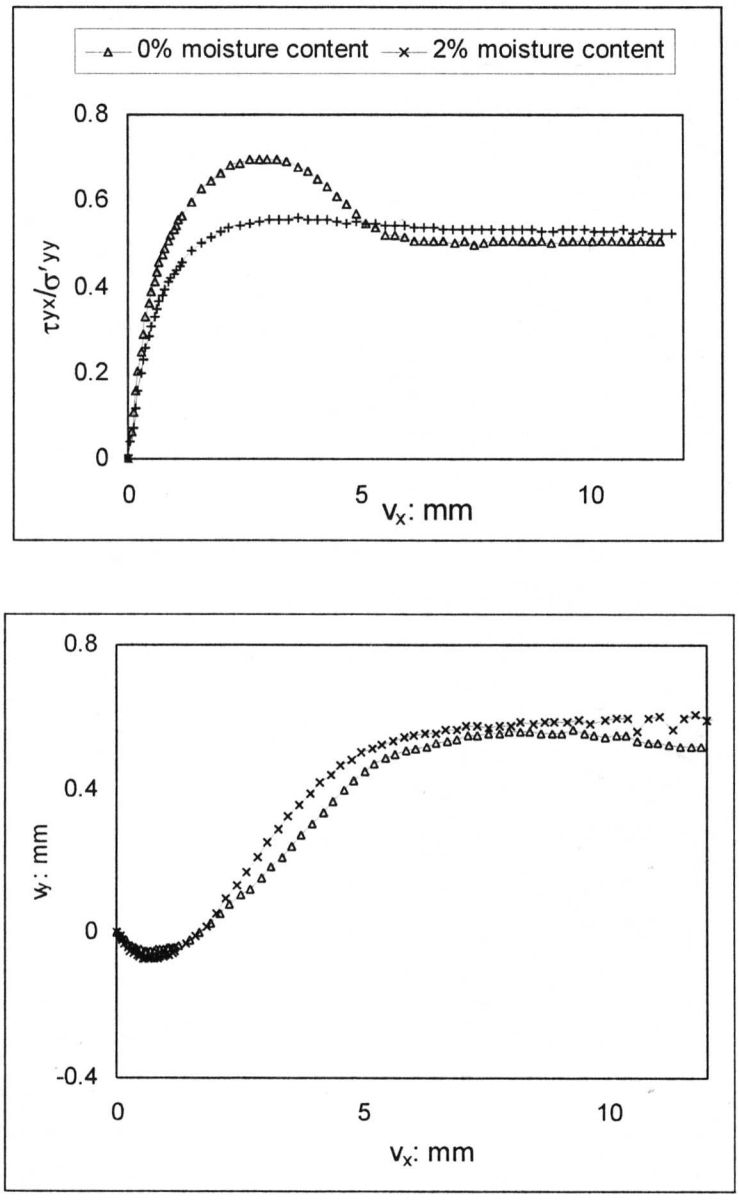

Figure 3.11: Moisture content comparison for Grenoble sand in direct shear (100 kPa normal stress)

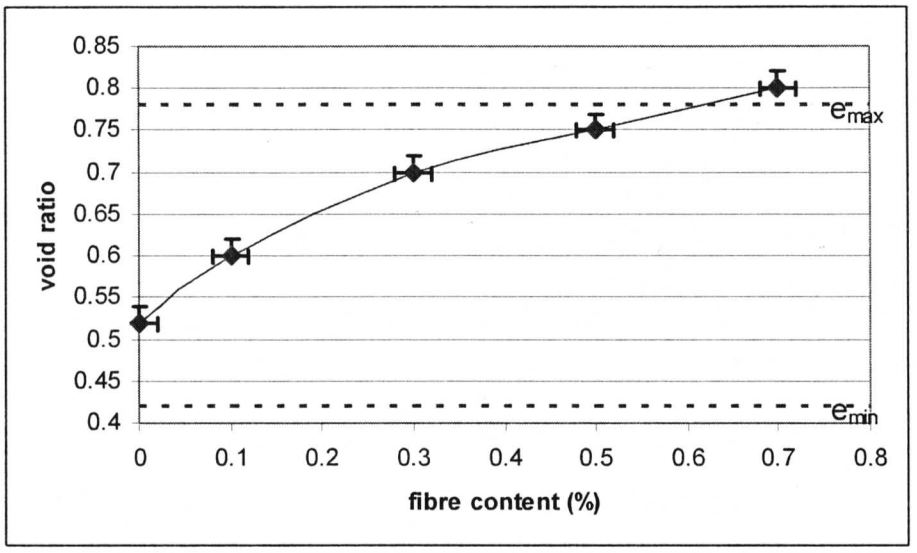

Figure 3.12: Void ratio limits of Grenoble sand with fibres

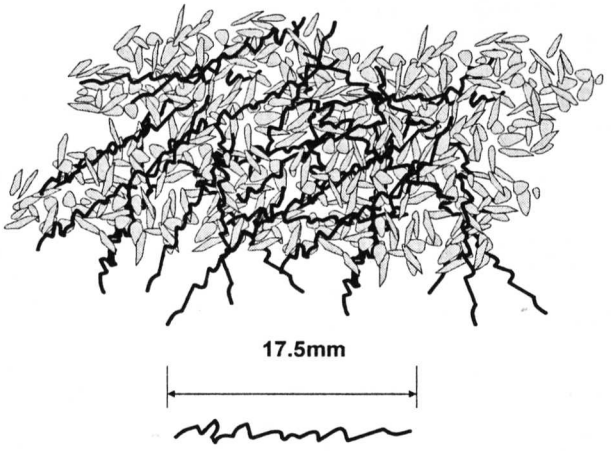

Figure 3.13: Schematic drawing of Hostun sand reinforced with *LokSand* fibres

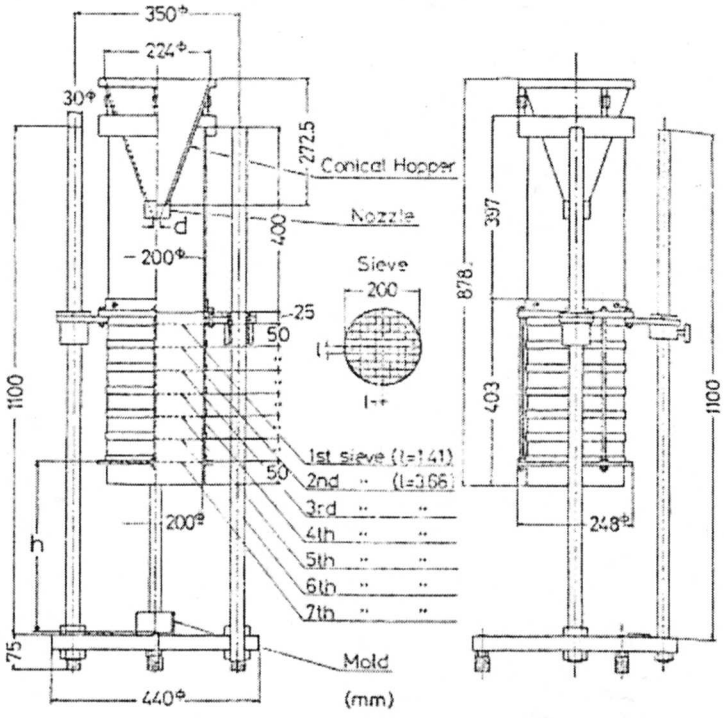

Figure 3.14: Muira and Toki multiple sieve pluviation apparatus
(after Muira and Toki, 1982)

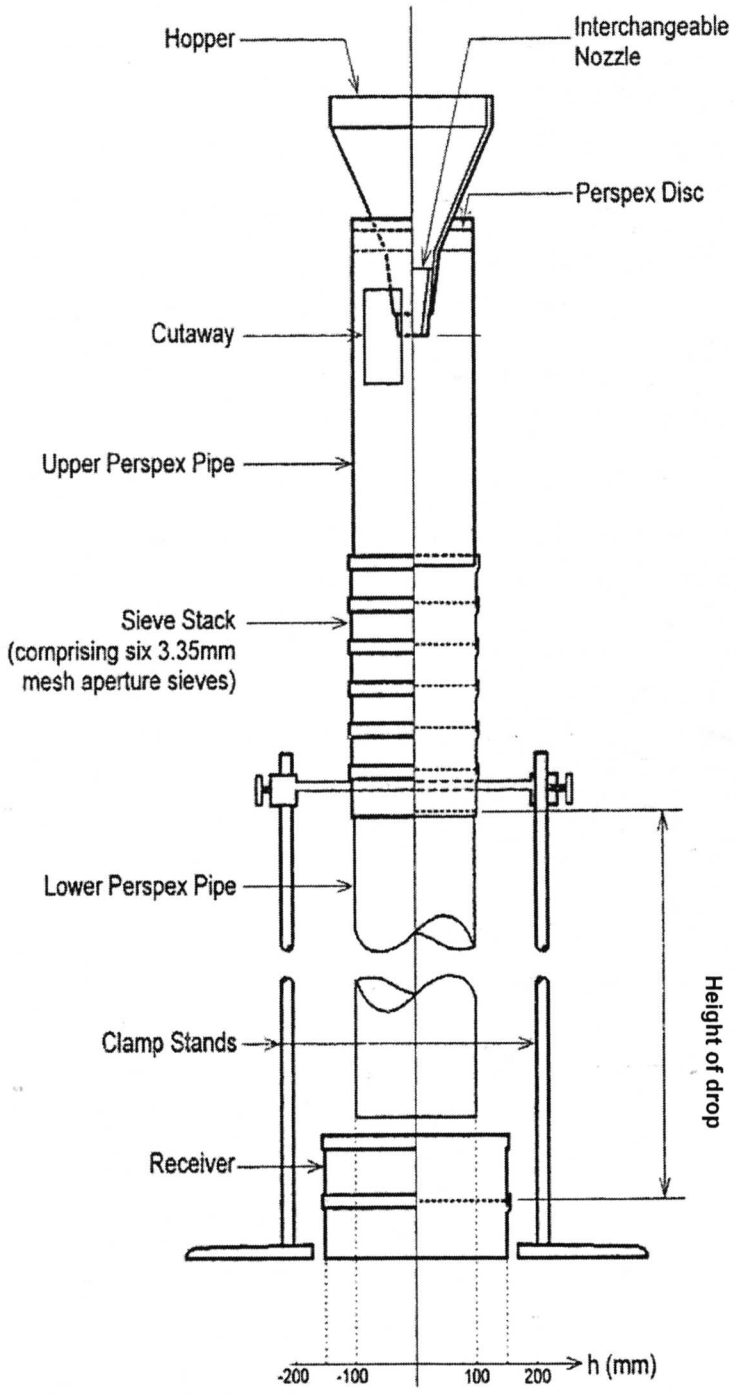

Figure 3.15: Configuration of the multiple sieve pluviator

(from Dietz, 2000)

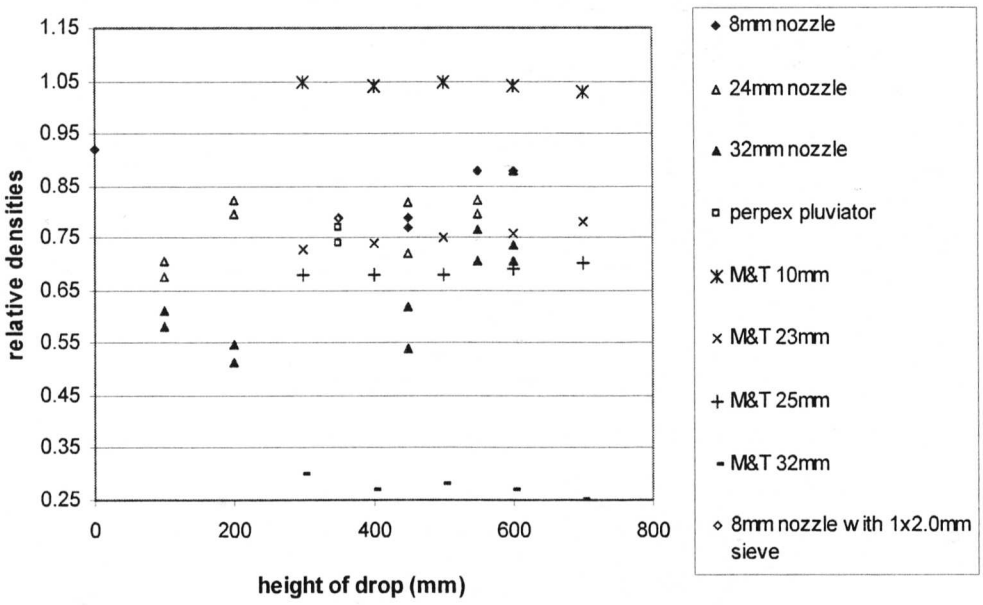

Figure 3.16: Relative densities achieved by pluviation

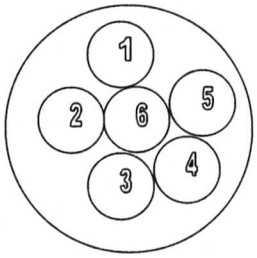

Figure 3.17: Pluviation cup placement

	Multi-sieve pluviator (6 x 3.35mm)			Perspex pluviator with 2.0mm mesh			Multi-sieve pluviator with single 2.0mm sieve		
	Test # 1	Test # 2	Test # 3	Test # 1	Test # 2	Test # 3	Test # 1	Test # 2	Test # 3
cup #	relative density			relative density			relative density		
1	0.88	0.88	0.94	0.79	0.82	0.79	0.91	0.88	0.88
2	0.91	0.88	0.94	0.85	0.82	0.79	0.91	0.88	0.94
3	0.88	0.88	0.94	0.91	0.88	0.82	0.82	0.94	0.88
4	0.94	0.96	0.99	0.91	0.88	0.85	0.88	0.91	0.94
5	0.85	0.94	0.88	0.79	0.79	0.79	0.79	0.88	0.88
6	0.79	0.77	0.79	0.77	0.74	0.74	0.79	0.79	0.79

Table 3.2: Relative densities of samples in cups after pluviation

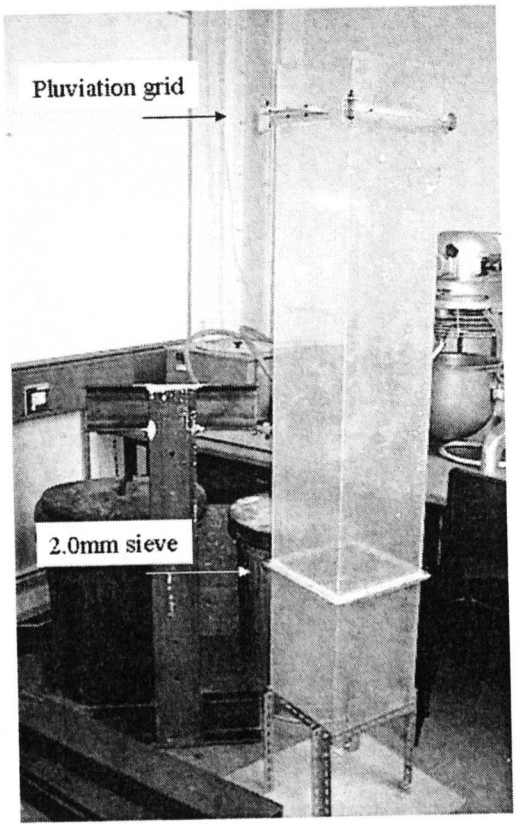

Figure 3.18: Perspex pluviator

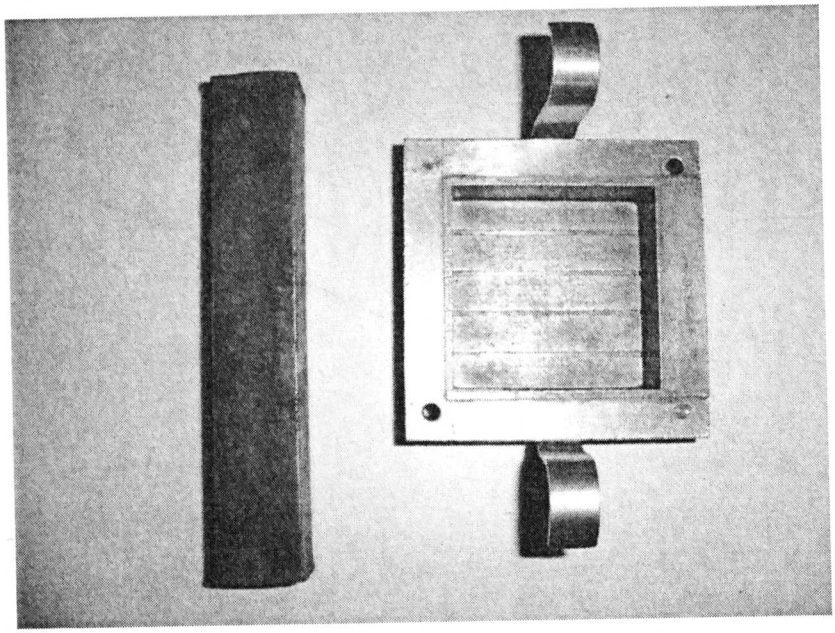

Figure 3.19: Steel bar and shear box (plan view)

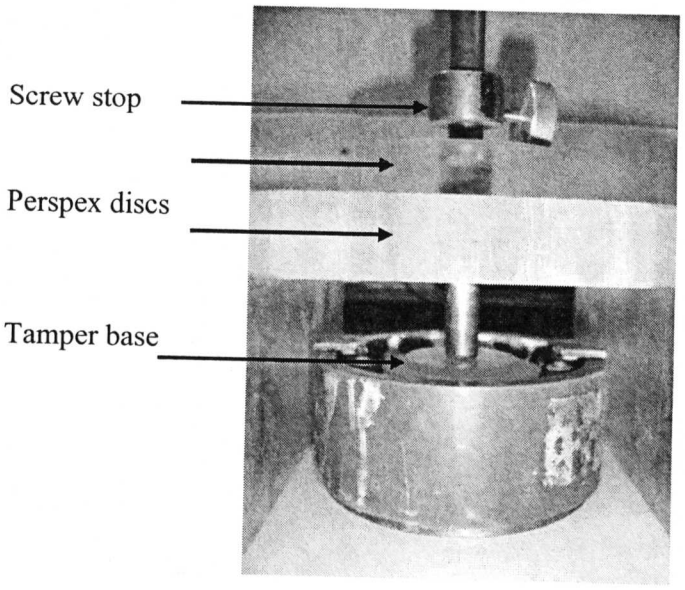

(a) oedometer cell

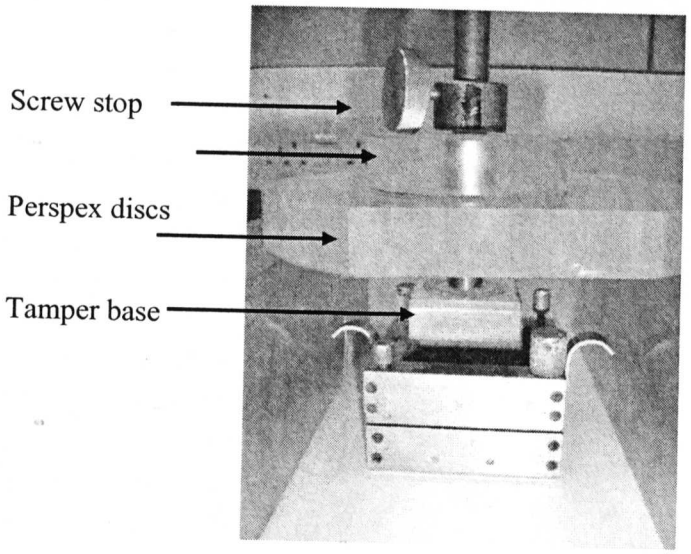

(b) shear box

Figure 3.20: Tamping devices

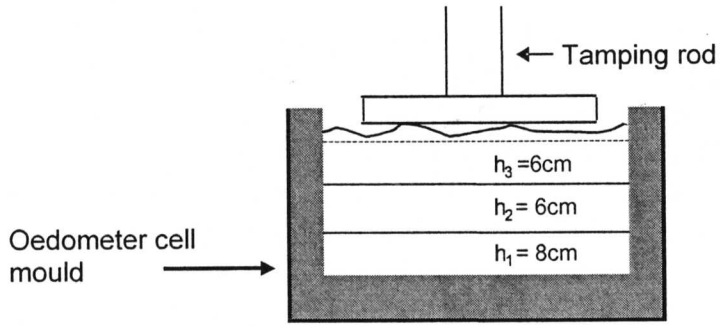

Figure 3.21: Layer heights for compression tests
(110 and 120g sample masses)

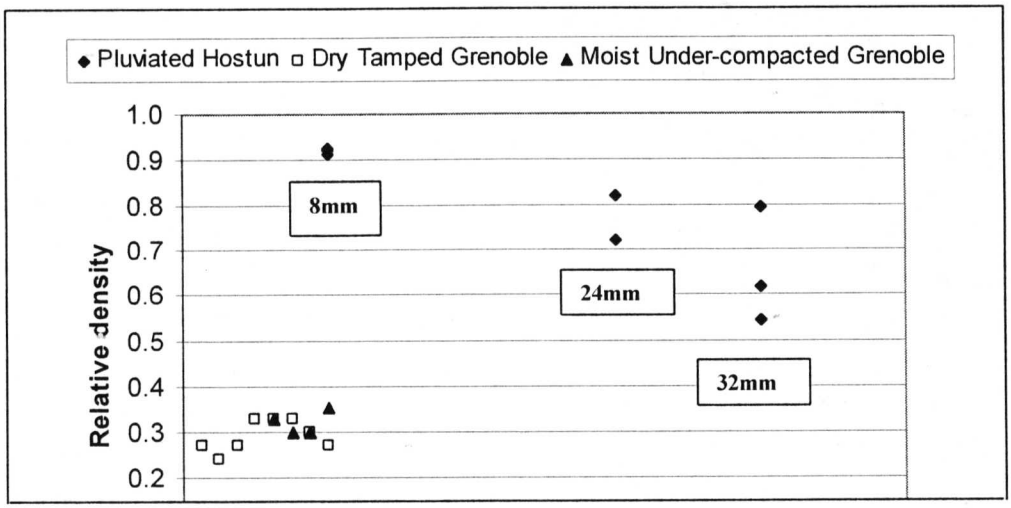

Figure 3.22: Relative density comparisons for Grenoble and Hostun sand sample preparation

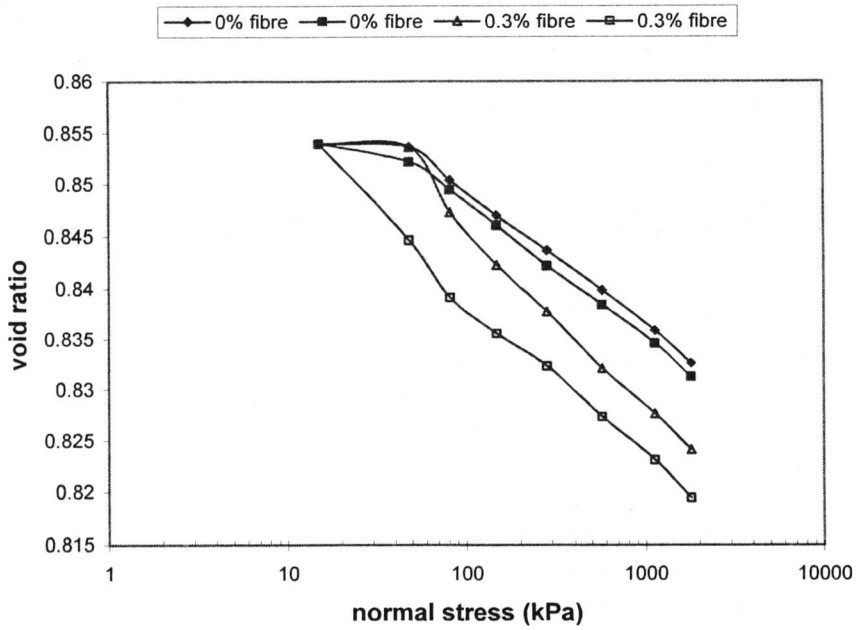

Figure 3.23: One-dimensional compression test results Hostun sand - spooned assembly

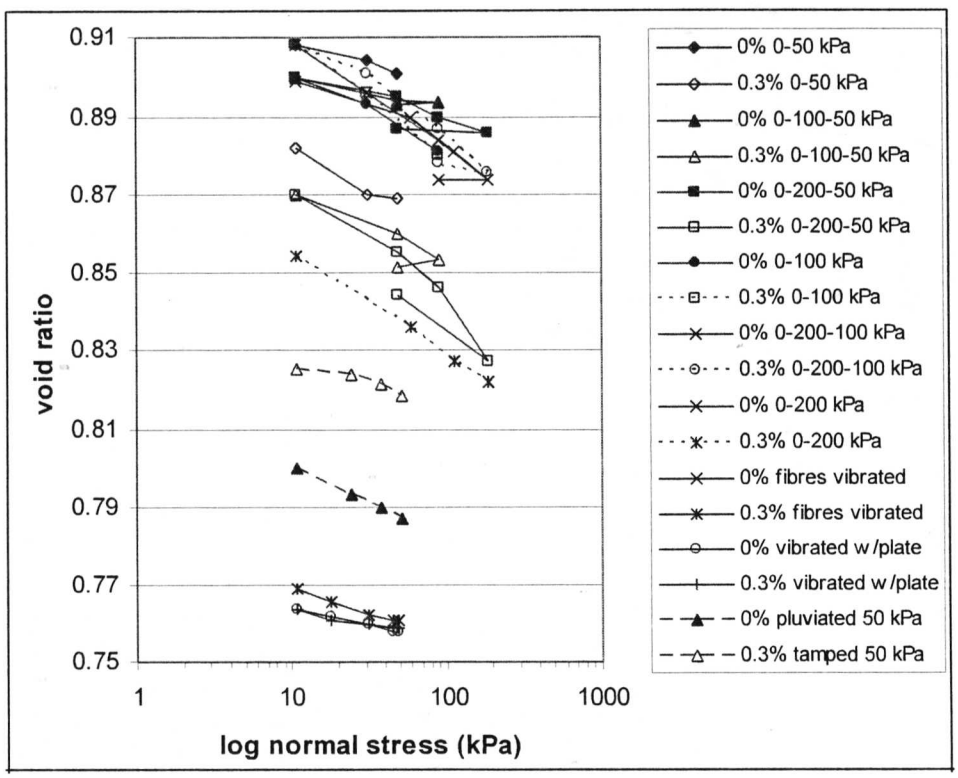

Figure 3.24: Compression of pre-stressed Hostun sand

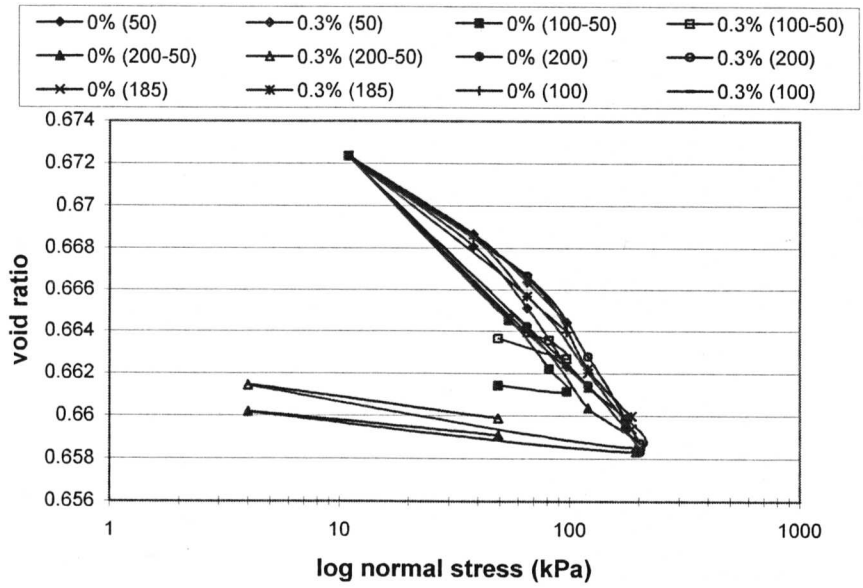

Figure 3.25: Compression of pre-stressed Hostun sand samples vibrated with a top plate

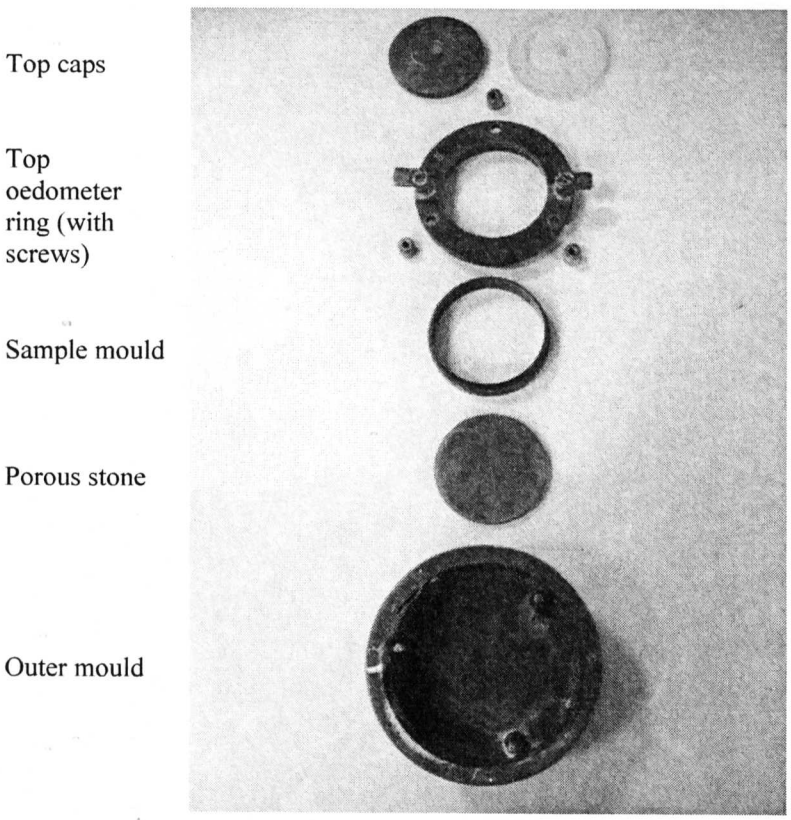

Figure 3.26: Components of the oedometer cell (including both the Perspex and bronze top caps)

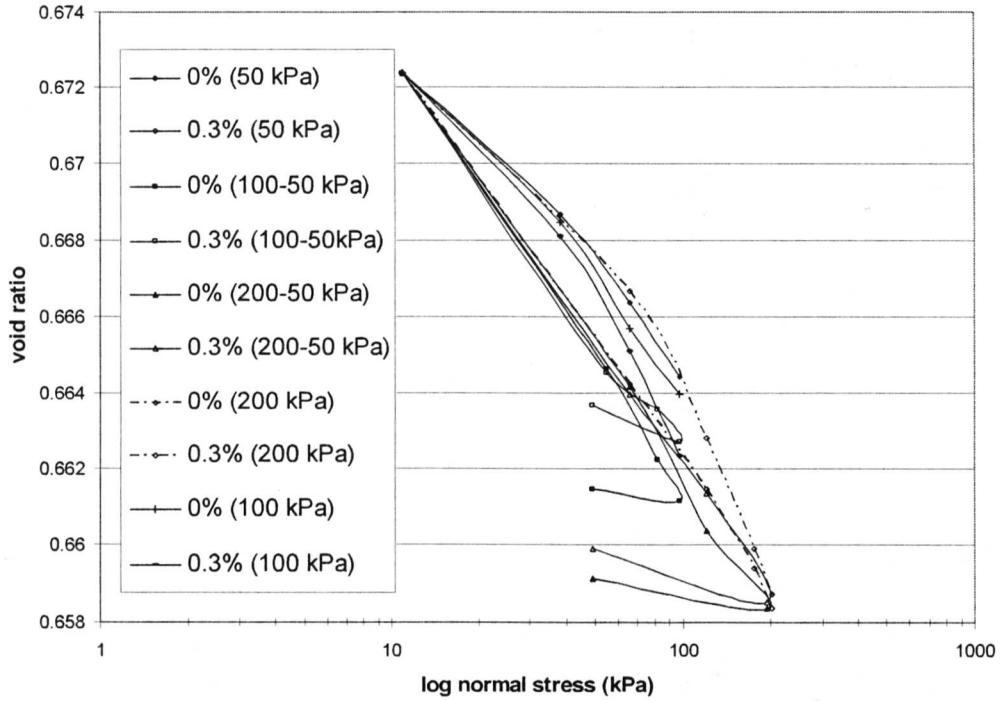

Figure 3.27: One-dimensional compression of pre-loaded samples

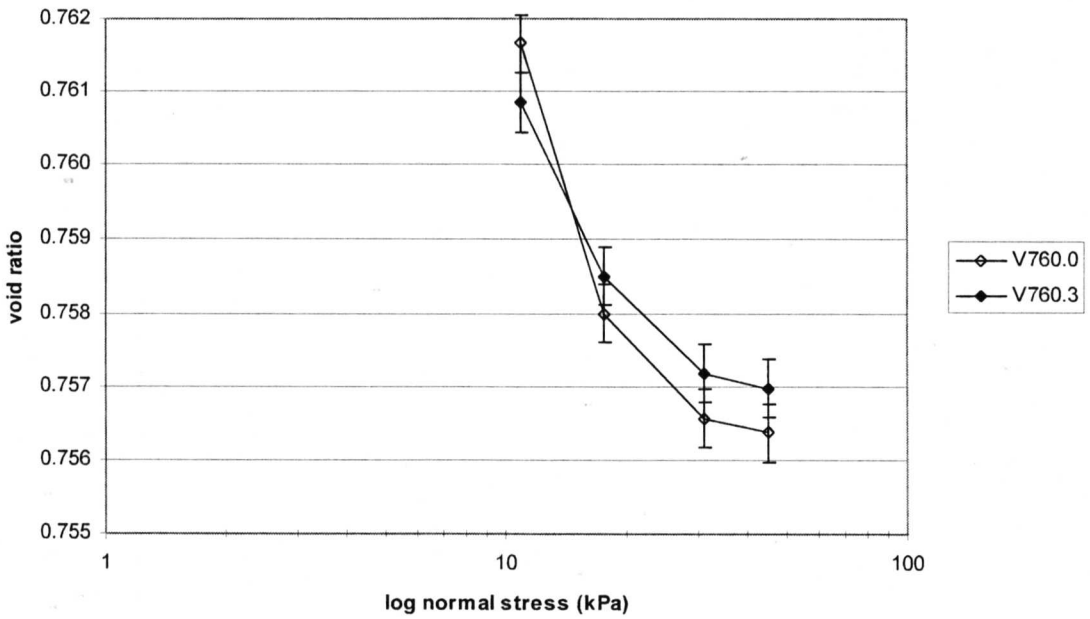

Figure 3.28: Repeatability graph for top cap tests (loose samples)

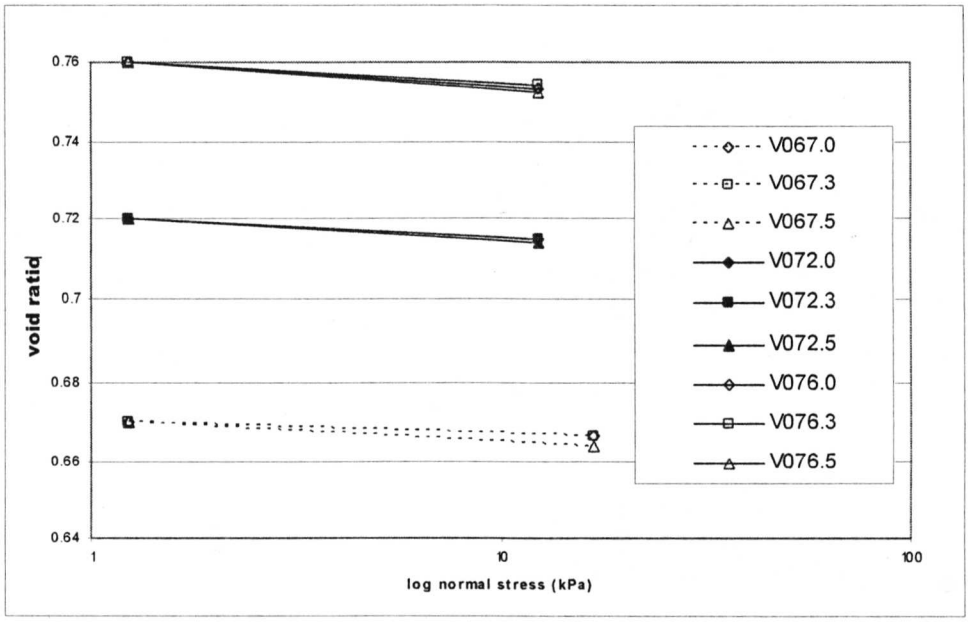

Figure 3.29: One-dimensional compression during the placement of the shear box top cap and load hanger

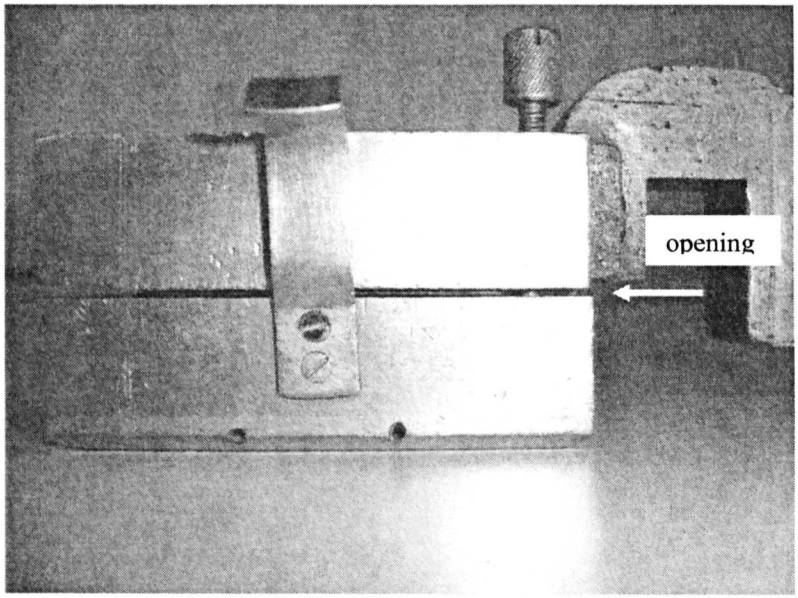

Figure 3.30: Side elevation of shear box with 2mm opening

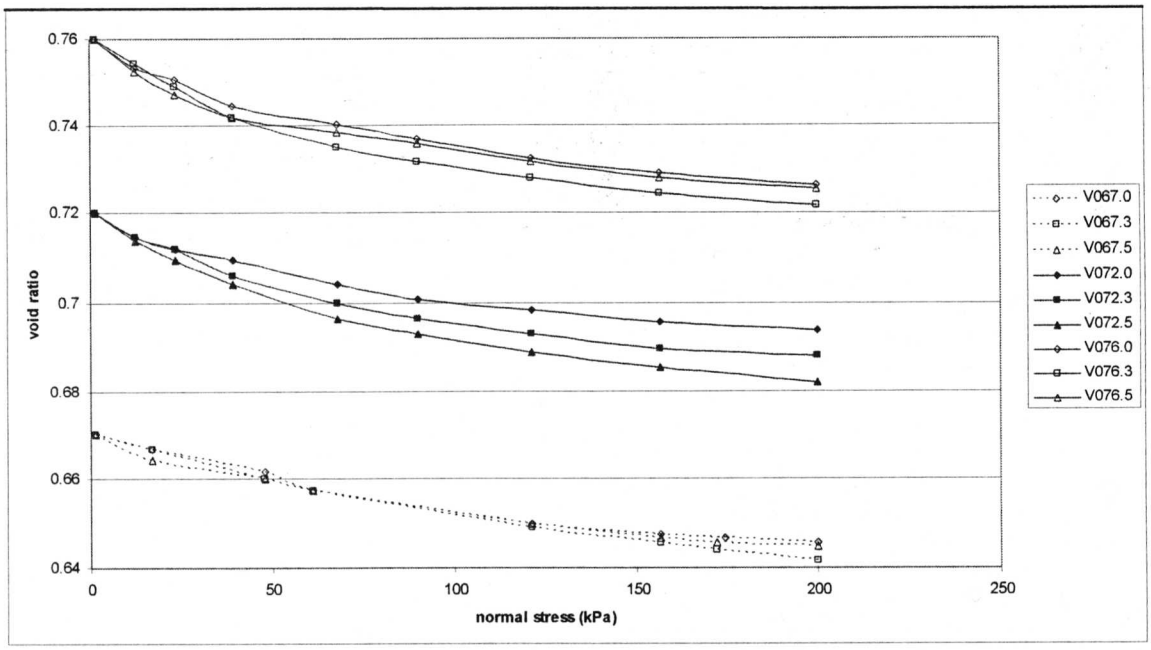

Figure 3.31: Compression of vibrated samples

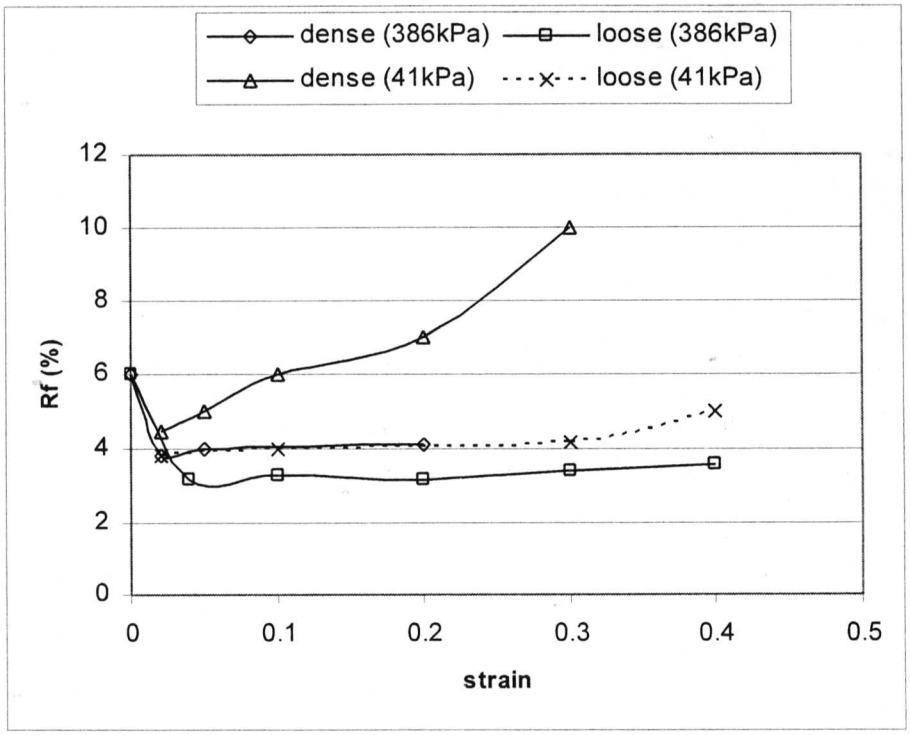

Figure 3.32: Wall friction ratio of percentage horizontal shear force R_f versus strain α

(after Stroud, 1971)

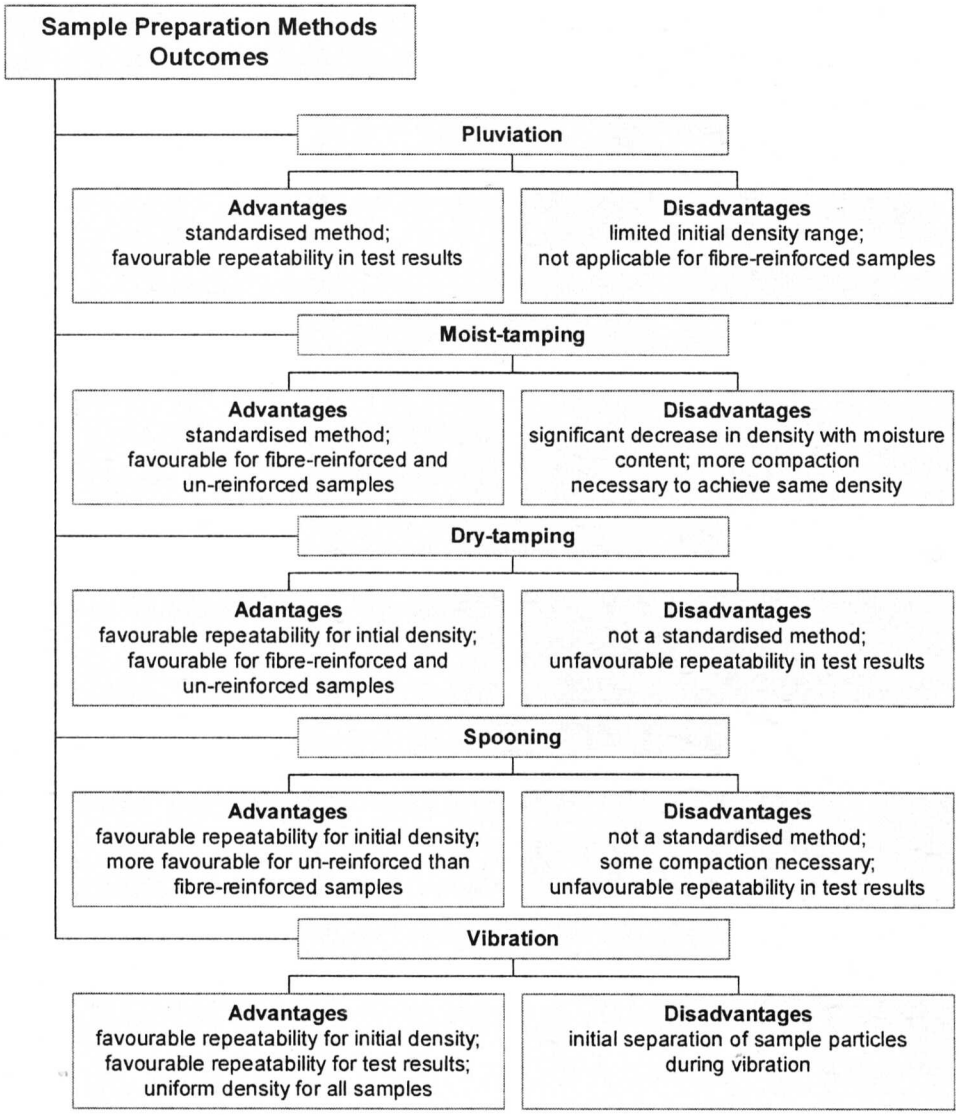

Figure 3.33: Sample preparation methods outcomes

4.0 Proctor Compaction Tests

4.1 Light Proctor compaction

The Proctor compaction test is a basic soil test employed to learn the maximum dry density and the optimum moisture content of a soil. Although *LokSand* fibres are used to resist deformation from dynamic loads, some type of compaction is necessary in the placement of moist soils reinforced with these fibres in the field to ensure the density of the fibre-reinforced soil layer. Proctor compaction tests were attempted in order to release trapped air from laboratory samples and compare the effects of a range of fibre contents and moisture contents on the maximum dry density values.

Light compaction tests were carried out according to BS1377: Part 4: 1990, clause 4, test 12 using Hostun sand with various fibre concentrations at various moisture contents. Each test sample was prepared with pre-determined fibre content from a single batch. The samples were oven-dried and re-mixed after each test before the moisture content of the mixture was increased for subsequent tests. The oven temperature range was from 102 to 105°C which is below the melting temperature for the fibres (150°C).

The inclusion of moisture content and fibre content increased the amount of voids in Hostun sand samples during mixing. Soil permeability affects the degree of coupling between the solid and fluid phases of a soil material and it plays an important role in the initiation and development of strain localisation (Liu et al, 2005). The optimum moisture content and the optimum dry density of *LokSand*-reinforced Hostun sand samples were found from plotting the Proctor tests results according to their fibre content.

4.1.1 Equipment description

A Proctor compactor was used throughout this study. Figure 4.1 shows the components of the apparatus in section. The Proctor compactor consisted of a circular steel 2.5kg hammer, having a facing diameter of 50mm and 450mm in length. A mechanical release gave the hammer a free vertical fall to the sample mould, which rested on a heavy solid base that mechanically rotated a few degrees horizontally in between releases to ensure uniform compaction. A counter controlled the hammer release and, hence, the number of blows of the hammer.

The circular test mould used for all tests had an internal diameter of 105mm and internal height of 115.5mm. A detachable base plate and extension collar provided additional accessibility for sample preparation and removal. Additional items used in the sample

preparation included a 20mm BS test sieve and receiver, a high-temperature oven, a balance accurate to 1g, a soil container, a spoon, a metal straight edge and a water pipette.

4.1.2 Sample preparation

The samples were prepared with 0.0, 0.1, 0.3, 0.5, and 0.7% *LokSand* fibre content by weight. To obtain the most representative data for the shear test samples, the *LokSand* fibres tested in compaction were cut from the original 35mm to 17.5mm length. The 1.8 kg soil samples were first sieved through a single 20 mm BS test sieve and then mixed by hand in a container. The fibre and moisture contents were weighed separately and hand-mixed with the Hostun sand. Each sample was separated into equal thirds by weight and each third was compacted in succession in the mould. Total samples were compacted in 3 layers with 27 blows of the hammer per layer. No other tamping or vibration was used in the samples' assembly.

The hammer had a maximum height of drop of 300mm to the base of the mould. Each layer surface was scarified so that the position of the layers would not be conspicuous upon test completion. The final layer surface was not higher than 5mm above the top of the mould, as suggested in Head (1992). A metal straightedge was used to level the sample with the top of the mould and remove the excess soil. The weight of the compacted sample was recorded while inside the test mould, and then the weight of the mould was subtracted from the total weight measurement.

A representative portion of each sample was removed to verify the moisture content and determine the dry density by calculation. The portions were placed in an oven overnight and the weight difference between moist and dry conditions was recorded. The test results were plotted as dry density values versus the moisture content, as measured from the representative oven-dried sample portions.

4.2 Compaction results

4.2.1 Hostun compaction

The results of all tests are plotted on graphs of dry density against moisture content in Figure 4.2. Air voids lines of 15%, 20% and 30% were also plotted on the compaction curve for Hostun sand samples. The air voids percentages were calculated by dividing the volume of air by the total volume of the soil. The results show that the samples were compacted to approximately 30% air voids (denoted as 30% Va in Figure 4.2) by light Proctor compaction. Decreasing density was seen with added moisture content beyond the peak dry density value for all Hostun sand test samples.

Figure 4.3 is a basic diagram of the proportion of the volume of air (Va), water (Vw) and soil (Vs) for the maximum dry density (a) and a sample with a greater moisture content (b) and the same volume of air. In this example, the samples would have had the same compactive effort, but different moisture contents. As the amount of compaction increased, the moistened sand mixed with fibres became denser due to the expulsion of air voids. In laboratory experimentation the fibres seemed to 'hold' the sand particles together from confinement within the mould during compaction compared to un-reinforced samples where the sand particles showed no such cohesion.

The dry density values rose up to a maximum dry density value as the moisture content increased from zero. Beyond the maximum dry density value, the samples became less dense with increased moisture contents due to greater saturation. The samples with 0.1% fibre content gave similar results to the un-reinforced samples (denoted as 0.0% f.c. in Figure 4.2). As the fibre content increased beyond 0.1%, the dry density of the reinforced Hostun sand samples decreased at all moisture contents. At low moisture contents a difference in fibre content of 0.2% by weight corresponded to a decrease in dry density of approximately 0.015 Mg/m^3. The greatest difference (0.05 Mg/m^3) in dry density between fibre-reinforced and un-reinforced sand was found at the peak dry densities, with moisture content of approximately 8%.

All Hostun sand samples exhibited a peak dry density at moisture contents between 7 and 8%. Figure 4.4 shows the peak dry density values for the fibre contents tested. The maximum dry densities for the un-reinforced sand and the sand with 0.7% fibre content were 1.540 Mg/m^3 and 1.505 Mg/m^3 respectively. The test results for Hostun sand samples reinforced with *LokSand* fibres are comparable to those for the fibre-reinforced sand produced by Fibresand Limited. Fibresand is prepared by mechanically mixing 35mm long *LokSand* fibres and granular soil with a moisture content of approximately 6% for commercial use.

4.2.2 Comparison with other test results

Bailey (2000) tested straight 35mm long *LokSand* fibres mixed in Berry Hill sand as provided by Fibresand Limited. The comparison of the soil properties for Berry Hill and Hostun sand is shown in Table 4.1. Based on the soil properties, Berry Hill can be summarised as uniformly graded sub-rounded sand, while the Hostun sand is uniformly graded and sub-angular. The two sands behaved differently in compaction with Hostun sand experiencing a distinct dry density peak and Berry Hill sand showing two dry density peak values for 0% fibre content.

The results obtained for the un-reinforced Berry Hill sand in Figure 4.5 are scattered (Bailey, 2000). Peak dry density values were reported to have occurred between 6 and 9% moisture content for 0%, 0.3% and 0.45% fibre content. The increase in fibre content resulted in an increase in the dry density up to 0.45% fibre content. The 0% fibre content samples showed scattered results without a definite peak value. The 0.3% fibre content samples seemed to reach a peak dry density of approximately 1.53Mg/m^3 after 9% moisture content and then neither increased nor decreased from that value. The 0.45% fibre content samples had increasing dry density values with increasing moisture contents. The inclusion of fibres increased the dry density at all moisture contents compared to the un-reinforced Berry Hill sand.

The effect of the fibres in the Proctor light compaction test results with Berry Hill sand obtained by Bailey (2000) was the opposite to that in the test results with Hostun sand. The greatest difference in dry density between fibre-reinforced sand and un-reinforced sand was slightly greater than the Hostun sand samples (-0.06 Mg/m^3) at a moisture content just below the maximum dry density value (approximately 5% moisture content). The maximum dry densities for Berry Hill samples with 0% fibre content, at the lower peak, and 0.45% fibre content samples were 1.48 Mg/m^3 and 1.52 Mg/m^3 respectively, with corresponding moisture content of 8%.

The Berry Hill samples showed a flattened peak on the dry density-moisture content curve. The imprecise peak dry density values in Figure 4.5 could be the result of poor sample preparation. Bailey's reinforced samples were initially prepared by industrial mixers in order to replicate field conditions. It is possible that the fibre reinforcements may not have been evenly distributed throughout the soil in all test samples, as the same test soil was oven dried and then re-used in Proctor compaction tests. The plain sand samples did not show a decisive peak value, so it is difficult to compare their behaviour with the fibre-reinforced Berry Hill sand samples.

The fibre-reinforced Hostun sand samples showed maximum dry density curves with good correlation to the un-reinforced sand sample behaviour at all moisture contents. The fibre-reinforced Berry Hill samples were more densified by light compaction than the un-reinforced sand samples, but the Hostun sand samples were made less dense with the inclusion of fibres in light compaction. It was concluded that the fibre-reinforced Hostun sand samples would require a greater compactive force to achieve the same dry density value than un-reinforced samples. This could be due to the different soil particle shapes and fibre lengths. Together with the different shape of the fibres (straight or crimped), these three variables are known to

affect the soil densities. The effects of different sample preparation methods can also produce different compaction curves depending on the sample preparation method.

4.3 Summary

Proctor compaction tests were attempted to determine the effects of a range of fibre and moisture contents on the dry densities of Hostun sand samples. The optimum dry densities for 0.0, 0.1, 0.3, 0.5, and 0.7% *LokSand* fibre-reinforced Hostun sand were all found at between 7 and 8% moisture content by dynamic compaction. The light Proctor compaction test results showed good repeatability for samples compacted to approximately 30% air voids. The dry density-moisture content relationship of test samples was compared with other fibre-reinforced sand samples that showed less favourable repeatability. The spurious compaction curves for Berry Hill sand was thought to be the result of poor sample preparation.

Increased fibre contents produced samples with lower dry density values in the compaction tests of Hostun sand samples. The fibres' ability to confine the soil particles translated into less soil escaping the Proctor mould during compaction and a greater compactive effort was driven onto the particles. Although the compactive influence of each blow of the hammer was increased as a result of the soil confinement, the fibres resisted deformation. A difference in fibre content of 0.2% by weight resulted in a dry density decrease of approximately 0.015 Mg/m^3 for low moisture contents.

In small-scale laboratory tests the inclusion of crimped fibres increased density compared with the un-reinforced Hostun sand at all moisture contents. The maximum dry density values ranged from 1.540 to 1.505 Mg/m^3 for fibre content of 0.3% and greater. Beyond the peak value the moisture contents were very low and void ratios were high as the dry density values reduced.

The behaviour of the samples in dynamic compaction is extremely useful in order to observe the deformation characteristics of the fibre-reinforcements. The magnitude of normal stress and type of load application used in this test is closer to the stress conditions the fibres are manufactured to resist in the field. Light Proctor compaction tests are useful for the basis of comparisons with the one-dimensional deformation characteristics and with the work done by Bailey (2000).

The results of light dynamic compaction showed that the inclusion of fibre reinforcements in Hostun sand decreased the samples' dry density values. The one-dimensional compression tests in the oedometer apparatus described in Figures 3.25 and 3.26 also showed lower

densities achieved by the fibre-reinforced sand samples. As a greater amount of (low-stress) compaction was required in the sample preparation of fibre-reinforced sand samples in order to achieve the same initial density values as un-reinforced sand samples, in Proctor tests an equal amount of dynamic compaction produced LokSand-reinforced samples with lower densities than plain Hostun sand at all moisture contents.

Fibres have proven to increase and sustain plastic deformation at large normal stresses. The moistened fibre-reinforced sand samples subjected to light Proctor compaction resisted the vertical deformation most at higher moisture contents. As can be seen in Figure 4.2, the fibre-reinforced Hostun sand samples had lower dry densities than un-reinforced samples in the range of 13 - 18% moisture content. More friction tended to exist between the soil particles in un-reinforced samples drier than their optimum moisture content. Un-reinforced soils wetter than the optimum moisture content exhibit less internal friction in compaction as the voids fill with water rather than air. However, the Hostun sand samples reinforced with fibres showed increased internal friction with moisture contents from their optimum value (7-8%) and greater (up to 18%) when tested in dynamic compaction.

4.4 Tables and figures

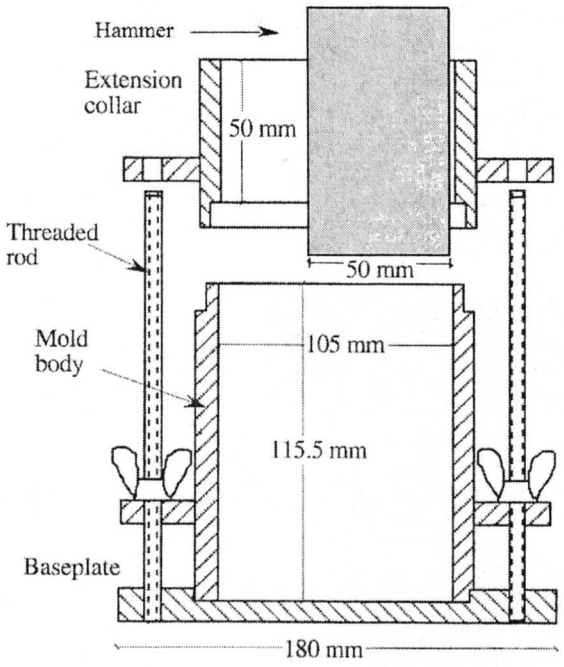

Figure 4.1: Proctor compaction mould section

(from Bardet, 1997)

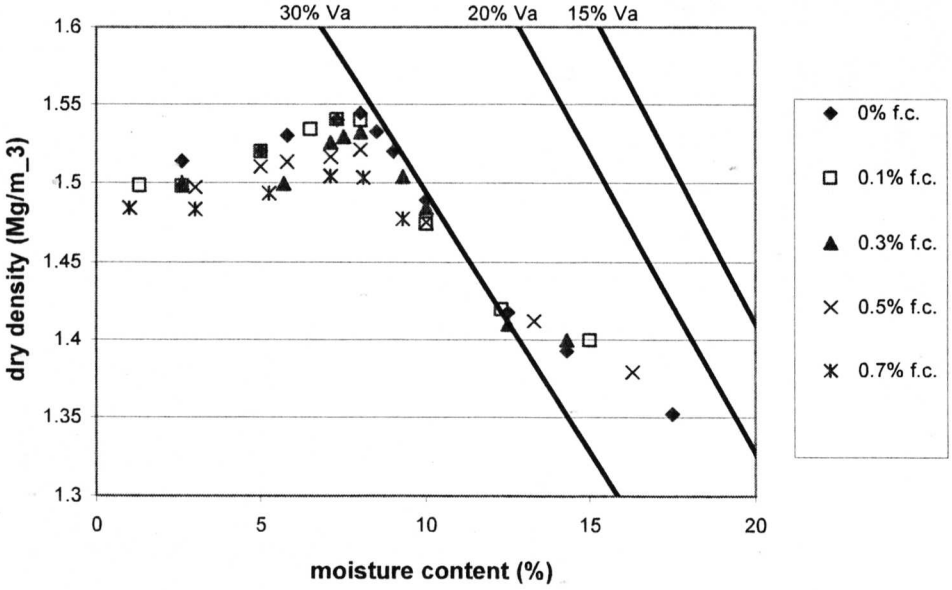

Figure 4.2: Proctor Light Compaction results

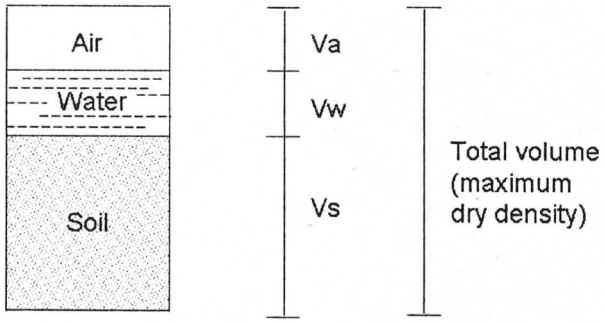

(a)

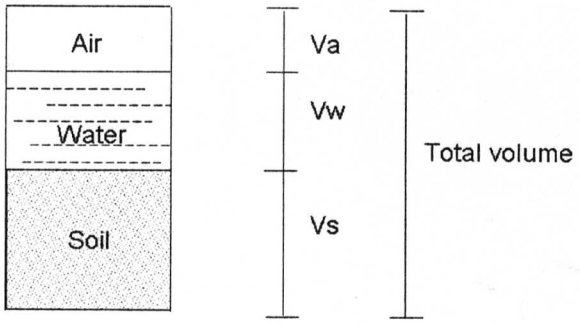

(b)

Figure 4.3: Model Proctor soil samples

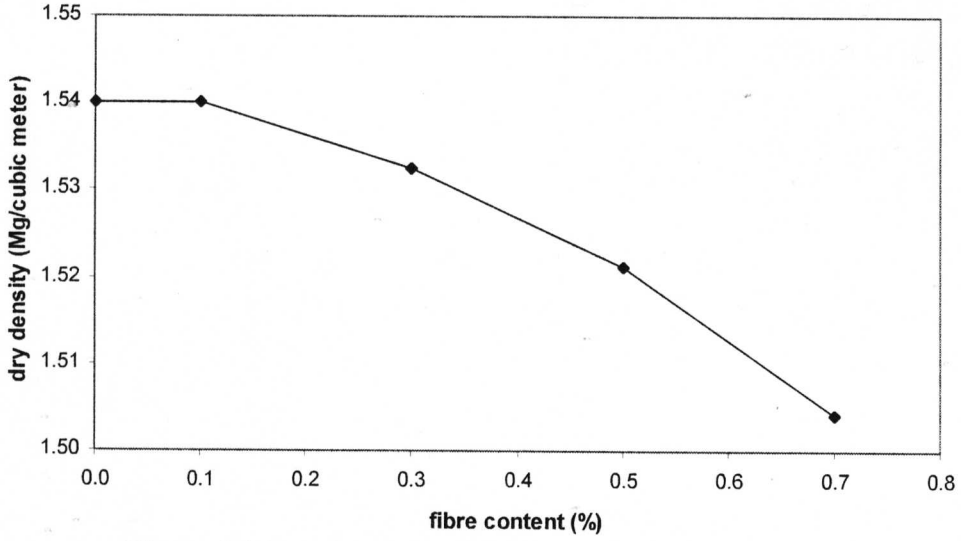

Figure 4.4: Maximum dry density versus fibre content Hostun sand

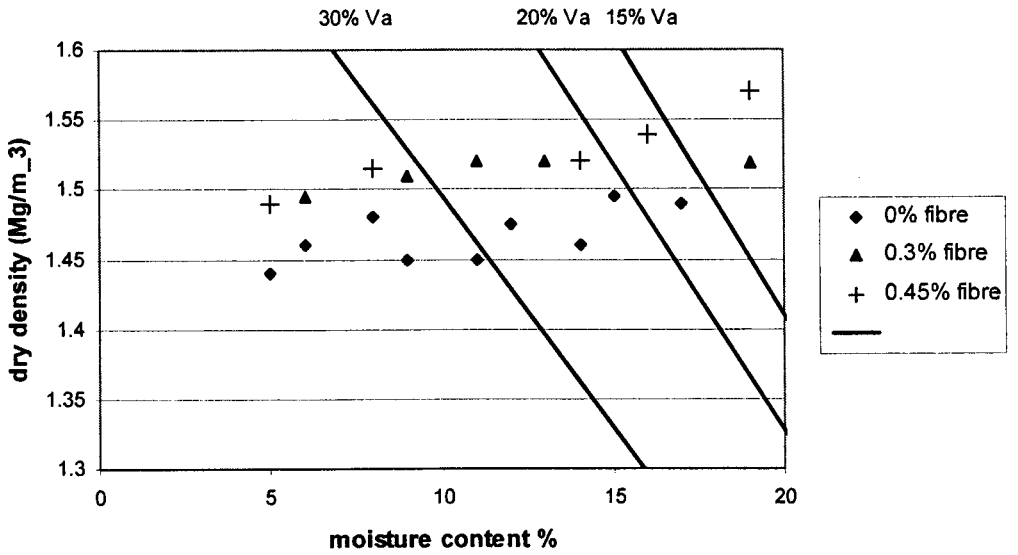

Figure 4.5: Light compaction by Proctor on Berry Hill sand

(after Bailey, 2000)

Table 4.1: Soil properties for two sands

Sand	G_s (Mg/m^3)	D_{10} (mm)	D_{50} (mm)	D_{60} (mm)	Cu	Shape
Hostun	2.65	0.23	0.40	0.45	2.0	Sub-angular
Berry Hill	2.64	0.32	0.36	0.37	1.16	Sub-rounded

5.0 Experimental results and discussion

In this chapter the results of the one-dimensional compression and direct shear tests are discussed. Details of the mechanical behaviour of the test sands with and without the inclusion of crimped polypropylene fibres tested in direct shear are included. The experimental results of samples reinforced with various percentages of fibre are presented and the effects of the fibre contents are discussed. Samples were loaded with vertical loads larger than the loads used for subsequent direct shear tests in order to assess the possible confining effects that a large normal pre-load can have on a sample's shear stress-deformation characteristics. The peak and critical stress states of sheared samples are presented along with their volumetric deformations based on the initial densities and normal stress values. The peak internal angles of friction were compared according to normal stress, initial density value and fibre content of samples.

Observations of *LokSand*-reinforced Hostun sand samples characteristics are compared with published direct shear test results for similar laboratory samples. The fundamental soil mechanics of the samples determined in this chapter will form the basis for the evaluation of the model in Chapter 6. A general summary of the laboratory results concludes this chapter.

5.1 Overview of results

Both traditional and modified sample preparation methods have been used to prepare fibre-reinforced test samples with different initial densities. The information provided by the low-stress sample preparation compaction results (vibration, moist- and dry-tamping) offer a picture of the fibre-reinforced sand deformation behaviour under static vertical stresses compared to un-reinforced sand. In the Light Proctor dynamic compaction test results, the blow count of the dynamic compaction lowered the sample densities. The inclusion of fibres has appeared to confine soil particles in both moist and dry conditions, while also allowing greater vertical deformation to take place when subjected to normal stresses. As was seen in the one-dimensional compression test results for MGS samples with 2% moisture content in Figure 3.10, a certain amount of compression must take place in the sample preparation in order to adequately confine the fibre-soil bond within samples (and in the case of MSG sand, a great deal of compression was necessary in order to bring samples within the void ratio limits of the soil).

The fabrication process can significantly change the mechanical properties of the interface region between the fibres and the soil grains in the form of residual stresses and volumetric changes as the test results in this chapter will show. Both the initial density of a sample and the normal stress value altered the interface bond strength.

The information about the shear strength and the reinforcing mechanisms of a fibre-sand mix can be measured in a multitude of ways for a variety of different soil characteristics. The direct shear response of samples with different normal stress levels and fibre contents follows. The normal stresses of 50, 100 and 200 kPa were applied in order to compare the peak and critical state stress values as well as the increased internal angles of friction for different confining stresses. The normal stress value of 200 kPa was used for the sake of completeness as in reality, this would be not a likely load. All vertical deformations were related to the sample density and the volume change considerations were reported in terms of void ratio and dilatancy effects. The differences of the typical response to normal stresses for fibre-reinforced samples and un-reinforced samples in shear have been evaluated and compared with other researchers' data.

The pre-loading of samples with vertical loads larger than the loads used for subsequent shear tests was attempted in order to assess the possible confining effects that a large normal pre-load can have on a sample's volume change characteristics. The pre-loading resulted in an initial confining stress for the soil-fibre interface in hand-spooned samples before they were sheared with 50 kPa normal stress. The flexible lightweight fibres did not contribute to the compressive stiffness of test samples; however, the fibre-reinforcements have been seen to be able to resist shear stress in experimentation depending on the confining stress value.

Direct shear tests results for *LokSand*-reinforced Hostun sand were compared with the behaviour of reinforced soil in direct shear reported by Bailey (2000). Bailey (2000) tested different sands with *LokSand* fibre reinforcements, similar to those used in this study, in direct shear with high normal stresses. The similarities and differences in sample behaviour were explored based on the strength and deformation characteristics of the reinforcements.

5.2 Light compaction behaviour

5.2.1 Dry density values based on fibre content

It was seen in Chapter 4 that the fibre-reinforced Hostun sand samples had lower dry densities than un-reinforced samples in the range of 13 - 18% moisture content. This behaviour was accredited to the fibres' ability to resist deformation and confine soil particles when subjected

to large loads. The reinforcing effect of the fibres in moist Proctor test samples seemed to occur in the region around 12% moisture content. The dynamic compaction increased the densities of Hostun samples with greater fibre and moisture contents. When comparing reinforced and un-reinforced samples subjected to equal amounts of compaction, dynamic compaction mobilised the tensile strain of fibres within a sand mass after a moisture content of 12% and resisted vertical deformation to produce samples with lower dry densities than un-reinforced samples (see Figure 4.2). This behaviour can be interpreted as another example of fibres improving the deformation resistance of granular soils once an optimum density value that sufficiently confines the sand particles is achieved.

5.3 One-dimensional compression behaviour

5.3.1 Compression characteristics of fibre-reinforced sands

A series of one-dimensional compression tests were conducted on samples spooned and pre-loaded or vibrated in the shear box to observe the effects of different preparation techniques. The independent variables used in the measurement of pre-stress deformation were vertical stress, the compacted void ratio, the weight of the test apparatus top cap and the as-compacted pre-stress loads. The samples were loaded with normal stress values chosen to pre-compress the samples by the normal load values that they will have in direct shear tests. After loading, the vertical recovery of the samples fabricated by the spooned preparation was recorded at 50 kPa normal stress. The pre-loaded samples are denoted as (100-50 kPa) and (200-50 kPa) in the graph legend. The results are compared with samples that have not been pre-loaded, denoted as fibre content (% by weight), V (vibrated preparation method), and 50, 100 or 200 kPa (normal stress). The vertical displacements of the samples from one-dimensional compression test results are shown in Figure 5.1.

A "yield stress" was taken as the point of the greatest curvature on the compression curve. For the test results shown in Figure 5.1, the fibre-reinforced samples experienced yield at lower normal stress values compared to the un-reinforced samples. The samples' deformation behaviour was considered as a representation of the samples' internal stability, therefore the region that shows a "yield" marks a point of sample instability. The vibrated samples generally compressed under static normal loads less than the pre-stressed samples prepared by spooned assembly. These two tests had different initial densities, as spooned samples could not be prepared to medium-dense or dense void ratio values. This is assumed to be due to the fibres offering a greater confinement to the sand particles than samples that were hand-spooned into the test mould without any type of initial compression or densification.

The test samples pre-loaded with 100 and 200 kPa had a lower initial void ratio at 50 kPa normal stress than the samples not pre-loaded. The un-reinforced samples had a void ratio value of 0.667 at 50 kPa, but this value for 50 kPa normal stress dropped to 0.661 and 0.659 after a pre-load of 100 and 200 kPa respectively. This shows that there was greater vertical deformation between samples pre-loaded at 100 and 200 kPa (void ratio difference = 0.006) than between samples with 50 and 100 kPa (void ratio difference = 0.002). As would be expected, the results showed that un-reinforced sand samples pre-loaded with 200 kPa were much denser than samples pre-loaded with 100 kPa. The dry un-reinforced Hostun sand samples with an initial void ratio of 0.667 showed greater vertical deformation at smaller loads and less deformation at larger loads. These samples were more compressible at lower stresses for this initial void ratio, but the repeatability of the compression characteristics was extremely favourable.

The samples reinforced with 0.3% fibre content exhibited slightly higher void ratio values under 50 kPa normal stress (0.667, 0.664 and 0.660 at 50, 100 and 200 kPa respectively) compared to the un-reinforced samples. The 0.3% fibres demonstrated slightly greater resistance to deformation than plain sand. The samples pre-loaded up to 100 or 200 kPa also demonstrated a recovery of some of the vertical displacement when the load was removed. The post-stress recovery of these samples from 100 or 200 kPa to 50 kPa is evident in the graph.

The vibrated fibre-reinforced samples showed greater compressibility than vibrated plain sand samples. Comparing their compression trend with the pre-loaded samples, the vibrated fibre-reinforced samples did not deform as much as the spooned samples. It is possible that the fibres in the vibrated samples had a greater confinement due to vibration compared to the spooned samples.

5.3.2 Effect of initial density

In Figure 5.1, the greatest scatter was seen in the compression curves of samples under normal stresses greater than 50 kPa. In Figure 5.2 the vertical deformation of vibrated samples (fibre length = 17.5mm) previously presented in Figure 3.31 is now shown on a logarithmic scale of normal stress. The densest and loosest samples show a small range of scatter for void ratio values at 200 kPa stress, while the medium density samples show the largest scatter. For the two lowest initial densities, the samples deformed more with increasing fibre content.

5.3.3 Effect of fibre length

The one-dimensional compression behaviours of samples reinforced with fibres of both the original 35mm length and the modified 17.5mm length are shown in Figure 5.3. The vertical deformation under normal stresses of 10 to 50 kPa was extremely similar for both fibre lengths. The greatest disparity between the 35 and 17.5mm fibre length deformation results was seen in the loosest sample at approximately 18 kPa where the fibre length did not significantly affect the vertical deformation of dense samples. The overall conclusion that can be drawn from this series of tests is that the reinforcing effects of the fibres were not mobilised in one-dimensional compression for either of the fibre lengths under small normal stresses. In order to observe improved vertical deformation resistance from reinforced samples compared to un-reinforced samples, the compression loads would have to be greater.

5.4 Pre-loaded samples

5.4.1 The significance of stress history

The load carrying capacity of soil reinforcements operates best with large loads, so pre-loading of fibre-reinforced samples was attempted to compare the peak stress ratios with smaller loading conditions. In the pre-load sample preparation, higher stresses were required to compress fibre-reinforced sands to achieve the same density as un-reinforced sand. A small amount of confinement attributed to pre-loads greater than 50 kPa mobilised the tensile deformation of the fibre-reinforcements before shear took place. Soil reinforcements are usually pre-stressed or pre-loaded in the field, but published literature rarely describes such sample preparation processes in detail. The pre-loading of a series of shear test samples was regarded as a sample preparation method and the significance of the stress history for these pre-loaded samples can be seen in this section.

In the case of the Mohr circle, the tangent $\tau = \sigma \tan \phi' + c'$ is shown as the shear failure plane for soil. Very small and very large normal stresses can give incorrect values for the failure envelope when modelling the soil behaviour. This occurrence may be due to lower stresses that may not sufficiently confine the fibres with the soil particles. It may also be due to higher normal stresses that could potentially crush the soil particles hence, degrading the particles in the shear zone and effectively lowering the shear strength value. The normal stress values chosen for this thesis should adequately confine test samples without crushing the sand particles, as Colliat et al (1988) found the average crushing strength of Hostun sand to be ~ 10 MPa.

According to critical state soil mechanics theory, there is a unique void ratio value for each state of effective stress at critical state that is independent of initial state and the mode of shearing. The evolution of critical state for fibre-reinforced sand samples was evaluated over a range of initial conditions. The evolution of strain localisations to critical state for dense sands has typically been considered to occur only within a shear band, however fibre inclusions can spread the volumetric strains throughout a dense sample according to their physical locations. Finno and Rechenmacher (2003) found that the relationship between void ratio and effective stress at critical state is dependent upon the consolidation history and the initial state of sand.

The evaluate the consolidation history of fibre-reinforced sands, spooned samples were pre-loaded with 100 or 200 kPa normal stress before the shearing commenced to pre-load the samples' granular structure. The pre-load values were chosen to pre-compress the samples by the normal load value that they will have in direct shear tests. After loading, the vertical recovery was recorded at 50 kPa normal stress. The vertical displacements of the samples from one-dimensional compression test results were shown in Figure 5.1. In order to observe the effects of pre-load stress history in fibre-reinforced samples, a portion of the pre-load was removed to leave a total of 50 kPa normal stress as the applied confining stress. The samples were then sheared under 50 kPa normal stress.

5.4.2 Pre-loaded direct shear tests

Different stress ratio values and dilatancy behaviour for fibre-reinforced and plain sand samples in direct shear were characterised by their prior loading conditions. The direct shear test results are shown in Figure 5.4 for 100 kPa pre-load and Figure 5.5 for samples with 200 kPa normal stress pre-load. All samples were prepared to have an initial void ratio value of 0.672 in the test mould. The vertical deformations after placement in the test apparatus were similar for both fibre contents (fc = fibre content in the table below), although this behaviour is counter-intuitive. The initial void ratios for the pre-loaded samples immediately before shear commenced were as follows.

Pre-load intensity	Initial void ratio 0% fc	Initial void ratio 0.3% fc
0 kPa	0.668	0.668
100-50 kPa	0.661	0.664
200-50 kPa	0.659	0.660

The stress ratio of pre-loaded samples steadily increased in shear as the horizontal displacement increased. The samples without pre-load reached a peak stress ratio by the point of 3mm horizontal displacement in both graphs, before reducing to their residual stress values which were approximately 8% lower than the peak value. Samples with 0.0% and 0.3% fibre reinforcement sheared at 50 kPa normal stress did not reach peak shear strength values at the void ratio value tested, as the stress ratios continued increasing until the end of the tests. The peak stress ratios for all samples are shown below.

Pre-load intensity	Peak stress ratio 0% fc	Peak stress ratio 0.3% fc
0 kPa	0.656	0.937
100-50 kPa	0.688	1.199
200-50 kPa	0.728	1.095

Increasing the confining stress of samples in the form of pre-load resulted in increased angles of friction for all samples. The peak internal angles of friction for Hostun sand samples increased by +1.5° with 50 kPa increased pre-load value (100 – 50 kPa) and +2.8° with 150 kPa pre-load increase (200 – 50 kPa). The samples reinforced with 0.3% fibre content had peak friction angles twice these values (+3° with 50 kPa increased pre-load and +6.8° with 150 kPa pre-load increase) as seen in the table below.

Pre-load (kPa)	0 % fibre content angle of friction (degrees)	0.3% fibre content angle of friction (degrees)
50	33	38
100 – 50	34.5	41.8
200 - 50	36.2	43

Figure 5.6 shows the angles of friction for samples plotted according to their pre-load stress value. From these failure envelopes of samples tested under 50 kPa normal stress, the average peak internal angle of friction for fibre-reinforced samples was 40.9°, an average increase of +6.3° from the average plain sand friction angle (34.6°) due to 0.3% fibre content. This behaviour introduces a failure envelope for the range of confining stresses from 50 to 200 kPa for samples with the same initial density tested in shear under the same normal stress. The results of this investigation show that the confining stress influences the internal angle of friction for samples tested under the same normal stress in shear. From the range of confining stress values shown, a model for the critical confining stress of dense samples under 50 kPa

normal stress in direct shear can be developed based on the average peak internal angle of friction for fibre-reinforced and un-reinforced Hostun sand samples (see 6.3.1).

Average angles of friction	0% fibre content	0.3% fibre content
	34.6°	40.9°

For samples with an initial void ratio of approximately 0.67, a higher confining stress in the form of normal stress pre-load increased the angle of internal friction mobilised on the shear plane, as well as the angle of dilatancy and, hence, strengthened the samples tested with 50 kPa normal stress. The stress-dilatancy behaviour seen in Figures 5.7 and 5.8 demonstrated that samples with an applied pre-load dilated less during shear. The samples initially dilated linearly, and after the peak stress value the increased dilation depended on the amount of fibre reinforcement. Samples with higher fibre content dilated more than less reinforced samples in all cases.

The inclusion of fibres improved the soil stiffness and enabled Hostun sand samples to achieve superior shear strength values at large displacements. The model used to illustrate the relationship between stress ratios and the rates of dilation for plane strain can be seen in Figure 5.9. According to this graph, the peak angles of dilatancy increased when the confining stress increased from 50 kPa (no pre-load) to 200 kPa pre-load (denoted as 200-50 kPa in the legend). The results for 100 kPa pre-load (denoted as 100-50) showed a slight decrease in dilatancy. The peak friction angles increased with the addition of fibre content and with increasing pre-load values for all tests. The samples showed increased strength during shear up to peak values according to the initial densities of the samples.

The angles of dilation were higher for the fibre-reinforced samples, which confirm that the reinforced samples are able to deform more and mobilise the tensile strain of the fibres while reaching their peak stress ratio. The angles of dilatancy decreased from 9° to 8° for the reinforced 50 and 100-50 kPa samples respectively and their un-reinforced angles of friction were quite similar. This suggests that an optimum confining stress for Hostun samples with 0.0 and 0.3% fibre content lies between the initial pre-load values of 100 and 50 kPa for samples with initial void ratio of 0.67, sheared with 50 kPa normal stress.

The pre-loaded samples were tested in shear to provide an indication of the effect of the confining stress value. The three different stress histories demonstrated different stress-deformation characteristics depending on the normal stress value before shear. Pre-compression is used in the field to densify the fibre-reinforced soil mass and strengthen the

interface bond between the two materials. This small-scale study reflected the strengthening effects of pre-loading. Increasing the confining stress mobilised the fibre reinforcements to sustain higher peak shear stress values for greater shear displacements. Let us now turn our attention to the volume changes that took place in the samples when the stress ratio values increased.

5.4.3 Volume changes due to pre-load

The stress ratios were plotted against the volumetric deformation (dy/dx) of the pre-loaded samples to compare their volume changes in Figures 5.7 and 5.8. Two tests of each sample (denoted as 'a' and 'b' in the legend) were shown for completeness. The reliability of the data points on the graphs were verified by the repeatability of the test results and the agreement amongst the trend lines. As in the test results mentioned earlier in this section, the samples' fibre contents were 0.0 and 0.3% by weight. The similar volumetric expansion of the 100-50 kPa pre-loaded fibre-reinforced and un-reinforced samples in Figure 5.7 are best observed by their trend lines. The stress ratios for the reinforced samples were approximately 0.07 greater than the un-reinforced Hostun sand samples. The reinforced samples expanded approximately by 0.04 more than the plain sand.

The reinforced sands in Figure 5.8 did not show the same volumetric trend as the plain sands with 200-50 kPa pre-load. All the reinforced and plain samples showed a steeper increase in the stress ratio values compared with the 100-50 kPa samples, and the trend lines for the samples with and without fibre content were almost parallel. In fact, the trend line for the 0.3% samples showed volume expansion occurring at lower stress ratio values than the un-reinforced samples. The reinforced samples expanded approximately 0.075 more than the plain sand samples, but at a stress ratio value of about 0.05 less than the plain sand. In these graphs the delay in pre-loaded fibre-reinforced sands reaching their peak stress with 50 kPa confining stress compared to plain sand was apparent. Significantly, the fibre-reinforced 200-50 kPa samples showed lower stress ratio values than the un-reinforced samples until large deformations had been generated. This trend demonstrates that the inclusion of fibres allows a sample to deform while absorbing internal shear stresses, especially at larger normal (confining) stresses.

The amount of pre-load seemed to determine the stress-deformation mechanism of the samples with 0.0 and 0.3% fibre contents. The plain sand samples with pre-load showed a slight increase of stress ratio at larger shear displacements compared with samples not pre-

loaded. This behaviour indicated that a similar stress ratio increase would be seen for fibre-reinforced samples due to the increased confinement of the samples. The inclusion of fibres normally results in increased stress ratio values for sand samples in shear at large displacements, but these samples did not actually achieve a critical state before the end of testing. The pre-load was applied to ascertain whether there was a confining stress value that could be used in sample preparation as part of a stress history in order to confine the fibre within the sand particles and achieve higher peak and critical stress states. Although slightly higher peak stresses were achieved in pre-loaded samples (see Figures 5.4-5.5), critical states were not.

5.5 Behaviour of fibre-reinforced sand in shear

5.5.1 The significance of confining stress

A range of confining stresses was used the *LokSand*-reinforced Hostun sand samples in order to observe the effects of a set of normal stresses on the shear strength values and to potentially distinguish a critical confining stress for the samples. Figure 5.10 shows the peak shear stress values achieved in direct shear plotted against the normal stress value for all initial densities and fibre contents. The main conclusions that can be drawn from this figure are summarised as follows.

- Samples with higher normal stresses achieve higher peak stresses in all Hostun sand samples.
- Fibre-reinforced samples showed the greatest increased peak stress ratio values at lower (50 kPa) confining stress.
- The samples with the lowest initial densities generated the highest peak shear stresses.

Further investigation of the normal confining stresses of samples will be discussed throughout this chapter. It will be seen that the peak stress ratios tended to move towards the critical state values for less dense samples. Critical confining stresses for different initial densities will be determined for the peak stress values according to the horizontal displacement, initial sample density value and fibre content. The confining stress and initial density values proved to be correlated.

5.5.2 Effect of initial density

A range of strength parameters was found for the *LokSand*-reinforced Hostun sand samples according their initial sample densities. In the stress-deformation graphs shown in this

chapter, a general trend that is seen is that the samples with the highest initial density achieved peak stress ratio values at smaller horizontal displacements than the samples with lower initial densities. Figure 5.10 has shown that for all initial densities, increasing the fibre content increased the peak stress ratio values in direct shear. The initial density values are featured a great deal in the description of the stress-deformation behaviour of all samples at both peak and critical stress states.

5.5.3 Effect of fibre content and length

The shear tests described thus far have all contained fibres 17.5mm in length. This is a modified length for the *LokSand* fibres. The fibres used in these studies were trimmed to ensure the employment of their tensile strength in 60 x 60mm shear box tests. Preliminary shear tests of *LokSand*-reinforced Hostun sand with the original 35mm length fibres as supplied were initially tested for this study in a 100 x 100mm shear box. The samples with fibres 35mm long did not show a definite peak in the stress-displacement curve for the normal stress values used.

Figure 5.11 shows the stress-deformation of samples prepared by vibration under a small normal load and sheared with 50 kPa normal stress. The "L" and "S" after the legend headings indicate whether the fibres were long (35mm) or short (17.5mm). The two fibre lengths were plotted on the same graph in order to demonstrate the difference that the fibre geometry has on their ability to confine the Hostun sand grains. The samples with longer fibres did not exhibit a definite peak stress value although reinforced and un-reinforced samples were prepared to the same initial densities (as shown). Due to the apparent higher initial density and volume fraction of samples reinforced with fibres of original length (35mm), the shorter fibres were used so that critical stress states could be observed for samples with dense, medium and loose initial densities. (All fibres were crimped as supplied.)

The volume fraction of fibre-reinforced samples was introduced earlier. Increasing the volume fraction of the fibres (fibre content by weight) in a sand sample can decrease the density of reinforced samples. An increase of the fibre length had the same affect on the shear strength properties as increasing the fibre content, which was that distinguishable peak shear strengths (and therefore critical stresses) could not be observed for all initial densities and normal stresses. Increased shear strength values for fibre-reinforced samples compared with un-reinforced sand samples demonstrate the existence of mobilised tensile strength within the reinforcements. The shear displacement at which the peak shear stress is attained is of great importance in order to analyse the fibre-sand particle interaction.

5.5.4 Stress-deformation characteristics

For dense samples especially, the stress ratios of the shear samples initially increased rapidly with the horizontal displacement, then decreased as the peak stress ratio value was mobilised. The more highly stressed samples generally exhibited greater dilatancy and a less obvious peak value, or rather, a prolonged peak state that will be used as critical state values. This phenomenon was seen particularly in the looser samples. Increased normal stress values decreased the peak stress ratio value and increased the horizontal displacement at which the peak was reached. The horizontal displacement corresponding to the post-peak critical state stress ratio values reduced as the normal stress values increased. The stress-deformation characteristics are shown in Figures 5.12 – 5.14 for a series of samples with initial void ratio values of 0.67, 0.72 and 0.76 (which were initial relative density values of 0.87, 0.75 and 0.65 respectively) where the normal stresses (50, 100 or 200 kPa) were constant during shear.

The vertical-horizontal displacement data in Figures 5.12 – 5.14 show the initial contraction of the samples followed by the dilation of samples as upward displacement. The initial sample density value tends to dictate the amount of the initial contraction as well as the value of shear displacement at which the dilation commences. As the vertical to horizontal displacement values progress from the peak stress ratios towards a constant value, the sample is approaching its critical state. The samples with initial void ratio of 0.67 (Figure 5.12) showed stress-deformation behaviour closest to what is expected for critical states.

The peak and critical stress states will first be considered according to their corresponding volumetric deformations for the shear test samples. Due to the continued deformations in the majority of the samples, it can be postulated that few of the samples achieved true critical states. Therefore, representative critical states for the samples will be established in order to understand the roles that the fibres' tensile strength, sample density and the normal stress values play in the shear strength parameters for Hostun sand.

The fibre contents in dry Hostun sand samples enabled the samples to achieve higher peak shear stresses. Figures 5.12 – 5.14 show the stress-deformation data for tests according to their initial density value. Considering first the dense samples (e_i=0.67, RD = 0.87), the peak stresses increased more for samples with greater fibre content. For low stress samples (50 kPa confining stress), an addition of 0.3% fibre content increased the peak stress ratio (PSR) by approximately +20% and an addition of 0.5% fibre content increased the PSR by approximately +33%. These increases are quite substantial for low confining stresses. The medium density samples (e_i=0.72, RD = 0.75) showed peak strength increases of 17% and 26% with 0.3% and 0.5% fibre content, respectively. The loosest samples (e_i=0.76, RD =

0.65) showed PSR increases of 14% and 28% with 0.3% and 0.5% fibre content, respectively. This showed that the denser a sample is, the greater the reinforcing effect of the fibre can be observed as an increased peak shear stress value for low stress shear tests. The amount of the increased peak strength reduced with increasing initial densities in the reinforced samples with 50 kPa confining stress.

The un-reinforced dense sample with the medium confining stress value (100 kPa) reached its PSR value (0.8) at 2mm shear displacement and gradually decreased towards a critical stress ratio value slightly greater than the un-reinforced Hostun sand with low normal stress. The presence of fibres increased the PSR values (0.82 for both 0.3 and 0.5% fibre contents) and the critical stress ratios were marginally less (0.76 and 0.77) for samples with 0.3% and 0.5% fibre contents, respectively. The un-reinforced medium dense samples showed a distinct peak (0.67) followed by a lower critical stress ratio (0.61), which demonstrates the lower shear stress values obtained from samples with higher initial void ratio values. Again both sets of fibre-reinforced samples had similar critical stress ratios to each other, and greater than the un-reinforced sand. However the stress ratio steadily increased towards this peak value after 6mm shear displacement for the samples with 0.3% fibre content, while the 0.5% fibre content samples first peaked at approximately 2mm shear displacement. The loosest un-reinforced samples reached PSR at 4mm shear displacement and the critical stress ratio was only marginally lower. The 0.3% fibre content attained peak stress ratio at 4mm shear displacement and again the 0.5% fibre content reached a higher peak at approximately 3mm shear displacement followed by a slightly lower critical value.

The high normal stress samples (200 kPa) without fibre-reinforcement achieved similar peak and critical stress ratio (CSR) values to the 100 kPa samples with dense and medium initial densities. The loosest samples (e_i=0.76) achieved slightly lower critical stress ratio. The reinforced dense samples had increased PSR values according to fibre content (PSR= 0.79 for 0.3% and PSR= 0.81 for 0.5%), as did the CSR values (CSR= 0.73 for 0.3% and CSR= 0.80 for 0.5% fibre content). The reinforced medium samples had virtually identical stress ratio-shear displacement curves where the peak stress ratio and critical stress ratio were similar (CSR=0.68 for 0.3% and CSR= 0.71 for 0.5%). The loosest un-reinforced samples experienced a PSR value slightly lower than the same density with 100 kPa confining stress at approximately 4mm shear displacement, then a CSR nearly equal to that of samples with 50 kPa normal stress. The loose samples with 0.3% fibre content gradually achieved PSR towards the end of the test, while the 0.5% fibre content samples peaked at 3mm shear displacement.

For samples with 0.5% fibre reinforcement, the lowest confining stress value always achieved the highest peak stress ratio of all tests. It could be argued that the exception to this rule is the sample 100V760.5 that had PSR=0.80 compared to 50V760.5 PSR=0.79, but the early peak behaviour of the 100V760.5 sample is considered to be an unique performance for 0.5% fibre-reinforced sands with 100 kPa confining stress, as the critical stress ratio value was lower than that of 50V760.5. Not surprisingly, it can be difficult to obtain consistent uniform stress-deformation behaviour during direct shear tests on loose samples.

An "equivalent" shear stress ratio is usually used to compare the strength parameters of reinforced soil with un-reinforced soil. For the "equivalent" stress ratio values used here, the stress ratio of fibre-reinforced samples was divided by the stress ratio of plain Hostun sand. Figures 5.15 – 5.17 show the equivalent stress ratios for fibre-reinforced samples according to their initial densities. The dense samples (Figure 5.15) showed the sharpest decline in the equivalent peak stress ratio values from 50 to 100 kPa normal stress. The equivalent stress ratios of the two fibre contents seemed to almost converge at 200 kPa normal stress. This convergence at 200 kPa normal stress was seen for all three initial densities. The samples with 0.3% fibre content gave the largest equivalent peak stress ratio for all tests.

Figures 5.18 – 5.20 show the equivalent critical state stress ratios for fibre-reinforced samples according to their initial densities. Samples with 0.3% fibre content gave the largest equivalent critical stress ratio for all tests. For all initial densities the greatest contrast in the equivalent critical state stress curves was seen at 100 kPa normal stress, with scatter from 1.15 to 1.35 for 0.3% fibre content and from 1.05 to 1.15 for the 0.5% fibre content. This behaviour was seen mostly in looser samples where the equivalent peak stress ratio was similar to the critical state stress. Convergence of the equivalent stress ratios for the majority of samples at 200 kPa normal stress resulted from the similarity between peak and critical stress ratio values.

5.5.5 The internal angle of friction

The peak shear stresses of a soil are plotted against the normal stress values to define the failure envelope for a soil. The coefficients of variation for the test data were not great enough to drastically alter the values presented here. Figures 5.21-5.23 show the failure envelopes for the samples according to their initial void ratio values. "Best fit" lines were drawn from the origin for 0.0% and 0.5% fibre contents to highlight the envelopes. The averages of the peak internal angles of friction for the three normal stresses were found from all experimentation

and shown in Table 5.2. The most important feature in these graphs is that the fibre-reinforced samples do not schematically show a value for the cohesion of the fibre-reinforced sand samples, as is sometimes mentioned in literature. For the moment, we will consider the internal angles of friction as the basis of shear strength comparisons.

The densest un-reinforced samples gave a friction angle of ϕ'_p 36.1° for Hostun sand. The internal angles of friction decreased as the samples' initial void ratio values increased. The friction angles of fibre-reinforced samples increased for all sample densities, with the samples with the greatest fibre content increasing the most. In general, an increase of approximately 0.25% fibre content equated to approximately 2° increase in shear resistance for Hostun sand samples under small normal stresses at all initial densities in direct shear.

Modified failure envelopes were drawn in solid lines for reinforced tests results with the failure envelope not passing through the origin in order to analyse the intercept of reinforced samples in Figures 5.24 – 5.26, while the dashed lines showed bi-linear failure envelopes that passed through the origin. The solid trendlines showed the average intercept for samples with 0.5% fibre content. These solid trendlines showed that the 0.5% fibre-reinforced samples intercepted the shear strength axis at 17 kPa, while the plain Hostun sand samples intercepted the shear axis at the origin. The intercept for samples with 0.3% fibre content was approximately 5 kPa. These readings are only speculative as they are based on linear failure envelopes for the reinforced samples. The shear stress intercept has been described in literature as an "apparent cohesion" that the fibres give to sand samples, although this definition implies that samples posses a value of shear stress with 0 normal stress. The failure envelope for reinforced sands must be bi-linear or curved so that an increased internal angle of friction that originates from zero stresses can be depicted graphically (as shown in Figure 5.27). The reinforcing effect of the fibres can be qualified more easily from observing their dilatancy response.

5.5.6 Dilatancy response

The mobilisation of tensile strain in the fibres depends to a large extent on the soil dilatancy. Dilating soils soften at large deformations, so we would expect localisation, softening and/or an unstable response in un-reinforced soils. A ductile material exhibits increased dilation in direct shear. Figures 5.28 – 5.30 plotted the stress ratio to the vertical over horizontal displacement for *LokSand* fibre-reinforced Hostun sand. The increase of the amount of reinforcement in shearing sand was shown to coincide with the angle of dilation. The fibre-reinforced samples have shown greater dilation after a peak stress value is reached.

The small initial contraction of the samples during the elastic phase transferred into dilation between 2 and 3mm horizontal displacement for all tests. After the peak stress ratio value was realised, the dilation continued in reinforced samples during the residual stress state. Previous researchers also found that reinforcements improved the shearing resistance of dense sand by reducing the vertical deformation caused by the shear force (see, for example, Bauer & Zhao, 1993; Gray & Ohashi, 1983; Vaid et al, 1981). The normal stress value did not greatly affect the peak and residual stress values for the reinforced and un-reinforced soils, but samples with higher normal stresses tend to reach a peak value at larger shear displacements. The greater fibre contents enabled dense samples to attain higher stress values. The dilatancy of the fibre-reinforced direct shear tests was also pre-determined by the fibre content value.

The fibres were mobilised when the mechanism that interlocks the fibres and sand grains had been superseded and loosened by dilatancy. The angle of dilatancy refers to the tangent of the vertical deformation increment over the horizontal deformation increment. Figures 5.28 – 5.30 show the peak angles of friction versus the peak angles of dilation for the three initial void ratio values separately. The peak angles of friction were used for each of the three normal stress values according to fibre content. From Figures 5.31 – 5.33 we saw that the dilation behaviour of each sample was mobilised at different rates and the tests differ in either fibre content or normal stress values, so the peak angles of dilatancy are merely representative of the stress-dilatancy relationship. The samples' journeys from negative (compressive) to positive (dilatant) volumetric displacements (on the dy/dx axis) represented the different deformations according to the stress ratio values.

Considering the densest samples first, the trend lines for 0.0% and 0.5% fibre content give a good estimation of the envelope within which the majority of data points lie. In this case, the peak angles of friction for 0.3% samples all lie in the region of 38-39°. For the medium density samples, the scatter was large enough to draw the trend lines for all three fibre contents. The trend lines were nearly parallel, so again a suitable envelope represented the increased dilation and friction with increased fibre contents. The loosest samples showed a less coherent stress-dilatancy correlation due to the large scatter of data points.

At peak stress ratio values the average cumulative volumetric changes were the greatest positive values for the data sets shown. Up to a peak stress ratio the volumetric strain was uniform for the entire sample volume, especially in dense samples. In the shear displacement following peak, the development of a region of rapid dilation was formed in the shear zone. The non-uniform stress distribution measurement was corrected for peak stress ratio values,

corresponding to shear displacements between 2 and 5mm horizontal displacement depending on the normal stress value, sample density and fibre content. Non-uniformities of volumetric strain become less pronounced at the point of peak stress ratio.

5.5.7 Comparison with Bailey's experiments

Despite the differences in shear box dimensions and test sands, the direct shear tests of Bailey (2000) are comparable with this study as the same fibres were used to reinforce the sand. Both sets of test samples used a random distribution of fibres, but the fibre-reinforced samples tested by Bailey were mechanically mixed before they were compacted in the test mould. Bailey compared dense samples of 0.0% and 0.45% fibre-reinforced Berry Hill sand in direct shear using normal stress values of 278 and 556 kPa. Bailey's research generally concentrated on large-scale tests, therefore higher stresses were used in her experiments. Figures 5.34 and 5.35 plot the shear stress values and vertical deformation against horizontal displacement. The peak and residual stress values are shown in the table below.

Stress values	**Stress ratio 0% fibre**	**Stress ratio 0.45% fibre**
278 kPa : Peak stress	0.88	0.95
278 kPa : Residual stress	0.63	0.86
556 kPa : Peak stress	0.73	0.90
556 kPa : Residual stress	0.70	0.77

Hostun (200 kPa)	$e_i = 0.67$	$e_i = 0.72$	$e_i = 0.76$
Peak stress ratio 0.0% fibre	0.78	0.70	0.67
Peak stress ratio 0.5% fibre	0.80	0.72	0.70
Residual stress ratio 0.0% fibre	0.65	0.63	0.60
Residual stress ratio 0.5% fibre	0.80	0.72	0.70

(based on Bailey, 2000)

The general conclusion that can be drawn is that fibre-reinforced Berry Hill samples exhibit greater peak shear strength and post-peak dilatancy than un-reinforced samples. Both the peak and residual stress ratios for the reinforced 278 kPa samples were higher than those for the 556 kPa samples. In the case of the un-reinforced sands, the residual stress was greater with a larger normal stress value. All samples reached a peak value, beyond which the reinforced samples exhibited steady residual stress state at large displacements.

The 0.5% fibre-reinforced Hostun samples with 200 kPa normal stress had similar stress ratio increases compared with direct shear test results for fibre-reinforced Berry Hill sand in Figure 5.34. The 0.5% fibre-reinforced Hostun sand samples reached peak stress ratio values of 0.80, 0.72, and 0.76 with 200 kPa normal stress depending on the initial void ratio values. The plain Hostun sand samples had peak stress ratio values of 0.78, 0.70 and 0.67 according to initial void ratio values. The Berry Hill sand with 278 kPa normal stress reached peak stress ratio values of 0.88 and 0.95 for un-reinforced and fibre-reinforced samples. The Berry Hill samples had higher peak stress ratios with 278 kPa normal stress than the Hostun sand samples with 200 kPa, although the increased peak stress ratio per kPa normal stress was equal for the two reinforced test sands.

The peak stress ratio value decreased with increasing initial void ratio value in the un-reinforced Hostun sand samples. The samples with 0.5% fibre reinforcement had higher peak stress ratio values than the un-reinforced samples in all tests. The peak stress ratios increased by 2% for the denser samples (e_i = 0.67 and 0.72) and by 3% for the loosest sample (e_i = 0.76). The peak stress ratio for the Berry Hill samples was increased by 7% by the addition of 0.45% fibres. The Berry Hill samples with 6% moisture content at 278 kPa normal stress had the initial densities of $e_{\text{un-reinforced}} = 0.79$ and $e_{0.45\%\text{ fibre content}} = 0.72$ after being compacted in three layers within the test mould. The inclusion of fibres increased the peak strength of the Berry Hill sand samples with 278 kPa normal stress.

Bailey's samples with 556 kPa normal stress were prepared to the same initial densities as the samples with 278 kPa normal stress and showed an increase in peak shear strength by 39% with the inclusion of 0.45% fibres (see Figure 5.35). This is a remarkably high shear strength increase. The peak stress ratio of the plain sand (PSR = 0.44) was increased by 11% (PSR = 0.49) due to the inclusion of fibres. The vertical deformation of reinforced samples increased by 120% compared to the plain Berry Hill sand samples and the residual stress increased by

39% in the reinforced samples. Both the reinforced and un-reinforced samples reached distinct peak and critical stress values.

The fibre-reinforced Berry Hill samples showed the following peak internal angles of friction:

Fibre content	ϕ'_p 278 kPa	ϕ'_p 556 kPa
0%	41.3	36.1
0.45%	43.5	42.0

The increase in shear resistance for fibre-reinforced samples with 278 kPa normal stress showed good agreement with the Hostun samples. This is especially the case when we consider the difference in the normal stress values. The 556 kPa samples are experiencing twice the normal stress, but the value of the internal angle of friction for both un-reinforced and fibre-reinforced samples is less. It is assumed from these values alone that either the fibre content is absorbing the internal stresses or the reinforced samples actually have less shear resistance strength. In order to confirm which one of these two conflicting solutions is correct, the dilatancy must be investigated.

The major difference between the fibre-reinforced Berry Hill sand samples (Figures 5.34 and 5.35) and the fibre-reinforced Hostun sand samples shown in Figures 5.12 - 5.14 is that the reinforced Berry Hill samples reached a distinct peak, followed by a lower residual stress ratio with 278 kPa normal stress. The reinforced Hostun samples reached a peak value that was equal to the residual stress ratio with 200 kPa normal stress. It is obvious that the reinforced Berry Hill samples exhibited dense behaviour in shear, while the reinforced Hostun samples with 200 kPa normal stress exhibited loose behaviour. This could be a result of the different sample preparation techniques.

The contribution of fibre reinforcements to the failure envelopes of the two sands in direct shear became apparent at the critical stress value, which increased with increasing amounts of reinforcement. Bailey mentioned the existence of a critical confining stress for fibre-reinforced samples:

> *The fibres' surface should also be as rough as possible to efficiently mobilise the soil-fibre bond and therefore the fibre strength and reduce the critical confining stress.*
>
> (Bailey, 2000)

The *LokSand* fibres were crimped along their length, which also increased the strength of the interface bond between the fibres and sub-angular Hostun sand. The surface of the *LokSand* fibres could be considered rougher than the fibres used by Bailey due to the crimping.

5.6 Validation of experimental results

5.6.1 The significance of sample preparation method

The objective of the testing program of LokSand-reinforced Hostun sand samples was to examine the behaviour over a range of sample densities, stress levels and sample preparation techniques. For the direct shear tests recorded in this thesis, random distribution was the preferred fibre orientation as randomly placed fibre reinforcements have proven to be most effective in resisting shear stress. The fibres were distributed evenly throughout the sample to ensure uniformity of the mix, despite the many directions into which the fibres extended within the sample volumes.

One set of experimental samples were pre-loaded before testing in one-dimensional compression and direct shear in order to assess the effects of different stress histories and increased confinement. The differences in the confining stress values demonstrated significant effects in the stress-deformation behaviour. The pre-loads of 100 and 200 kPa normal stresses increased the shear strength and dilatancy of samples compared with samples not subjected to a pre-load. The internal angles of friction for this set of test results were compared to reveal the range of internal angles of friction depending on the confining stresses and the average increase of the internal angles of friction due to 0.3% fibre content.

5.6.2 Validation of the internal angles of friction

A range of values given by Schanz and Vermeer (1996) for the peak internal angles of friction for Hostun sand in triaxial tests with 300 kPa confining stress were based on their initial sample densities (ϕ'_{loose} = 40 - 42° and ϕ'_{dense} = 34°). The critical state angle of friction was found to be $\phi'_{critical}$ = 34.4° for all samples. The angles of friction for the un-reinforced Hostun samples in direct shear were plotted with the triaxial sample estimations set out by Schanz and Vermeer (S&V) in Figure 5.36. The failure envelope for the average internal angles of friction for un-reinforced Hostun sand samples tested in direct shear with pre-load was included for completeness (see "trendline pre-load" in the legend).

There was small yet equal scatter on both sides of the failure envelope for un-reinforced samples based on the average un-reinforced pre-load tests in the region of ±1° at 50 kPa, ±2° at 100 kPa and ±4° at 200 kPa. The fibre-reinforced samples all fell within the limits of Schanz and Vermeer's estimations. Although the angles of friction from triaxial test results are usually underestimated by -2° compared with the angles for samples tested in direct shear, these results show good agreement due to the differences in confining stresses of the two types of test (triaxial = 300 kPa and direct shear = 50 – 200 kPa). The trendline for the pre-loaded 0.3% fibre-reinforced Hostun sand samples was extremely similar to the "S&V loose" samples failure envelope. The two trendlines are barely distinguishable from each other. This failure envelope would appear to be an upper limit for "loose" Hostun sands in shear, while the "S&V dense" samples appear to be a lower limit.

The previously stated formula for an increased angle of friction of +2° for every additional ~0.25% fibre-reinforcement in Hostun samples in section 5.5.5 compared with un-reinforced angles of friction (based on fibre content) was not valid for the average pre-load failure envelopes, even when tested with small normal stresses in direct shear. This indicates that an increase in the peak shear strength of Hostun sand samples depends on both the fibre content and the confining stress value. In order to fully understand the shear strength increases due to fibre reinforcements, the critical stresses for fibre-reinforced sands must be observed.

5.6.3 Critical state parameters for fibre-reinforced sand

The fibre content played a significant role in increasing the shear resistance of sand, which was observed in the increased angles of friction from direct shear test results. The tensile strain mobilised in the reinforcements contributed to the additional shear strength in the fibre-reinforced test samples. In previous research, models have been based on mechanistic approaches (see, for example, Maher and Gray, 1990), to quantify the 'equivalent shear strength' of the fibre-reinforced composite as a function of the thickness of the shear band that develops during failure. The void ratio values of shear samples at peak and critical stress states will be compared in order to gain a better understanding of the conditions necessary to mobilise this tensile strain.

Figures 5.37 - 5.39 show the voids ratio values reached at peak shear stresses plotted against the normal stress values. The dense samples showed a decreasing density-normal stress relationship and their trend lines converged in the region of void ratio = 0.672 at approximately 80 kPa normal stress. The medium density samples showed more disparate

results. The loosest samples showed better agreement of a decreasing peak void ratio value with increasing normal stress values for the fibre-reinforced sands, while the un-reinforced samples showed a constant peak void ratio for all normal stress values.

Figures 5.40 - 5.42 show the voids ratio values at their observed critical states plotted against the normal stress values for each sample density. The densest samples showed the best convergence nearest 200 kPa normal stress. The medium samples also showed convergence nearest 200 kPa. The samples with the highest initial void ratio values showed the most disparate set of results, therefore a different method for presenting the test results was adopted. Figures 5.43 - 5.45 show the voids ratio values at their observed critical states plotted against the normal stress values according to fibre content in order to compare the critical state lines for each density according to the amount of sample reinforcement.

The critical state line (CSL) was used as a reference condition for the Hostun sand behaviour, characterised by the samples with the same fibre contents at their highest confining stresses. The CSL can be extrapolated back to the void ratio axis. This model is a proposal for the measurement of the strength increases imparted to soil by fibres based on the fibre content and the sample density at critical state from the experimental results. From the graphs, it is apparent that the critical state line starts with void ratios higher than initial void ratios at low confining stresses. As the confining stresses increase, the critical void ratio decreases. From this representation of the test data, a critical confining stress exists that sufficiently confines the optimum void ratio for achieving peak shear stress values. This critical confining stress can be estimated for a sample according to the initial void ratio value and fibre content. Other features include the following:

- The greater the confining stress value, the lower the critical confining stress value for un-reinforced sands.

- For all densities, increasing the fibre content increased the critical stress ratio values.

- For un-reinforced Hostun sands, the critical state lines shown in Figure 5.43 are at a similar angle of inclination (based on best fit). The angles of inclination remain almost constant with greater fibre contents (as seen in Figure 5.43-5.45). The distance between the void ratio values for the different initial density sets decreases as the fibre content increases.

- The tensile strength of the fibres can be mobilised at low confining stresses due to the relatively large internal movements that take place at large shear displacements. The increase in strength was related to the void ratio at critical state as a physical representation of the fibre tensile strength mobilised by the sand particles' deformations.

5.6.4 Strain-softening behaviour

One aspect of the strain-softening behaviour of sand is the dilatancy at large shear displacement relative to the dilatancy at peak shear resistance value. The post-peak strain behaviour of a sample is only as strong as its weakest zone, or failure zone in the case of direct shear. In the direct shear of plain sand it is only the failure zone that is likely to be stressed to the critical state. In the case of fibre-reinforced sands, the fibres spread the shear zone throughout the sample volume and, therefore, more dilation occurs in fibre-reinforced samples because more sand is taking part in shear.

The post-peak increase of vertical deformations in reinforced samples was due to the larger volume of fibres being mobilised as the samples deformed. For the fibres to mobilise within the 60 x 60mm shear box, approximately 3mm shear displacement was required, depending on the normal stress value, sample density and fibre content. The random distribution of fibres in samples was expected to give a random distribution of fibre directions, so not all the fibres will be oriented in a direction that contributes to shear resistance. Some fibres may have been bent during the sample fabrication in layers. Since not all fibres will be favourably oriented to oppose shear, not all of the fibre content within the shear zone of a sample will be mobilised. As the fibre-sand mixture begins to deform, an increasing number of fibres are mobilised. As the sample continues to deform, the mobilisation of fibre tensile strain continues until the fibres have been fully mobilised or the test terminates (whichever occurs first). Upon visual inspection after the laboratory tests were completed, none of the fibres used in the experimentation were found to be broken.

From the point of view of the strain-softening behaviour, the following conclusions were drawn from the shear tests results:

- It appeared that at large shear displacements the tensile characteristics of the fibres were mobilised at lower normal stresses due to the relatively large volumetric changes taking place within the sample.

- Even if the tensile force of the fibres did not appear to have been fully mobilised in tests (in the cases where the peak and critical stress ratios were equal) the fibres were still able to linearly increase the peak stress ratio values according to the fibre content compared to un-reinforced sand samples and prevent a loss of strength once achieving the peak stress ratio.

5.7 Summary

The performance repeatability of peak shear values and dilation characteristics were favourable for all tests. In direct shear tests on reinforced sand, it is normally found that the shearing resistance in the soil increases at higher normal stresses. These tests of Hostun sand with *LokSand* fibres have shown this hypothesis to be correct. The relationship between the confining stress value and the initial density value for fibre-reinforced samples has been demonstrated.

Notable conclusions from observing the laboratory experimentation include the observation of the importance of the stress history on fibre-reinforced samples, manipulation of the test data and agreement with published test results.

- The vibrated fibre-reinforced samples did not deform as much as the spooned samples on one-dimensional compression.

- The reinforcing effects of the fibres were not mobilised in one-dimensional compression tests for samples reinforced with the original 35mm fibre length nor for samples reinforced with the modified 17.5mm fibre length under small normal stresses.

- A series of direct shear tests was pre-loaded by normal stresses higher that the applied normal stress during shear in order to compare the effect of stress history of the samples. The pre-loaded samples did not achieve peak stress values at smaller shear displacements although the pre-stress acted as an applied confining stress to the fibre-reinforced samples. The pre-stress increased the shear resistance contribution of the fibres in samples sheared with 50 kPa normal stress.

- The amount of initial vertical deformation of the fibre-reinforced samples at the start of the direct shear test was found to be dependent on the fibre content.

- In general the fibre-reinforcement increased the peak strength of the sand, which occurred at greater shear displacements, and reduced the post-peak reduction in strength compared with sand alone. The reinforced sand samples also showed increased dilation of the sample compared with the un-reinforced sand. The interlocking mechanism of sand grains with reinforcements was mobilised when the critical stress value had been superseded and the samples dilated in all tests mentioned.

- The internal angles of friction increased with increased normal stress values as well as with increased fibre content for all sample densities. The angle of friction appeared to increase by approximately 2° for approximately every 0.25% fibre content increase. The model showed favourable agreement with the test results of fibre-reinforced Berry Hill sand.

- Good agreement was shown between the peak shear stress behaviour laboratory experimentation of LokSand fibre-reinforced Hostun sand in direct shear and published fibre-reinforced Berry Hill sand direct shear tests. The Hostun sand samples showed less post-peak softening than the Berry Hill samples.

- A series of representative critical state lines was adapted from the data for the un-reinforced and fibre-reinforced samples in direct shear in order to predict the critical confining stress for a given sample density and fibre content.

5.6 Figures for Laboratory Experimentation

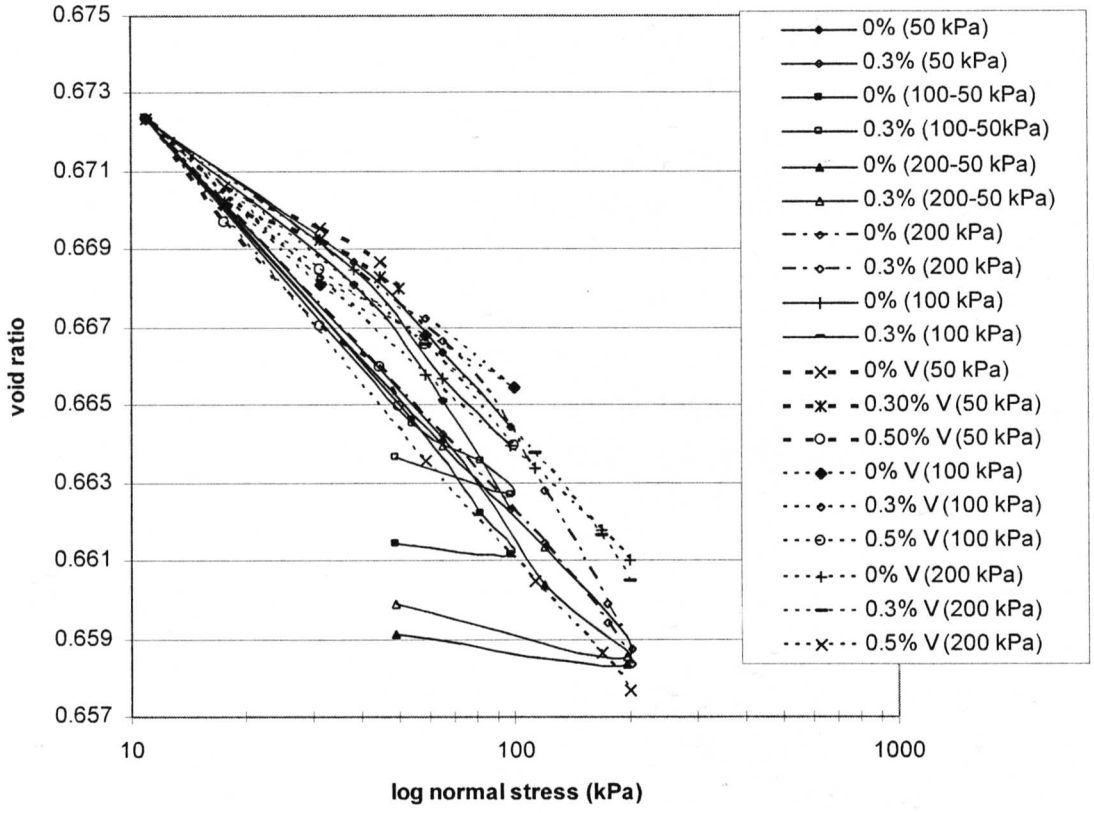

Figure 5.1: One-dimensional compression of vibrated samples and samples with pre-load

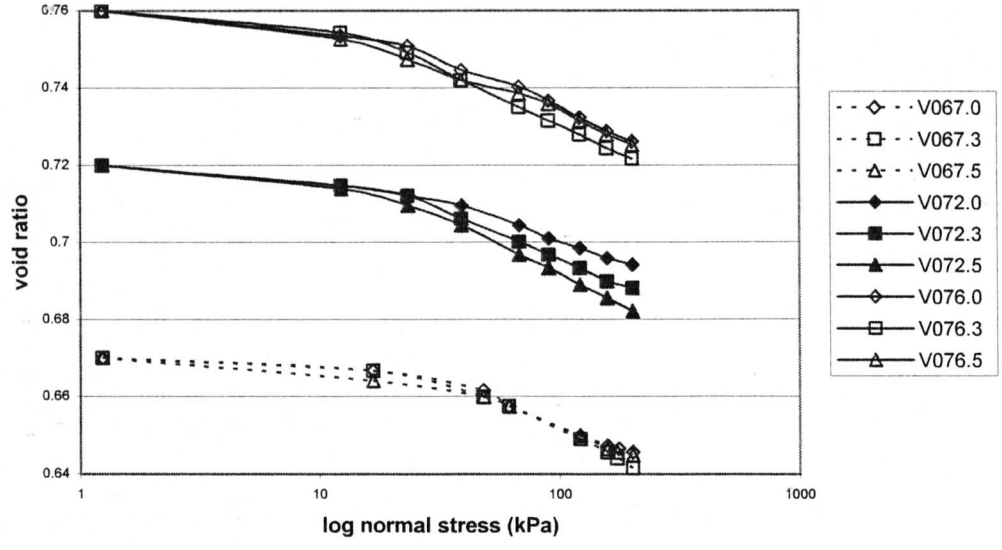

Figure 5.2: One-dimensional compression of vibrated samples

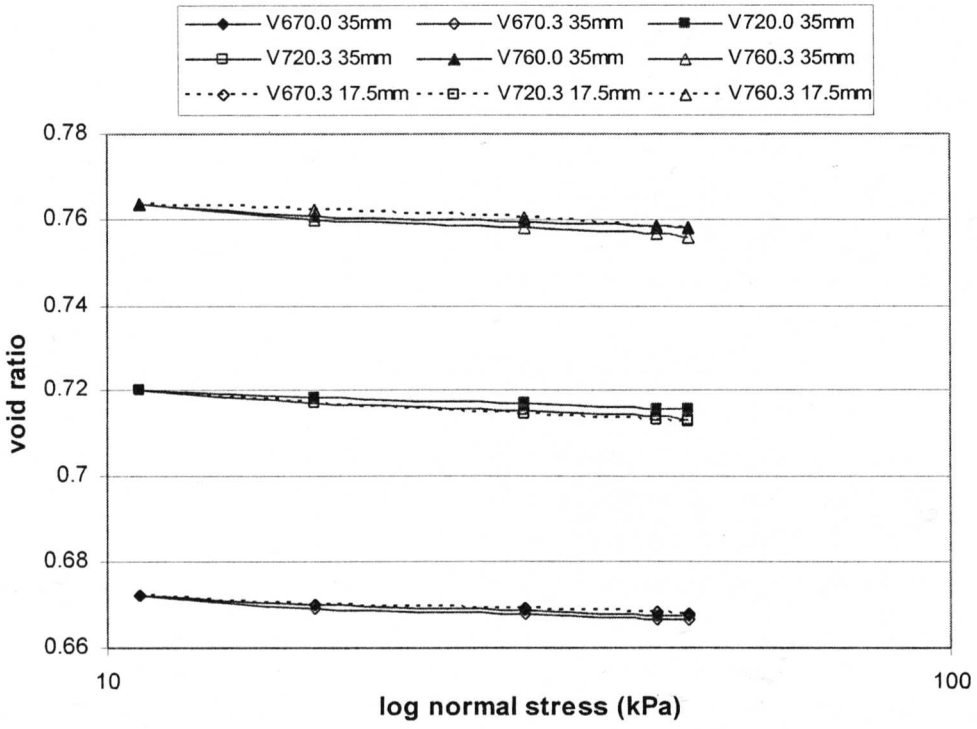

Figure 5.3: One-dimensional compression tests for 35 and 17.5mm fibre lengths

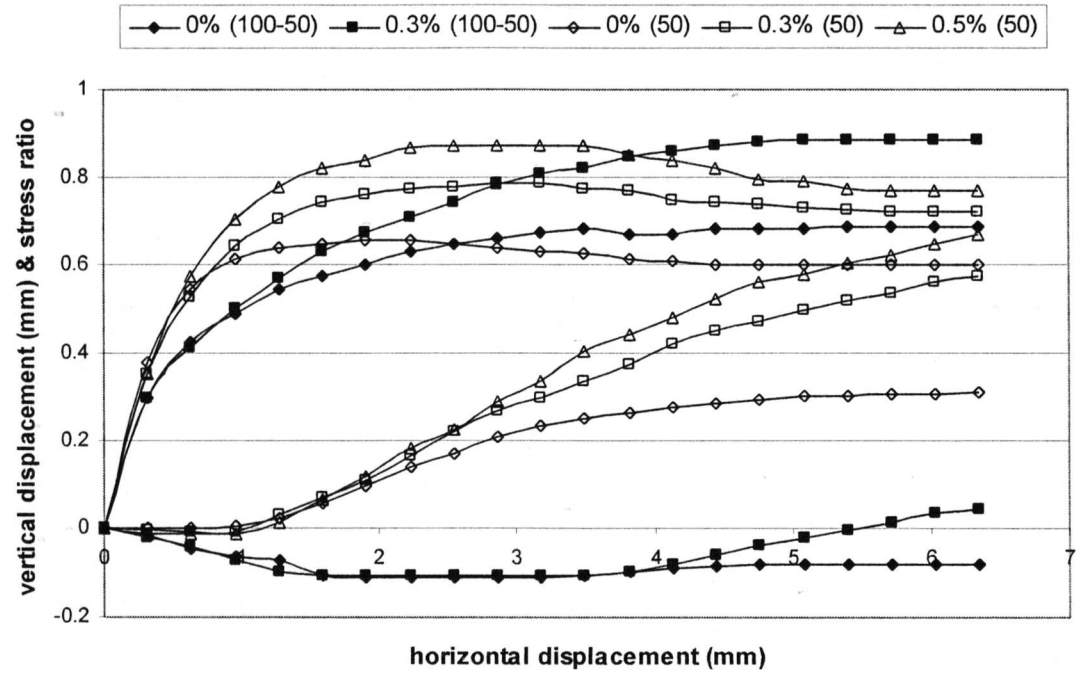

Figure 5.4: Stress-dilatancy curves for 100-50 and 50 kPa normal stress

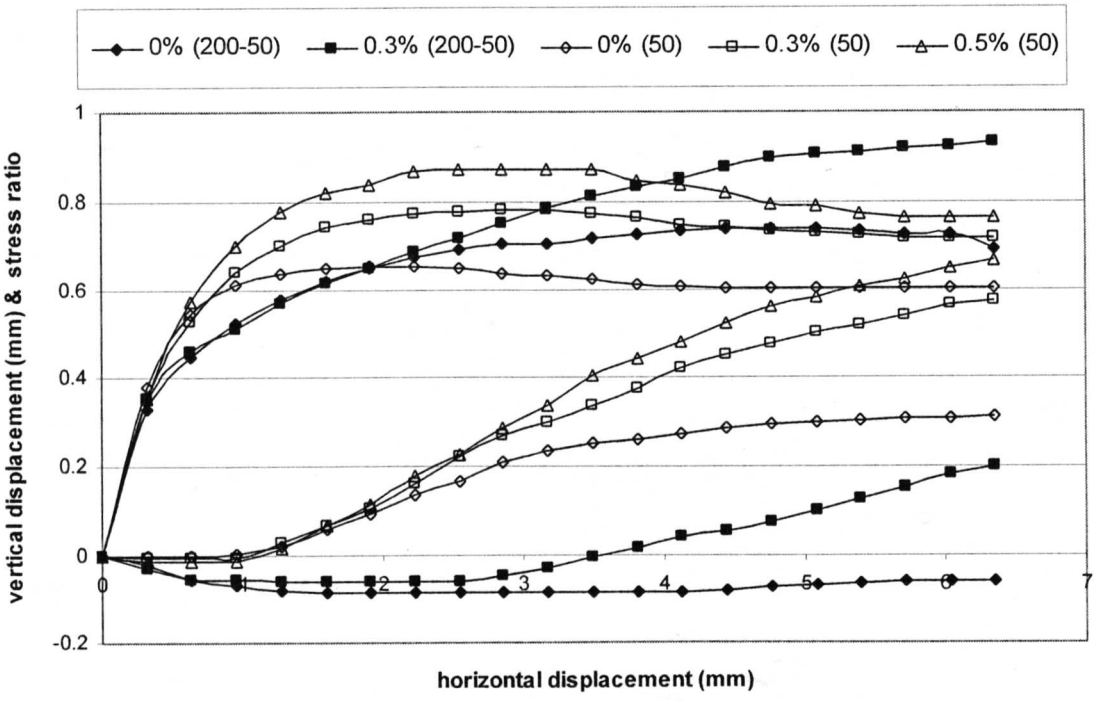

Figure 5.5: Stress-dilatancy curves for 200-50 and 50 kPa normal stress

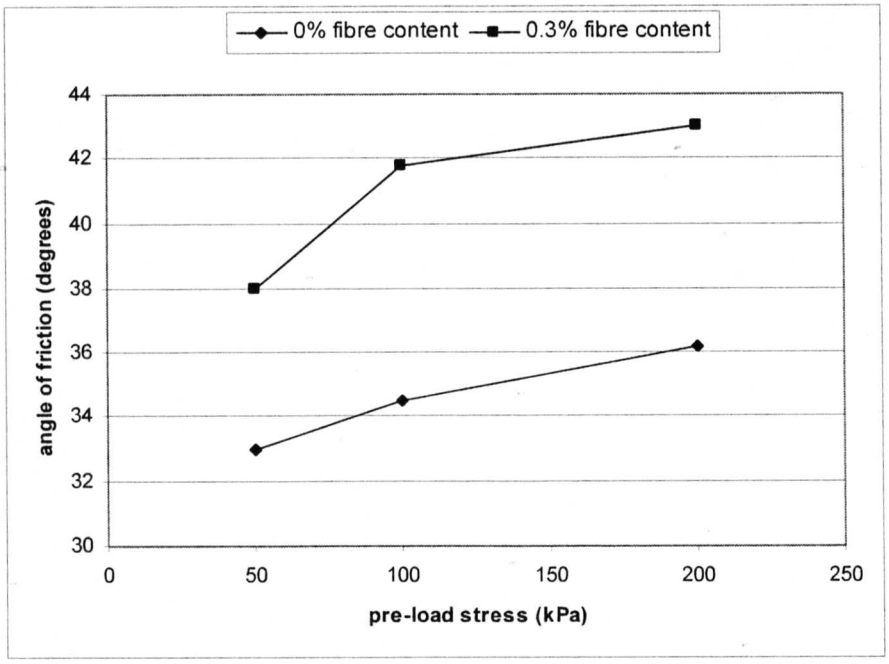

Figure 5.6: Angles of friction according to pre-load stress value

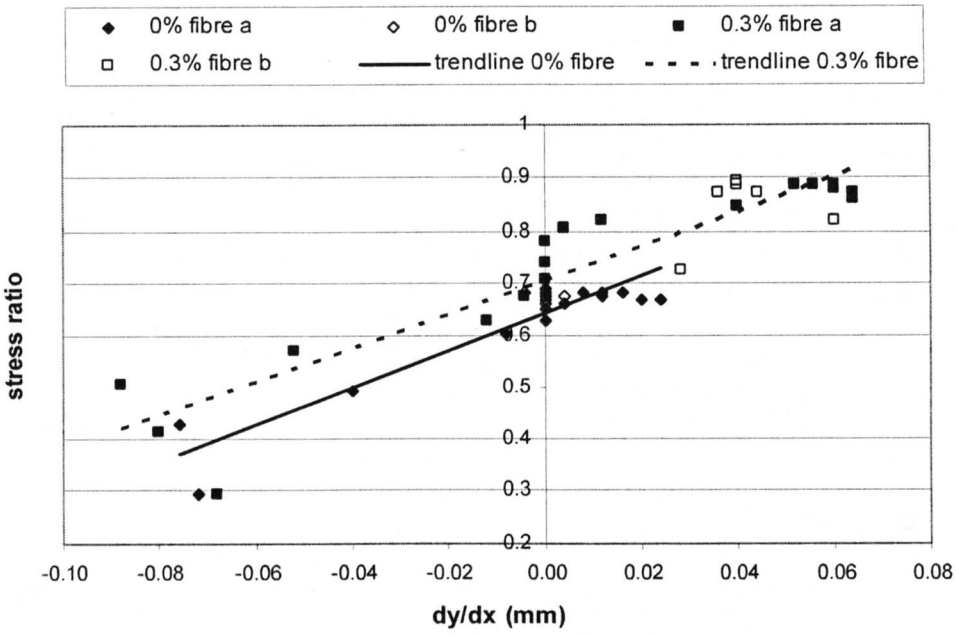

Figure 5.7: Stress ratio to volume change 100-50 kPa

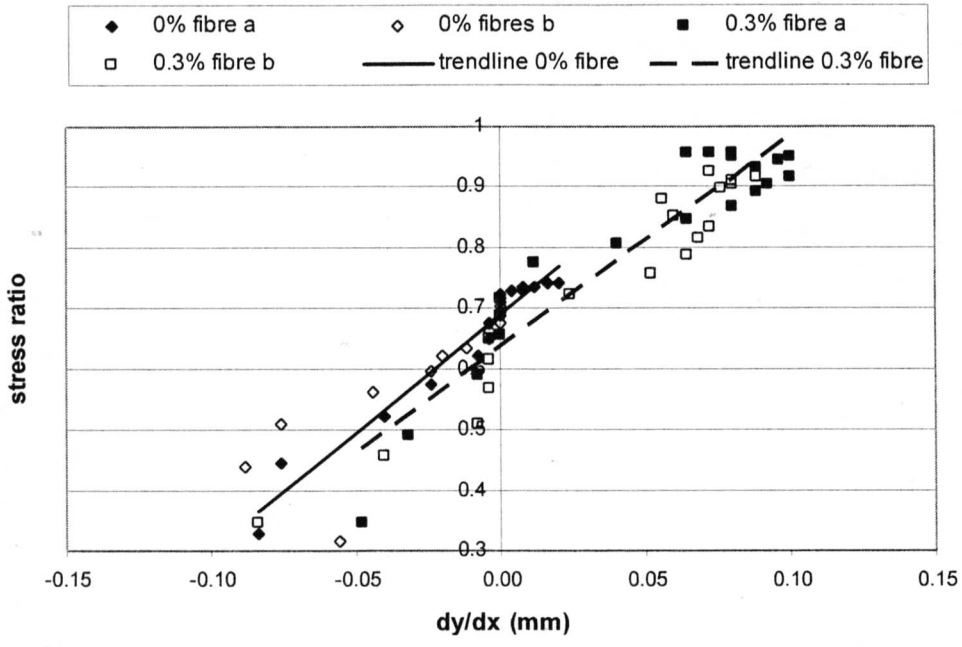

Figure 5.8: Stress ratio to volume change 200-50 kPa

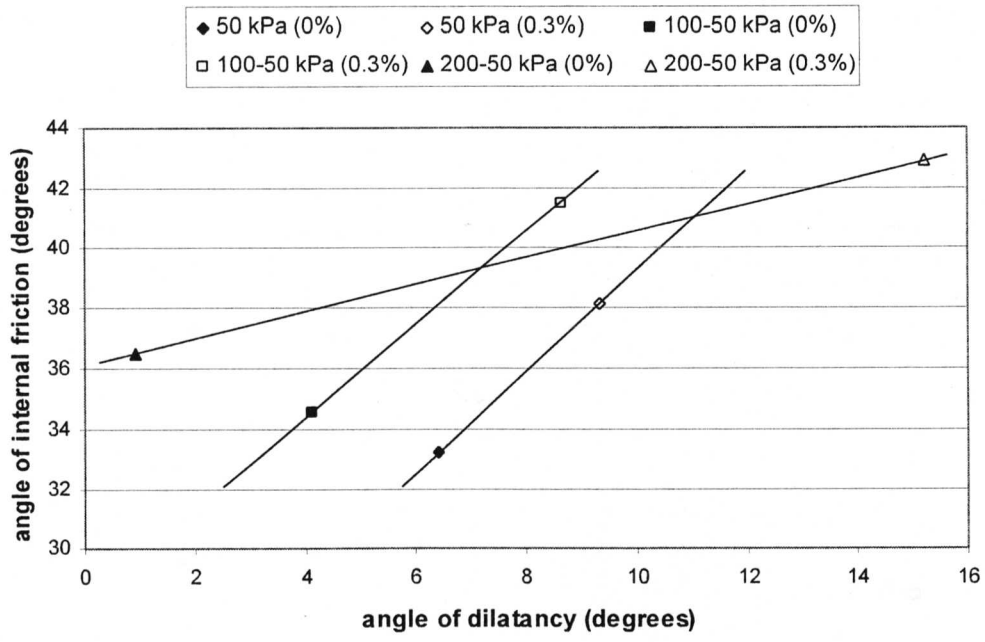

Figure 5.9: Peak angle of friction to peak angle of dilatancy graph (pre-load)

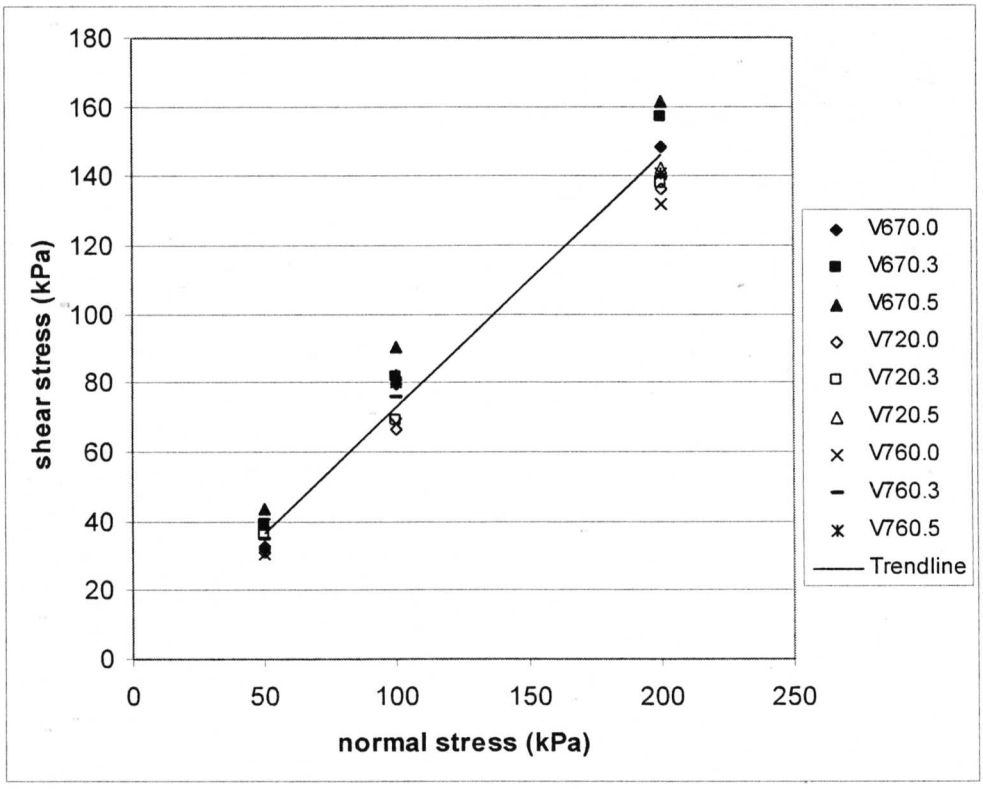

Figure 5.10: Peak shear stresses versus normal stresses in direct shear

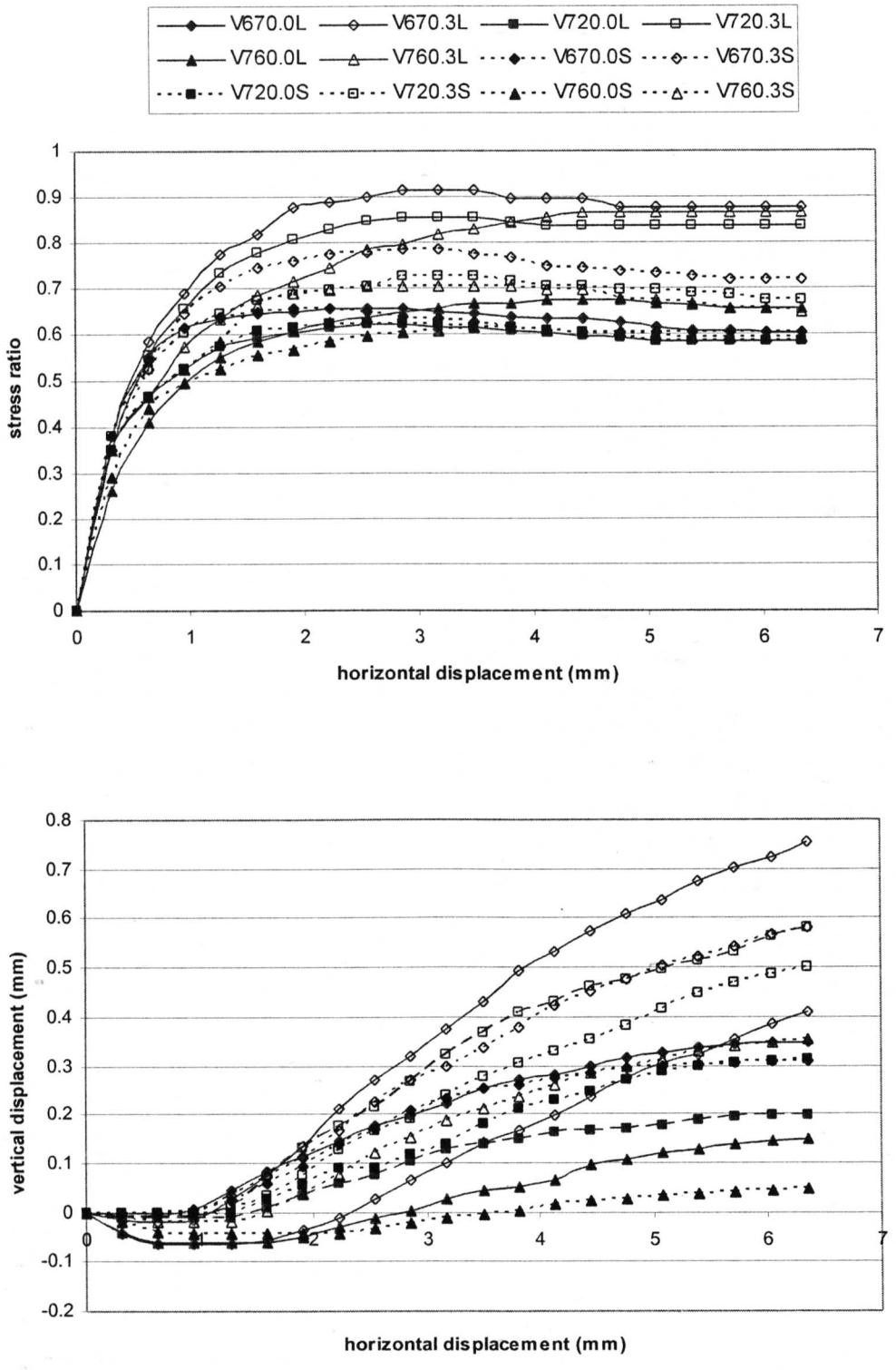

Figure 5.11: Stress-deformation for Hostun samples with fibre lengths of 35mm (L) or 17.5mm (S)

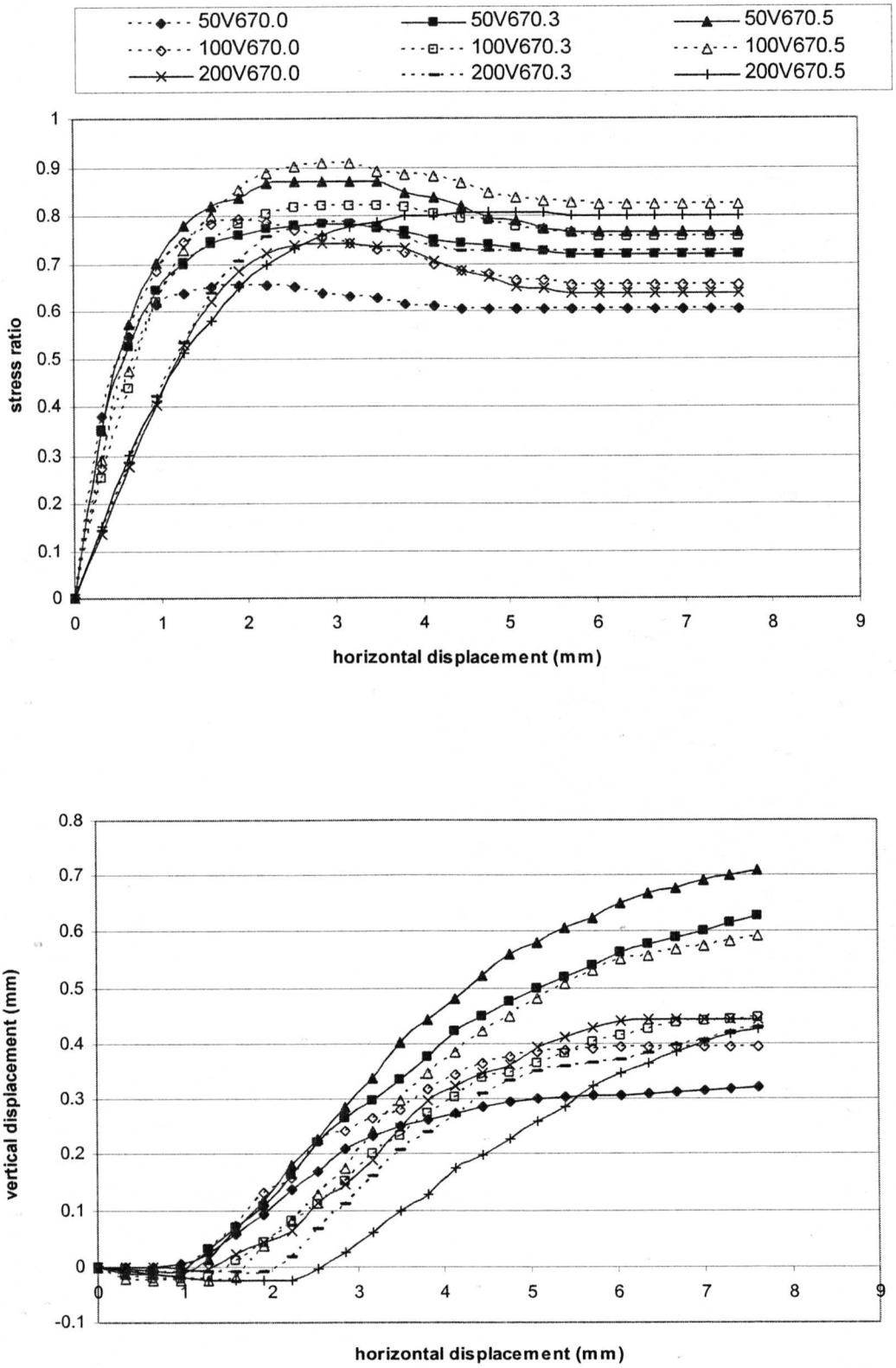

Figure 5.12: Stress ratio and vertical displacement versus horizontal displacement (e_i=0.67)

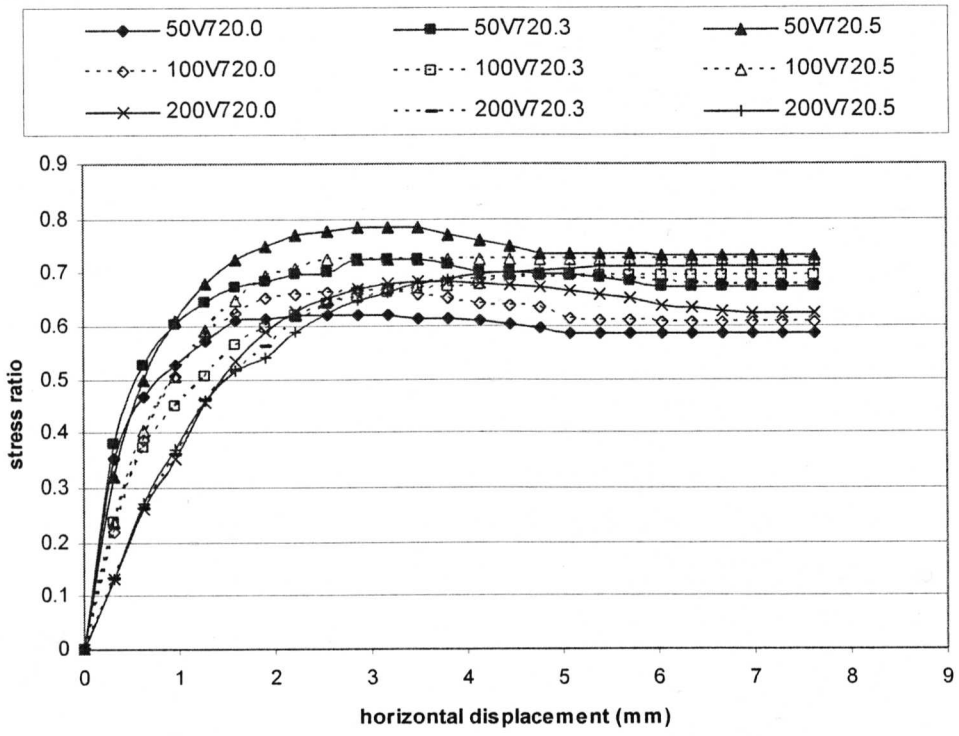

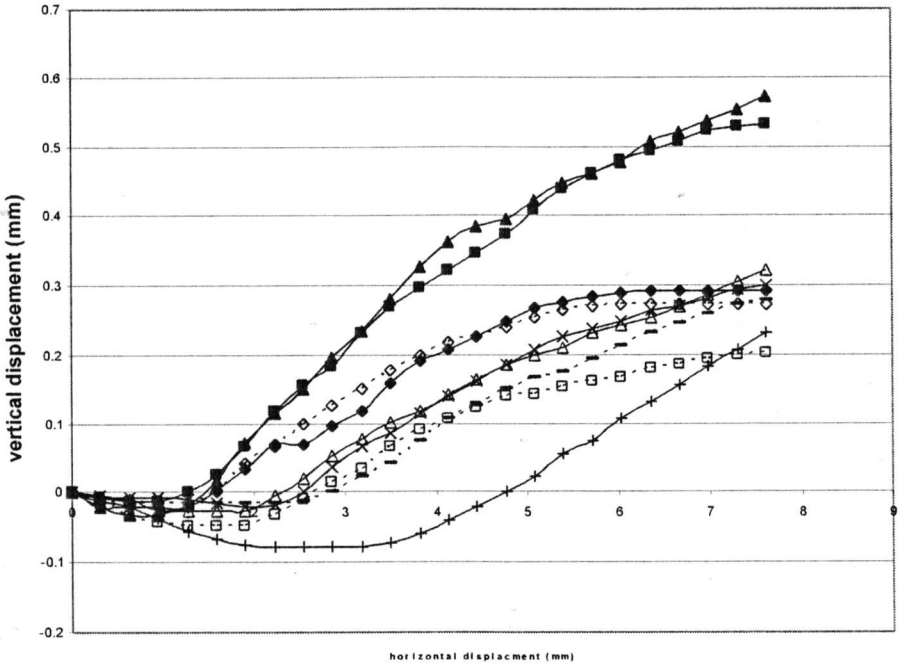

Figure 5.13: Stress-deformation for fibre-reinforced Hostun sand samples $e_i = 0.72$

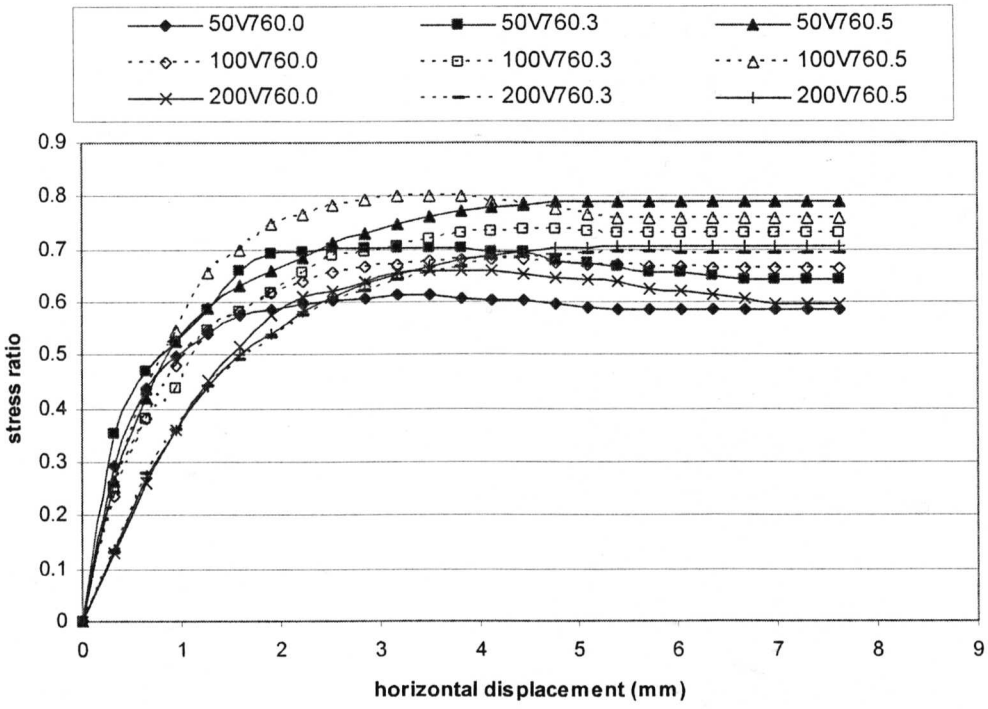

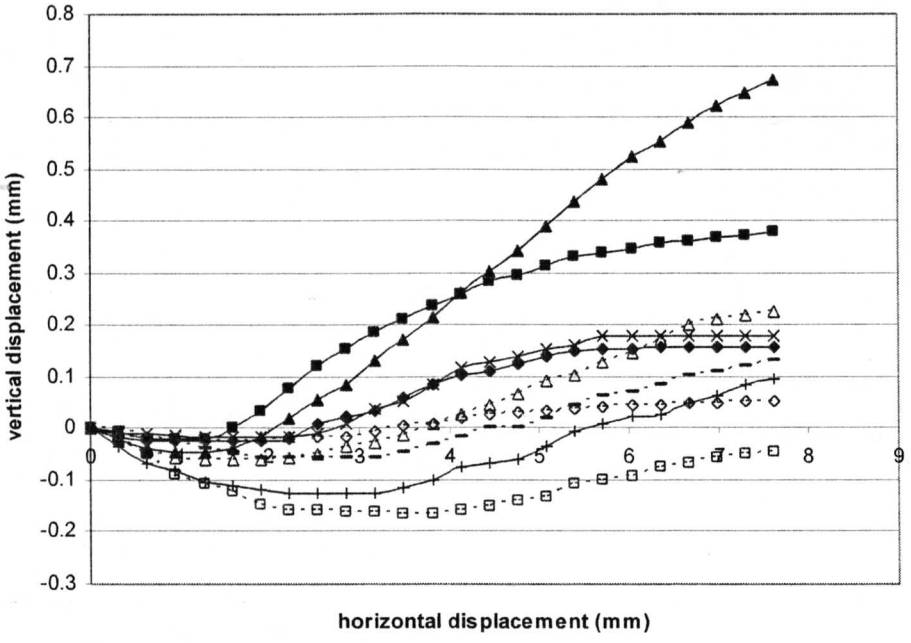

Figure 5.14: Stress-deformation for fibre-reinforced Hostun sand samples $e_i = 0.76$

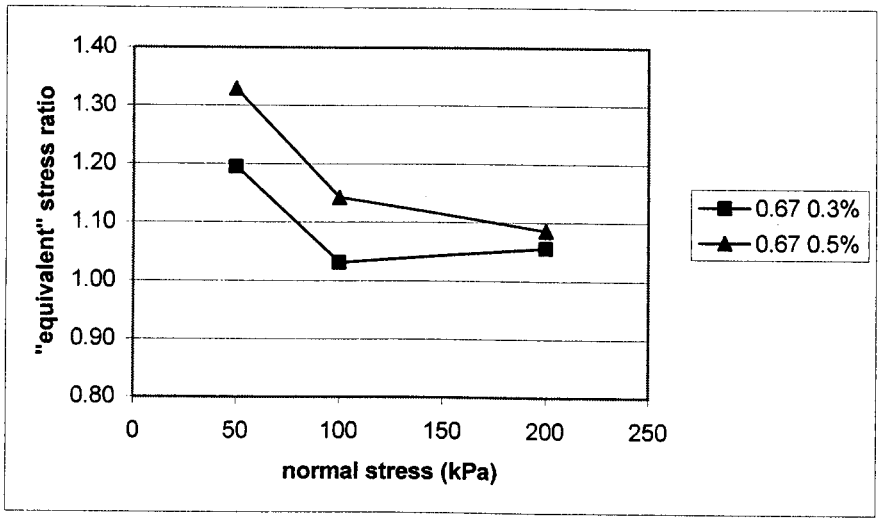

Figure 5.15: Equivalent peak stress ratio (e_i = 0.67)

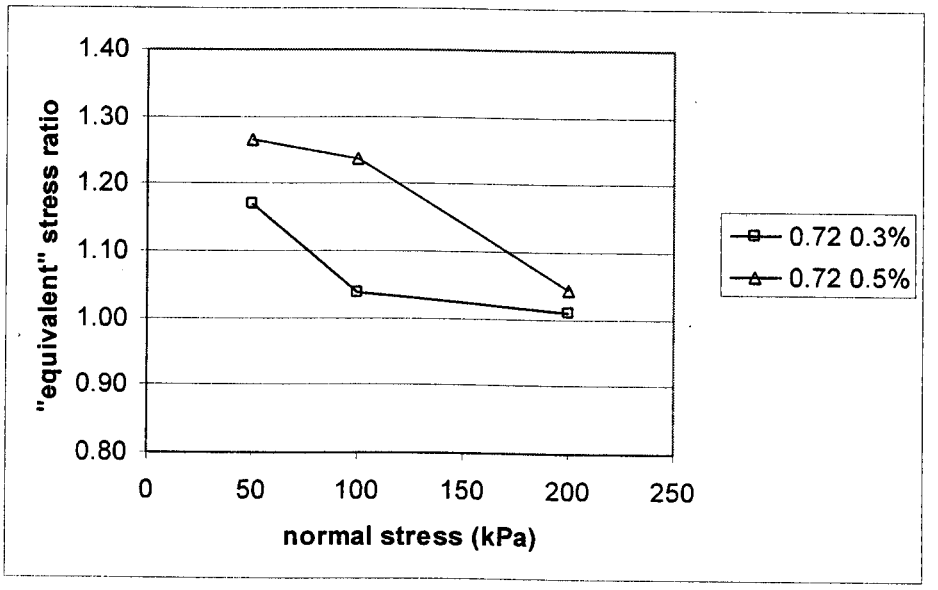

Figure 5.16: Equivalent peak stress ratio (e_i = 0.72)

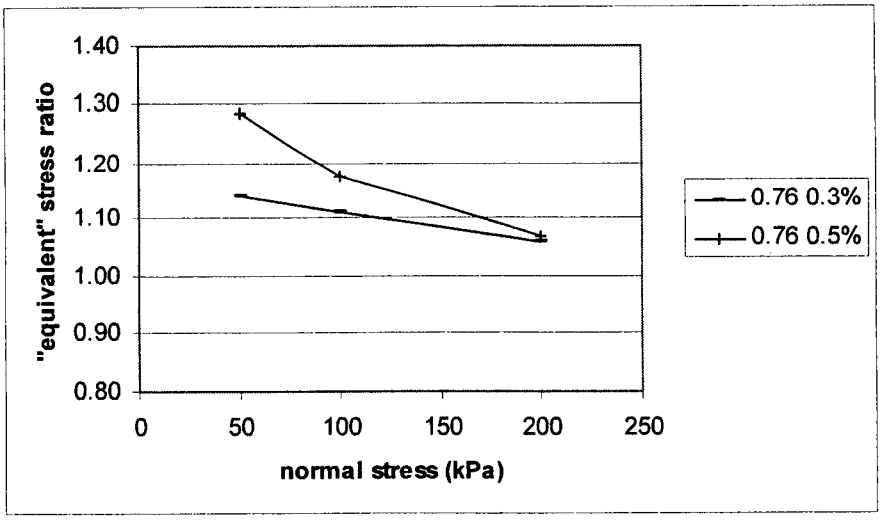

Figure 5.17: Equivalent peak stress ratio (e_i = 0.76)

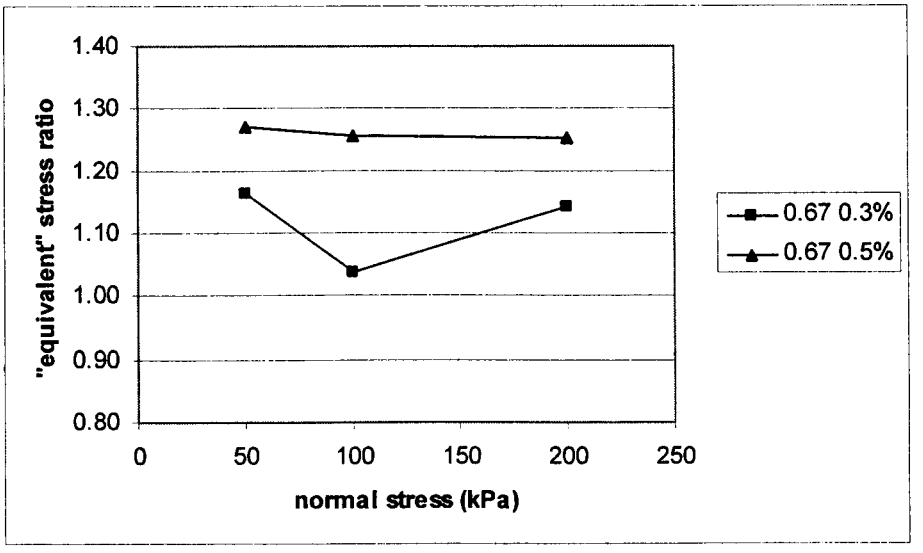

Figure 5.18: Equivalent critical state stress ratio (e_i = 0.67)

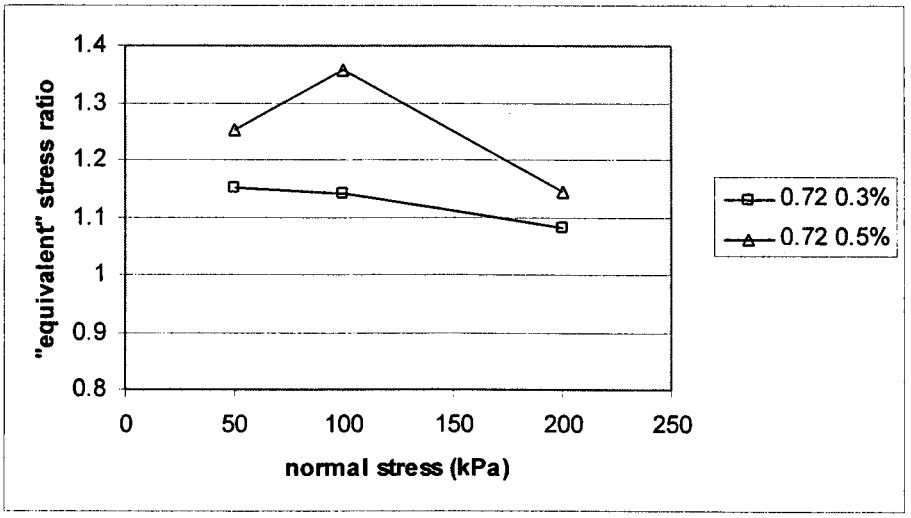

Figure 5.19: Equivalent critical state stress ratio ($e_i = 0.72$)

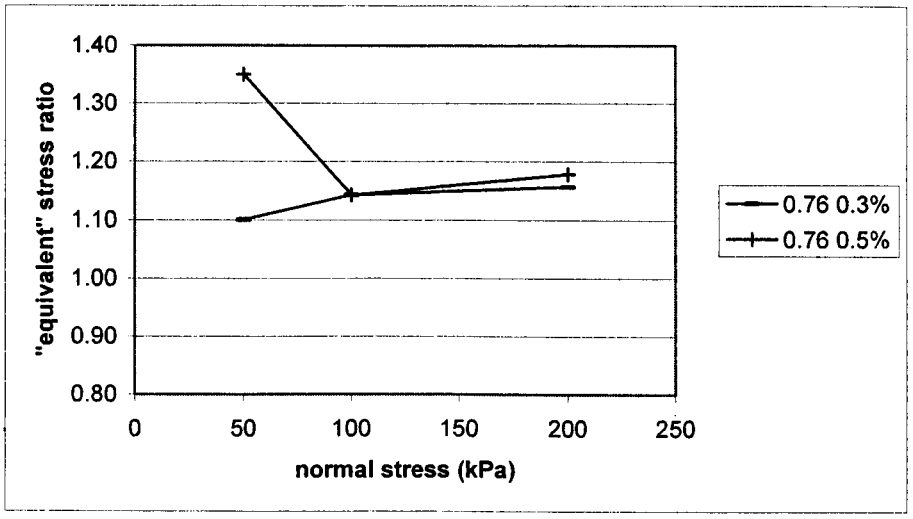

Figure 5.20: Equivalent critical state stress ratio ($e_i = 0.76$)

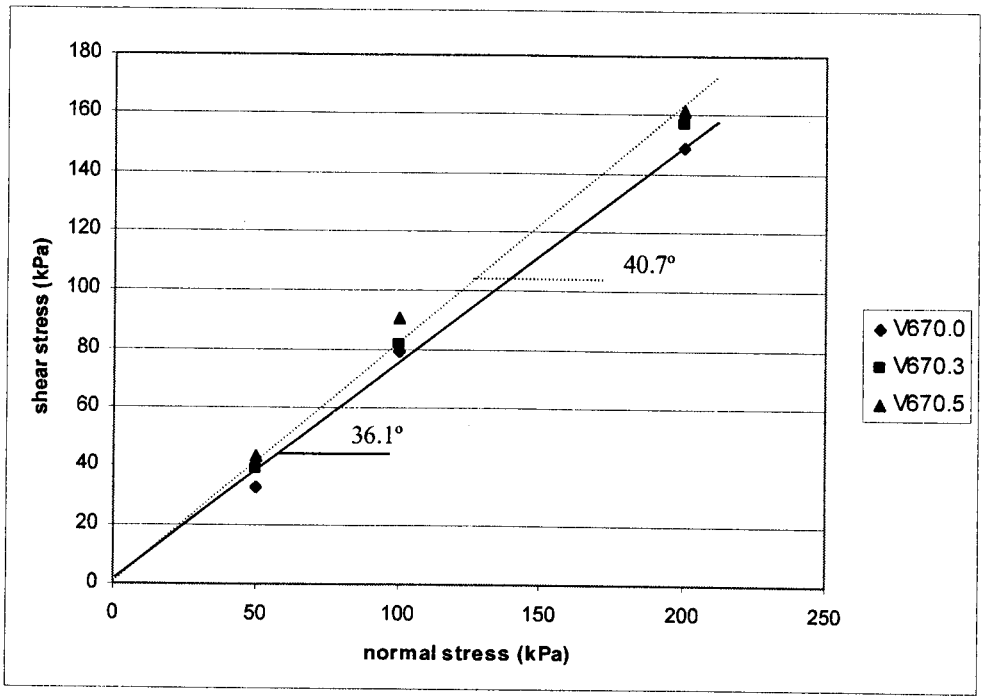

Figure 5.21: Failure envelope e_i=0.67

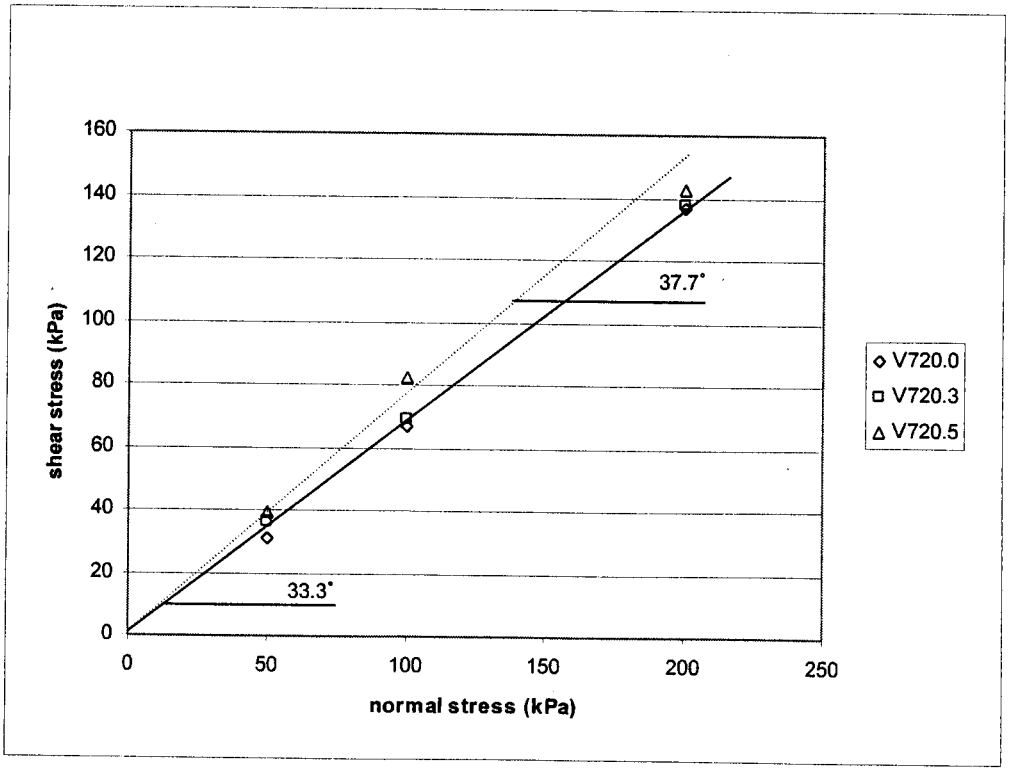

Figure 5.22: Failure envelope e_i=0.72

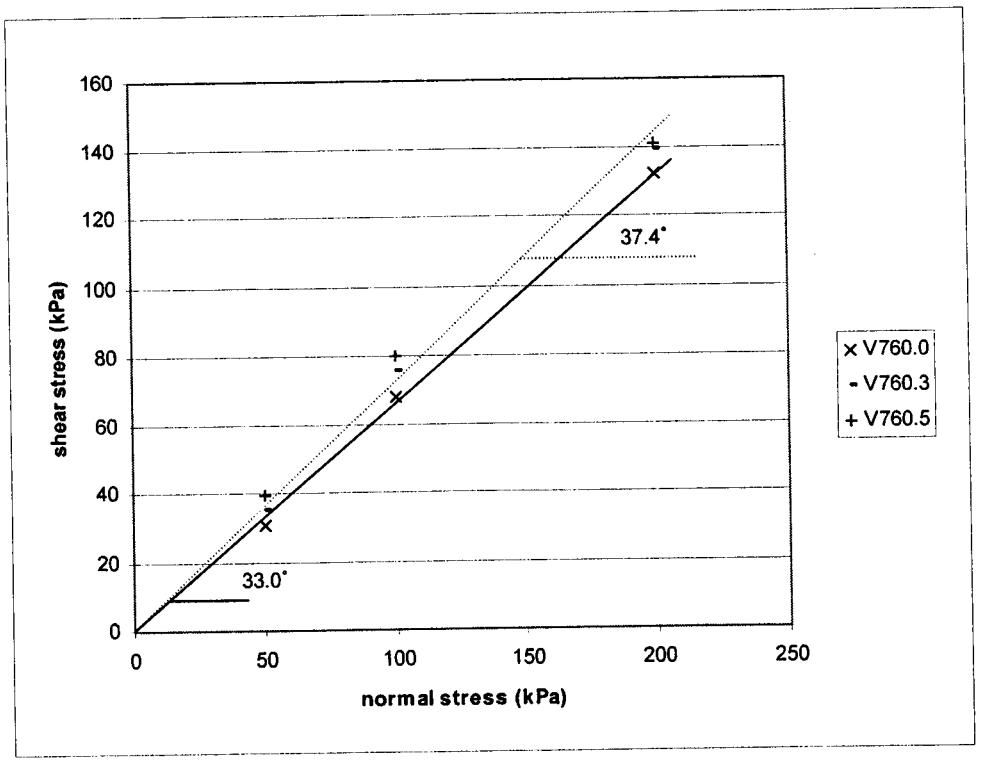

Figure 5.23: Failure envelope e_i=0.76

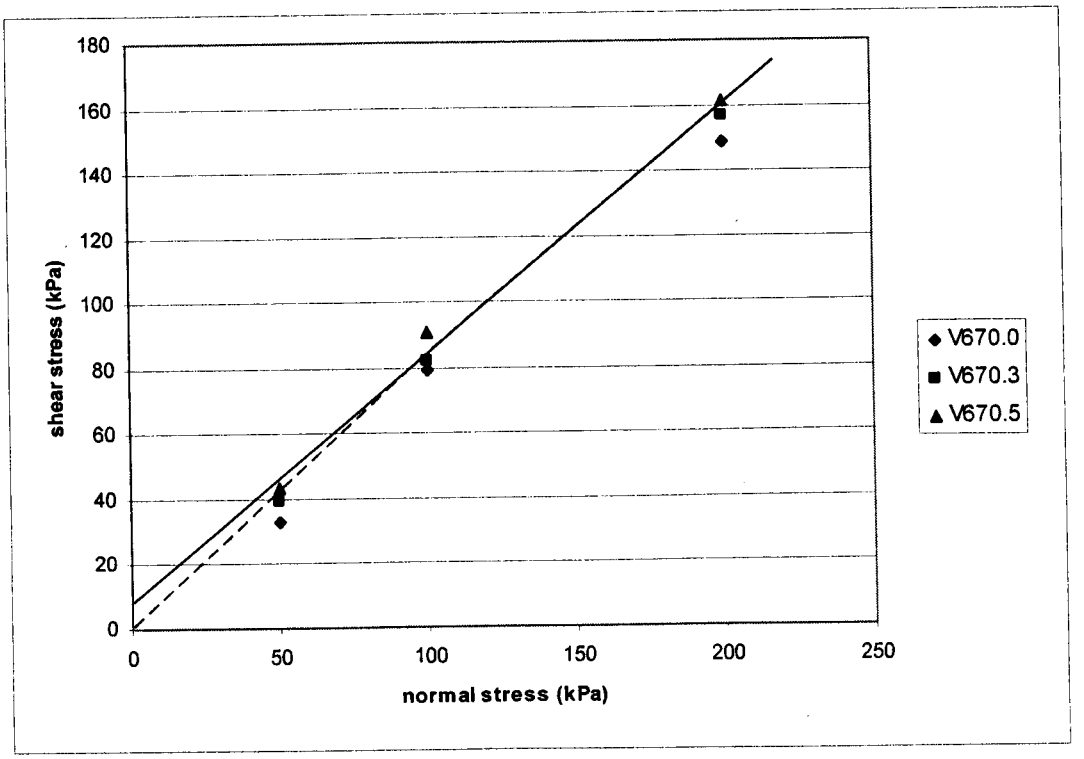

Figure 5.24: Modified failure envelope e_i=0.67

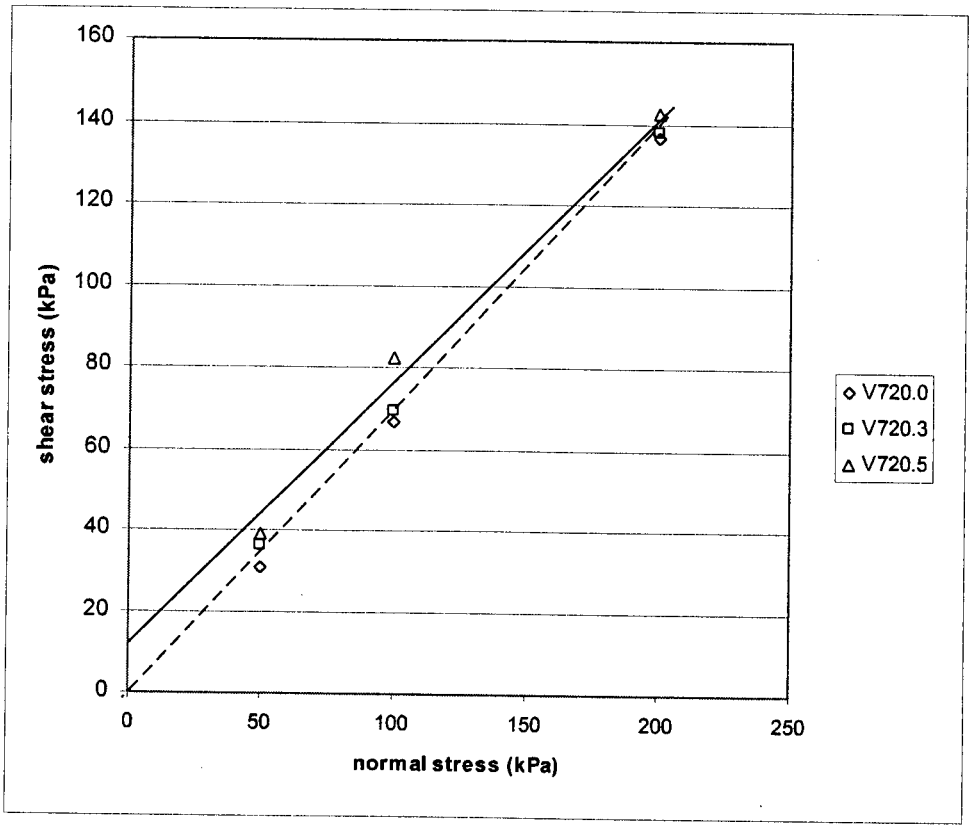

Figure 5.25: Modified failure envelope e_i=0.72

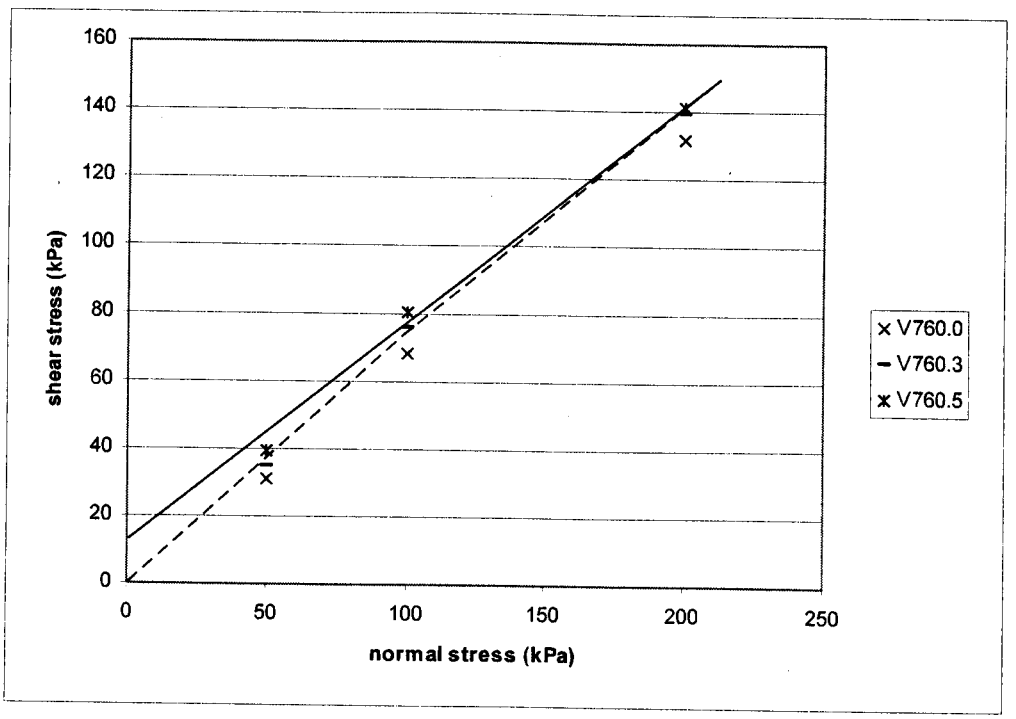

Figure 5.26: Modified failure envelope e_i=0.76

0.67			0.72			0.76		
0%	0.3%	0.5%	0%	0.3%	0.5%	0%	0.3%	0.5%
36.1	38.5	40.7	33.3	35.1	37.7	33.0	35.7	37.4

Table 5.2: Peak angles of internal friction (averages of 50-200 kPa) for three densities

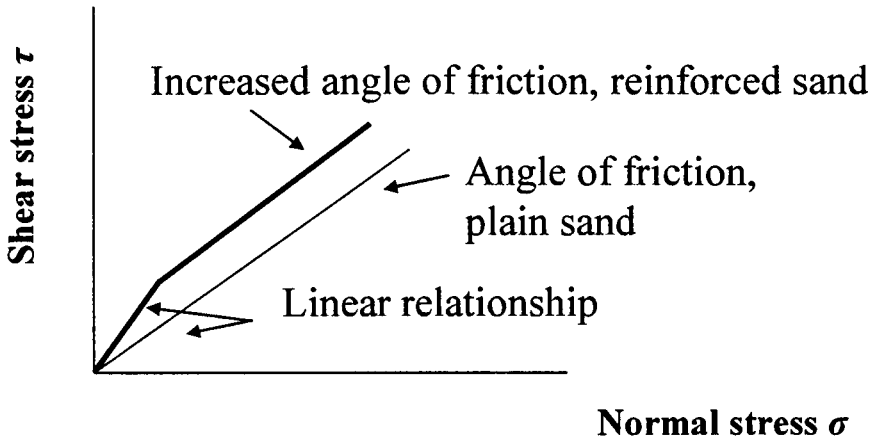

Figure 5.27: Non-linear failure envelope for reinforced sand

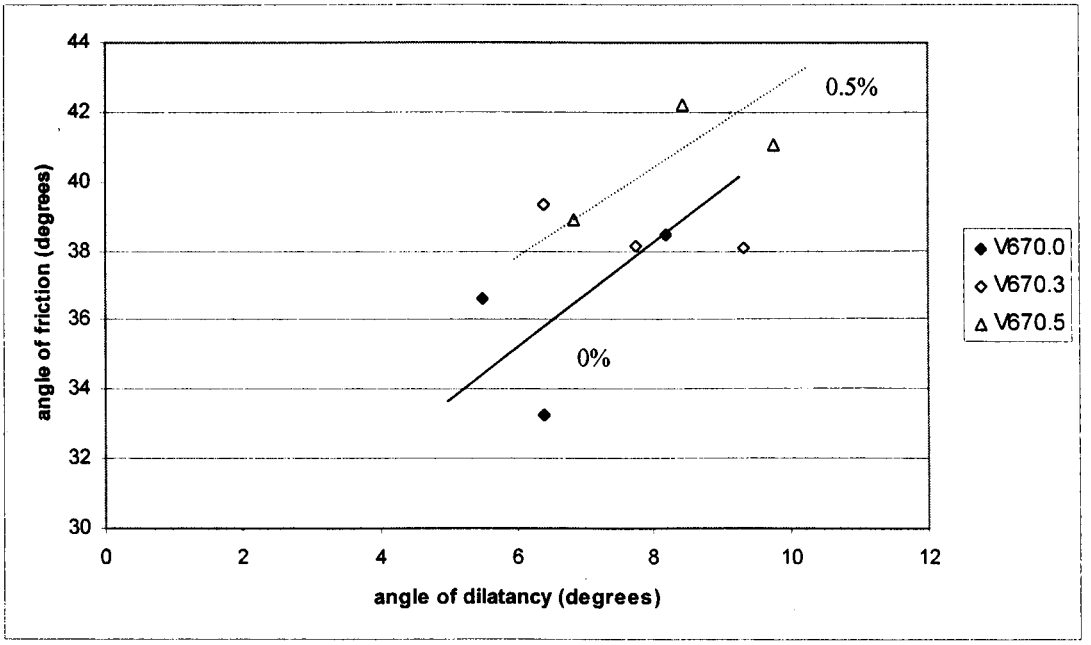

Figure 5.28: Peak angles of friction to dilatancy e_i=0.67

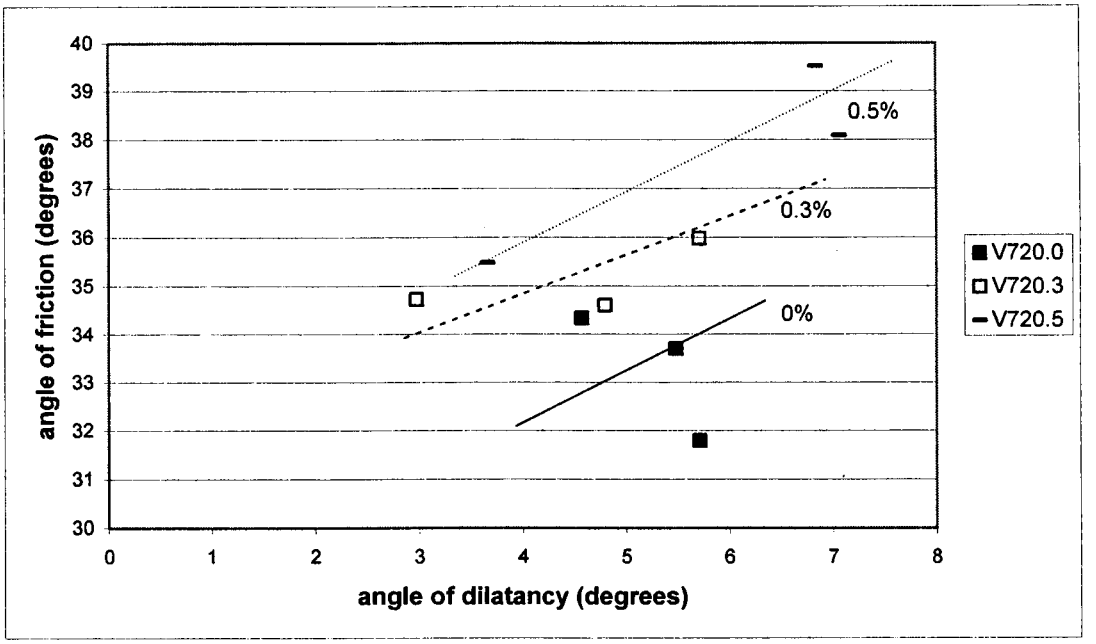

Figure 5.29: Peak angles of friction to dilatancy e_i=0.72

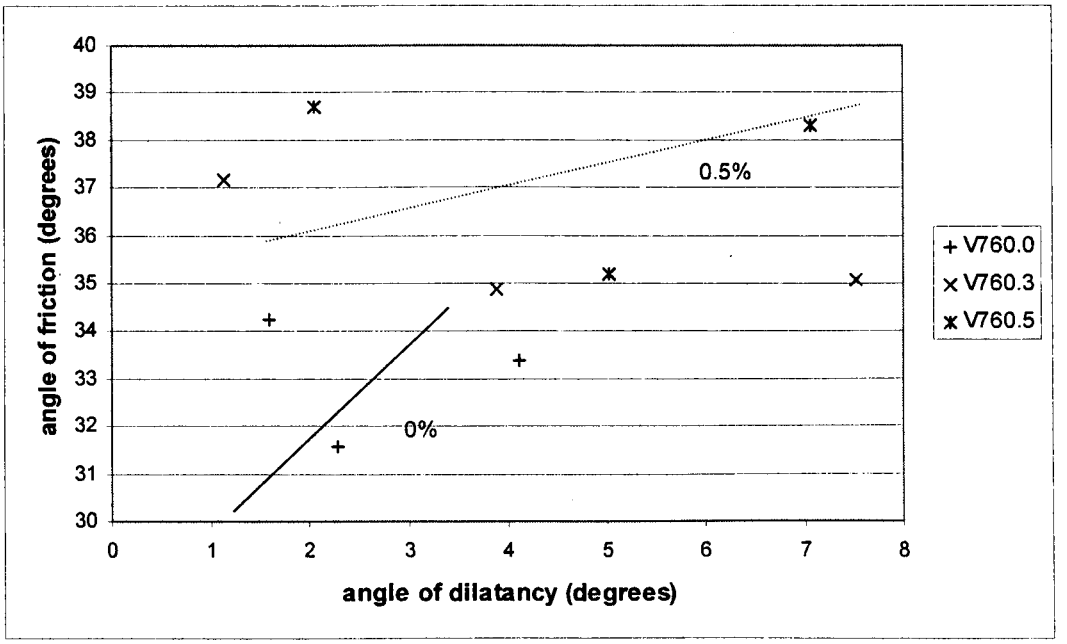

Figure 5.30: Peak angles of friction to dilatancy e_i=0.76

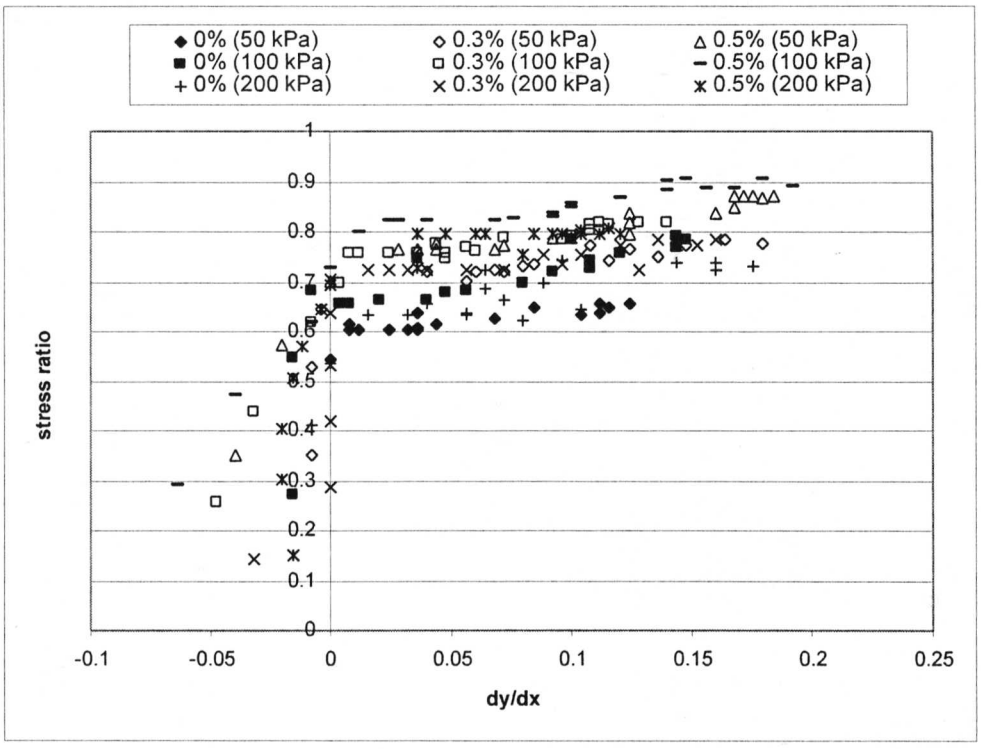

Figure 5.31: Dilation rate for e_i=0.67

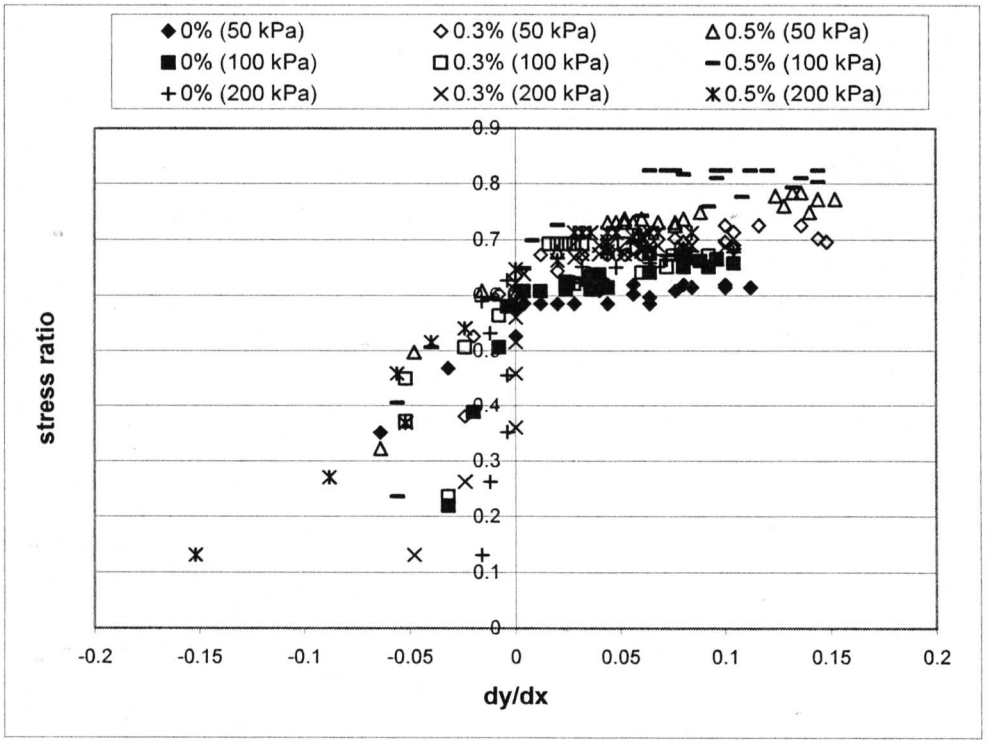

Figure 5.32: Dilation rate for e_i=0.72

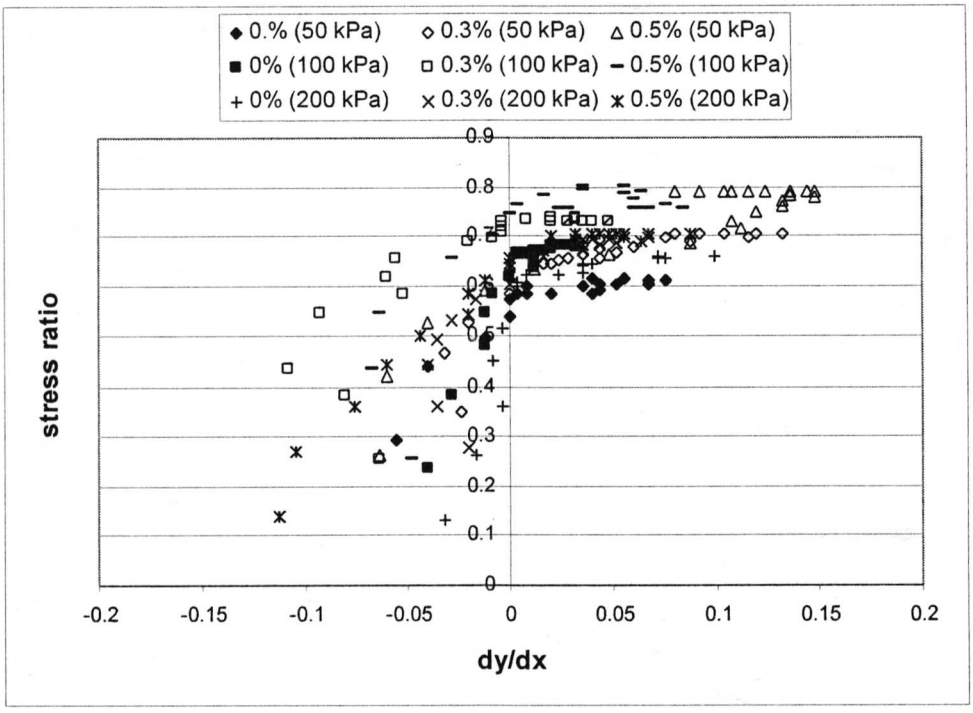

Figure 5.33: Dilation rate for e_i=0.76

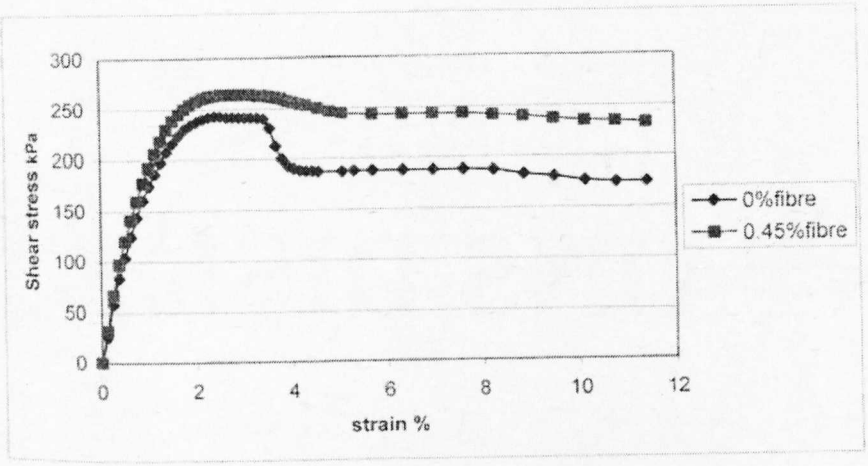

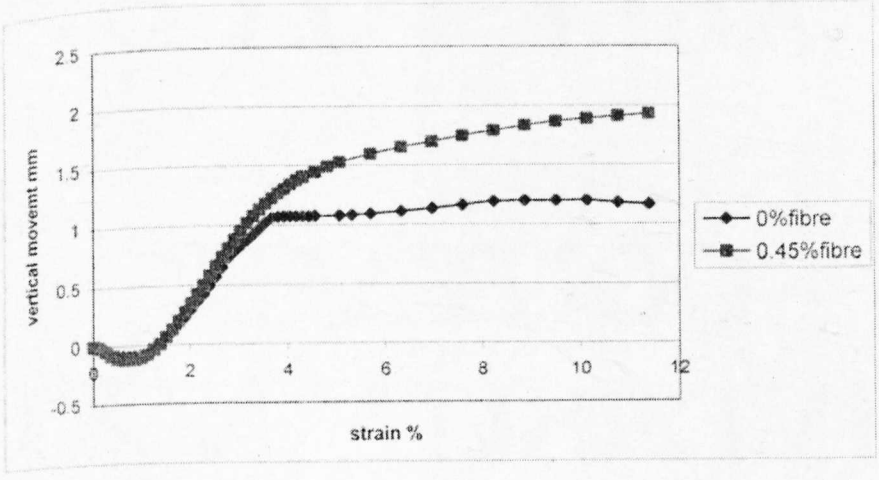

Figure 5.34: Direct shear tests with 278 kPa normal stress
(after Bailey, 2000)

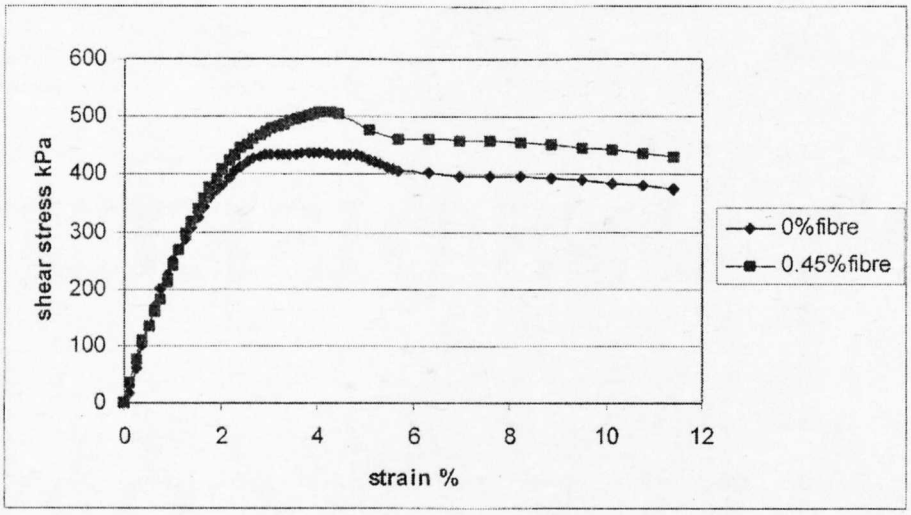

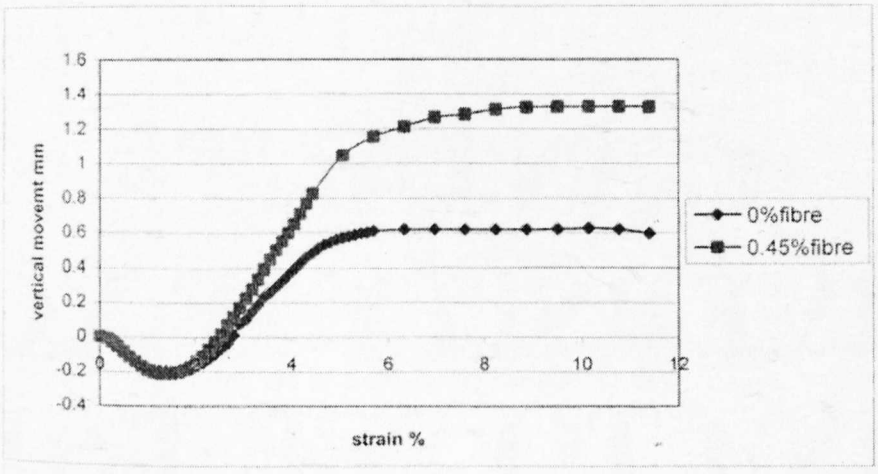

Figure 5.35: Direct shear tests with 556 kPa normal stress
(after Bailey, 2000)

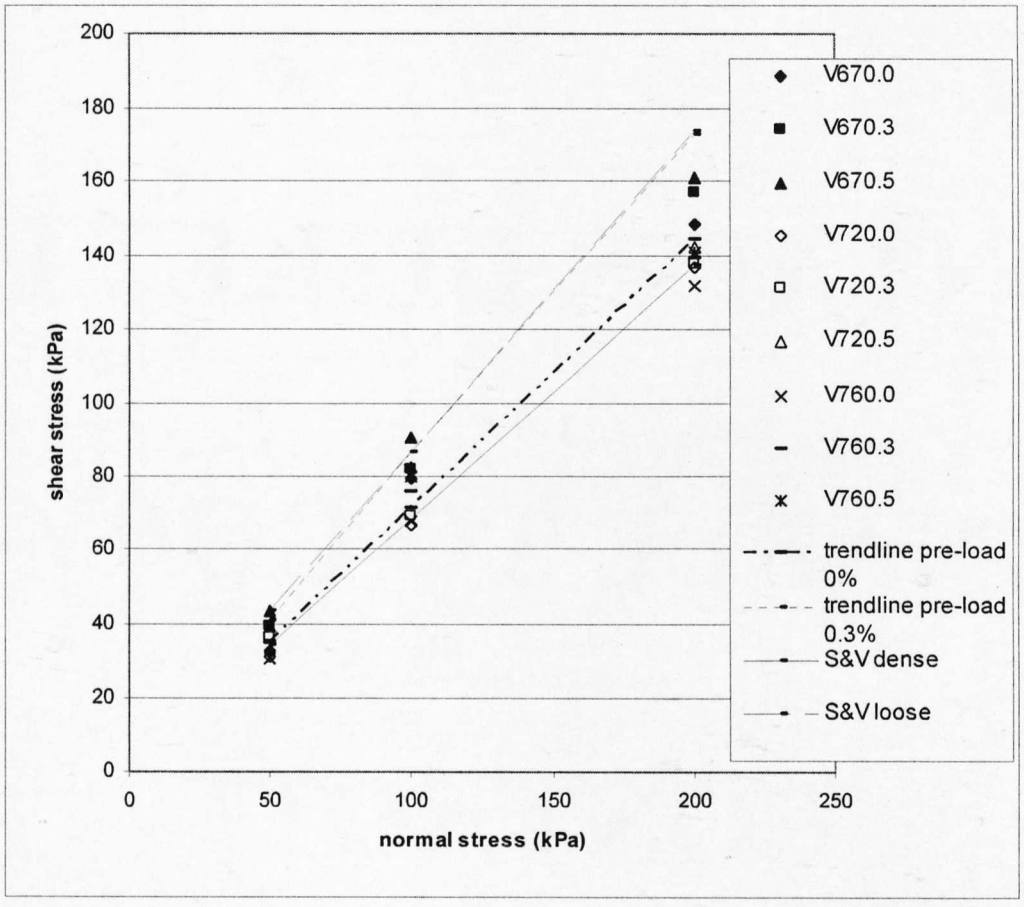

Figure 5.36: Failure envelopes for Hostun sand samples in direct shear with triaxial test results by Schanz and Vermeer (1996)

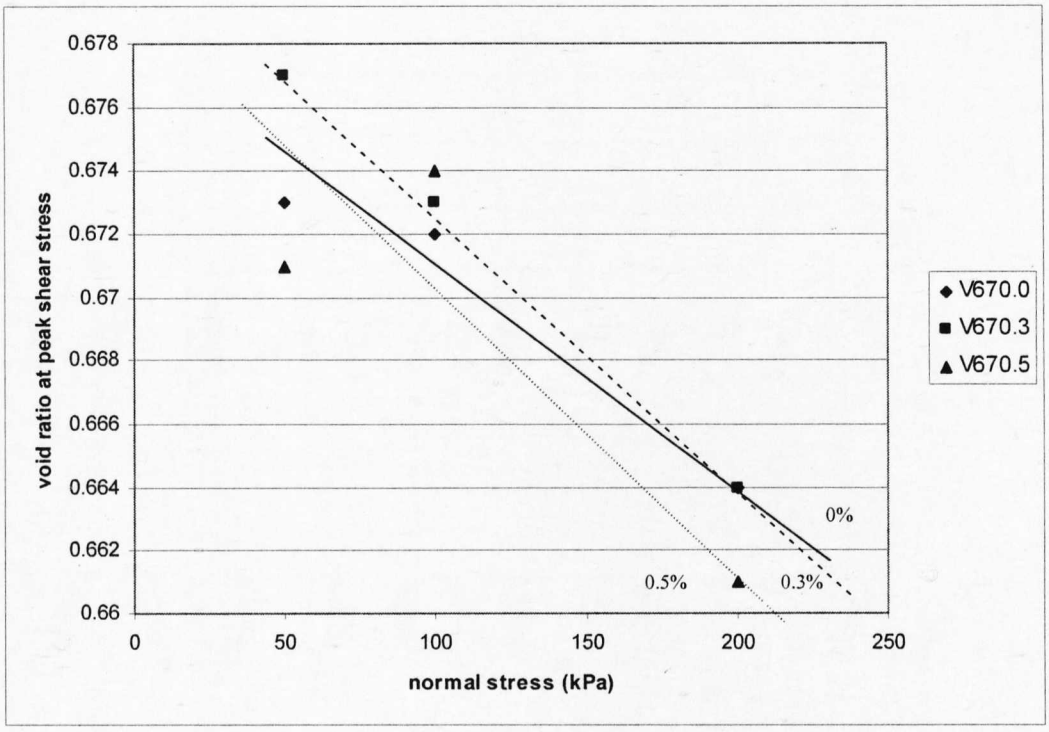

Figure 5.37: Void ratios for peak stress ratio values e_i=0.67

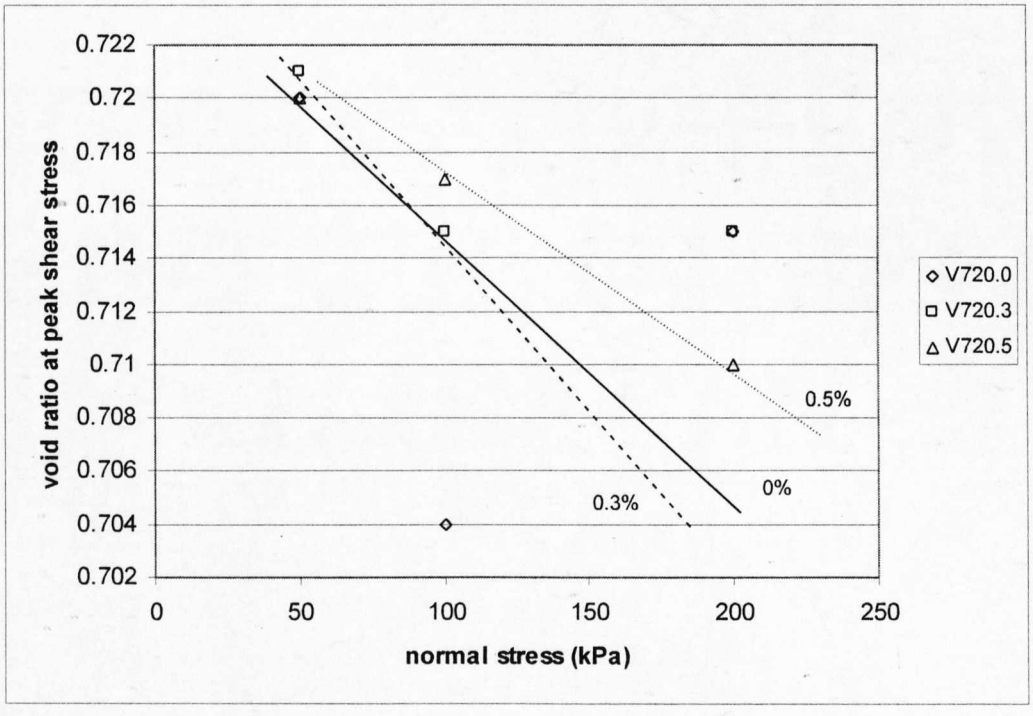

Figure 5.38: Void ratios for peak stress ratio values e_i=0.72

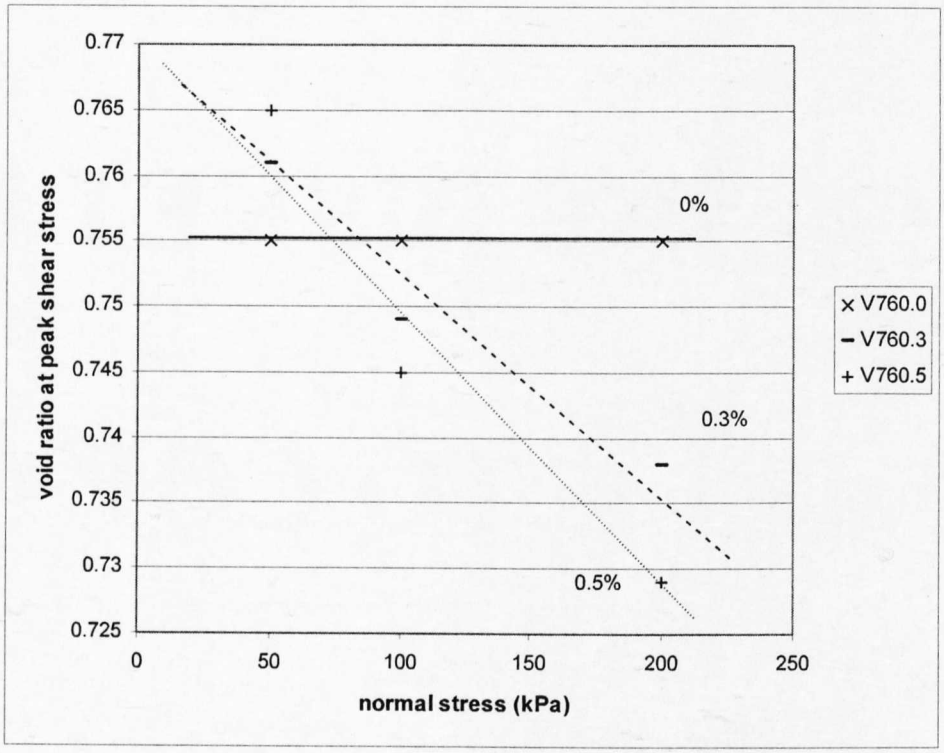

Figure 5.39: Void ratios for peak stress ratio values e_i=0.76

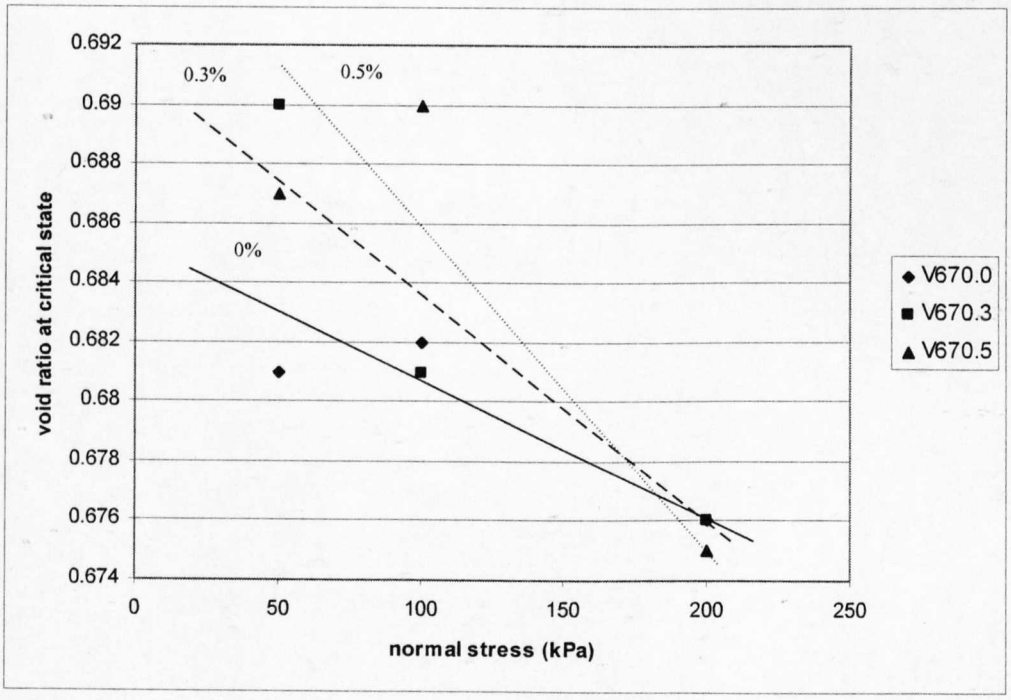

Figure 5.40: Void ratios for critical stress ratio values e_i=0.67

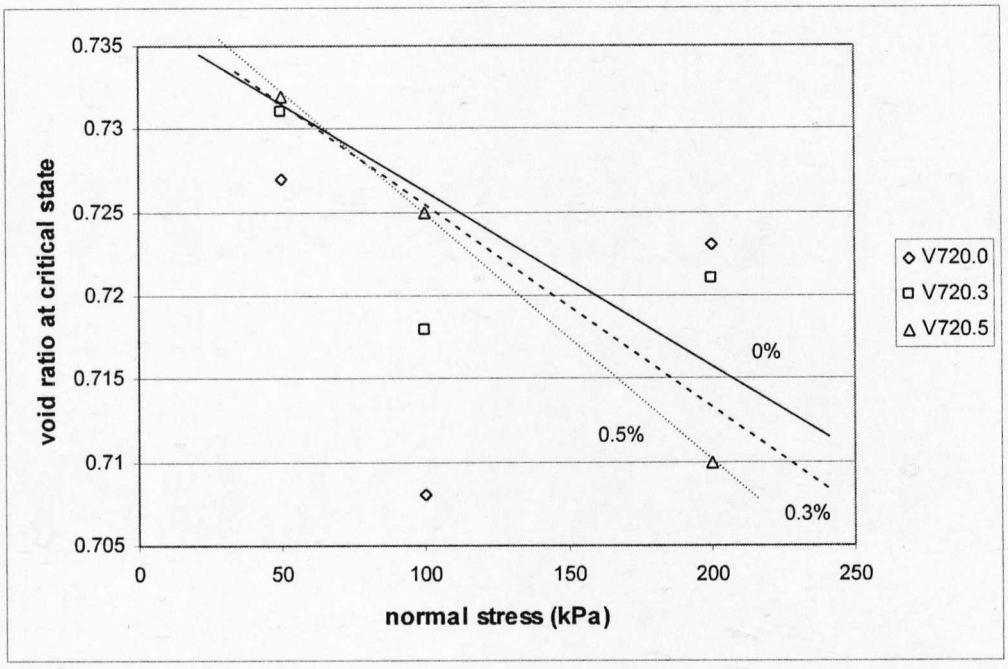

Figure 5.41: Void ratios for critical stress ratio values e_i=0.72

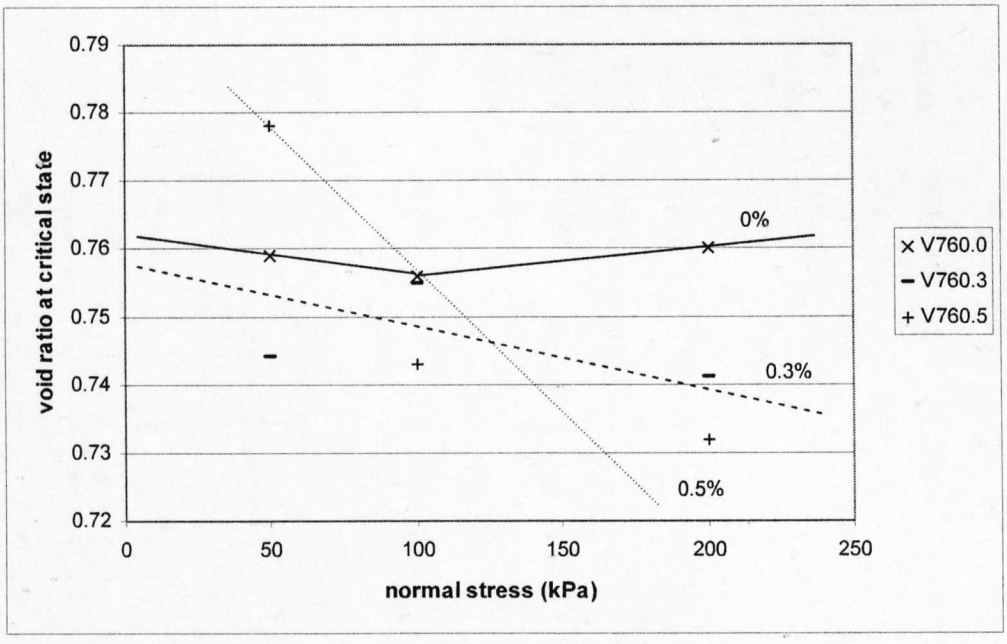

Figure 5.42: Void ratios for critical stress ratio values e_i=0.76

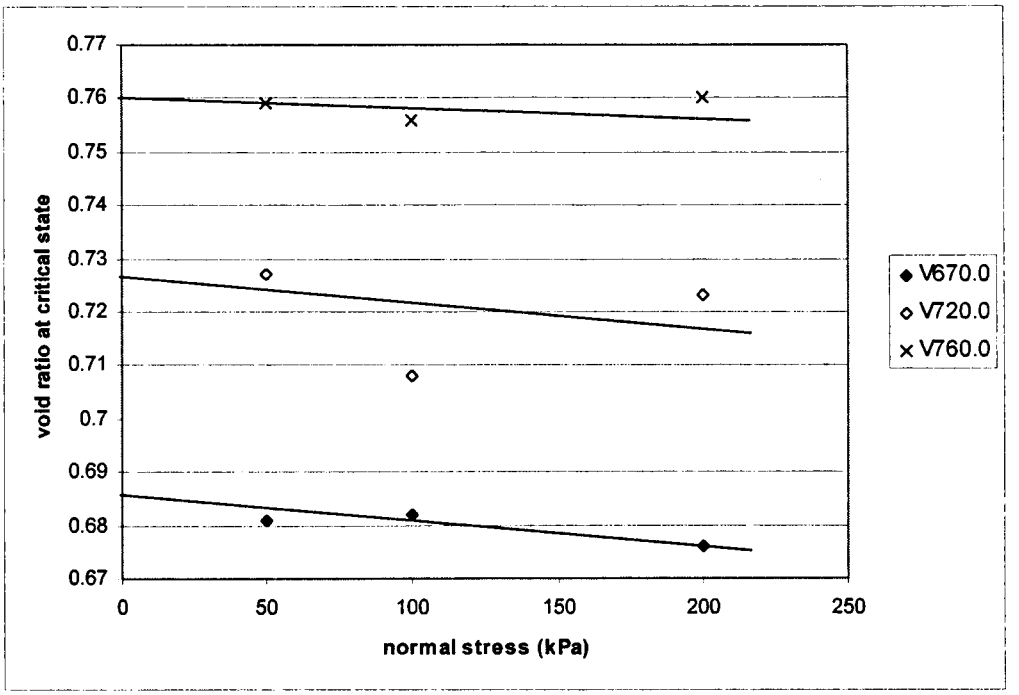

Figure 5.43: Critical state lines for 0% fibre content

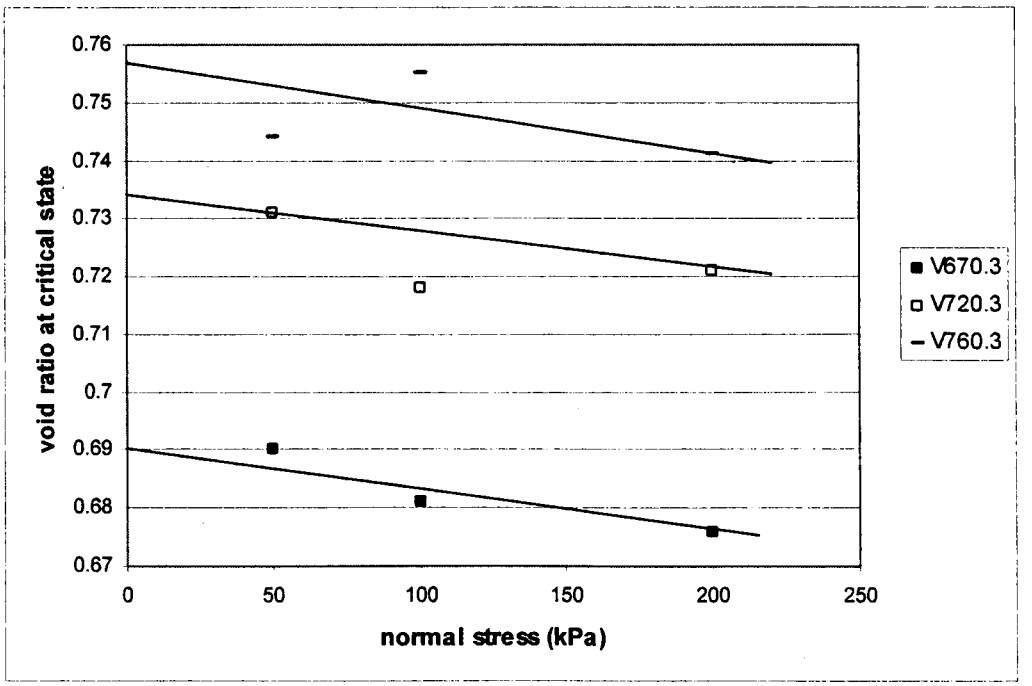

Figure 5.44: Critical state lines for 0.3% fibre content

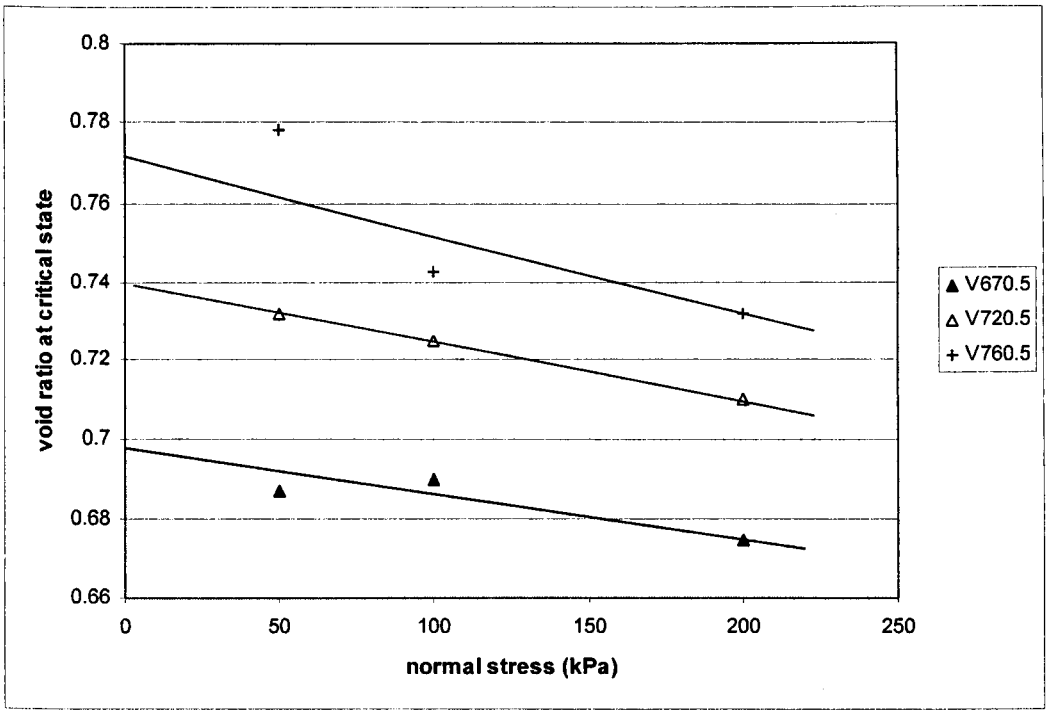

Figure 5.45: Critical state lines for 0.5% fibre content

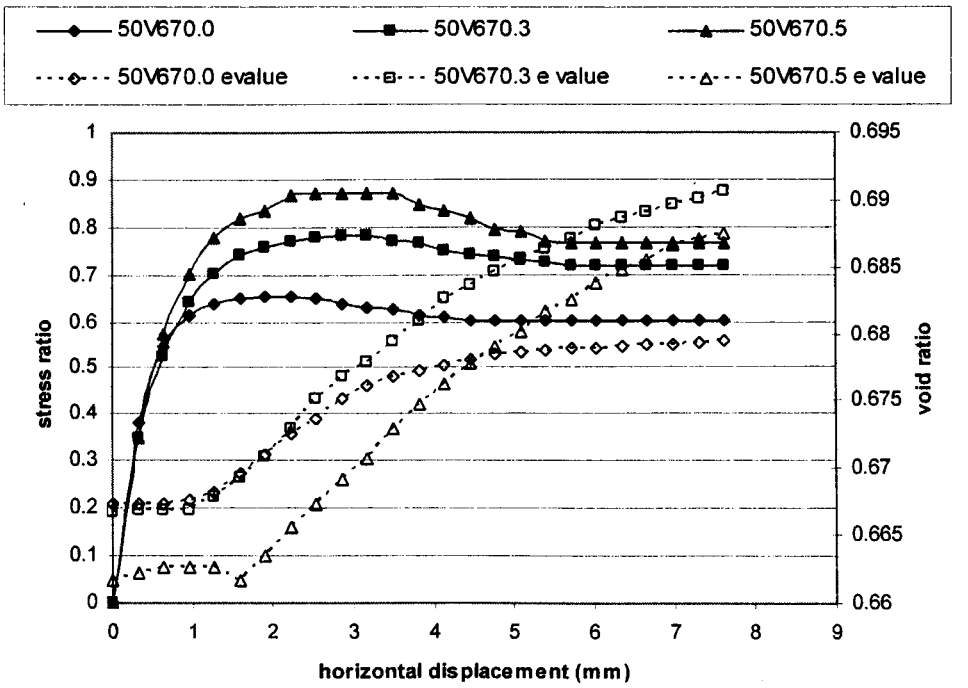

Figure 5.46: Stress ratio to void ratio (e_i=0.67)

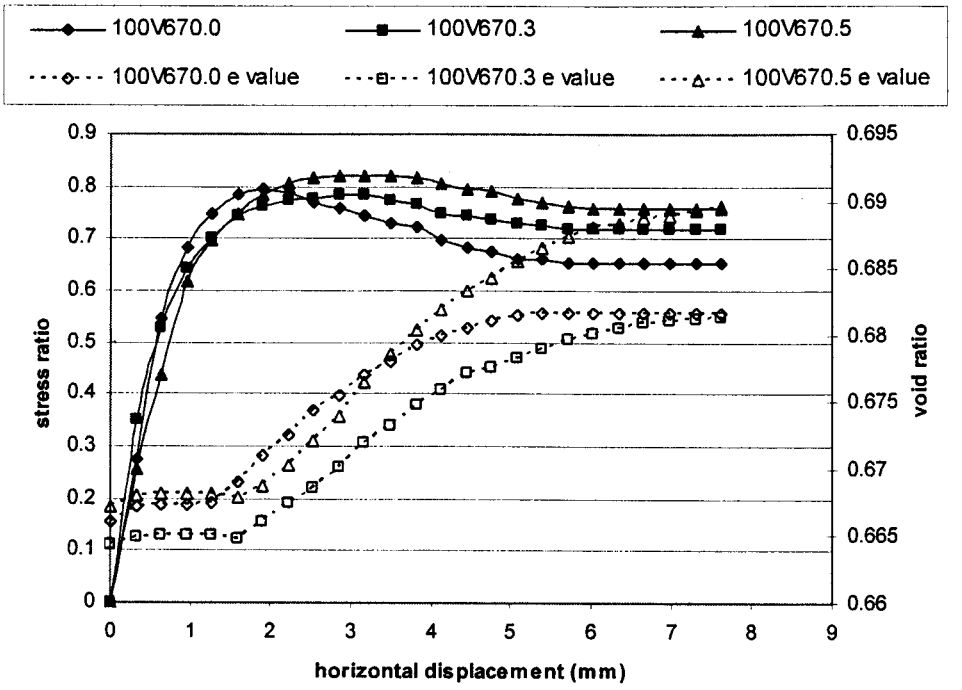

Figure 5.47: Stress ratio to void ratio (e_i=0.72)

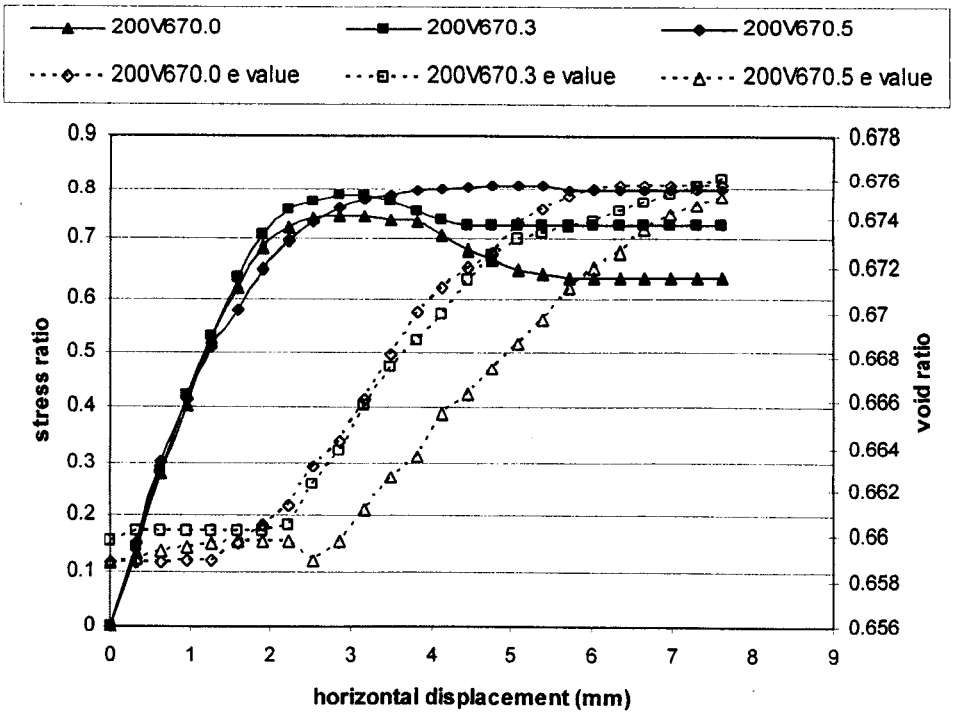

Figure 5.48: Stress ratio to void ratio (e_i=0.76)

6.0 Fibre-reinforced sand performance models

6.1 Introduction

The mechanical effects of different initial sample conditions on the peak and critical shear strength of fibre-reinforced sands have been observed and discussed in the experimental results in the previous section. In this chapter, a model is presented to demonstrate how the addition of fibres increases the shear strength of a sample and increases the ductility of the composite. The experimental results are compared with the theoretical predictions. The process of developing a model for the fibre-reinforced sand behaviour in shear consisted of the following stages.

1. Define the peak and critical states of stress for plain sand.

2. Compare the volumetric strains associated with different stages of shearing resistance in direct shear tests.

3. Observe the confining effects of the normal stress value based on the failure envelope.

4. Identify a critical confining stress for direct shear samples that relates to a marked change in the shear stress to normal stress envelope and the sample density.

5. Establish a model failure envelope for reinforced sands according to fibre content.

6. Determine the effects that the inclusions of fibres have on strain localisation in the shear zone.

7. Distinguish the relationship between the change of internal angle of friction and the change of sample density.

First the main principles for comparing the shear strength for plain sand samples in direct shear tests are described. The strength parameters of homogeneous Hostun sand samples at peak and critical stresses are defined to gain an understanding of the soil behaviour in shear. The volume changes at large shear displacements are then studied as part of the model investigation of critical state soil behaviour with respect to sample density. Finally a model for the performance of fibre-reinforced sand samples in direct shear is presented.

The proposed framework for fibre-reinforced sands consists of the following assumptions. Each of these assumptions will be discussed further and justification for each will be given.

- The Hostun sand exhibits the characteristics of a soil described by the Mohr-Coulomb failure criterion, which means that the assembly of soil particles are considered perfectly plastic.

- Random orientations of evenly distributed fibres are assumed within the reinforced samples. Not all fibres within a sample contribute to the shear resistance due to the various orientations.

- No fibres appear to stretch or break when observed after tests. A small amount of fibre stretching was assumed with respect to minuscule "straightening" effects of the crimped fibres.

- No sand particles are crushed in direct shear, although the normal stress values are sufficient to confine the fibres.

- During peak shear all fibres in the shear plane are fully stressed and therefore, the tensile strain of shear-resisting fibres is fully mobilised from the onset of the peak stress state until the end of testing.

All fibres are assumed to contribute to the confinement of sand particles during shear. It is assumed that the stress within samples is equally distributed to all the fibres in the shear zone that contribute to shear resistance. These assumptions yield a less conservative result compared with calculations of shear strength for fibres at a certain orientation to the shear plane only, while at the same time allow for a simple force distribution for investigation.

6.2 Fundamental direct shear model

6.2.1 Critical states of shear stress

The normal stress in direct shear provides confinement for a soil sample. The peak and critical stress behaviour has been shown to depend on the confining stress value and the sample density. A state parameter is used to correlate these two test variables with the critical state values for Hostun sand. Figure 6.1 shows a representation of a samples' void ratio value (-) in relation to the steady state line for the sand. Figure 6.2 shows a representation of the

strength to state parameter values for plain sand. These fundamental relationships will be used to compare predicted values with experimental results in this chapter.

The void ratio values for the samples at peak and critical states were implemented into the state parameter model in order to determine its relevance to a performance framework for fibre-reinforced sands. The shear test results for plain sand direct shear test samples in Figures 6.3 and 6.4 show the void ratio values at peak shear and critical state stresses respectively. The void ratios at peak (Figure 6.3) generally decreased with confining stress values increasing from 50 to 200 kPa. Dense samples showed a gradual decline in void ratio value and the loose samples showed no change in the void ratio at peak stress. The medium density samples showed a sharp drop in the peak void ratio curve at 100 kPa which indicated that the sample was in its most dense condition at that point of the test. The void ratio at critical state is expected to show a relationship with the confining stress for plain sand samples. The void ratios at critical state (Figure 6.4) showed 100 kPa to be the confining stress that corresponds to the densest condition for the 0.72 and 0.76 initial void ratios (for all experimental results). The dense samples (e_i = 0.67) showed that 100 kPa confining stress gave the least dense condition at critical state.

A state parameter was introduced by Been and Jeffries (1985) that related the change of sample density to the critical state stress value. In Figure 6.5 the average void ratio values at initial and critical state for each test were plotted against the logarithmic mean normal stress value. The average void ratio values (initial and critical) used in this figure were the mean values for the values obtained under the three normal stresses of 50, 100 and 200 kPa. It is necessary to use the mean normal stress value in the determination of a state parameter as this parameter is defined on a plane of constant mean stress. The critical state lines ("CS e = *initial void ratio*" in the legend) were shown for the critical state void ratios of shear samples from 50 to 200 kPa normal stress (the void ratio values at 100 kPa were omitted for clarity). The state parameter of a sample at any point during a test is simply the vertical offset of the initial void ratio from the CS line.

Figure 6.6 shows the peak stress ratio values for 50 and 200 kPa normal stress plotted against the samples' state parameter values. The stress ratios were used to normalise the sand's behavioural response with respect to stress. The dense and medium samples showed an increase in the state parameter value as the peak stress ratio increased, therefore the sample densities at peak stress changed according to the confining stress value. The loose sample showed the same state parameter value for both normal stresses as the sample's density at peak remained the same for both confining stresses. The state parameter values for dense and

medium samples indicated that the peak stress ratios were approaching critical states at higher normal stresses. The loose samples' state parameter values also represented behaviour similar to critical state as the value -0.003 can be described as "slightly negative" according to Been and Jefferies' criterion (see Been and Jefferies, 1985). For all samples (irrespective of the initial density value) the peak stress ratio was reached when the normal (confining) stresses were greater than the mean normal stress value.

The shear stress value at critical state is related to the normal stress by a function of the critical state angle of friction. Figure 6.7 shows the peak angles of internal friction as functions of the state parameter. The trend lines crossing from negative to positive mark the change from dilation to contraction or vice versa according to the state parameter. Angles of friction that tend to fall in the regions closest to zero (both positive and negative) represent the state parameter values that indicate dilative behaviour. This trend shows good agreement with the stress-deformation behaviour of the samples in direct shear.

The average of the state parameters for the test samples at critical state are shown in Table 6.1 according to their initial void ratio. The mean normal stress of 117 kPa was calculated for the test set of normal stresses that included 50, 100 and 200 kPa. The dense and loose samples had positive values at 117 kPa mean normal stress, while the medium samples showed a negative state parameter value. Negative state parameter values generally indicate significant sample dilation and positive values indicate little dilation within the samples before reaching critical state, as there is a dependency of the state parameter, ψ_A, on volumetric strain. Figure 6.8 shows the dilation rate at peak stress ratio as a function of the state parameter for the three initial Hostun sand densities. The peak dilation rates were chosen as they correspond to the greatest phase transformation within the soil in direct shear tests. Again an increase was observed for the dense and medium samples, while the state parameter for loose samples remained constant.

Although the state parameter model provides a relationship for the friction angle and dilation rate to a physical state for un-reinforced soil, the benefits of fibre reinforcements are best observed at large displacements. The volumetric strain of plain Hostun sand samples at large shear displacements was observed with respect to their shear strength values.

6.2.2 Volumetric strain at large displacements

The critical state for sands tends to develop at large shear displacements. The amount of shear displacement that takes place until the peak and critical stress values are realised in a soil

depends on the sample density and the normal stress value. The angle of friction for a soil, as determined by peak stress values, is related to the volume changes from shear displacement and vertical displacement in direct shear. A basic parameter that describes this relationship will be used to compare the Hostun sand test samples.

In direct shear tests, the total volume change of a sample does not explicitly represent the volume change in the shear zone. The shear zone can be dilating while the volume changes are absorbed by the compression of the surrounding soil. Strain "softening" at large displacements can be revealed through the mobilised friction angle, ϕ'. The difference between the peak and critical shear strain states was defined as $\Delta\varepsilon^{-p}$ (units = mm) and used by Shuttle and Smith (1988) in the following formula to define a softening parameter (H').

$$H' = \Delta\phi' / \Delta\varepsilon^{-p}$$

The strain-softening parameter can be used to determine the change of the angle of friction based on the strain and vice versa.

The global volume change evolution was observed in the Hostun sand samples from the stage of an initial contraction followed by dilation until the peak stress was reached in the region of 2 to 3mm shear displacement. Post-peak the dilation reduced to zero as the vertical deformation remained stable while shear displacement continued to the end of tests. The range of global volume change values at large shear displacements decreased with increased initial void ratio. The largest global volume changes at large displacements were observed in the samples with larger normal stresses.

Initial void ratio	***dy/dx* range**
0.67	0.04 to 0.17
0.72	0.06 to 0.12
0.76	0.08 to 0.10

The peak mobilised friction angles were observed in the range of ϕ'_{peak} = 31.0 to 38.4°, while the critical state angles ranged ϕ_{cv}' = 31.0 to 33.5°. The volume change from initial state to peak stresses ranged from 1.9 mm to 3.8 mm shear displacement and in the change from initial state to critical stress state, the shear displacement ranged from 4.5 to 7.3 mm for the Hostun sand samples (depending on their initial densities and normal stress values).

In Figure 6.9 the strain softening parameter for the dense samples increased with increased normal stress, while the "medium" density samples increased from 50 to 100 kPa then decreased. The parameter decreased in loose samples from 50 to 100 kPa, then increased from 100 to 200 kPa. A similar strain-softening parameter that depends on a sample's confining stress has been developed for the fibre-reinforced samples.

6.3 Fibre-reinforced direct shear model

6.3.1 Confining stress

The normal stress values used for testing reinforced sands in the literature tended to be low. The typical normal stress values in literature were between 20 and 200 kPa. The low normal stress range used in this thesis was within the limits of published triaxial and direct shear tests. The largest confining stresses used in triaxial tests were 400 kPa (Bailey, 1997; Bouazza et al, 1994; Ranjan et al, 1996) and 600 kPa (Michalowski and Zhao, 1996), to name a few. Bouazza et al found that a critical confining stress that was common to samples reinforced with either randomly oriented fibres or geotextiles (110 kPa $<\sigma_{crit}<$ 125 kPa). In the case of $\sigma_3 < \sigma_{crit}$, it was postulated that the sand failed before the reinforcement because of the extensibility of the latter.

The normal stress provides confinement to the fibres and sand particles within the samples in the direct shear test. The shear strength envelope for fibre-reinforced sands has a bi-linear shape (as was shown in Figure 5.27). A "threshold" confining stress is defined as the point at which the tangent of shear stress over normal stress changes its angle of inclination. The threshold or confining stress in reinforced soils signifies a break point at which the slippage of the reinforcement in relation to the surrounding soil begins in shear. The value of the critical confining normal stress and the corresponding increase of shear strength beyond that point depend on the properties of the reinforcements, but the shear strength envelopes tend to be parallel to each other for normal stresses above the critical normal stress (Qui et al, 2000).

Based on these findings, an understanding of the stress-deformation behaviour of fibre-reinforced sands in direct shear relies on the determination of a critical normal stress value in order to predict the change of the shear strength envelope. The critical confining stress together with the sample density describes the state of the fibres' confinement within a soil and hence, the amount of increased shear strength produced by the fibres.

Figures 6.10 – 6.12 show the failure envelopes of samples with and without fibre reinforcements according to their initial density values. All envelopes are shown as beginning

at zero shear and normal stress in order to compare the difference inclinations of the shear stresses in the smaller normal stress ranges. The maximum curvature in the failure envelopes of all fibre-reinforced Hostun sand samples occurred at approximately 100 kPa normal stress. From 100 to 200 kPa normal stress, the failure envelopes of all samples were virtually parallel depending on their initial density values. In Figure 6.12 the loose samples show the clearest change in the failure envelope at 100 kPa. At normal stresses lower than 100 kPa, the fibre-reinforced samples' shear strength envelopes were inclined at higher angles of inclination than the un-reinforced samples.

The critical confining stress for reinforced and plain sand samples varied according to the initial densities. Depending on their confinement within a sample, the fibre reinforcements' tensile properties are mobilised in shear and the shear strength of the fibre-sand samples increases. In order to ascertain a critical confining stress for each sample density, the pre-loaded sample test results were included in the investigation for a critical confining stress. Figure 6.13 shows the failure envelopes for pre-loaded samples (shown as 100-50 and 200-50 in the legend as before) with the vibrated samples that were prepared to the same initial density value ($e_i \sim 0.67$). The vibrated samples' strength envelopes increased with increased fibre content. The pre-loaded samples' strength envelopes increased with increased fibre content and with increased confining stress, in the form of a pre-load. Higher confining stresses increased the strength envelope of direct shear samples; the greatest strength increases were found in the samples with the greatest fibre-reinforcement.

Due to the different stress history of the pre-loaded samples, the void ratios at the peak stresses were used as a reference for these samples. The critical confining stress for samples will therefore be determined according to the samples' void ratio at the point of maximum curvature on the shear stress-normal stress failure envelope. The peak void ratio values for the samples with 50 kPa normal stress are given below.

Initial void ratio	**Void ratio at peak 0% fibre content (σ_n = 50 kPa)**	**Void ratio at peak 0.3% fibre content (σ_n = 50 kPa)**
0.67	0.673	0.677
0.72	0.720	0.726
0.76	0.755	0.702
0.67 (100 – 50 kPa pre-load)	0.658	0.6735
0.67 (200 – 50 kPa pre-load)	0.664	0.669

The change of the void ratio values from initial to peak stress conditions are shown below along with their peak shear stress values. The samples with 0.3% fibre content had increased shear strength for all initial void ratios, with the greatest increases seen in the samples with pre-load. The dense samples and pre-loaded samples show the least change in void ratio value from initial to peak stress states. This indicated that when a sample was dense or when the confining stress was increased in the form of pre-load, the change of void ratio from initial to peak stress conditions was less than that of samples with higher initial void ratios. The void ratio values at peak for these tests will be used later to define the critical confining stress value for the pre-load samples, as the tests were all sheared with the sample normal stress value of 50 kPa.

Initial void ratio	**Δe at peak (σ_n = 50 kPa) 0% fibre content**	**Δe at peak (σ_n = 50 kPa) 0.3% fibre content**	**Peak shear stress (kPa) 0% fibre content**	**Peak shear stress (kPa) 0.3% fibre content**
0.67	0.003	0.007	32.78	39.22
0.72	-0.1	0.006	31.00	36.30
0.76	-0.145	-0.058	30.75	35.10
0.67 (100 – 50 kPa pre-load)	-0.012	0.0035	34.42	44.25
0.67 (200 – 50 kPa pre-load)	-0.006	-0.001	37.04	46.54

An equivalent stress ratio has been used in this thesis to define the ratio of the peak shear strength of reinforced sand to that of un-reinforced sand. Figures 6.14 and 6.15 show the equivalent stress ratios at peak and critical states, respectively, as functions of the state parameter. The state parameter method does not easily lend itself to an investigation of fibre-reinforced shear samples, so Figures 6.16 and 6.17 show the void ratio to equivalent peak stress ratio for shear samples. The test results indicated that the fibre-reinforced samples had increased strength under the following conditions:

- as the void ratio decreases, which results in the increase of the total contact area between the sand and reinforcement;
- as the normal stress value increases and
- as the amount of fibre reinforcement increases.

The above considerations of the fibre-sand strength mechanisms indicate that the volume increase associated with the shearing of fibre-reinforced sand should become smaller with the increase in strength caused by the inclusion of fibre reinforcements. Figure 6.17 shows the change of void ratio values from initial to critical state conditions plotted against the equivalent stress ratios at critical state. The greatest void ratio change occurring between initial and critical state conditions was observed in the dense reinforced samples. The samples' change in density would suggest that the fibre-sand bond was weak due to the sample dilation, when in fact the increased dilation is a reinforced samples' response to increased stress. The greater increases in strength and dilatancy characteristics were seen for sands having more contact with the fibre reinforcements by means of a greater confining stress value.

The presentation of experimental results using a state parameter does not fully explain the internal deformations for fibre-reinforced sands in direct shear as a result of the confining stress value. Simpler representations are given in Figures 6.18 and 6.19 for the void ratio values at peak and critical states plotted on a logarithmic scale of normal confining stress. The increased shear strength with the addition of fibre content was apparent for all test results. The relationship between the confining normal stress and the shear stress-dilatancy can be described more accurately by the internal angle of friction and the volumetric response at peak and post-peak shear displacements.

6.3.2 Internal friction

The internal angles of friction of the fibre-reinforced samples increased with increasing fibre content according to the initial density values. The increase of the internal friction angle was generated from the increased peak stress ratios described in the preceding section. Figure 6.20 shows the internal angles of friction for fibre-reinforced samples at peak shear stress as a function of the state parameter. Alternative models for the relationship between the increased internal angles of friction for fibre-reinforced soils and the fibre content are required.

A value for the increased shear strength of soil reinforced by plant roots (S_r) in the shear zone was introduced by Wu et al (1979) where the tensile strength of the plant roots at pullout (T_r) was multiplied by the area ratio of the roots in the shear zone (A_r/A). An approximation of 1.2 was used to account for shear stress acting at an inclination of 90° to the shear plane (θ).

$$S_r = T_r \frac{A_r}{A}\left[\cos\theta \tan\phi + \sin\theta\right]$$

approximates to

$$S_r = 1.12\ T_r\ (A_r/A)$$

for the angle orientation to shear plane range $40^\circ \leq \theta \leq 70^\circ$ and

for the internal angle of friction range $20^\circ \leq \phi \leq 40^\circ$ in direct shear.

In the equation presented here, the increased shear strength of sand reinforced by fibres is considered for the entire shear box volume as the fibre distribution is considered to be uniform throughout the sample, and the orientations of the fibres with respect to the shear plane are random (see Figure 6.21). A modification to the formula above is to use the volume fraction for the fibre contents which becomes

$$\Delta\tau = S_f = 1.12\ T_f\ V_f$$

S_f = 1.12 x 3.2 x 0.5 = 1.79 N/mm = **4.88 kPa** for 0.3% fibre content by weight and

S_f = 1.12 x 3.2 x 0.8 = 2.77 N/mm = **7.56 kPa** for 0.5% fibre content by weight

These calculations show good agreement with the experimental results for the increased shear strength that fibre-reinforcements gave to the Hostun sand samples in direct shear as presented in Chapter 5. However, this calculation of increased shear strength at peak stress state does not account for the volume changes during shear.

As the internal angle of friction in shear is a function of the stress ratio, the increases of the equivalent stress ratios were plotted against the fibre contents in peak and critical state stress conditions in Figures 6.22 and 6.23. The highest peak stress ratio values were achieved by the samples with the lowest confining stresses, while the samples with 100 kPa normal stress showed the greatest increase of peak stress ratio values between the two fibre contents. At critical state the dense samples showed the most consistent stress ratio increase with confining stress increases, and again a marked stress ratio increase was observed in samples with 100 kPa confining stress. The increases of the stress ratios at critical state were more erratic as the majority of low initial density samples reinforced with 0.5% fibre content had the same stress ratio values for peak and critical states.

6.3.3 Strain localisation

The presence of fibres tends to flatten out the peak stress values in direct shear. There generally is not an abrupt transition between the elastic and plastic phases for reinforced soils.

The critical states for such samples are not easily identified at smaller shear displacements. The fibres improved the ductility of the samples by minimising strain localisations within the sample volume at large displacements. The fibres strengthened the potential planes of weakness in strain. The isotropic strain characteristics displayed by the samples depended on their initial density values.

Localisation of deformation in the form of narrow zones of shearing can develop in granular soils during processes of flow. Shear localisation can occur inside materials as a single shear zone or a regular pattern of shear zones. The initiation of the localisation can take place before the peak in the overall stress-strain curve; the shear band is not simultaneously initiated at every point, but it propagates from an initiating point with a constant direction for plain sands (Desrues et al, 1985). In the case of sand reinforced with a random placement of flexible fibres, the fibres can minimise localised deformations within a direct shear sample by either suppressing strain localisation or by spreading the volumetric strains throughout the sample beyond the zone of greatest shear resistance.

The determination of the thickness of a shear zone is of great importance for a realistic estimation of the forces transferred from the fibre-soil mass in the shear zone to the rest of a sample volume. The thickness of a dominant shear band is not a fixed value while the shear band is developing in plain sand. The shear band constantly varies and new sand particles are continuously added as the shear band propagates as well as after its full development. With a random fibre distribution, fibres that contribute to the shear resistance can cross the shear plane in a number of orientations to the shear force (as was seen in Figure 6.21). A shear band cannot freely pass through a fibre due to its rigidity (Qui et al, 2000). This suggests that a thicker shear zone consisting of a greater number of small shear bands develops as the tensile strain increases in shear. The main parameters that can alter the dimensions of the shear zone for plain sand include the grain size distribution, the initial void ratio and the confining stress; for fibre-reinforced samples, the fibre content and orientations are additional parameters that affect the size of the shear zone.

The onset of localisation and the development of a complete localisation structure inside triaxial specimens tested by Desrues et al (1996) were clearly revealed by the density maps in the case of the dense samples. Conversely it was difficult to observe localisation in the loose specimens because the density in the localised strain zones did not change significantly. They found a strong tendency for the local void ratio to stabilise after a large jump during the first stage of the localisation development, and remarkably good agreement between the final void ratio values of the different tests.

> "The final plateau observed in the volumetric strain-axial strain curves for dense dilating samples is not physically relevant; it can be interpreted not as the manifestation of a limit void ratio, but as an effect of the strain localisation process inside the specimen."

They summarised that the limit void ratio shown in their test results was dependent on the confining stress level. They also found that any major heterogeneity breaking the symmetry of a sample would induce the selection of one direction as the preferred plane strain direction.

The strain softening parameter H' was used to describe the behaviour of the un-reinforced Hostun shear samples in Figure 6.9. Figure 6.24 shows the strain softening parameter for all fibre contents according to their initial samples densities. The parameter was calculated by $H' = \Delta\phi'/\Delta\varepsilon^{-p}$ which is the change in friction angle over the change in the shear displacement from peak to critical state. The samples with 100 kPa normal stress again showed inconsistencies with the increasing parameter values from 50 to 200 kPa normal stresses. The dense samples gave the highest values of H' as they experienced the greatest change in internal friction angle within the shortest shear displacement range (from peak to critical state). Loose samples gave lower values of H' as there was little difference between the peak and critical angles of friction over a greater shear displacement range.

For sand samples, the strain softening parameter can provide a relationship necessary for a fundamental model of the shear strength and displacement; however for sand samples reinforced with a random distribution of fibres, the strain softening behaviour tends to change after a critical confining stress value is reached. The mechanism of the fibre tensile strain resisting strain localisation within a sand sample has a direct effect on the increase of the peak shear strength, and also increases the ultimate shear strength. The increased shear strength of reinforced samples at both peak and post-peak was due to the tensile strain provided by the fibre content.

6.3.4 A performance model for fibre-reinforced sands

The shear-deformation response of fibre-reinforced sands differed from un-reinforced sands, especially after a critical confining stress value. The failure envelopes of fibre-reinforced sands have been described as non-linear with a "break point" in the internal angle of friction occurring at the confining stress value. For the range of normal stress values and initial sample densities used in this set of experiments, the critical confining stress was found to be in the region of 100 kPa. The experimental results for Hostun sand samples under small

normal stresses in direct shear generally demonstrated approximately 2° increase in the peak internal angle of friction with an increase of approximately 0.25% fibre content at all initial densities. The model for the shear behaviour of fibre-reinforced sand samples relies on the sample variables of initial densities, the confining stress values and the fibre content to predict the shear strength characteristics.

The failure envelopes for fibre-reinforced sands were modelled on the plain sand behaviour where the increase of shear stress (S_f) was calculated and added to the shear stress values from the critical confining stress value onwards; in these tests the confining stress value = 100 kPa. The increased shear stress due to reinforcement was determined by the model introduced by Wu et al (1979) to be +5.23 kPa for 0.3% fibre content and +8.39 kPa for 0.5% fibre content. These stress increases were applied to the 100 and 200 kPa shear stress values on the un-reinforced sand peak stress envelope. For small normal stresses, the shear stress values were determined by extrapolation from 0 to 100 kPa. The predicted failure envelopes for fibre-reinforced samples were plotted against the experimental results in Figures 6.25 – 6.27 in order to observe the accuracy of the performance framework based on the formula mentioned. The predicted values were compared to the fibre-reinforced test results on a failure envelope in Figures 6.28 to 6.30. The modelled behaviour for fibre-reinforced samples shows favourable agreement with the failure envelopes of the experimental results.

The model for the void ratio parameter at critical states combines the theories for the strain-softening parameter, H' and state parameter ψ_{SP}. The change of internal angle of friction from peak to critical state was divided by the void ratio value at critical confining stress for the sample density to give a void ratio parameter H'_e based on the critical state void ratio.

$$H'_e = \Delta\phi' / e_{ccs}$$

$$\text{where } e_{ccs} = e_{fc} - e_{0\%}$$

The void ratio value of un-reinforced samples at their critical confining stress ratio, $e_{0\%}$, was subtracted from the void ratio values of fibre-reinforced samples at critical state e_{fc} to calculate the difference between the critical void ratio at critical confining stress e_{ccs}.

Figure 6.26 shows the range of void ratio parameter values from 0 to 5 for the fibre-reinforced shear samples with the normal stress range of 50 to 200 kPa. The dense samples showed the highest void ratio parameter values for both fibre contents at low normal stresses. The

medium density and loose samples with 0.3% fibre content showed no change in void ratio parameter with increased normal stress value. The medium density samples with 0.5% fibre content showed a marked decrease in void ratio parameter with increased normal stress values. The loose samples with 0.5% fibre content gave zero values for the void ratio parameter as there was no void ratio difference between their peak and critical void ratio values.

Samples of medium initial density gave a constant void ratio parameter value of 3 for the range of normal stress values. The dense samples generally had higher void ratio parameter values, but as these values declined with larger normal stresses and higher fibre contents, the most significant stress-strain behaviour lies in this range. It is the range of void ratio parameter values that is of greatest importance, and secondly the constant values. The loosest samples did not achieve a peak angle of friction greater than critical state, therefore the benefits of fibre reinforcements were not fully realised for this sample density.

The void ratio parameter uses the void ratio value at critical confining stress to provide a stable density condition related to the failure envelope. The ratio of the change of the internal friction angles to the change of the critical void ratio values due to the addition of fibre content gives a parameter that can be used to predict the increased angle of a sample's failure envelope or density compared to plain sand samples.

6.4 Summary

This chapter set out to define the performance of fibre-reinforced sands in shear and to predict their stress-deformation behaviour. The following conclusions were drawn from the predictions and the laboratory experimental results.

- The fibres enhanced the shear strength and tensile strain properties of Hostun sand in direct shear at both peak and critical states. Increasing the fibre content increased the peak and critical shear stresses for all samples.

- Equivalent stress ratios were used to compare the increased shear states of stress of fibre-reinforced samples with the un-reinforced Hostun sand samples.

- The volumetric strains of sand samples in direct shear were associated with the difference of the shear displacements at peak and critical stress states.

- The fibres were considered to absorb localised shear bands in the shear zone in conditions of strain softening so that the global void ratio changes could be compared.

- The absence of localised strains within the reinforced shear tests samples was due to the confining action that the fibres presented to the sand grains.

- Increasing the confining stress increased the peak and critical shear stress for all samples.

- The critical confining stress values were determined based on the point of greatest curvature on $\tau - \sigma_v$ graphs for the three initial densities and compared with published critical stress levels for similar normal stress ranges.

- The stress-deformation behaviour of samples with a stress history of pre-loading before shearing commenced under 50 kPa normal stress provided additional information for the change of peak and critical state void ratio values under different confining stress values.

- A formula for the increased shear strength of samples in direct shear according to the tensile strength of the fibres, the volumetric fibre content and the critical confining stress showed favourable agreement with the experimental results.

- A void ratio parameter was developed that compared the changes in void ratio values at critical state with the critical void ratio, according to fibre content.

6.5 Figures

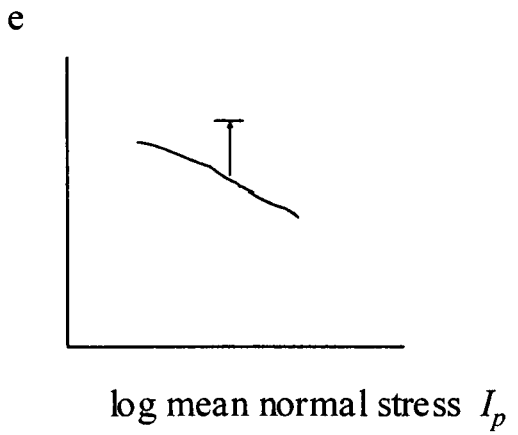

Figure 6.1: A void ratio value greater than the steady state line of void ratio to log mean normal stress

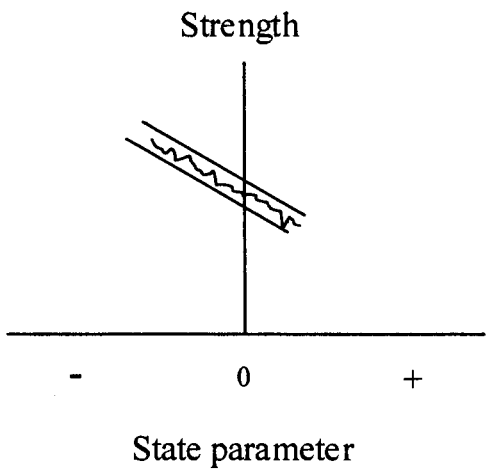

Figure 6.2: Relationship between soil strength and state parameter values

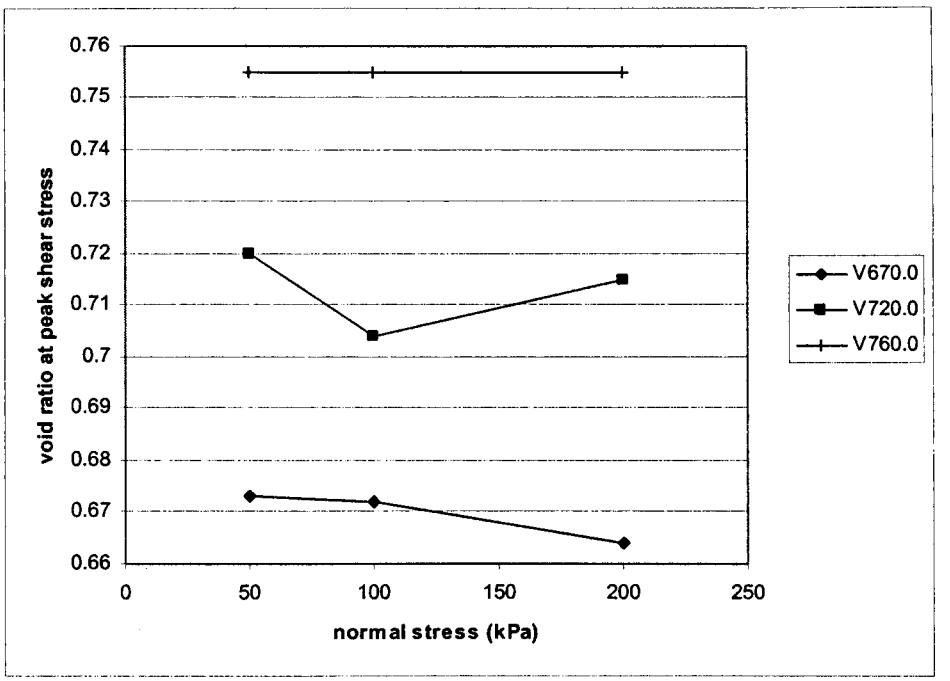

Figure 6.3: Peak stress void ratio values

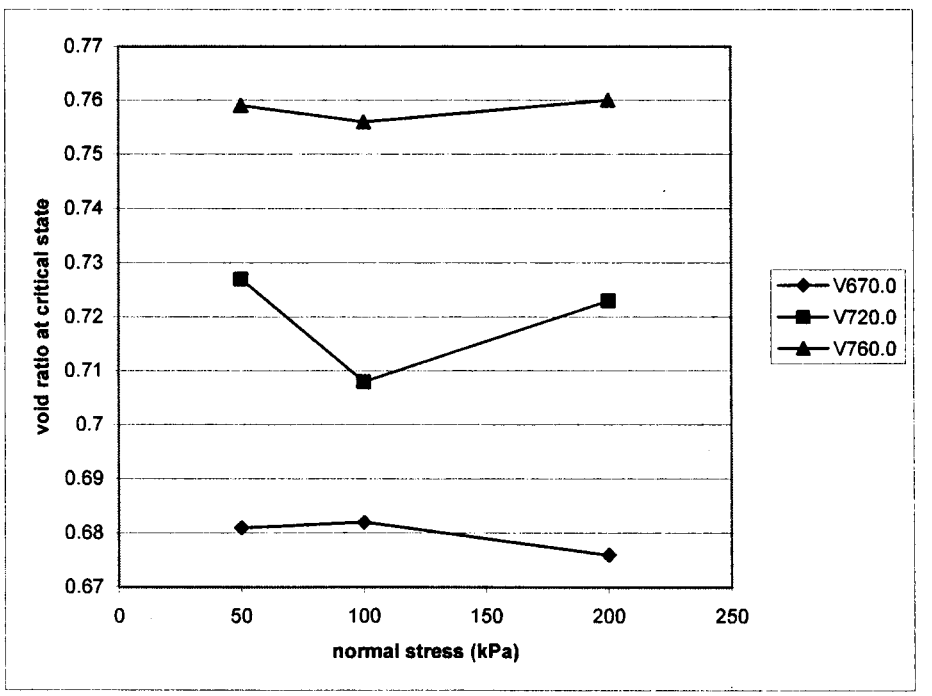

Figure 6.4: Critical state void ratio values

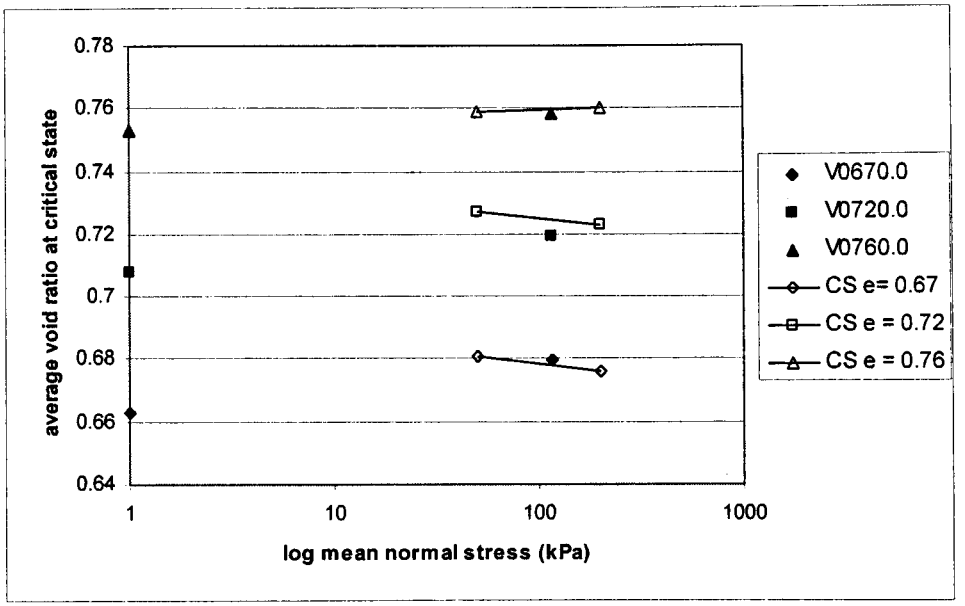

Figure 6.5: State parameter relationship for Hostun sand

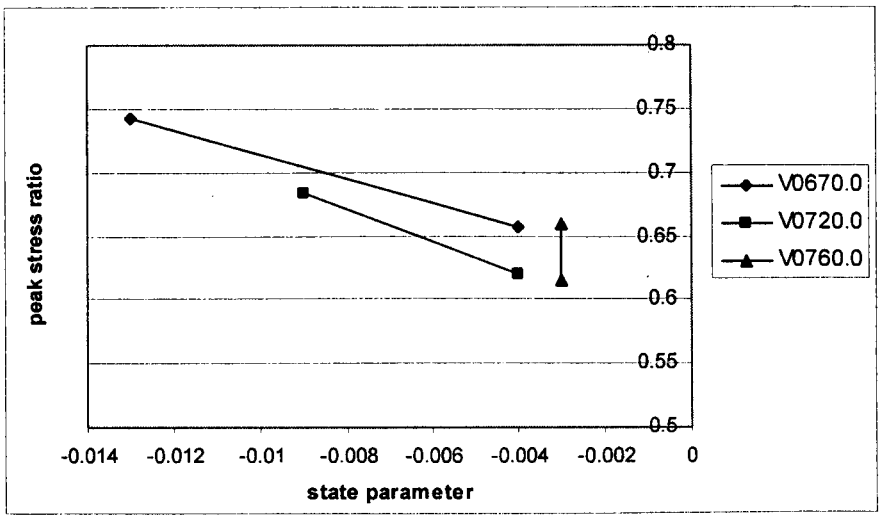

Figure 6.6: Peak stress ratio as a function of state parameter values

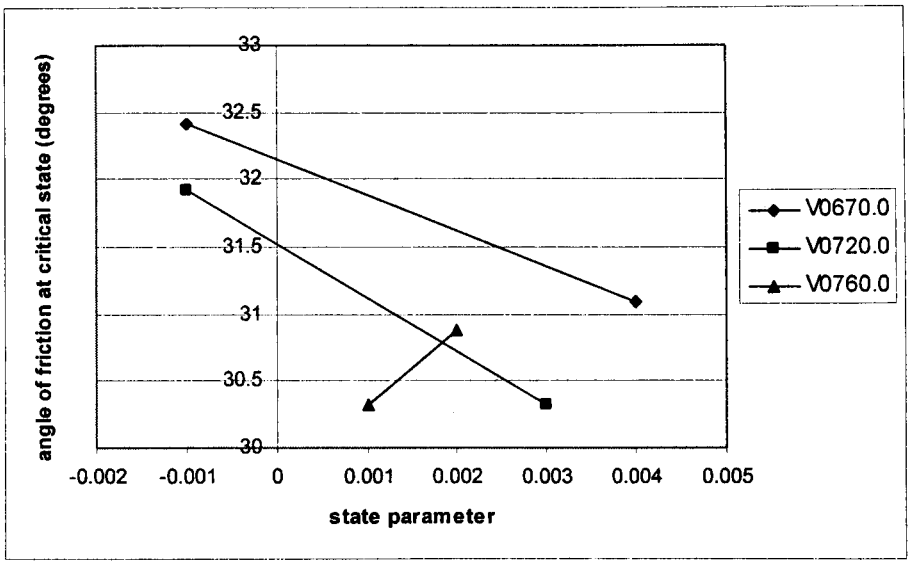

Figure 6.7: Angle of friction at peak stress ratio as a function of state parameter

Initial void ratio value	State parameter
0.67	-0.00267
0.72	0.004667
0.76	-0.00033

Table 6.1: State parameter values for Hostun sand samples at critical state (117 kPa normal stress)

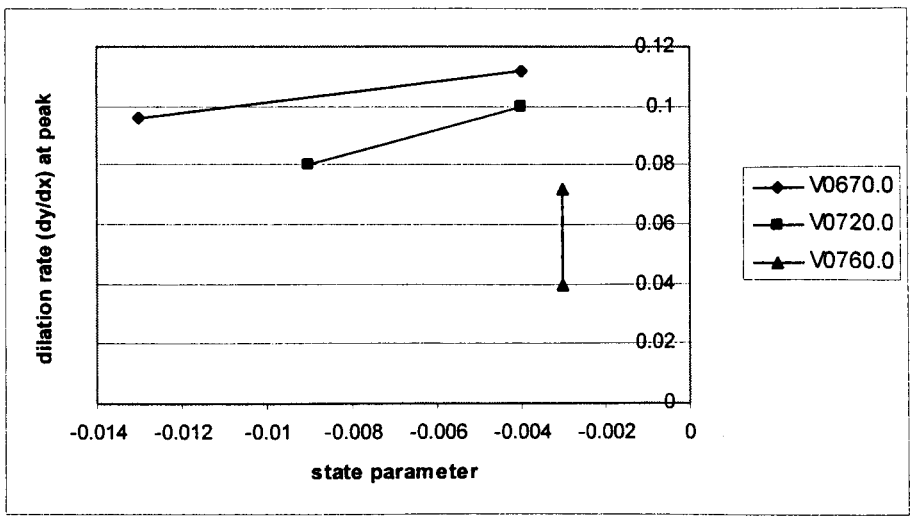

Figure 6.8: Dilation rate at peak stress ratio as a function of state parameter

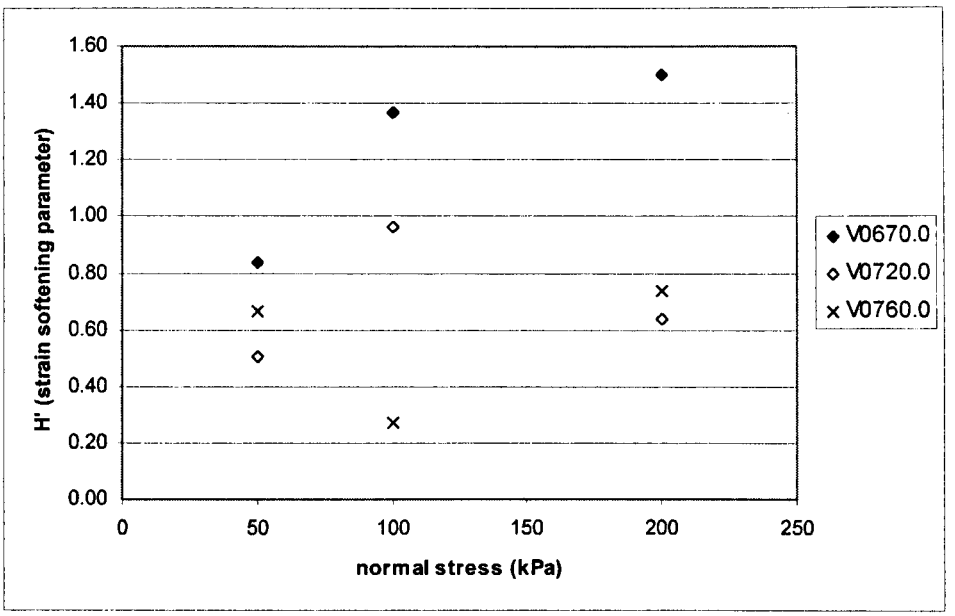

Figure 6.9: Strain-softening parameter for Hostun sand

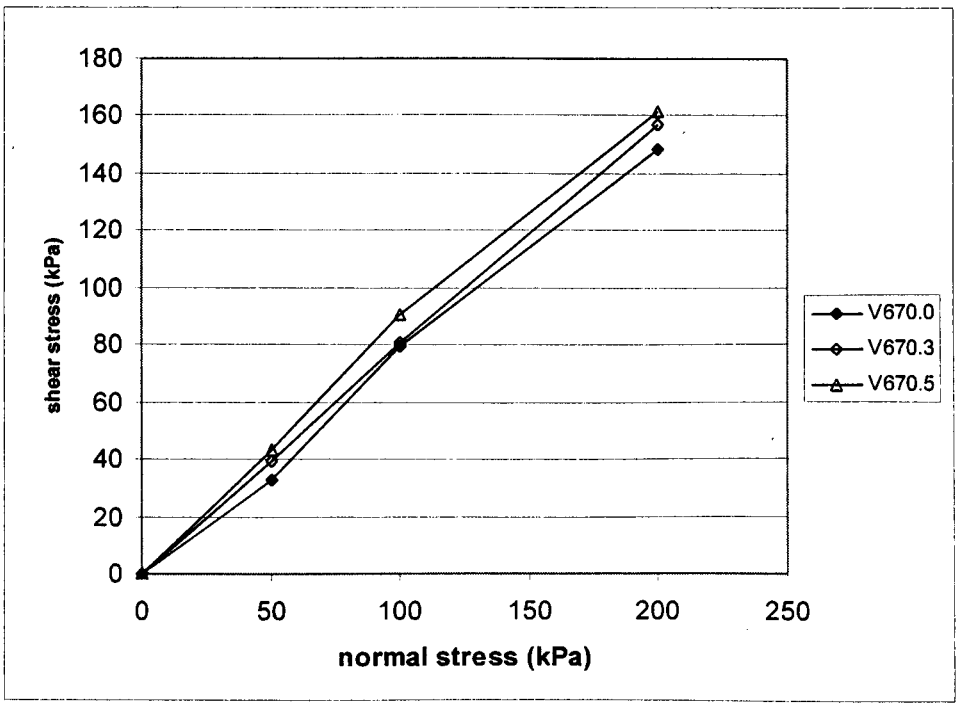

Figure 6.10: Failure envelope for Hostun sand (e_i = 0.67)

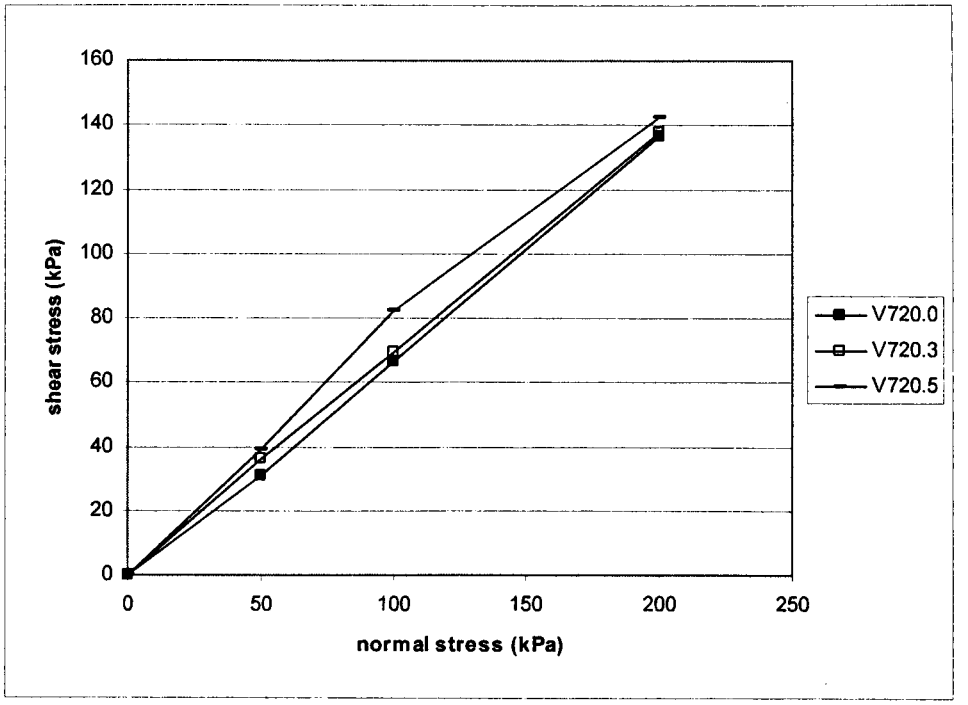

Figure 6.11: Failure envelope for Hostun sand (e_i = 0.72)

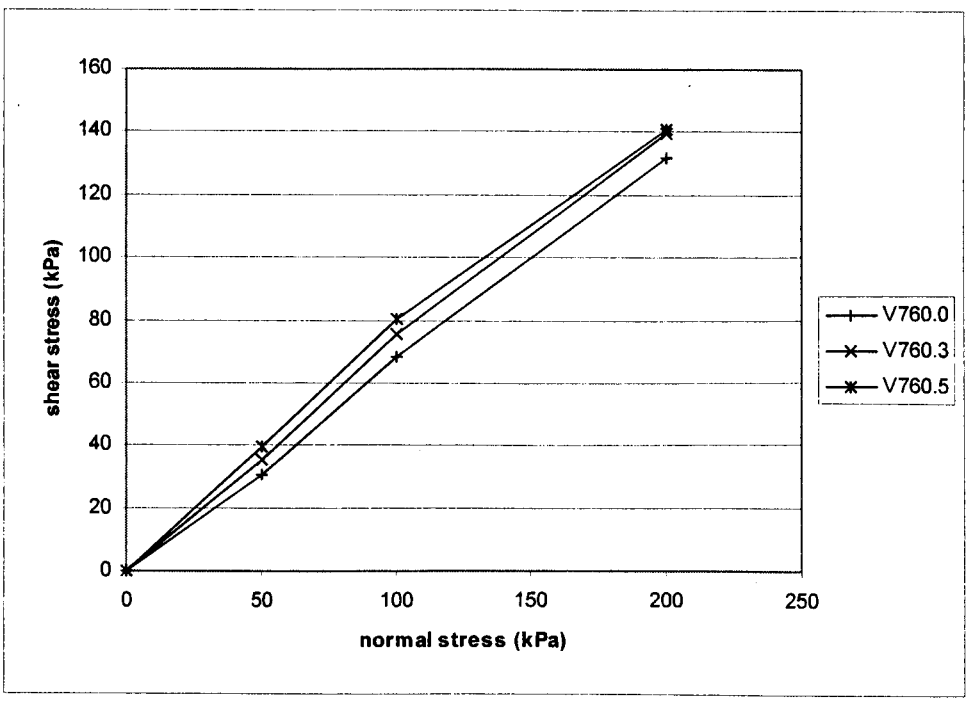

Figure 6.12: Failure envelope for Hostun sand (e_i = 0. 76)

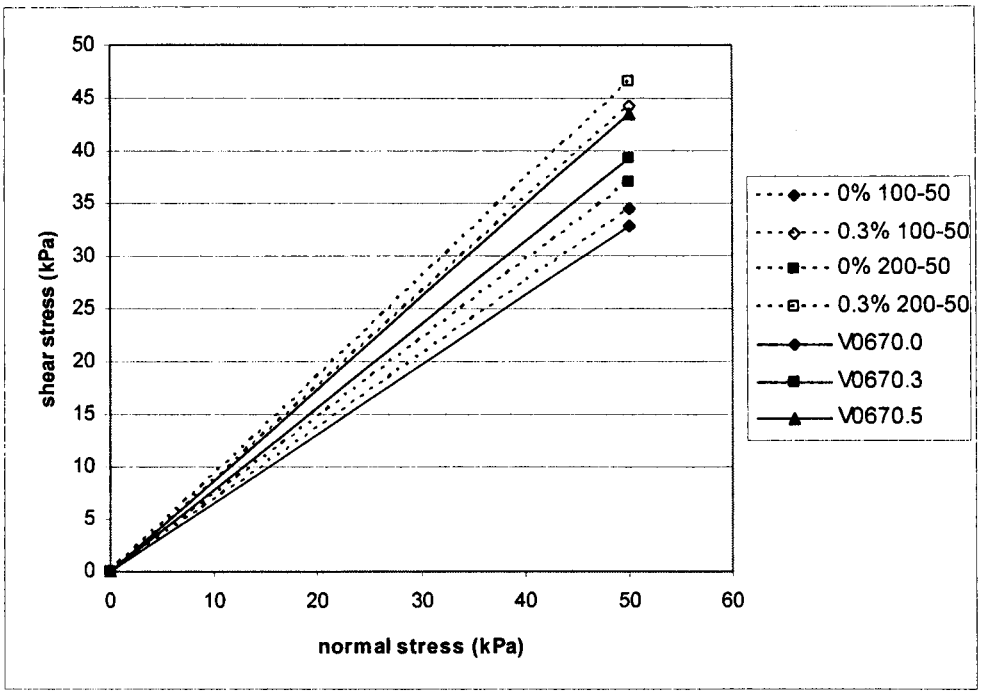

Figure 6.13: Failure envelopes 0 to 50 kPa normal stress for vibrated and pre-loaded samples

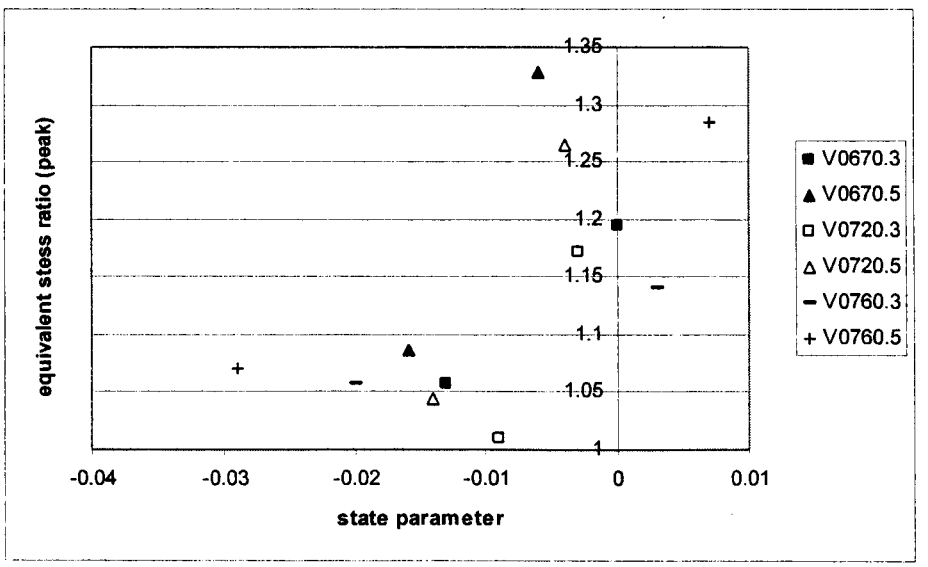

Figure 6.14: Equivalent stress ratio (peak) as a function of state parameter

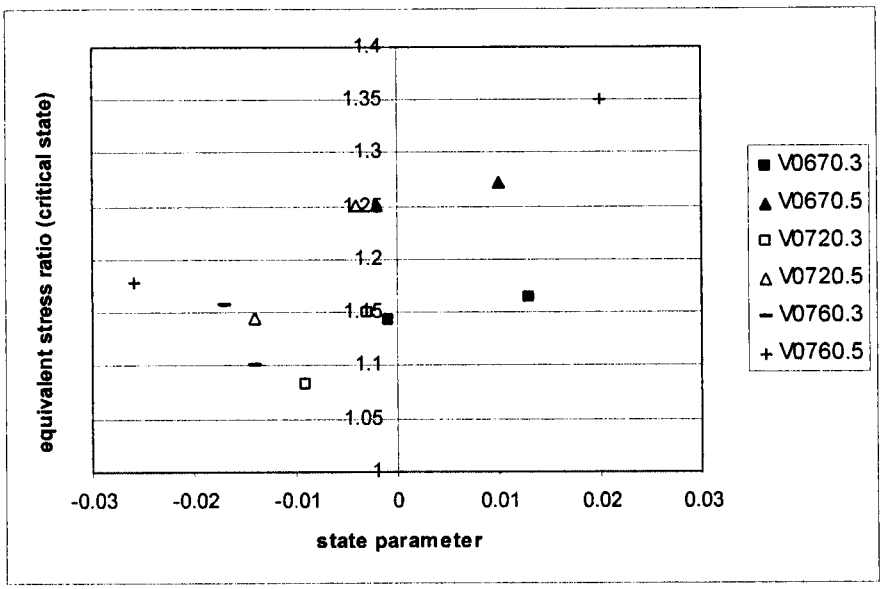

Figure 6.15: Equivalent stress ratio (critical state) as a function of state parameter

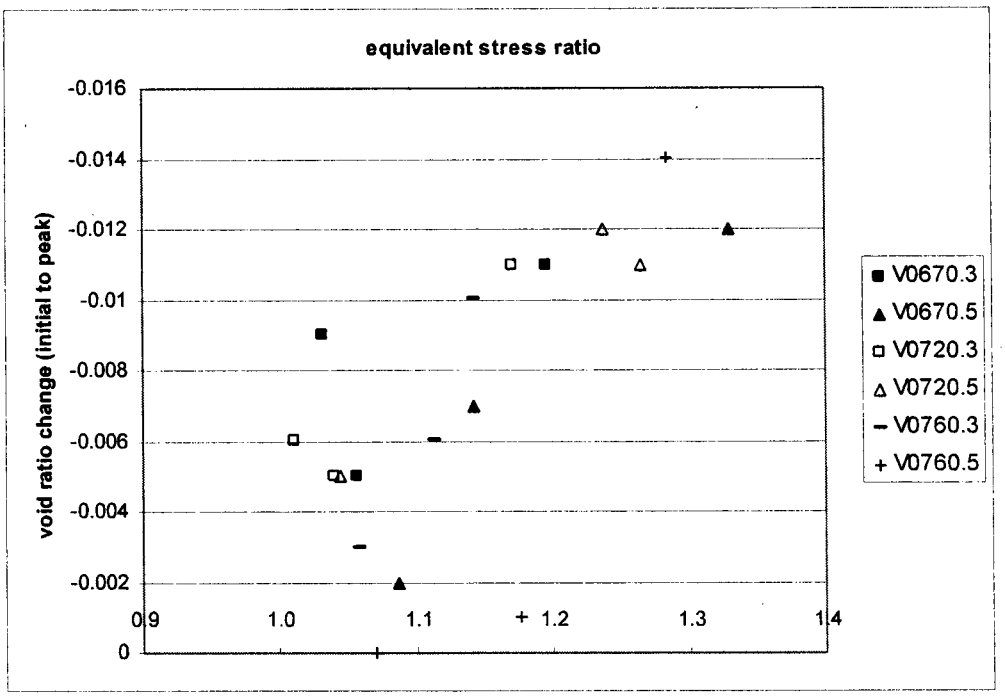

Figure 6.16: Void ratio change to equivalent stress ratio at peak

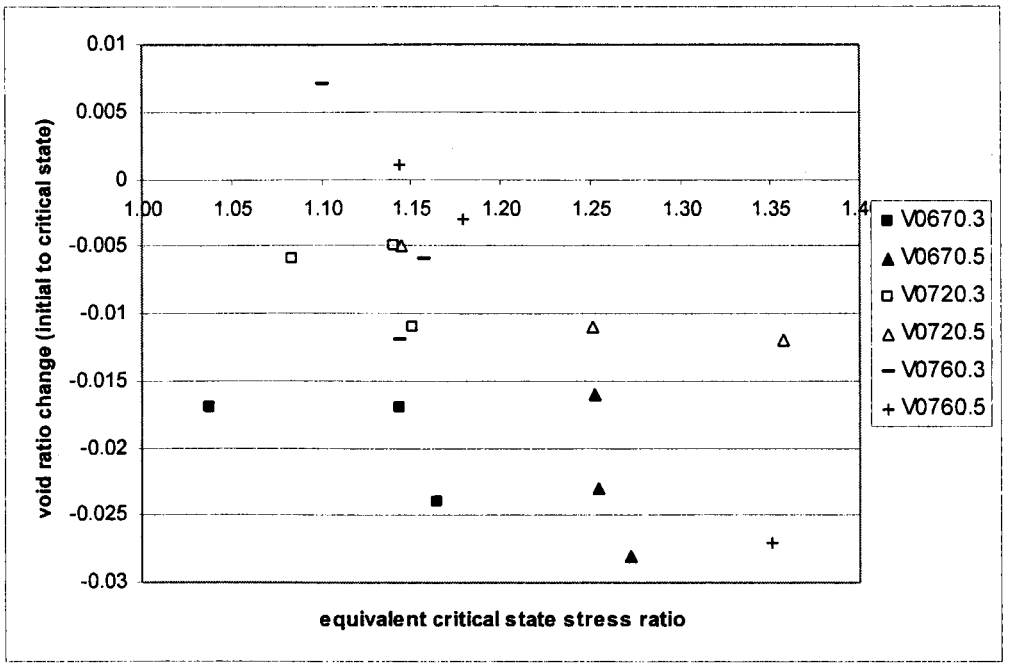

Figure 6.17: Void ratio change to equivalent stress ratio at critical state

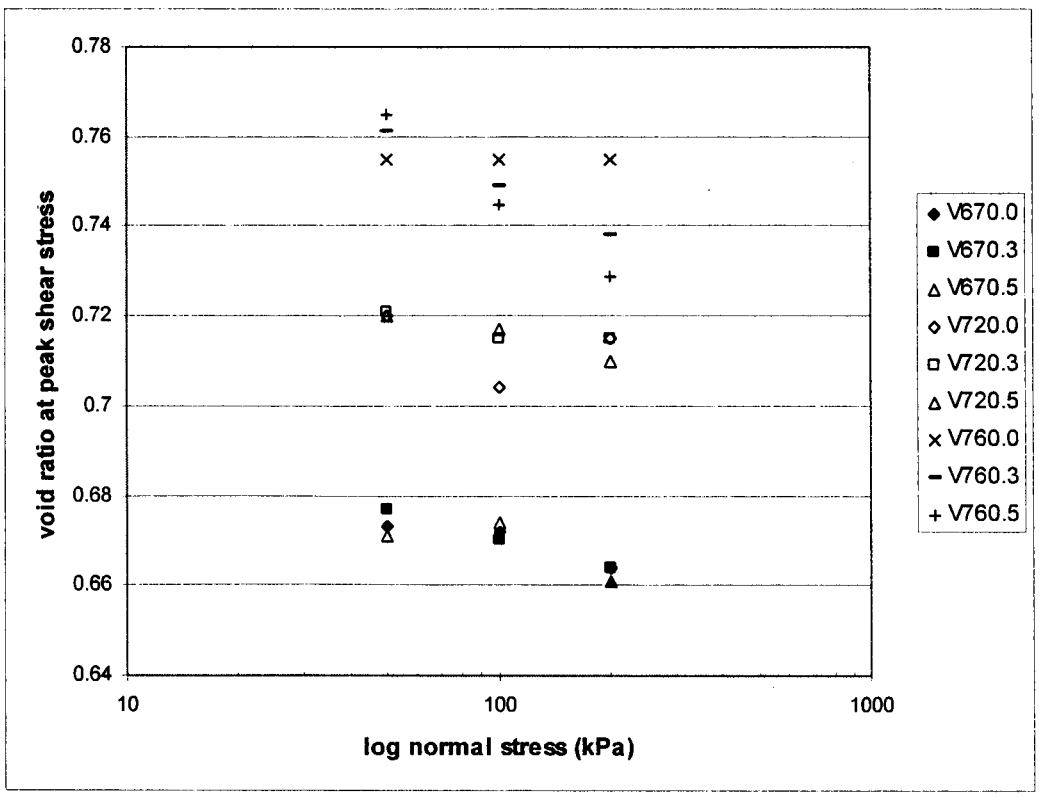

Figure 6.18: Void ratio values at peak stress ratio

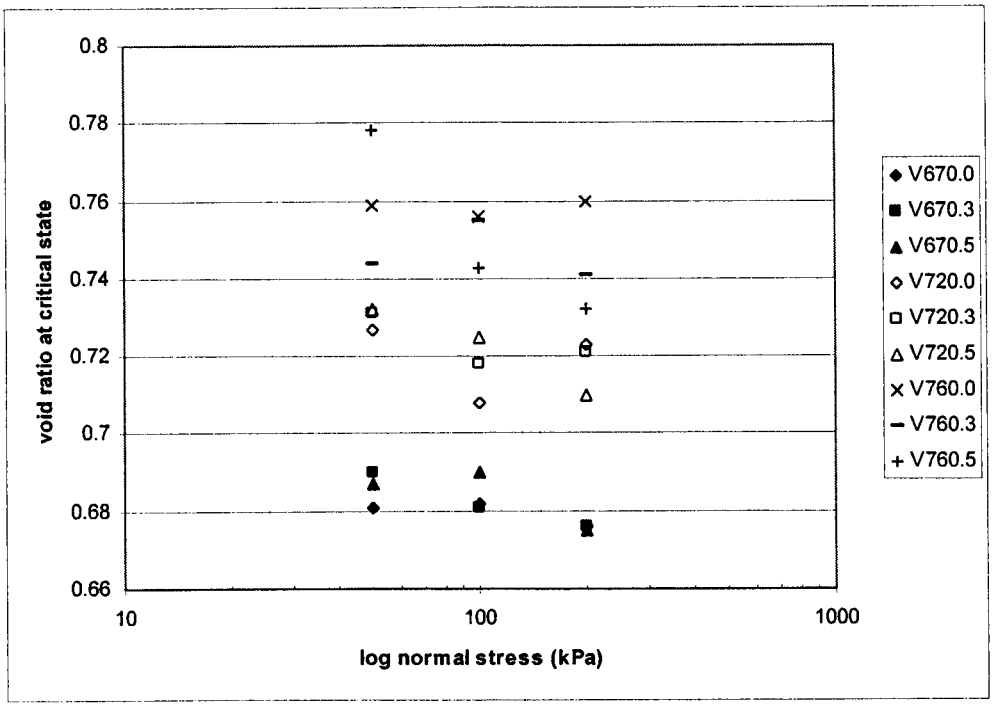

Figure 6.19: Void ratio values at critical state

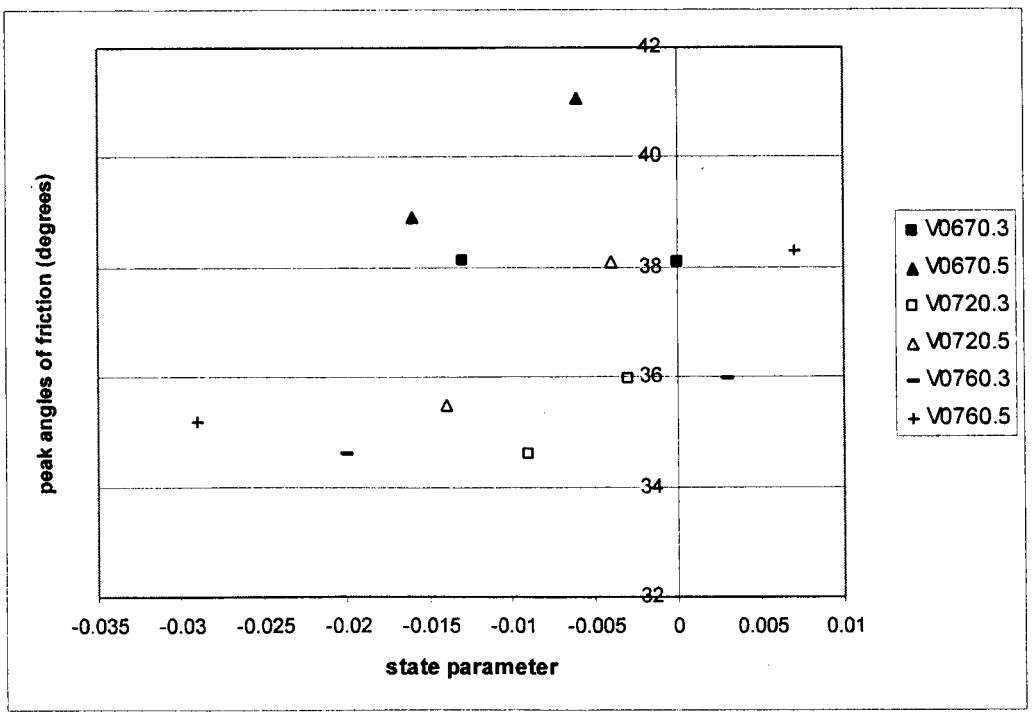

Figure 6.20: Peak internal angles of friction as functions of state parameter for fibre-reinforced sands

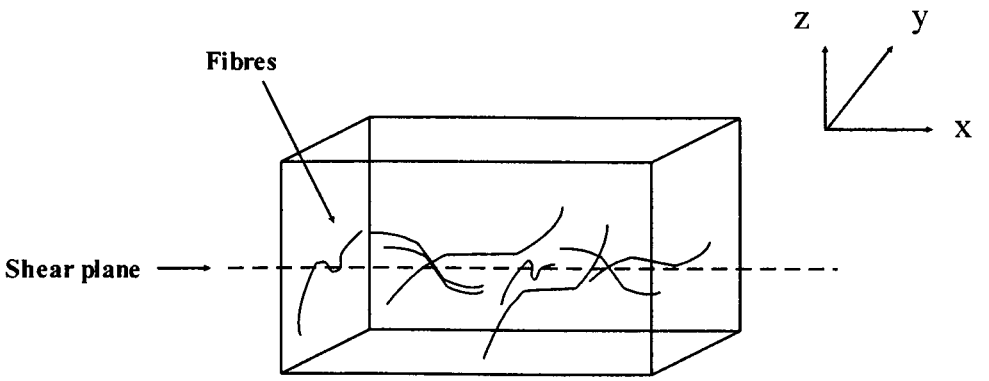

Figure 6.21: Schematic relationship of random fibre orientation within the shear zone of a direct shear sample

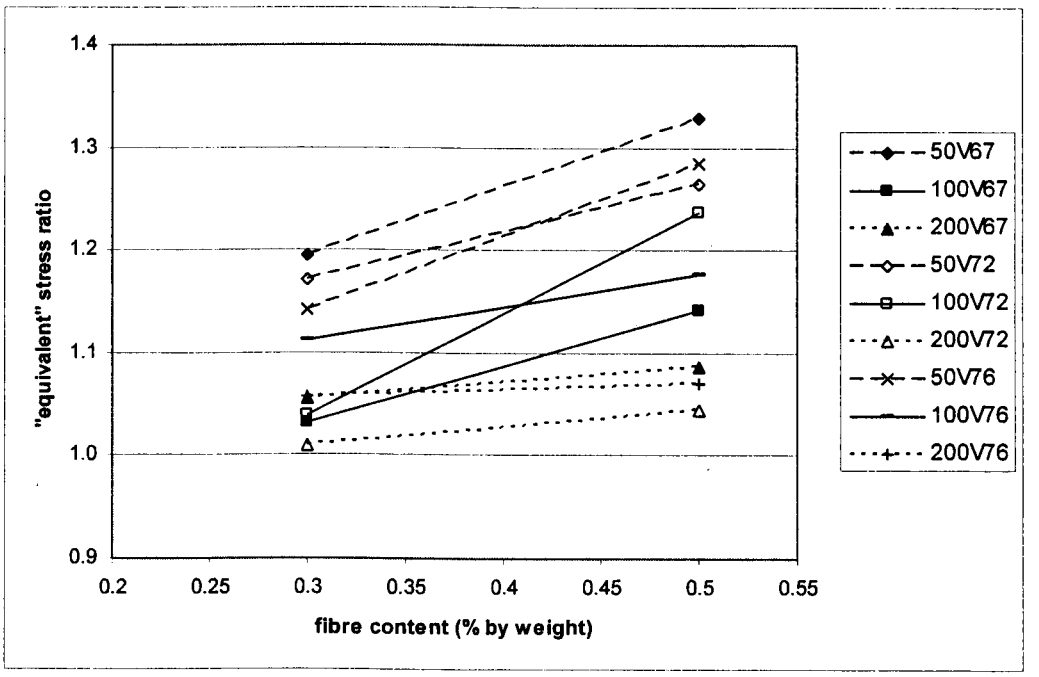

Figure 6.22: Equivalent stress ratio to fibre content (peak)

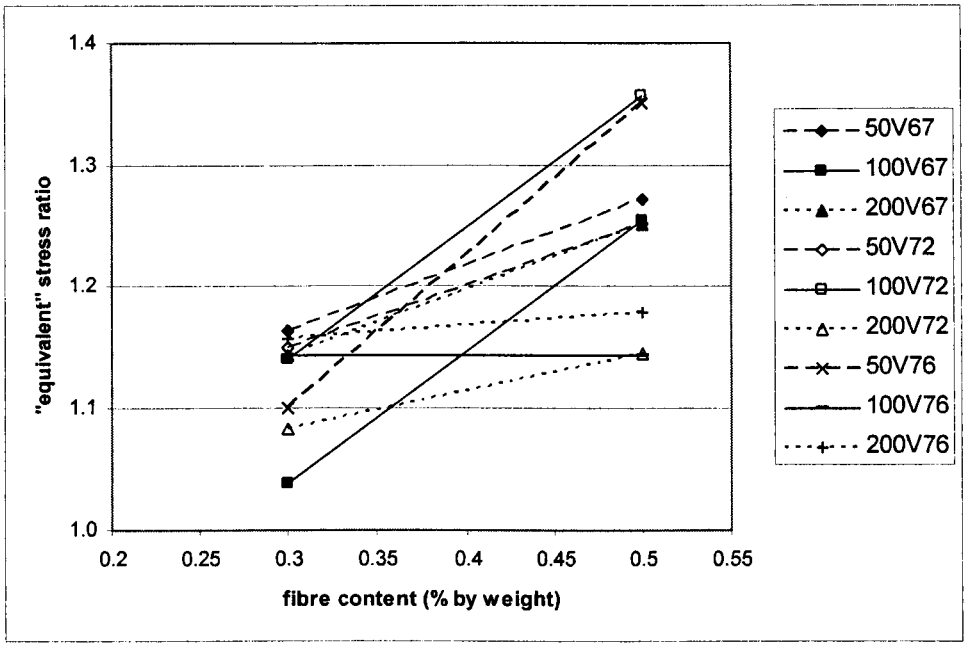

Figure 6.23: Equivalent stress ratio to fibre content (critical state)

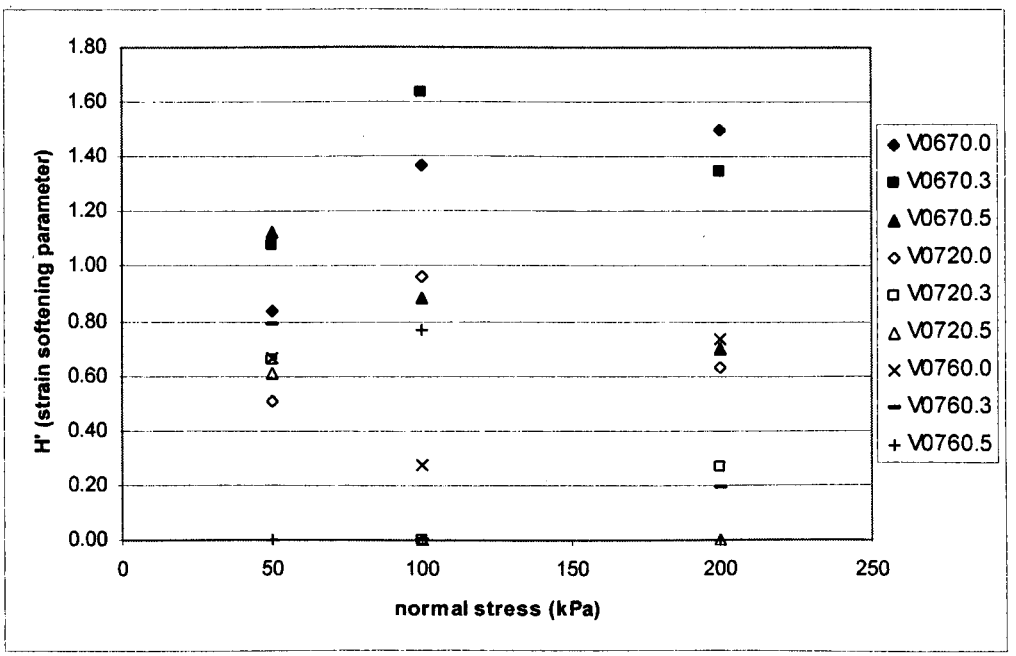

Figure 6.24: Strain-softening parameter (all fibre contents)

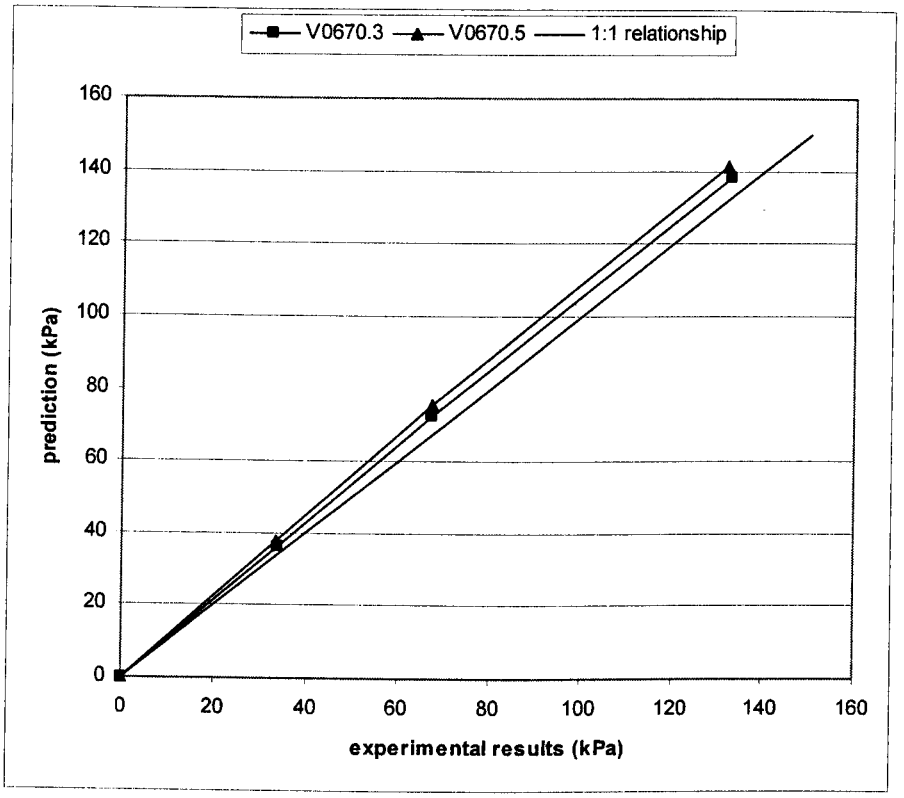

Figure 6.25: Predicted shear envelope versus experimental results (e_i = 0.67)

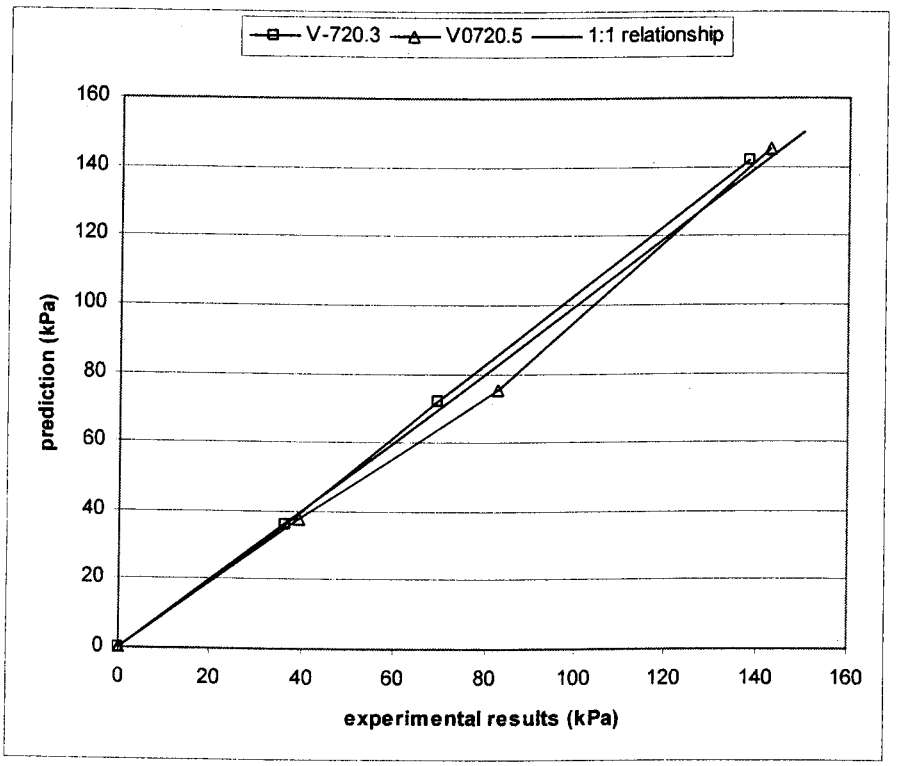

Figure 6.26: Predicted shear envelope versus experimental results (e_i = 0.72)

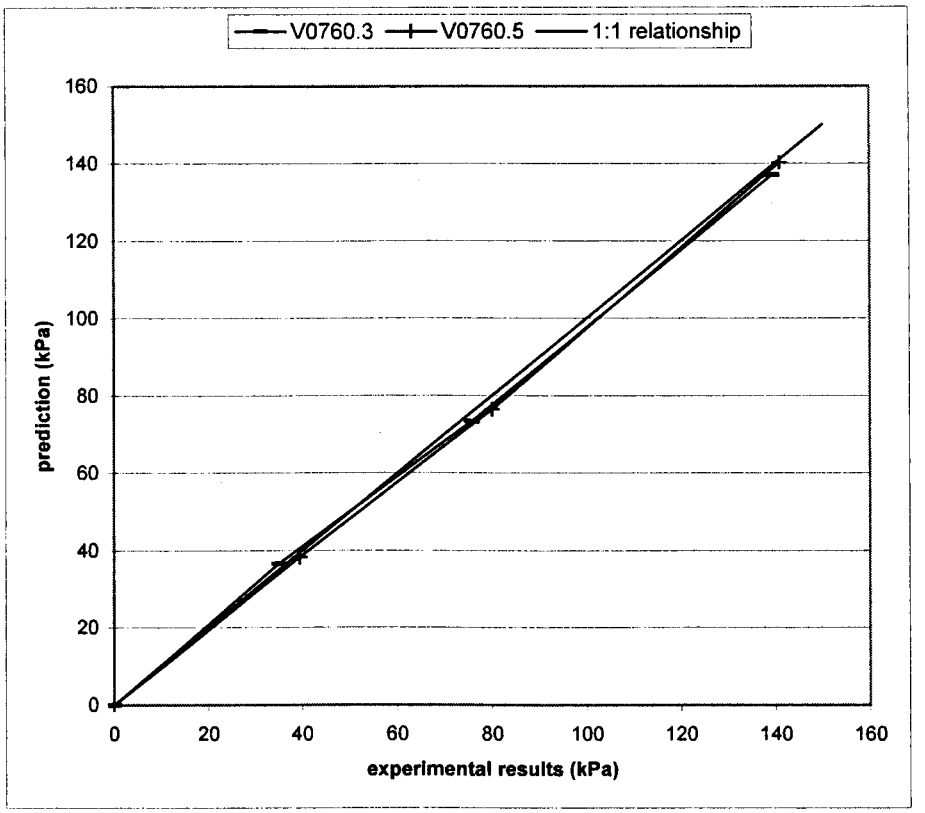

Figure 6.27: Predicted shear envelope versus experimental results (e_i = 0.76)

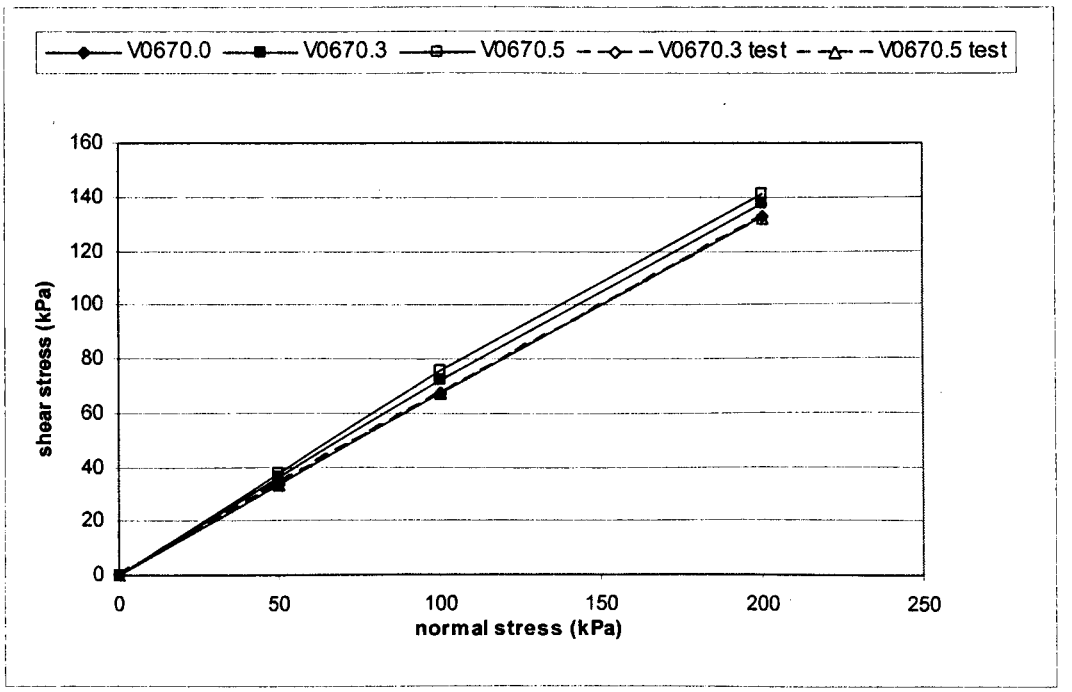

Figure 6.28: S_f model (e_i = 0.67)

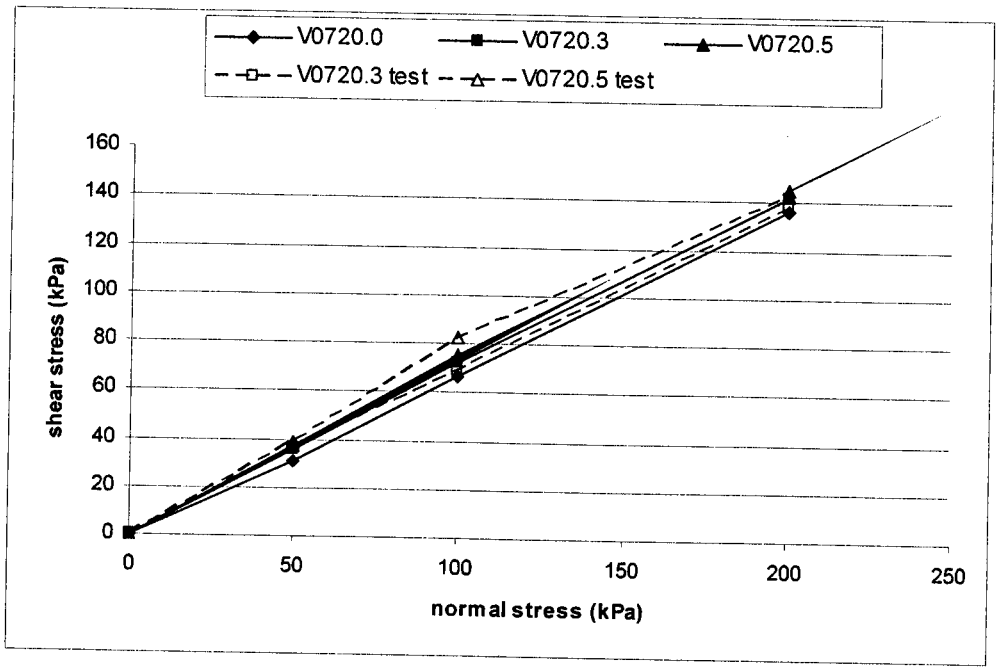

Figure 6.29: S_f model ($e_i = 0.72$)

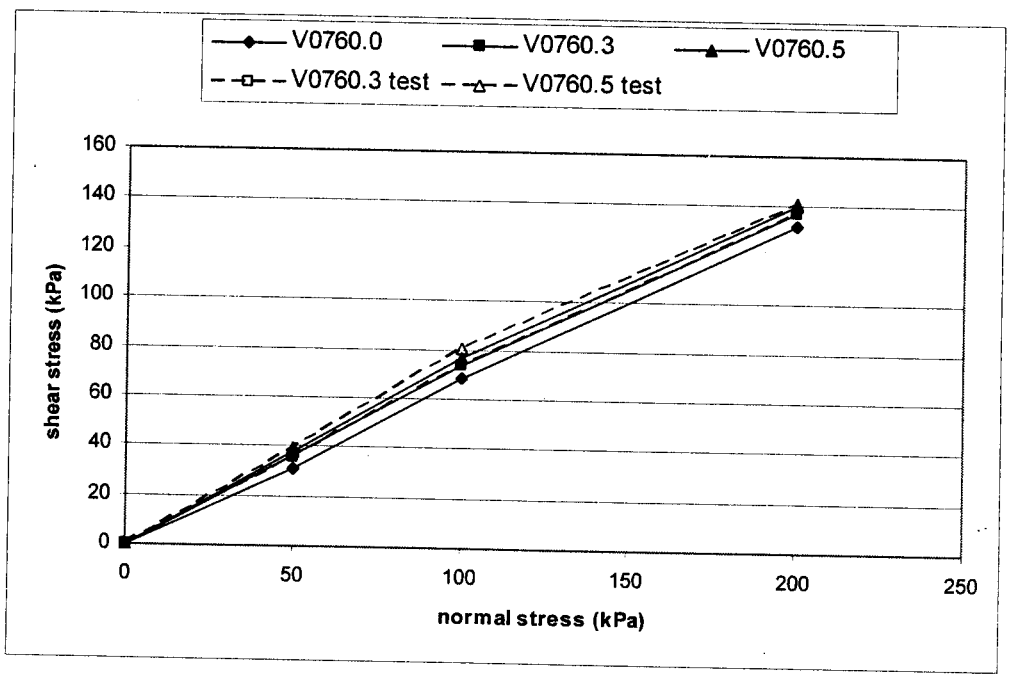

Figure 6.30: S_f model ($e_i = 0.76$)

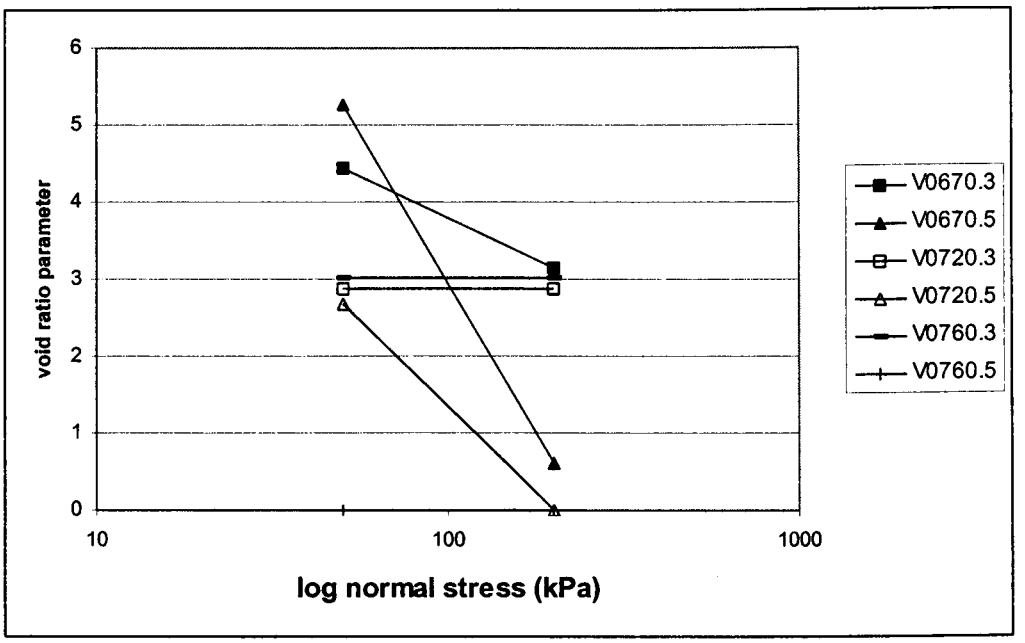

Figure 6.31: Void ratio parameter for fibre-reinforced samples

7.0 Review of performance framework

7.1 Main conclusions

The purpose of the current research was to deepen the understanding of stress-deformation behaviour of fibre-reinforced sand and to explore the influence of initial sample density values, normal stress values and fibre contents. In order to explain the soil mechanics of *LokSand*-reinforced Hostun sand samples, the following tasks were undertaken:

- An assessment of the state of the art for reinforced soils and the limitations of laboratory experiments to date.

- Assessments of the performance of fibre-reinforced sands applicable to direct shear testing in particular.

- Identification of the soil strength parameters that are affected by the inclusion of flexible lightweight fibres.

- Assessment of the validity and applicability of one-dimensional compression tests, dynamic compaction and direct shear tests for the determination of the relevant soil strength parameters.

- Evaluation of the validity and applicability of different sample preparation methods for fibre-reinforced sands and the significance of their possible adverse effects on sample behaviour with special consideration for the initial sample density values.

- An analysis of the stress-deformation response of one-dimensional compression and direct shear laboratory test results and the establishment of a performance framework for fibre-reinforced sands in direct shear.

- Exploration of potential modifications to existing modelling approaches and testing techniques for fibre-reinforced sands in one-dimensional compression and direct shear.

Conclusions were specified in individual chapters. However, the most significant conclusions and suggestions for future research work evolving from the various aspects of the current research are summarised in the following sections.

7.2 Benefits of this research

There have been numerous models proposed for peak strength and critical state values for sands. No models of this type have been published for randomly-distributed fibre-reinforced sands in direct shear. The stress-dilatancy response of fibre-reinforced sands is highly dependent on initial density values and confining stress values. Less attention is usually given to the fibre content, however this thesis proves that the volume fraction of the fibre content can influence the stress-deformation response of granular soils.

An effective amount of repeatable sample densification was discovered for the samples so that for any given fibre content, the initial sample density can equal that of an un-reinforced sample (for comparison purposes). This enabled the author to produce samples with a range of confinement conditions for the fibre-sand mixes. The geometry of the fibres and the width of shear bands/zone for test samples were considered and incorporated into both the sample preparation methods and the formulation of a performance framework for the increased shear strength. The strain localisation within shear bands that usually dictates the failure mechanism for sands in direct shear seemed to have little effect on the randomly-distributed fibre reinforcements.

A concept for the investigation of fibre-reinforced sands has been mentioned by Shuttle and Smith (1988) who found that the shear strength envelope of a soil was not only a function of the state of stress, but also a function of the relation of the internal material state to the critical state. The model introduced in this thesis relates the internal material state of fibre-reinforced sands to the confining stress and sample density at critical state.

The effect of fibre content on the Mohr-Coloumb shear strength envelope (including the internal angle of friction) has been detailed and compared with test results in literature. The internal friction angles for the un-reinforced and fibre-reinforced sands found from direct shear tests tended to parallel the un-reinforced sand behaviour at high normal stresses (200 kPa), with an increased friction angle of about 2° for each fibre content of approximately 0.25% by weight for all initial sample densities. At low normal stresses (50 kPa) the internal friction angles for fibre-reinforced samples were significantly greater than for the un-reinforced samples. A critical normal stress value was discovered that signified the mobilisation of the tensile strain of the fibre reinforcements. This critical normal stress value separated the shear strength envelopes into two failure planes.

7.3 Limitations of the research and further work

The analysis of critical state values for fibre-reinforced sands should be continued in a substantially larger shear box and in the triaxial cell. An increased model scale could help to overcome some of the non-uniformity problems experienced in the fabrication of small-scale tests.

Ideas for future work include:

- Soil tests that could continue the analysis of one-dimensional compression for fibre-reinforced soils include settlement tests for plates or footings.

- Larger scale tests could be conducted on saturated samples or samples tested at the optimum moisture content and further stress analysis could be undertaken in triaxial tests.

- The failure stresses could be compared with the pull-out resistance of the fibres under similar conditions.

- Modelling of the inter-particle forces in one-dimensional compression and shear tests using fibre-reinforced sands would be extremely beneficial to the section of geotechnical engineering dealing with soil micromechanics as a whole and soil strengthening in general.

7.4 Closure

This chapter has presented findings of small-scale direct shear tests from sample preparation to the manipulation and analysis of the experimentation. The systematic approach to all material and mechanical factors relating to fibre-reinforced soil strength has been considered and described. The usefulness of each sample and test variable has been examined and evaluated. The purpose of the scrutiny of material variables was to quantify the stress-deformation characteristics that can be attributed to material properties of the fibres or the soil separately.

8.0 References

Al-Refeai, T.O. (1991): Behaviour of granular inclusions reinforced with discrete randomly oriented inclusions, Geotextiles and Geomembranes, Vol.10, pp. 319-333

Bailey, R. (2000): The properties and applications of fibre-reinforced sand in geotechnical structures, PhD thesis, University of Paisley

Bailey, R. & Knox, R.A. (1997): The strength properties of fibre-reinforced sand, Proceedings of 3rd International Conference on Ground Improvement Geosystems 1997, pp. 349-357

Bauer, G.E. & Zhao, Y. (1993): Evaluation of shear strength and dilatancy behaviour of reinforced soil from direct shear tests, Geosynthetic soil reinforcement testing procedures, ASTM Publication code number 04-011900-38, STP1190, pp.138-151

Been, K. (1998): The critical state line and its application to soil liquefaction, In Physics and Mechanics of Soil Liquefaction, Balkema, Rotterdam; Lade, P.V. & Yamamuro, J.A (eds.), pp. 195-204

Been, K., Jefferies, M.G., Hachey, J. (1991): The critical state of sands, Geotechnique, Vol. 41, No. 3, pp. 365-381

Bell, F.G. (1993): Engineering treatment of soils, E & FN Spon, London, ISBN 0-419-17750-7, Chapter 8

Bishop, A.W. (1966): The strength of soils as engineering material, Geotechnique, Vol. 16, No. 2, pp. 91-130

British Standards Institution (1994): Sample preparation/Classification of soils, BS 1377: Parts 1, 2, 4, 6 and 8

British Standards Institution (1990): Light Proctor compaction, BS1377: Part 4, clause 4, test 12

British Standards Institution (1994): Code of practice for earth retaining structures, BS 8002: Part 2, clause 2, test 4

Bolton, M.D. (1986): The strength and dilatancy of sand, Geotechnique, Vol. 36, pp. 65-78

Bouazza, A., Amokrane, K., Aberkane, T. (1994): Granular soil reinforced with geotextile and randomly orientated fibres, 5th International Conference on Geotextiles, Geomembranes and Related Products, Singapore, pp. 391-394, ISBN: 981 005 8217

Burgoyne, C. (2001): FRPRCS-5: Fibre-reinforced plastics for reinforced concrete structures, Thomas Telford Ltd., London, Vol. 1, ISBN: 0-7277-3029-0

Casagrande, A. (1938): The shearing resistance of soils and its relation to the stability of earth dams, Proceedings of Soils and Foundations Conference of the U.S. Engineer Department, Boston

Casagrande, A. & Carillo, N. (1944): Shear failure of anisotropic materials, Proc. Boston Society of Civil Engineering, Vol.31, pp. 74-87

Cheng, Y.P., White, D.J., Bowman, E.T., Bolton, M.D. and Soga, K. (2001) The observation of soil microstructure under load, Powders and Grains, 2001: Proceedings of the 4th international conference on micromechanics of granular media, Sendai, Japan, 21-25 May, 2001, Ed. Y. Kishino, pp. 69-72

Colliat, J-L., Desrues, J. & Foray, P. (1988): Triaxial testing of granular soil under elevated cell pressures, AMTM, Special Technical Publication 977 on Advanced Triaxial Testing of Soil and Rock, pp. 290-310

Concrete Society (1973): Fibre-reinforced cement composites report, Materials Technology Division of the Concrete Society, London, Technical report No. 51.067

Cresswell, A., Barton, M.E., Brown, R. (1999): Determining the maximum density of sands by pluviation, Geotechnical Testing Journal, Vol. 22, No. 4, pp. 324-328

Desrues, J., Chambon, R., Mokni, M. and Mazerolle (1996): Void ratio evolution inside shear bands in triaxial sand specimens studies by computed tomography, Geotechnique, Vol. 46, No. 3, pp. 529-546

Desrues, J., Lanier, J. and Stutz, P. (1985): Localization of the deformation in tests on sand sample, Engineering Fracture Mechanics, Vol. 21, No. 4, pp. 909-921

Dietz, M.S. (2000): Developing an holistic understanding of interface friction using sand within the direct shear apparatus, PhD thesis, University of Bristol

Di Prisco, C. & Nova, R. (1993): A constitutive model for soil reinforced by continuous threads, Geotextiles and Geomembranes, Vol. 12, pp. 161-178

Doanh, T. & Ibraim, E. (2000): Minimum undrained strength of Hostun RF sand, Geotechnique, Vol. 50, No. 4, pp. 377-392

Finno, R.J. & Rechenmacher, A.L. (2003): Effects of consolidation history on critical state of sand, Journal of Geotechnical and Geoenvironmental Engineering, ASCE, Vol. 129 (4), pp. 350-360

Fredlund, D.G. & Morgenstern, N.R. (1978): The shear strength of unsaturated soils, Canadian Geotechnical Journal, Vol. 15 (3), pp. 313-321

Gajo, A. & Piffer, L. (1999): The effects of preloading history on the undrained behaviour of saturated loose sand, Soils and Foundations, Vol. 39, No. 6., pp. 43-54

Gray, D.H. & Al-Refeai, T.O. (1986): Behaviour of fabric- versus fibre- reinforced sand, Journal Geotechnical Engineering, ASCE, Vol. 112 (8), pp. 804-820

Gray, D.H. & Ohashi, H. (1983): Mechanics of fibre reinforcement in sand, Journal of Geotechnical Engineering, ASCE, Vol. 109 (3), pp. 335-353

Hardin, B.O. (1987): 1-D strain in normally consolidated cohesion-less soils, Journal of Geotechnical Engineering, ASCE, Vol. 113, No. 12, pp. 1449-1467

Harr, M.E. (1977): Mechanics of particulate media, McGraw-Hill, New York, 553p

Harrison, A.T. (2000): Earthquake-induced liquefaction of fibre-reinforced sands, BEng dissertation, University of Wales, Cardiff

Hoare, D.J. (1979): Laboratory study of granular soils reinforced with randomly oriented discrete fibres, Proceedings of international conference on the use of fabrics in geotechnics, Vol. 1, Paris, pp. 47-52

Hollaway, L.C. & Leeming, M.B. (1999): Strengthening of reinforced concrete structures using externally-bonded FRP composites in structural and civil engineering; Woodhead, Cambridge Press

Hryciw, R.D. & Irsyam, M. (1993): Pullout stiffness of elastic anchors in slope stabilization systems, ASCE, Journal of Geotechnical Engineering, Vol. 118, No. 6, pp. 902-919

Jewell, R.A. (1989): Direct shear tests on sand, Geotechnique, Vol. 39, pp. 309-322

Jewell, R.A. & Wroth, C.P. (1987): Direct shear tests on reinforced soil, Geotechnique, Vol. 37, No. 1, pp. 53-68

Jones, C.J.F.P. (1996): Earth reinforcement and soil structures, Thomas Telford, Chapter 4

Jones, M., McKinley, J., Ogden, G. and Ellis, G. (2001): The strength properties of fibre reinforced soil, The XVth international conference on soil mechanics and geotechnical engineering, Istanbul, September 2001

Jones, M. (2004): The properties of crimped fibre-reinforced soil and their use in the provision of grass surface roads, PhD thesis (unpublished), University of Wales, Cardiff

Juran, I. & Christopher, B. (1989): Laboratory model study on geosynthetic reinforced soil retaining walls, Journal of Geotechnical Engineering, ASCE, Vol. 115, No. 7, pp. 905-926

Karihaloo B.L. (2000): Mechanics of Short-Fibre-Reinforced Cementitious Composites and their Application to Retrofitting, *Proc of Int Conf on Composites in Transportation Industry*, Bandyopadhyay, S. ed., University of New South Wales Sydney Press 1, pp. 282-290 ISBN 0-7334- 0698X

Karakouzian, M., Huydma, N., Avar, B. (2001): Observations and nomenclature of shear bands formed in granular soils, The Electronic Journal of Geotechnical Engineering, http://www.ejge.com/2001/Ppr0103/Abs0103.htm

Ladd, R.S. (1978): Preparing test specimens using undercompaction, Geotechnical Testing Journal, Vol. 1, No. 10, pp. 16-23

Lade, P.V., Liggio, C.D., Yamamuro, J.A. (1998): Effects of non-plastic fines on minimum and maximum void ratios of sand, Geotechnical Testing Journal, Vol. 21, No. 4, pp. 336-347

Lawton, E.C., Khire, M.V., Fox, N.S. (1993): Reinforcement of soils by multioriented geosynthetic inclusions, Journal of Geotechnical Engineering, ASCE, Vol. 119, No. 2, pp. 257-273

Leflaive, E. (1985): Soil Reinforced with continuous yarns: the Texsol, Proceedings of 11th International Conference on Soil Mechanics and Foundation Engineering, Vol. 3, pp. 1787-1790

Leshichinsky, D. & Boedeker, R.H. (1989): Geosynthetic reinforced soil structures, Journal of Geotechnical Engineering, ASCE, Vol. 115, No. 10, pp. 1459-1478

Li, X.S., Dafalias, Y.F., Wang, Z.L. (1999): State-dependent dilatancy in critical-state constitutive modelling of sand, Canadian Geotechnical Testing Journal, Volume 36, pp. 599-611

Liu, X., Scarpas, A., Blaauwendraad, J. (2005): Numerical modelling of non-linear response of soil Part 2: Strain localisation investigation on sand, International Journal of Solids and Structures, Vol. 42, No. 7, pp.1883-1907

Lo Presti, D.C.F., Pedroni, S., Crippa, V. (1992): Maximum dry density of cohesionless soils by pluviation and by ASTMD4253-83: A comparative study, Geotechnical Testing Journal, Vol. 15, No. 2, pp. 180-189

Lo Presti, D.C.F, Berardi, R., Pedroni, S., Crippa, V. (1993): A new travelling sand pluviator to reconstitute specimens of well-graded silty sands, Geotechnical Testing Journal, Vol. 16, No. 1, pp.18-26

Maeda, K. & Miura, K (1999): Confining stress dependency of mechanical properties of sands, Soils and Foundations, Vol. 39, No. 1, pp. 53-67

Maher, M.H. & Gray, D.H. (1990): Static response of sands reinforced with randomly distributed fibres, Journal of Geotechnical Engineering, ASCE, Vol. 116, No. 11, pp. 1661-1677

Maher, M.H. & Ho, Y.C. (1993): Behaviour of fibre-reinforced cemented sand under static and cyclic loads, Geotechnical Testing Journal, Vol. 16, No. 3, pp. 330-338

Maher, M.H. & Ho, Y.C. (1994): Mechanical properties of kaolinite/fibre soil composite, Journal of Geotechnical Engineering, ASCE, Vol. 120, No. 8, pp. 1381-1393

Maher, M.H. & Woods, R.D. (1990): Dynamic response of sand reinforced with randomly distributed fibres, Journal of Geotechnical Engineering, ASCE, Vol. 116, No. 7, pp. 1116-1131

McDowell, G.R. & Harireche, O. (2002_a): Discrete element modelling of soil particle fracture, Geotechnique Vol. 52, No. 2, pp. 131-135

McDowell, G.R. & Harireche, O. (2002_b): Discrete element modelling of yielding and normal compression of sand, Geotechnique, Vol. 52, No. 4, pp. 299-304

McGown, A., Andrawes, K.Z., Hytiris, N., Mercere, F.B. (1985): Soil strengthening using randomly distributed mesh elements, Proceedings of 11th International Conference on Soil Mechanics and Foundation Engineering, Vol. 3, pp. 1735-1738

McGown, A., Yogarajah, I., Andrawes, K.Z., Saad, M.A. (1995): Strain behaviour of polymeric geogrids subjected and repeated loading in air and in soil, Geosynthetics International, Vol. 2, No. 1, pp. 341-355

Michalowski, R.L. & Zhao, A. (1996): Failure of fibre-reinforced granular soils, Journal of Geotechnical Engineering, ASCE, Vol. 122, No.33, pp. 226-234

Miura, S. & Toki, S. (1982): A sample preparation method and its effects on static and cyclic deformation-strength properties of sand, Soils and Foundations, Vol. 22, No. 1, pp. 61-77

Muira, S. & Toki, S. (1984): Anisotropy in mechanical properties and its simulation of sand sampled from natural deposits, Soils and Foundations, Vol. 24, No. 3, pp. 69-84

Miura, K., Maeda, K., Toki, S. (1997): Method of measurement for the angle of repose in sands, Soils and Foundations, Vol. 37, No. 2, pp. 89-96

Miura, K., Miura, S., Toki, S. (1986): Deformation behaviour of anisotropic dense sand under principal stress axes rotation, Soils and Foundations, Vol. 26, No. 1, pp. 36-52

Muller, G. (1967): Methods in Sedimentary Petrology, Hafner Publishing Co., New York, section 3.52

Mulilis, J.P., Seed, H.B., Chan, C.K., Mitchell, J.K., Arulanandan, K. (1977): Effects of sample preparation on sand liquefaction, Journal of Geotechnical Engineering, Vol. 103, No. GT2, pp. 91-106

Nakata, Y., Kato, Y., Hyodo, M., Hyde, A.F.L., Murata, H. (2001): One-dimensional compression behaviour of uniformly graded sand related to single particle crushing strength, Soil and Foundations, Vol. 41, No. 2, pp.39-51

Netralvali, A.N., Krstic, R., Crouse, J.L., Richmond, L.E. (1993): Chemical stability of polyester fibres and geotextiles without and under stress, Geosynthetic Soil Reinforcement Testing Procedures, ASTM STP 1190, S.C. Cheng, ed., American Society for Testing and Materials, Philidelphia, pp. 207-217

Noorany, I. & Uzdavines, M. (1989): Dynamic behaviour of saturated sand reinforced with geosynthetic fibres, Geosynthetics 1989 Conference, San Diego, CA, pp. 385-396

Ola, S.A. (1989): Stabilisation of lateritic soils by extensible fibre reinforcement, Engineering Geology, Vol. 26, pp. 125-140

Qui, J.Y., Tatsuoka, F. and Uchimura, T. (2000): Constant pressure and constant volume direct shear tests on reinforced sand, Soils and Foundations, Vol. 40, No. 4, pp. 1-17

Palmeira, E.M. & Milligan, G.W.E. (1989): Large scale direct shear tests on reinforced soil, Soils and Foundations, Vol. 29, No. 1, pp. 18-30

Ranjan, G., Vasan, R.M. and Charan, H.D. (1996): Probabilistic analysis of randomly distributed fibre-reinforced soil, Journal of Geotechnical Engineering, ASCE, Vol. 122, No. 6, pp. 419-426

Rethatí, L. (1998): Probabilistic solutions in geotechnics, Elsevier, London, ISBN: 0-444-98960-9, Chapter 1

Reiner, M.F., Seed, R.B., Nicholson, P.G., Jong, H.L. (1990): Steady state testing of loose sands: limiting minimum density, Journal of Geotechnical Engineering, Vol. 116, No. 2, pp. 332-337

Roscoe, K.H., Schofield, A.N., Wroth, C.P. (1958): On the yielding of soils, Geotechnique, Vol. 47, No. 2, pp. 22-53

Saada, A.S., Liang, L., Figueroa, J.L. and Cope, C.T. (1999): Bifurcation and shear bands propagation in sands, Geotechnique, Vol. 49, No. 3, pp. 367-385

Santoni, R.L., Tingle, J.S., Webster, S.L. (2001): Non-traditional stabilization of silty sand, U.S. Army Research and Development Center

Scarpelli, G. & Wood, D.M. (1982): Experimental observations of shear band patterns in direct shear tests, Proceedings of the IUTAM conference on deformation and failure of granular materials, pp. 473-484

Schultze, E. (1972_a) Frequency distributions and correlations of soil properties, statistics and probability in civil engineering, Oxford University Press

Schultze, E. (1972_b) Some aspects concerning the application of statistics and probability to foundation structures, Proceedings of second international conference on applications of statistics and probability in soil and structural engineering, Vol. 2, pp.457-494

Scott, C.R. (1980): An introduction to soil mechanics and foundations, Applied Science Publishers, Chapters 6 & 7

Shewbridge, S.E. & Sitar, N. (1996): Formation of shear zones in reinforced sand, Journal of Geotechnical Engineering, ASCE, Vol. 122, No. 11, pp. 873-885

Shukla, S.K. & Chandra, S. (1994): The effect of pre-stressing on the settlement characteristics of geo-synthetic-reinforced soil, Geotextiles and Geomembranes, Vol. 13, No. 8, pp. 531-543

Shuttle, D.A. & Smith, I.M. (1988): Numerical simulation of shear band formation in soils, International Journal for Numerical and Analytical Methods in Geomechanics, Vol. 12, pp. 611-626

Siddiquee, M.S.A., Tanaka, T., Tatsuoka, F., Tani, F., Morimoto, T. (1999): FEM simulation of scale effect in bearing capacity of strip footing on sand, Soils and Foundations, Vol.39, No. 4, pp.93-109

Stroud, M.A. (1971): The mechanical behaviour of sand at low stress levels in the simple shear apparatus, PhD thesis, University of Cambridge

Tatsuoka, F. (1987): Discussion on the strength and dilatancy of sand, Journal of Geotechnical Engineering, ASCE, Vol. 37, No. 2, pp. 219-226

Tatsuoka, F., Ochi, K., Fujii, S., Okamoto, M. (1986a): Cyclic undrained triaxial and torsional shear strength of sands for different sample preparation methods, Soils and Foundations, Vol. 26, No. 3, pp. 23-41

Tatsuoka, F., Sakamoto, M., Kawamura, T., Fukushima, S. (1986b): Strength and deformation characteristics of sand in plane strain compression at extremely low pressures, Soils and Foundations, Vol. 26, No. 1, pp. 65-84

Tatsuoka, F., Sato, T., Park, C.S., Kim, Y.S., Mukabi, J.N., Kohata, Y. (1994): Measurements of elastic properties of geomaterials in laboratory compression tests, Geotechnical Testing Journal, Vol. 17, pp. 80-94

Timoshenko, S. & Goodier, J.N. (1951): Theory of Elasticity, McGraw-Hill Book Company, London, Second edition, pp. 255-256

Vaid, Y.P., Bryrne, P.M., Hughes, J.M.O. (1981): Dilation angle and liquefaction potential, Journal of Geotechnical Engineering, ASCE, Vol. 107, No. GT7, pp. 1003-1008

Vaid, Y.P., Chung, E.K.F., Kuerbis, R.H. (1990): Stress path and steady state, Canadian Geotechnical Journal, Vol. 27, No. 1, pp. 1-7

Vaid, Y.P. & Negussey, D. (1984): Relative density of pluviated sand samples, Soils and Foundations, Vol. 24, No. 2, pp. 101-105

Vaid, Y.P. & Negussey, D. (1988): Preparation of reconstituted sand specimens, Advances Triaxial Testing of Soil and Rock, ASTM STP 977, American Society for Testing and Materials, Philidelphia, pp. 405-417

Vaid, Y.P., Sivathayalan, S., Stedman, D. (1999): Influence of specimen-reconstituting method on the undrained response of sand, Geotechnical Testing Journal, Vol. 22, No. 3, pp. 187-195

Vidal, H. (1969): The earth army, Annals of the Technical Institute of Building and Public Works, Materials, Vol. 38, Nos. 259-260, pp. 1-59

Waldron, L.J., (1977): The shear resistance of root-permeated homogeneous and stratified soil, Journal of Soil Science Society of America, Vol. 41, pp. 843-849

Waldron, L.J. & Dakessian, S. (1981): Soil reinforcement by roots: Calculation of increased soil shear resistance from root properties, Journal of Soil Science Society of America, Vol. 132, pp. 427-435

Waldron, L.J., Dakessian, S., Nemson, J.A. (1981): Shear resistance enhancement of 1.22-meter diameter soil cross-sections by pine and alfalfa roots, Journal of Soil Science Society of America, Vol. 47, pp. 9-14

Wood, D.M. (1990): Soil Behaviour and Critical State Soil Mechanics, Cambridge University Press, ISBN 0-521-33782-8, pp. 226-253

Wu, T., McKinnell, W.P., Swanston, D.N. (1979): Strength of tree roots and landslides on Prince of Wales Island, Alaska, Canadian Geotechnical Journal, Vol. 16, pp. 19-33

Wu, T., McOmber, M., Erb, R.T., Beal, P.E. (1988_a): Study of soil-root interaction, Journal of Geotechnical Engineering, ASCE, Vol. 109, No. 3, pp. 1351-1375

Wu, T., Beal, P.E., Chinchun, L. (1988_b): In-situ shear test of soil-root systems, Journal of Geotechnical Engineering, ASCE, Vol. 114, pp. 1376-1393

Yasin, S.J.M., Umetsu, K., Tatsuoka, F., Arthur, J.R.F., Dunstan, T. (1999): Plane strain strength and deformation of sands affected by batch variations and different apparatus types, Geotechnical Testing Journal, Vol. 22, pp. 80-100

Yee, C.S. & Harr, R.D. (1977): Influence of soil aggregation on slope stability in the Oregon Coast Ranges, Environmental Geology, Vol. 1, p.367-377

Zornberg, J.G. (2002_a): Discrete framework for limit equilibrium analysis of fibre-reinforced soil, Geotechnique, Vol. 52, No. 8, pp. 593-604

Zornberg, J.G. (2002_b): Peak versus residual shear strength in geo-synthetic-reinforced soil design, Geosynthetics International, Vol. 9, No. 4, pp. 301-318

Zornberg, J.G., Sitar, N. and Mitchell, J.K. (2000): Limit equilibrium as a basis for design of geosynthetic reinforced slopes, Closure, Journal of Geotechnical and Geoenvironmental Engineering, ASCE, Vol. 126, No.3, pp. 286-288

9.0 Appendix

9.1 Top cap bending stiffness

The thickness and rigidity of the top caps were taken into consideration when reporting the vertical deformation in order to quantify any possible flexural rigidity that could affect the deformation behaviour of the reinforced samples. The bending stiffness of the top caps used in compression and shear tests depends on the materials of which they were made. The top cap used in the sample preparation for one-dimensional compression tests was made of Perspex and weighs 55.7g. Perspex has a Young's modulus of 2.9 GPa (according to www.engineering.usu.edu). The top cap used in the sample preparation for direct shear tests was made of mild steel and weighed approximately 360g. Mild steel has a Young's modulus of 212 GPa (Vogel, 1988).

There is an assumption that a more flexible top cap causes greater deformation by unequal load distribution in a similar manner as the flexibility of a raft foundation on a reinforced soil layer can produce non-uniform settlements. In both oedometer and shear box tests the points of contact for the load hangers were at the centre of the top cap. The fibre reinforcement spreads the point load throughout the volume of the sample.

The Poisson's ratio, Young's modulus and dimensions of the Perspex top cap were used in the calculation of the bending stiffness. The possible reactions and bending moments from the soil and indeed the porous stone or steel base that the samples rest on from the application of a point load, in this case the point of contact of the load hanger via a stabilising rod were calculated. Based on the values of the bending moments for the small-scale tests, the deflections due to bending stiffness were not found to be of a significant order.

9.2 Critical void ratio comparisons

Normal compression occurs from the continuous fracture of a sample's smallest (and usually strongest) particles, which fill local voids and protect the intrinsically weaker larger particles (McDowell, 2002). At high stresses the rate of reduction of voids ratio with log stress reduces as the sample becomes more rock-like at low void ratio values. The effect of the normal stress on the bond between soil and reinforcements is an increased confinement of the sand particles. This creates an apparent cohesion that the reinforcements impart to the soil. The reinforcement spreads the vertical load throughout the sample volume, which causes a deeper and wider mobilisation of soil strength in one-dimensional compression tests.

For granular soils subjected to one-dimensional compression, the compression curve is usually plotted as the void ratio against the logarithm of applied normal stress. Following

yield an approximately linear normal compression line emerges termed NCL, the normal consolidation line. In Figure 9.1 (repeated from chapter 2, Figure 2.39) the locations of particle breakages for two dry un-reinforced sand samples tested in a miniature oedometer are circled. It can be seen that the sample with the lowest normal stress did not suffer particle breakage. McDowell and Harireche (2002_a) believed that the point of maximum curvature on a plot of volume against the logarithm of stress is a suitable definition of yield, and that linear normal compression lines emerge as a result of particle breakage. Hardin (1987) related the yield point to the initial particle size distribution and particle shape, but not to the tensile strength of the particles.

If a single soil particle can be considered as an agglomerate of spheres bonded together, it can be possible to assume that the yielding in one-dimensional compression corresponds to the onset of fracture of bonds between the spheres that make up a grain of sand. The fracture of bonds can be observed as a "slip" between the original positions of the soil particles under stress. In Figure 9.2, the amalgamation was subjected to rotation, gravity and random spheres were removed for a more realistically natural particle model. If a fibre-reinforced soil sample can be considered as an amalgamation of sub-angular Hostun sand particles interspersed with flexible polypropylene fibres, it can be possible to verify that the yield point (as defined as the point of maximum curvature) in one-dimensional compression corresponds to the onset of fracture between the soil grains and fibres. Beyond yield an approximately linear normal compression line emerges. The slope of the compression plot reduces at high stress levels, because although some bond breakage may still occur, soil particles cannot fracture and fill voids indefinitely.

The inclusion of fibre reinforcements in a granular soil increases the tensile resistance of the mix. The tensile resistance of soil grains in usually measured indirectly by compressing a particle between flat platens until particle breakage occurs. The Weibull (1951) distribution of strength was modelled for a single particle d loaded diametrically between flat platens by a force F, the characteristic induced tensile stress $\sigma = F / d^2$. Weibull (1951) defined the probability of a particle's survival of this compression test for granular soils as P_s, in the following formula:

$$P_s(d) = \exp\left[-\left(\frac{\sigma}{\sigma_0}\right)^m\right]$$

where the value of normal stress (σ_0) at which 37% of particles survive failure is a function of the particle size of d diameter and m is the Weibull modulus. The Weibull modulus was used by McDowell and Harireche (2002_a) to calculate a normal stress value proportional to the average tensile strength as a function of the particle size by the following relationship:

$$\sigma_{yield} \sim \sigma_{tensile_{(average)}} \sim d^{-3/m}$$

McDowell and Harireche (2002_b) found the yield stress to be proportional to 37% particle tensile strength and equal to a factor of approximately 0.14-0.17 times the 37% tensile strength based on the survival probability P_s for granular soils.

In Figure 9.3 the yield stresses for silica sands in one-dimensional compression were defined according to their particle diameter size d. The expected yield stress was found to be proportional to the average particle tensile strength; therefore the yield stress should be inversely proportional to particle size (McDowell, 2002) by the following formula:

$$\left(\frac{\frac{d_{\min} + d_{\max}}{2}}{0.5} \right) \times \sigma_{yield} = \sigma_{tensile(average)}$$

For an aggregate of 0.5mm silica particles the yield stress would be approximately equal to 33 MPa ({[(0.3+0.6)/2]/0.5} × 37 MPa = 33 MPa). The 37% tensile strength for 0.5 mm diameter silica particles was found to be 147 MPa, so if the yield stress is assumed to be 0.25 times the 37% tensile strength, a yield stress of 37 MPa could be expected.

It is postulated that a "yield stress" in one-dimensional compression was shown for the reinforced samples (σ = 23 kPa) was less than the un-reinforced sample (σ = 39 kPa) in the samples with initial density e_i = 0.72. In Figure 9.4 the vertical "yield" stress value (shown in the region between dashed vertical lines) decreased as the initial void ratio values increased. It is well known that the yield stress can be related to the initiation of particle crushing, and that after yield the degree of particle crushing can increase rapidly. Nakata et al (2001) found a relationship between the yield stresses of sand samples in compression to a single particle's tensile strength in crushing. The relationship between the tensile strength in crushing of a single particle versus the tensile strength in crushing of a soil sample cannot be exactly

modelled due to the complexities of microscopic versus macroscopic scales of stresses for particles.

The characteristic tensile stress acting on a single particle embedded in a sample, was calculated by Nakata et al (2001) by the following:

$$V_s = \frac{1}{1+e}$$

where V_s is the volume of the solids in a unit volume of soil and e is the void ratio. The number of sand particles in a cubic volume, N, can be determined by the simplified assumption of the average volume of a single particle, V_{sp}.

$$N = \frac{V_s}{V_{sp}}$$

In a unit cubic volume containing N particles, the number of particles per unit cross-sectional area is calculated as $(N^{1/3})^2$ and the F_{sp} force acting on a single particle in the specimen is then given by dividing the normal stress σ by the number of particles across a plane of unit cross section:

$$F_{sp} = \frac{\sigma}{N^{2/3}}$$

The average volume of a single particle is taken based on the mean particle diameter; the measurement of the tensile stress is taken as a point load and the force on a single particle embedded in a soil sample was found to be:

$$F_{sp} = \sigma\left(\sqrt[3]{\frac{(1+e)\pi}{6}}\right)^2 d_{mean}^2$$

and the corresponding characteristic tensile stress is a function of the void ratio by the following:

$$\sigma_{sp} = \frac{F_{sp}}{d_{mean}^2} = \sigma\left(\sqrt[3]{\frac{(1+e)\pi}{6}}\right)^2$$

The characteristic tensile stress as a proportion of applied stress σ_{sp} increases as the void ratio increases. The relationship between the mean single particle crushing strength $(\sigma_f)_{mean}$ and the

characteristic tensile stress $(\sigma_{sp})c_{c=max}$ at the maximum compression index of a particle embedded in the granular mass was defined as:

$$(\sigma_{sp})c_{c=max} = \frac{F_{sp}}{d_{mean}^2} = (\sigma_v)c_{c=max}\left(\sqrt[3]{\frac{(1+e)\pi}{6}}\right)^2$$

Figure 9.5 shows the relationship between the ratio of 50% survival strength to characteristic tensile stress at maximum compression index versus the $e_{max} - e_{min}$ values. The area surrounded by a dashed line is the region where the mean single particle crushing strength $((\sigma_f)_{50} / (\sigma_{sp})c_{c=max})$ would be equal to the characteristic tensile stress of a particle embedded in a soil mass. The soil properties of the tests sands used by Nakata et al (2001) are shown in Table 9.1. A non-uniform distribution of inter-particle stress was taken into account when calculating the tensile stress acting on a single particle within a soil mass. The ratio of $(\sigma_f)_{50} / (\sigma_{sp})c_{c=max}$ was an indicator of the ratio of active to non-active particles. As the shape of the test grains became more angular and the surface roughness increased, the load distribution through the soil mass became more uniform. The one-dimensional test results for fibre-reinforced Hostun sand agreed with the conclusions of Nakata et al (2001) that the vertical yield stress increased with decreasing initial void ratio.

The reinforcing effects of the fibres are best seen in the increased shear strength that they provide to sand samples in direct shear. The mobilisation of the tensile force of the fibres is dependent on the confining stress. The tensile stress of the sand particles has been examined and now the tensile stress of both test materials will be investigated with respect to their contribution to increased shear strength.

The yield stress of un-reinforced sand was determined from one-dimensional compression tests. The average, characteristic and modified tensile strengths were calculated based on the compression data and presented. The tensile strength of the sand contributed to the increased shear resistance of fibre-reinforced soils. The void ratio corresponding to the yield tensile strength of the Hostun sand samples in one-dimensional compression was compared with the void ratio at peak shear stress for fibre-reinforced sands by the following relationship.

$$e_{SR\,(peak)} / e_{\sigma\,(yield)} \sim 1.0$$

The correlation between the void ratio values at peak stress ratio in shear and yield tensile stress from compression tests proved the theory that the sand particles contribute to the tensile strength of reinforced sand (in addition to the fibres' tensile strength) when sufficiently

confined. The results of the tensile strength comparisons based on the tensile strength of the sand particles can be seen in Tables 9.2 and 9.3. The void ratio at yield stresses were taken at the stress points of maximum deformation from the one-dimensional compression tests. The void ratios obtained from the peak stress states were considered to be the point at which the tensile strength of the fibre-reinforced sample as a whole was fully mobilised.

9.3 Tables / Figures

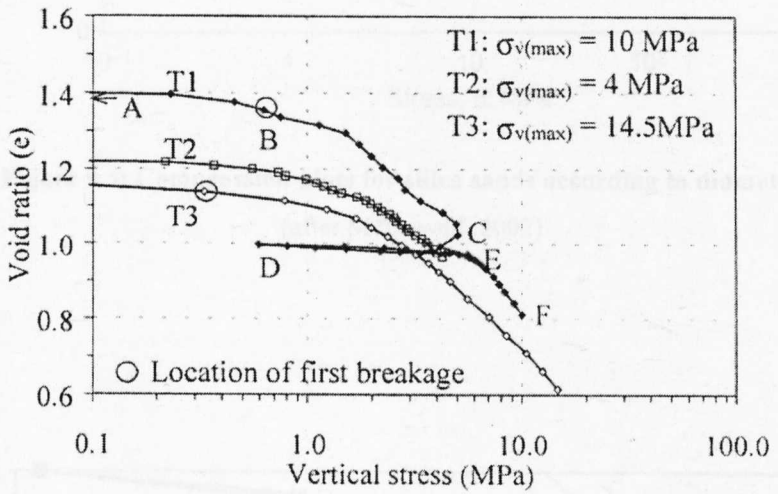

Figure 9.1: One-dimensional compression tests for three normal stresses

(after Cheng et al, 2001)

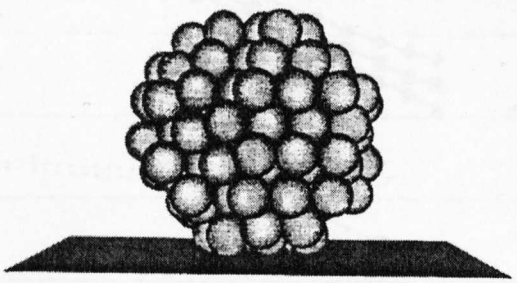

Figure 9.2: Amalgamation of 0.5mm diameter silica sand

(after McDowell, 2002)

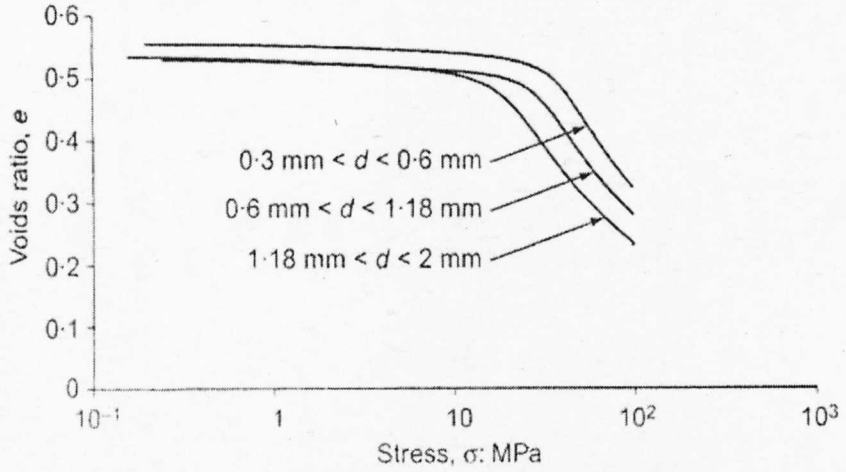

Figure 9.3: Compression plots for silica sands according to diameter *d*

(after McDowell, 2002)

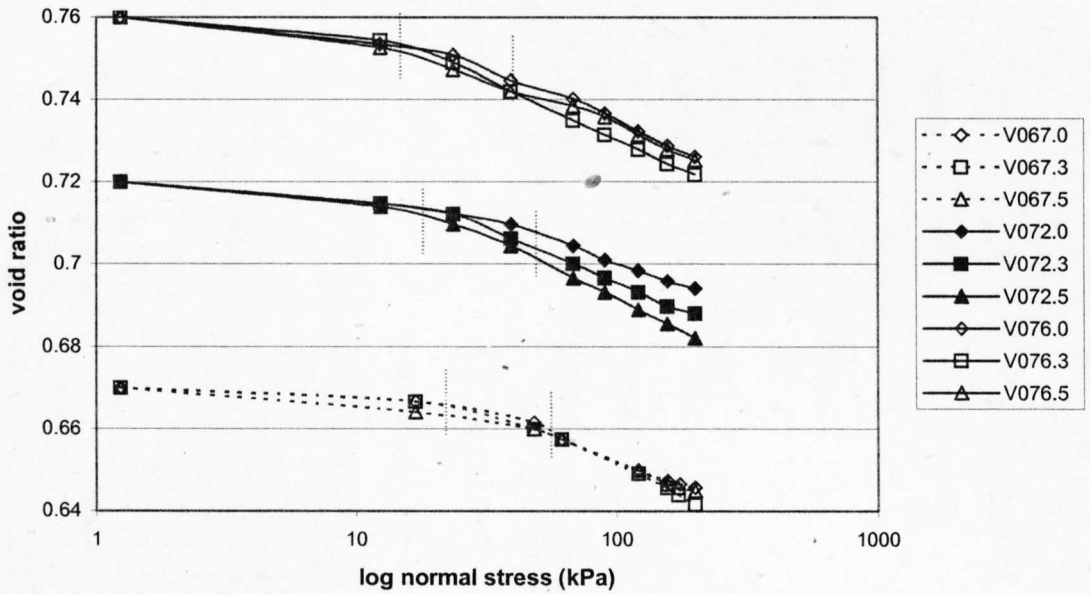

Figure 9.4: One-dimensional compression of vibrated samples (with yield)

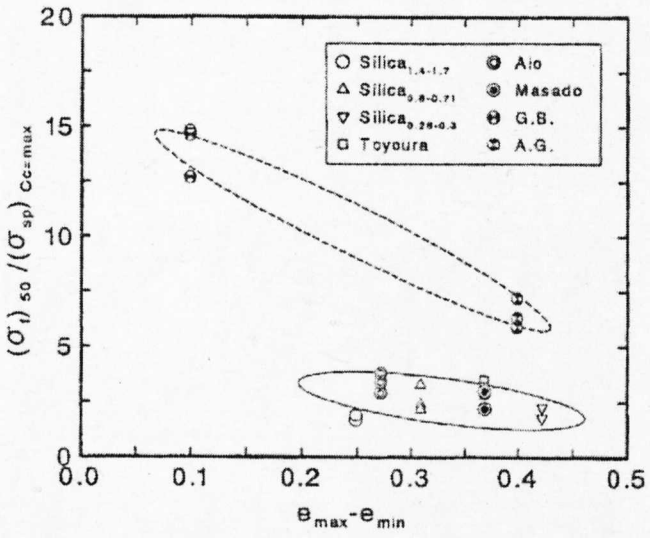

Figure 9.5: Relationship between σ_{sp} single particle tensile strength and void ratio
(after Nakata et al, 2001)

Material	Grains size (mm)	D_{r0} (%)	e_0	$(\sigma_v)_y$ (MPa)	$(\sigma_v)_{Cc=max}$ (MPa)	R
$Silica_{1.4-1.7}$	1.4–1.7	100	0.632	11.94	17.69	0.39
		87.6	0.666	9.63	17.86	0.62
		45	0.769	8.23	15.71	0.65
$Silica_{0.6-0.71}$	0.6–0.71	100	0.659	11.62	31.75	1.01
		96.6	0.666	13.44	34.86	0.95
		45	0.829	8.22	22.46	1.01
$Silica_{0.25-0.3}$	0.25–0.3	100	0.666	16.91	60.23	1.27
		45	0.898	10.41	44.73	1.46
Toyoura	0.106–0.25	100	0.617	17.46	49.89	1.05
		80	0.683	13.01	39.95	1.12
		45	0.812	8.73	42.21	1.58
Aio	0.85–2.0	100	0.695	5.26	13.34	0.93
		80	0.753	4.79	10.81	0.81
		45	0.845	2.64	9.58	1.29
Masado	1.4–1.7	100	0.838	2.23	7.44	1.20
		80	0.918	1.82	7.11	1.36
		45	1.045	1.68	9.12	1.69
Glass ballotini (G.B.)	0.85–1.0	100	0.600	26.49	27.33	0.03
		93	0.607	26.94	32.26	0.18
		45	0.648	27.00	27.33	0.01
Angular glass (A.G.)	0.85–1.0	100	0.744	4.78	10.46	0.78
		86	0.801	3.68	9.55	0.95
		45	0.956	2.08	8.06	1.36

Table 9.1: Test sand properties
(after Nakata et al, 2001)

$e_{initial}$=	0.67			0.72			0.76		
Fibre content (% by weight)	**0.0%**	**0.3%**	**0.5%**	**0.0%**	**0.3%**	**0.5%**	**0.0%**	**0.3%**	**0.5%**
σ_{yield} **(kPa)**	48	48	48	38	38	38	23	23	23

Table 9.2: Yield stresses for Hostun test samples

V670.0	e_{peak}	e_{yield}	Ratio e_{peak} / e_{yield}
50	0.673	0.66	1.0197
100	0.672	0.66	1.0182
200	0.664	0.66	1.0061
V720.0			
50	0.72	0.71	1.0141
100	0.704	0.71	0.9915
200	0.715	0.71	1.0070
V760.0			
50	0.755	0.75	1.0067
100	0.755	0.75	1.0067
200	0.755	0.75	1.0067
V670.3	e_{peak}	e_{yield}	Ratio e_{peak} / e_{yield}
50	0.677	0.658	1.0289
100	0.670	0.658	1.0182
200	0.664	0.658	1.0091
V720.3			
50	0.721	0.705	1.0227
100	0.715	0.705	1.0142
200	0.715	0.705	1.0142
V760.3			
50	0.761	0.745	1.0215
100	0.749	0.745	1.0054
200	0.738	0.745	0.9906
V670.5	e_{peak}	e_{yield}	Ratio e_{peak} / e_{yield}
50	0.755	0.75	1.0067
100	0.755	0.75	1.0067
200	0.755	0.75	1.0067
V720.5			
50	0.761	0.745	1.0215
100	0.749	0.745	1.0054
200	0.738	0.745	0.9906
V760.5			
50	0.765	0.742	1.0310
100	0.745	0.742	1.0040
200	0.729	0.742	0.9825

Table 9.3: Values for $e_{SR\ (peak)}$ shear stress and $e_{\sigma\ (yield)}$ one-dimensional compression